A Neotectonic Model of Taiwan, with a Focus on the Longitudinal Valley Suture

Thesis by

J. Bruce H. Shyu (Hao-Te Hsu)

In Partial Fulfillment of the Requirements

for the Degree of

Doctor of Philosophy

California Institute of Technology

Pasadena, California

2006

(Defended 22 November 2005)

© 2006

J. Bruce H. Shyu (Hao-Te Hsu)

All Rights Reserved

Acknowledgments

Seven years ago when I was writing my Master's thesis, I considered the acknowledgments to be the most important part of that thesis. Today, I still believe that this acknowledgment is the most important section of this dissertation. However, this acknowledgment could also be the section that is most difficult to write, since I may have to write a whole new thesis in order to thank everyone that has helped me through these years.

First of all, I want to express my utmost gratitude to my advisor, Kerry Sieh, for his generous support and guidance through the years, and his endless enthusiasm for the neotectonics of Taiwan, earth science, and the sciences in general. Without his intuitive decision to work on the general neotectonic picture of Taiwan after the earthquake, his meticulous working style in the field, and his painstaking corrections of my writing, this thesis would have never been produced. Furthermore, besides having learned tremendously from him in the scientific realm, I feel that I have benefited even more from countless casual discussions, whose topics have ranged from societal and political issues to the environment and even to how best to enjoy life. All of these shaped me not only into a scientist, but also into a better person, with a more international point of view.

I would like to thank my other thesis committee members, Jason Saleeby, Jean-Philippe Avouac, Mark Simons, and Joann Stock, for helping me through the years and for spending a great deal of time reviewing this dissertation and improving it significantly. Jason has been my academic advisor for these years and taught the first class that I took here at Caltech, a field class out in the desert. I am grateful for his patience and appreciation for me during that class, so that I was able to enjoy such a brand new environment and experience and strengthened my interest in pursuing geology in the field. Jean-Philippe helped me with the research that forms one chapter of this thesis, and he also taught me a great deal of the mathematics and physics of neotectonics,

which have long been my weakest points. Most of my knowledge about geodesy was obtained from valuable discussions with Mark, and I have learned a lot from Joann both in her classes and in discussions with her.

I would also like to thank all of the faculty members here in the GPS Division, Caltech, for teaching me so much during these six and a half years. In particular, I want to thank Dianne Newman, the advisor for one of my first-year propositions. Knowing nothing about microbiology at that time, I am grateful for her giving me the opportunity to work in her lab and for enlightening me on this subject, as well as for her understanding and encouragement of my decision to return to geology afterward. I have also learned enormously from John Eiler and Jess Adkins, advisors for my other first-year proposition, as well as from Joe Kirschvink and Brian Wernicke. I also want to thank George Rossman and Yuk Yung for their encouragement and support.

This thesis would not have come to exist without the tremendous help of my Taiwanese friends and colleagues. Yue-Gau Chen, the superman, is the most important unsung hero of this thesis. Not only did he provide all of the logistic and financial support, but he was also always there when I needed help. He has been a mentor, a colleague, and most importantly, a friend of mine throughout the years. Wen-Shan Chen provided the financial support for my Hsiukuluan River terrace investigations and taught me a lot about the Coastal Range geology. Typhoon Huang took care of the logistics and dealt with the landowners in eastern Taiwan. I am also grateful for the encouragement and support of Leh-Chyun Wu, Ping-Mei Liew, Ching-Hua Lo, Sun-Lin Chung, and other professors in National Taiwan University, without which I would not have finished this thesis.

The arduous and time-consuming field work that forms the basis of this thesis was aided by numerous friends and students in Taiwan. Among them, Ling-Ho Chung was my most important assistant and was in the field with me most of the time. We have tackled all kinds of roads and outcrops, mostly on motor scooters in the field. Yu Wang,

Kuang-Yin Lai, Ray Chuang, and other students of Yue-Gau's group helped with most of my field work in western Taiwan and some of the work in eastern Taiwan. Chung Huang, Po-Nong Li, Shin-Hua Huang, and Chih-Hao Chen helped the investigations and measurements in the Hsiukuluan River area. Yung-Chuan Chen helped me greatly in the Peinanshan area, and my works in the terrace pits were helped significantly by Barry Chih-Cheng Yang, I-Chin Yen, Neng-Wei Huang, and other students from Wen-Shan's group. Takuya Watanuki, who passed away this summer in a tragic accident, assisted me on several field trips in eastern Taiwan, and I have benefited from our discussions and enjoyed working in the field with him. I will always miss such a great friend.

Many local residents in eastern Taiwan have assisted me in the field. I want to thank Boss Hsieh of Rueisuei and Boss Huang of Lungtien for helping me dig the pits on the river terraces, Mr. Wu of Tewu for providing his own land and for arranging other suitable locations for the pit-digging, Mr. Hsieh of Chimei for providing his land for the pit-digging as well as for his hospitality in providing meals for me when I was in the area, and Reverend Pai and the Bunun Cultural and Educational Foundation for providing accommodation and their land and backhoe for the pit-digging. I want to thank in particular Teacher Huang and Teacher Cheng, the owner of the "House under the Hill" of Rueisuei, for their hospitality in providing me a warm, cozy and welcoming shelter in the field. Every time when I was heading toward the "House under the Hill," I felt as if I was heading home.

During the writing of this thesis, I have been benefited significantly from discussions with numerous colleagues, including Olivier Beyssac, Sara Carena, Yu-Chang Chan, Hui-Hsuan Chen, Wu-Cheng Chi, Hao-Tsu Chu, Meng-Long Hsieh, Jyr-Ching Hu, Jian-Cheng Lee, Wen-Tzong Liang, Chia-Yu Lu, Yoko Ota, Charlie Rubin, Colin Stark, Quocheng Sung, Louis Teng, David Wiltschko, and Shui-Beih Yu. Ya-Ju Hsu and Yih-Min Wu generously provided me with their geodetic and seismologic data along with valuable comments, and Char-Shine Liu provided the high-resolution

bathymetric data. Michaele Kashgarian of the Center for Accelerator Mass Spectrometry, at Lawrence Livermore National Laboratory, performed the radiocarbon dating of my charcoal samples from the river terraces. Several chapters of this thesis were improved significantly by the critical reading of many reviewers, including Hao-Tsu Chu, Thomas Fumal, Isabelle Manighetti, and Robert Yeats. Caltech proofreaders have provided valuable comments on the grammar and the overall consistency of this thesis, and Simon LeVay kindly helped me on the grammar of this acknowledgment.

I have been very fortunate to be able to study at Caltech, and I feel privileged to work among, interact with and learn from some of the finest scientists. Visiting professors and previous post-docs, including Paul Tapponnier, John Suppe, Çelal Şengör, Jamshid Hassan Zadeh, Anke Friedrich, Nadine McQuarrie, Eric Cowgill, Todd Ehlers, and Yann Klinger have significantly broadened my knowledge of many aspects of earth sciences. Danny Natawidjaja and Jing Liu, my previous officemates and groupmates, have taught me a lot about how to survive Caltech and how to work efficiently with Kerry. I am also grateful for both scientific and social interactions with, and encouragement and support from, the following persons: Elisabeth Nadin, Selene Eltgroth, Tanja Bosak, Eh Tan, Huirong Ai, Zhengrong Wang, Lingsen Zeng, Teh-Ru Alex Song, Laura Croal, Davin Malasarn, Sarah Miller, Zhimei Yan, Ying Tan, Qinya Liu, Sarah Minson, and my other classmates and fellow graduate students; Mariu Hernandez, Rowena Lohman, Nathan Niemi, Mike Oskin, and my other TAs; Martine Simoes, Mohamed Chlieh, Richard Briggs, Ryan Petterson, Charlie Verdel, Aron Meltzner, and other tectonic lunch group members; and Ashley Streig, Keegan Fengler, Jean Holiday, Sarah Venator, and other students from the Central Washington University. I have also learned a lot from the students of the four Ge112 classes, the one Ge177a class, and the three Ge122 classes that I have TA'ed. My life at Caltech was also enriched by many other friends of the Association of Caltech Taiwanese and our softball team, including Yu-Teng Chang, Ching-Tzu Chen, Po-Jui Chen, Wei-Ting Chen, Mu-Cheng Cheng, Chin-Wen Chou,

Serena Chung, Wei-Hsin Gu, Hung-Te Hsieh, Yu-Ting Huang, I-Ren Lee, Hsuan-Tien Lin, Ming-Shr Lin, Miao-Ling Lu, Mortada Mehyar, Victor Shih and Vanessa Lin, Borching Su, Bruce Tai, Tzer-jen Wei, Shau-Ming Wu, and Fu-Ling Yang.

The great working and learning environment at Caltech is produced and kept not only by the intelligent scientists and students, but also by the wonderful group of administrative and technical personnel. I want to thank JoAnne Giberson, Shaun Healy, and Jennifer Yu for keeping the GIS lab running smoothly, Jim O'Donnell and Susan Leising for providing a great library, Michelle Medley, Marcia Hudson, Carolyn Porter, Terry Gennaro, and the late Donna Sackett for their administrative support, and Heather Steele, Sheri Garcia, and other previous secretaries of Kerry's group, for taking care of everything!

Last but not least, I would like to thank my family. My parents have always been providing me with endless love, belief and encouragement, and I want to thank them for their understanding and support through the years, ever since I decided to transfer from engineering to geology. I also want to thank my brother and sister and in-laws, who are always there for me. And finally, I could have never finished this thesis without the love, care, companionship and support of my beloved wife, Shing-Lin Wang, who, through the years, has been always beside me through the difficulties, stresses, hard work, deadlines, and the occasional joyful achievement. I ascribe everything that I have accomplished to her.

Once again, I want to thank everyone who has helped me and cared about me through the years. May we all enjoy our life safely, happily, and joyfully, and may peace prevails on Earth.

Abstract

The disastrous effects of the 1999 Chi-Chi earthquake in Taiwan demonstrated an urgent need for better knowledge of the island's potential earthquake sources as well as their neotectonic context. Toward this end, we have utilized digital elevation models of the island to prepare a neotectonic map of Taiwan and proposed a neotectonic model for the orogen. Taiwan's numerous active faults and folds reveal that the active orogen is a tandem suturing and tandem disengagement of a volcanic arc and a continental sliver to and from the Eurasian continental margin. The collision and suturing in the southern part of the orogen and the post-collisional collapse and extension in the island's northern and northeastern flanks have produced eleven distinct neotectonic domains. Each domain is defined by a distinctive suite of active structures. In most of the domains, the size of the principal active fault is large enough to produce future earthquakes with magnitudes in the mid-7 range.

In order to further understand the suturing processes, we have focused the second part of our investigation on the Longitudinal Valley suture in eastern Taiwan. The earthquakes of November 1951 within this suture constitute one of the most destructive seismic episodes in Taiwan's history. The surface ruptures of the earthquakes consist of three distinct sections, two of which are along segments of the Longitudinal Valley fault. From fluvial terraces along the Hsiukuluan River, we have reconstructed a shallow listric geometry for the Longitudinal Valley fault. On the other hand, many uplifted lateritic fluvial terraces along the eastern flank of the Central Range indicate the presence of a west-dipping Central Range reverse fault. We believe the majority of the horizontal shortening across the Longitudinal Valley suture is accommodated by the slip on the Longitudinal Valley fault. The remaining horizontal convergence may be absorbed by a combination of slip on the Central Range fault and subsidence of the Longitudinal Valley floor. The along-strike difference in geometry of the two major faults along the

Longitudinal Valley is likely the manifestation of the northward maturation of the suturing of the Luzon volcanic arc to the Central Range continental sliver.

Table of Contents

Acknowledgments.....iii

Abstract.....viii

Table of Contents.....x
List of Figures.....xiv
List of Tables.....xvii

Introduction and Summary of Chapters.....1

Chapter 1 Tandem Suturing and Disarticulation of the Taiwan Orogen Revealed by Its Neotectonic Elements.....1-1
1.1 Abstract.....1-2
1.2 Introduction.....1-3
1.3 Neotectonic belts and domains of Taiwan.....1-3
1.4 The Taiwan orogen as accreting and disarticulating twin sutures.....1-7
1.5 Implications for future earthquake sources.....1-14
1.6 Concluding Remarks.....1-15
1.7 Acknowledgments.....1-17
1.8 References.....1-18

Chapter 2 Neotectonic Architecture of Taiwan and Its Implications for Future Large Earthquakes.....2-1
2.1 Abstract.....2-2
2.2 Introduction.....2-3
2.3 Neotectonic overview of Taiwan.....2-8
2.4 Neotectonic domains of Taiwan.....2-11
2.4.1 Eastern neotectonic belt.....2-13
2.4.2 Western neotectonic belt.....2-24
2.5 Discussion and earthquake scenarios.....2-43
2.6 Conclusions.....2-61
2.7 Acknowledgments.....2-62
2.8 References.....2-63

Chapter 3 Re-evaluation of the Surface Ruptures of the November 1951 Earthquake Series in Eastern Taiwan and Their Neotectonic Implications....3-1
3.1 Abstract....3-2
3.2 Introduction....3-3
3.3 Tectonic background of the Longitudinal Valley....3-6
3.4 The November 1951 earthquake series....3-8
3.5 Re-evaluation of the November 1951 ruptures....3-11
3.5.1 The Chihshang rupture....3-11
3.5.2 The Rueisuei rupture....3-15
3.5.3 The Yuli rupture....3-17
3.5.4 The Yuli rupture and the Longitudinal Valley fault....3-21
3.6 Discussion....3-23
3.6.1 The November 1951 earthquake series: a complex rupture event....3-23
3.6.2 What is the Yuli fault?....3-26
3.6.3 Implications for seismic hazard assessment....3-28
3.7 Conclusions....3-30
3.8 Acknowledgments....3-31
3.9 References....3-32

Chapter 4 Millennial Slip Rate of the Longitudinal Valley Fault from River Terraces: Implications for Convergence across the Active Suture of Eastern Taiwan....4-1
4.1 Abstract....4-2
4.2 Introduction....4-3
4.3 General geologic setting....4-7
4.4 River terraces of Hsiukuluan canyon....4-11
4.4.1 Distribution and characteristics....4-11
4.4.2 Age of terraces....4-15
4.4.3 Reconstructions of river patterns in the past....4-17
4.5 Incision and uplift rates along Hsiukuluan canyon....4-20
4.5.1 Shear stress profile along Hsiukuluan canyon....4-23
4.5.2 Fault-bend fold model....4-27
4.6 Discussion....4-30

4.6.1 Shortening across the Longitudinal Valley suture....4-30
4.6.2 Subsurface geometry of the Longitudinal Valley fault: The evolution of lithospheric sutures....4-35
4.6.3 Long-term uplift rates of the Coastal Range....4-39
4.6.4 Earthquake potential of the Longitudinal Valley fault....4-40
4.7 Conclusions....4-42
4.8 Acknowledgments....4-43
4.9 References....4-44

Chapter 5 Geomorphic Analysis of the Central Range Fault, the Second Major Active Structure of the Longitudinal Valley Suture, Eastern Taiwan....5-1
5.1 Abstract....5-2
5.2 Introduction....5-3
5.3 Geologic setting....5-6
5.4 Geomorphic analysis near the Wuhe Tableland....5-7
5.5 The Central Range fault south of the Taiping River....5-15
5.6 The blind Central Range fault south of Chihshang....5-19
5.7 Discussion....5-20
5.7.1 Geodetic and Seismic Evidence....5-20
5.7.2 Sense of Slip and Slip Rate of the Central Range Fault....5-22
5.7.3 The Evolution of the Longitudinal Valley Suture....5-24
5.7.4 The Central Range Fault and the Uplift of the Central Rang....5-26
5.8 Conclusions....5-27
5.9 Acknowledgments....5-29
5.10 References....5-30

Chapter 6 Neotectonic Geomorphology of Southernmost Longitudinal Valley Fault, Eastern Taiwan, and Its Tectonic Implications....6-1
6.1 Abstract....6-2
6.2 Introduction....6-3
6.3 Tectonic setting....6-6
6.4 Major geomorphic features at southernmost Longitudinal Valley....6-8
6.5 Neotectonic geomorphology of the Kaotai and surrounding terraces....6-10
6.6 Neotectonic geomorphology of the northern Peinanshan area....6-17
6.7 Neotectonic geomorphology of the southern Peinanshan area....6-22
6.8 Neotectonic geomorphology of the Pingting terraces....6-25

6.9 Discussion.....6-29
6.9.1 The Central Range fault at the southernmost Longitudinal Valley.....6-29
6.9.2 The southern termination of the Taitung Domain.....6-30
6.9.3 Stress release of the southernmost Longitudinal Valley fault.....6-31
6.9.4 Lichi Formation and the Longitudinal Valley fault.....6-32
6.10 Conclusions.....6-33
6.11 Acknowledgments.....6-35
6.12 References.....6-36

Chapter 7 Conclusions and Implications.....7-1
7.1 Neotectonic framework of Taiwan and earthquake scenarios.....7-2
7.2 Active tectonics of the Longitudinal Valley suture.....7-10
7.3 References.....7-14

List of Figures

Figure 1.1. Map of the active faults and anticlines of the Taiwan orogen.....1-4
Figure 1.2. Tandem suturing and tandem disarticulation of Taiwan.....1-8
Figure 1.3. Three schematic crustal cross sections across Taiwan.....1-9

Figure 2.1. A neotectonic snapshot of Taiwan and adjacent regions.....2-4
Figure 2.2. Examples of the geomorphic evidence for active structures.....2-7
Figure 2.3. Map of major active faults and folds of Taiwan.....2-12
Figure 2.4. Active-tectonic map of the Lutao-Lanyu Domain.....2-15
Figure 2.5. Active-tectonic map of the Taitung Domain.....2-17
Figure 2.6. Active-tectonic map of the Hualien Domain.....2-20
Figure 2.7. Active-tectonic map of the western part of the Ryukyu Domain.....2-23
Figure 2.8. Active-tectonic map of the Kaoping Domain.....2-27
Figure 2.9. Active-tectonic map of the Chiayi Domain.....2-29
Figure 2.10. Active-tectonic map of the Taichung Domain.....2-32
Figure 2.11. Active-tectonic map of the Miaoli Domain.....2-35
Figure 2.12. Active-tectonic map of the Hsinchu Domain.....2-38
Figure 2.13. Active-tectonic map of the Taipei Domain.....2-39
Figure 2.14. Active-tectonic map of the onland part of the Ilan Domain.....2-42
Figure 2.15. Simple cross sections proposed for the eleven tectonic domains.....2-48
Figure 2.16. Proposed major sources for future large earthquakes in and around Taiwan.....2-52

Figure 3.1. Taiwan is experiencing a transitory tandem suturing.....3-4
Figure 3.2. Shaded relief map showing the active structures in the Longitudinal Valley.....3-8
Figure 3.3. Map of previously published surface ruptures of the November 1951 earthquakes.....3-10
Figure 3.4. The Chihshang rupture.....3-12
Figure 3.5. The Rueisuei rupture.....3-16
Figure 3.6. The Yuli rupture.....3-18
Figure 3.7. Proposed extrapolation of the Yuli rupture of 1951 north of Yuli.....3-20
Figure 3.8. A schematic tectonic E-W cross section of the Longitudinal Valley.....3-28

Figure 4.1. The Taiwan orogen is being created by a tandem suturing.....4-4
Figure 4.2. Map of major structures in the middle part of the Longitudinal Valley...4-5
Figure 4.3. A GPS transect, topographic profiles, and major crustal structural features across Taiwan.....4-6
Figure 4.4. Map of Hsiukuluan canyon across the Coastal Range.....4-8
Figure 4.5. A schematic geologic cross section across the Longitudinal Valley.....4-10
Figure 4.6. Typical river terrace deposit exposures along Hsiukuluan canyon.....4-13
Figure 4.7. Detailed maps of the fluvial terraces of western Hsiukuluan canyon....4-16
Figure 4.8. Stratigraphic columns of all sampling sites.....4-18
Figure 4.9. Reconstruction of river channels along western Hsiukuluan canyon.....4-20
Figure 4.10. All of the river terraces projected along N80°W direction.....4-23
Figure 4.11. Shear stress calculations along Hsiukuluan canyon.....4-26
Figure 4.12. Fault-bend fold model of the Longitudinal Valley fault from the river terraces along Hsiukuluan canyon.....4-29
Figure 4.13. Subsurface geometry reconstruction of the Longitudinal Valley fault...4-30
Figure 4.14. Cartoon showing the effect of footwall subsidence on the calculation of the Longitudinal Valley fault slip rate.....4-33
Figure 4.15. Schematic crustal cross sections showing the evolution of the Longitudinal Valley suture.....4-37

Figure 5.1. The island of Taiwan is being created by a tandem suturing.....5-4
Figure 5.2. Map of major structures in the middle part of the Longitudinal Valley...5-5
Figure 5.3. Detailed map of geomorphic and neotectonic features on and around the Wuhe Tableland.....5-8
Figure 5.4. Index map of locations in the Wuhe Tableland area.....5-10
Figure 5.5. Selected photographs of the Wuhe Tableland area.....5-11
Figure 5.6. Selected topographic profiles in the Wuhe Tableland area.....5-12
Figure 5.7. Detailed map of geomorphic and neotectonic features south of the Wuhe Tableland.....5-16
Figure 5.8. Detailed map of geomorphic and neotectonic features between the Lele River and Chihshang.....5-17
Figure 5.9. Photograph and sketch of a large N-S trending ridge.....5-18
Figure 5.10. Photograph and sketch of a deformed alluvial fan surface.....5-19
Figure 5.11. Large incised alluvial fans south of Chihshang.....5-20
Figure 5.12. Schematic crustal cross sections showing our hypothesis for the evolution of the Longitudinal Valley suture.....5-25

Figure 6.1. The island of Taiwan is being created by a tandem suturing.....6-4
Figure 6.2. Map of neotectonic domains of Taiwan.....6-5
Figure 6.3. Major fluvial landforms near the southernmost Longitudinal Valley.....6-9
Figure 6.4. Detailed map showing geomorphic features and active structures of the Kaotai terraces area.....6-11
Figure 6.5. Selected topographic profiles of the Kaotai terraces area.....6-12
Figure 6.6. Field photographs of deformed bridges across the Peinan River.....6-16
Figure 6.7. Detailed map showing geomorphic features and active structures of the northern Peinanshan area.....6-18
Figure 6.8. Selected topographic profiles of the northern Peinanshan area.....6-19
Figure 6.9. Photographs of the landslide deposits east of the Peinan River.....6-22
Figure 6.10. Detailed map showing geomorphic features and active structures of the southern Peinanshan area.....6-24
Figure 6.11. Detailed map showing geomorphic features and active structures of the Pingting terraces area.....6-26
Figure 6.12. A schematic tectonic E-W cross section near the Peinanshan.....6-30

Figure 7.1. Map of major active faults and folds of Taiwan.....7-3
Figure 7.2. Proposed major sources for future large earthquakes in and around Taiwan.....7-4
Figure 7.3. Taiwan is experiencing a tandem suturing.....7-5
Figure 7.4. Major tectonic elements in southeastern Asia.....7-6
Figure 7.5. An alternative model for the E-W crustal cross section across central Taiwan.....7-8
Figure 7.6. Map of major structures in the central Longitudinal Valley.....7-11
Figure 7.7. Schematic crustal cross sections showing our hypothesis for the evolution of the Longitudinal Valley suture.....7-12

List of Tables

Table 2.1. Proposed major seismic structures of Taiwan.....2-54

Table 4.1. Measurements of the river terrace sediment thickness along Hsiukuluan canyon.....4-14

Table 4.2. Analytical results of all of the samples dated from river terraces along Hsiukuluan canyon.....4-19

Table 6.1. List and analytical results of the charcoal samples dated from the Peinanshan area.....6-13

Introduction and Summary of Chapters

The island of Taiwan, located at the boundary between the Eurasian and Philippine Sea plates, is a young collision belt that began to form in the last couple of million years. During this geologically short period of time, the island has been and continues to be produced and shaped by extremely high rates of convergence, uplift, erosion, and sedimentation. Numerous earthquakes must have also occurred frequently on the young island.

However, due to a short recorded history, the disastrous effects of large earthquakes have never come into the minds of the residents of the island, until the devastating earthquake of 1999 occurred. The earthquake, produced by more than 80 km of rupture on the Chelungpu thrust fault in central Taiwan, shook the entire island, and caused more than two thousand deaths on the island. Folding in the hanging-wall block of the fault produced impressive broad deformation of the ground surface and resulted in large areas of damage.

Many of these co-seismic phenomena could have been anticipated accurately if the earthquake source had been known in advance. For example, the trace of the Chelungpu fault that produced the 1999 earthquake was clear from its geomorphic expression well before its 1999 rupture, but it had not been mapped as an earthquake-generating active structure systematically. The basic subsurface geometry of the structure had been known for a long time, but important details had not been investigated using the patterns of deformation of fluvial terraces along the fault.

Prompted by this urgent need for a better understanding of the island's earthquake sources, we decided to systematically map the active structures of Taiwan. Based upon a 40-m resolution digital elevation model (DEM) and augmented by published structural, geodetic, and seismologic analyses and our own field investigations, we have produced a neotectonic map of the island. The characteristics of these active structures of the island

led us to realize that the Taiwan orogen is a product of a twin suturing and disarticulation of three lithospheric blocks: the Asian continental margin, the Luzon volcanic arc, and an intervening continental sliver that includes the Central backbone Range of Taiwan. Based on this neotectonic framework, the orogen can be separated into two neotectonic belts, each containing several neotectonic domains. In each domain, a distinct assemblage of active structures prevails.

The first two chapters of this thesis contain the discussion of these results. In the first chapter, we discuss the tandem suturing and disarticulation that are forming and breaking the island apart at the same time. In the second chapter, we describe in detail the two neotectonic belts of Taiwan, with a discussion on possible earthquake scenarios caused by these active structures in the future.

In eastern Taiwan, the Longitudinal Valley between the Central and Coastal Ranges is the suture between the docked Luzon volcanic arc and the continental sliver of the Central Range. Due to the high rate of convergence between these two blocks, the valley is one of the most tectonically active areas of the world, with numerous seismic activities and fast-slipping active structures. In order to further understand the suturing processes and the formation of the Longitudinal Valley, we have focused the second part of our investigation on mapping and analyzing the two major active structures along the valley: the east-dipping Longitudinal Valley fault and the west-dipping Central Range fault.

Chapters three to six of this thesis contain the results of these investigations. In the third chapter we provide the results of our re-evaluation of the surface ruptures of the November 1951 earthquake, which occurred in the central Longitudinal Valley, by examining old documents and reports and vintage photographs of the rupture and by conducting interviews of elderly residents who experienced the earthquake. In the fourth chapter we present our analysis of the subsurface geometry and the millennial slip rate of the Longitudinal Valley fault from geomorphic and structural analysis of river

terraces in its hanging-wall block. The fifth chapter contains results of our mapping and field investigation of the less-known Central Range fault. And finally, in the sixth chapter, we introduce our mapping and investigative results of the Longitudinal Valley fault near the southern end of the valley. The latter three chapters provide important information on the evolution of the Longitudinal Valley fault suture.

Chapter 1

Tandem Suturing and Disarticulation of the Taiwan Orogen Revealed by Its Neotectonic Elements

An edited version of this chapter has been published as:

Shyu, J.B.H., K. Sieh, and Y.-G. Chen, 2005, *Earth and Planetary Science Letters*, 233, 167-177.

1.1 Abstract

Taiwan's numerous active faults and folds demarcate distinct eastern and western neotectonic belts. The western belt results from the attachment and subsequent detachment of a sliver of continental lithosphere to the Eurasian continental margin. The eastern belt is the product of the same continental sliver docking with and then separating from the Luzon volcanic arc. Thus, the active Taiwan orogen is a tandem suturing and tandem disengagement of a volcanic arc and a continental sliver to and from the Eurasian continental margin. This progressive suturing and separation is a superb, living demonstration of the fundamental weakness of lithospheric sutures. Furthermore, this neotectonic architecture provides the basis for understanding the Taiwan's seismic sources.

Keywords: Taiwan, suture, neotectonics, seismic hazard, orogeny.

1.2 Introduction

Taiwan is a result of the collision of Eurasian and Philippine Sea plates [e.g., *Ho*, 1986; *Teng*, 1987, 1990, 1996]. Rapid rates of horizontal and vertical deformation [*Yu et al.*, 1997, 1999; *Hovius et al.*, 2000] and an abundance of seismic activity [*Bonilla*, 1975, 1977; *Hsu*, 1980; *Cheng and Yeh*, 1989] amply demonstrate the current vigor of the orogeny.

The 1999 Chi-Chi earthquake and its unanticipated effects on population and infrastructure focused much scientific and public attention on Taiwan and demonstrated the urgent need for a better understanding of the island's seismic sources [e.g., *Ma et al.*, 2000, 2001; *Chen et al.*, 2001; *Ji et al.*, 2001; *Johnson et al.*, 2001; *Kelson et al.*, 2001]. In particular, the spectacular rupture of the Chelungpu thrust inspired us to investigate the fault's neotectonic context.

Fortunately, coincident with the occurrence of the earthquake, a high-quality, high-resolution digital elevation model (DEM) of the island was produced. The DEM and new bathymetric maps afforded us the opportunity to conduct a broad survey of the geomorphic manifestation of active folding and faulting on the island and in nearby offshore regions. That geomorphologic investigation, augmented by consideration of published structural, stratigraphic, geodetic, and seismologic data, led to the production of a neotectonic map and cross sections of the island [*Shyu et al.*, 2005a].

Construction of the neotectonic map led, in turn, to the model of the Taiwan orogen that we present below. We discuss the details of the neotectonic architecture of the island in another lengthier paper [*Shyu et al.*, 2005a].

1.3 Neotectonic belts and domains of Taiwan

Figure 1.1 depicts the major active structures of Taiwan. The map shows that belts

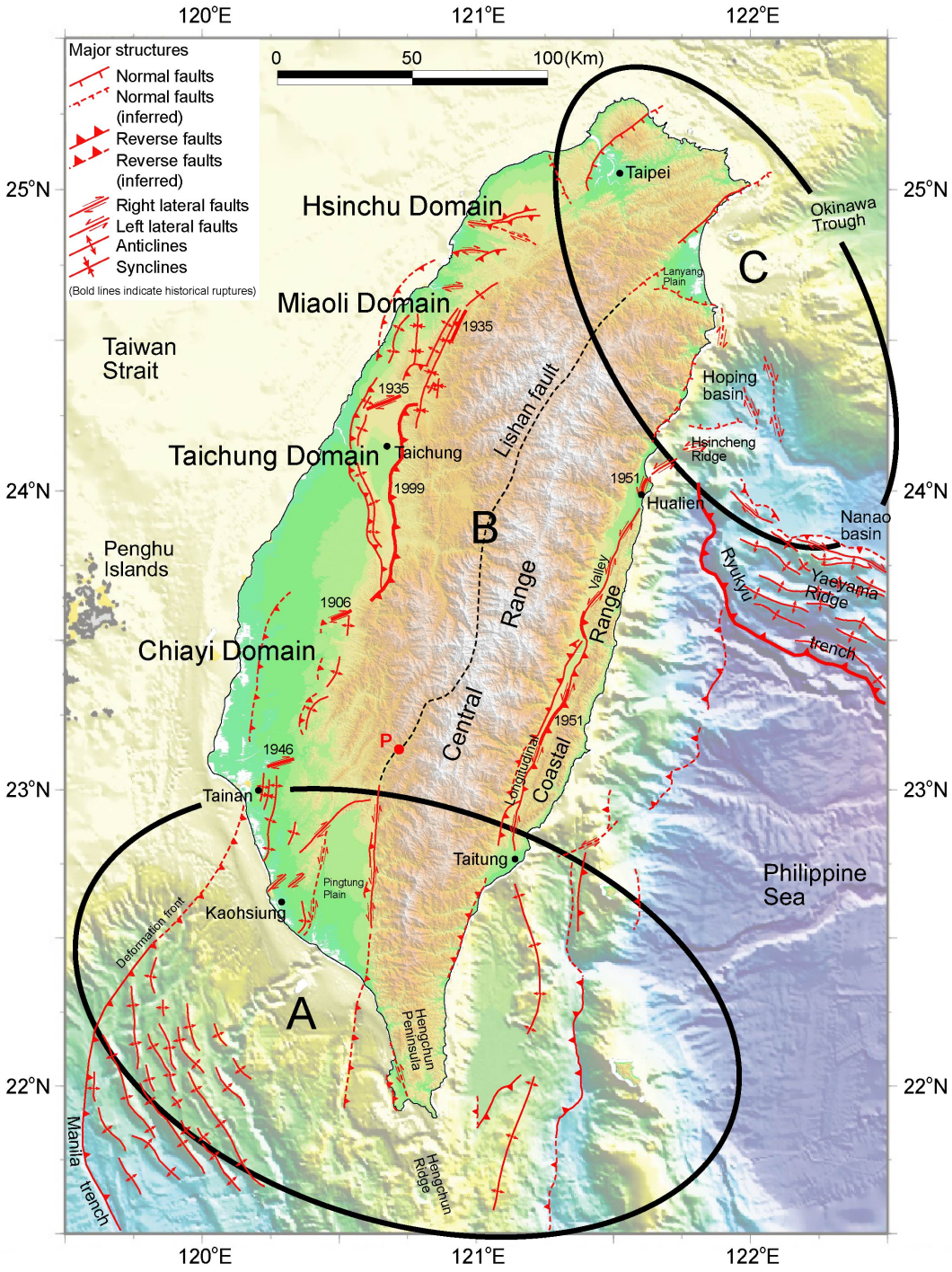

Figure 1.1. Map of the active faults and anticlines of the Taiwan orogen. Principal active faults and anticlines appear in red, and a key inactive fault appears as black dashes. Distinct western and eastern neotectonic belts flank the mountainous backbone of the island. The western belt reflects the docking of the Central Range (a continental sliver) to the Eurasian continental shelf. The eastern belt is the locus of docking of the Luzon volcanic arc to the same continental sliver. Collision is incipient across both belts in the south. Both sutures are coming undone in the north. A: Pre-collisional rapid and distributed convergence; B: Collision and suturing; C: Post-collisional collapse and extension; P: Outcrops of pillow lava along the western suture. Adapted from *Shyu et al.* [2005a].

of active structures flank the mountainous backbone of the island on both the west and the east. Along both the eastern and the western belts, characteristics of active deformation vary markedly. Deformation across the southern and northern quarters of the island and adjacent seafloor is, for example, much more diffuse than across the central half of the island.

In the south, large anticlinal ridges and thrust faults deform the seafloors south of Taitung and Kaohsiung (Figure 1.1). These are expressions of the deformation and consumption of oceanic crust on both sides of the island's southern peninsula. On the east side, oceanic crust of the forearc basin is clearly underthrusting beneath a major west-dipping thrust fault, which has long been known from both bathymetry and seismic profiles [e.g., *Lundberg et al.*, 1997; *Chang et al.*, 2001; *Malavieille et al.*, 2002]. On the west side, two major left-lateral oblique thrust faults bound the rapidly subsiding Pingtung Plain. Between Tainan and Kaohsiung are several active N-S trending folds and NE-SW striking right-lateral faults. These onland structures accommodate E-W shortening and southward extrusion [e.g., *Lacombe et al.*, 2001]. GPS geodesy across the two regions flanking the southern peninsula shows that each is shortening at about 40 mm/yr and that the western of the two is also extruding southward [*Yu et al.*, 1997].

North of Taitung and Tainan, active deformation is more localized. East of the Central Range, most deformation is confined to the narrow Longitudinal Valley and its flanks (Figure 1.1). The active left-lateral oblique Longitudinal Valley fault crops out along the eastern flank of the entire valley and dips steeply beneath the Coastal Range. Portions of this fault produced moderate earthquakes in 1951, 1995, and 2003 [*Chen and Rau*, 2002; *Shyu et al.*, 2005b; *R.-J. Rau*, unpublished data]. Along the southern half of the valley, an active reverse fault is also present along the western side of the valley [*Shyu et al.*, 2005a]. The Central Range is riding over the valley along this structure. GPS geodesy shows that the rate of closure of the southern half of the valley is about 40 mm/yr [*Yu et al.*, 1997]. Closure rates are much lower in the north, but left-lateral rates

of translation are similar in the north and south.

Between Tainan and Taipei, along the western neotectonic belt, shallow marine rocks of the continental shelf are being thrust onto the outer shelf of the Taiwan Strait [e.g., *Suppe and Namson*, 1979; *Suppe*, 1987]. This shortening has four distinct manifestations, which lead us [*Shyu et al.*, 2005a] to divide it into the Chiayi, Taichung, Miaoli, and Hsinchu Domains (Figure 1.1). Major blind thrust faults accommodate most of the shortening across the Chiayi and Miaoli Domains [*Suppe*, 1976; *Suppe and Namson*, 1979]. Several active folds are present in the hanging-wall blocks of these structures. In contrast, two major thrust faults dominate the Taichung Domain. Rupture of the eastern one, the Chelungpu fault, produced the 1999 Chi-Chi earthquake. Pre-1999 geodetic rates of strain across this domain were much smaller than rates to the south. A large earthquake in 1935 resulted from failure of a bending-moment backthrust within one of the synclines of the Miaoli Domain and a right-lateral accommodation structure between the Miaoli and Taichung Domains. Right-lateral accommodation structures on the edges of the Chiayi Domain produced large earthquakes in 1906 and 1946.

Active structures in the northern domains accommodate extension above the Ryukyu subduction zone (Figure 1.1). The Taipei Basin is a half-graben, bounded on the northwest by an active normal fault [*Teng et al.*, 2001] that extends offshore as a minor fault on the continental shelf. This is consistent with GPS measurements, which show that the Taipei Basin is extending at low rates. Slip on this normal fault may have resulted in creation of a marine incursion into the basin in 1694 [*Shieh*, 2000].

The Lanyang Plain is the westernmost, onland extension of the Okinawa Trough (Figure 1.1), which is opening as a back-arc basin at a rate of about 30-40 mm/yr [*Lallemand and Liu*, 1998]. Active fault zones on both the northwestern and southern flanks of the plain are geomorphically evident, but others are buried beneath the rapidly aggrading valley floor and seafloor.

South of the Ryukyu island arc are two submarine basins and a fold-and-thrust belt associated with the deformation front of the Ryukyu subduction zone (Figure 1.1). The Hoping basin is a triangular graben, bounded by normal faults on the west and south [*Shyu et al.*, 2005a]. Bathymetry and historical seismicity indicate that right-lateral strike-slip faults traverse the basin. These help to accommodate the southward opening of the Okinawa Trough and the translation of the deformation front and Ryukyu island arc.

1.4 The Taiwan orogen as accreting and disarticulating twin sutures

Traditionally, the Taiwan orogen has been viewed by most as a classic example of active arc-continent collision, between the Luzon arc and the Eurasian continental margin [e.g., *Barrier and Angelier*, 1986; *Suppe*, 1987; *Huang et al.*, 1997; *Malavieille et al.*, 2002; and references therein]. In such views, the intervening Hengchun Ridge is simply the accretionary wedge at the leading edge of the Manila trench (Figure 1.2).

However, the lack of a structural break between the Hengchun Ridge, Hengchun Peninsula, and the Central Range and the presence of pre-Cenozoic continental basement in the Central Range of Taiwan [e.g., *Ho*, 1988] suggest that this strip may not be just a simple accretionary prism. This observation has inspired many alternative models for the Taiwan orogen [e.g., *Hsu and Sibuet*, 1995; *Sibuet and Hsu*, 1997; *Wu et al.*, 1997; *Chemenda et al.*, 2001]. The pre-Cenozoic continental basement rocks in the Central Range led *Lu and Hsü* [1992] to suggest that the Central Range is a continental block, rifted away from southeastern China. Based on the structural continuity of the Central Range and the Hengchun Ridge, we think that they are, in fact, part of a thin sliver of continental lithosphere.

Moreover, this continental sliver may extend further to the east, as the basement of the westernmost part of the Ryukyu island arc. Except for a right-lateral tear, there

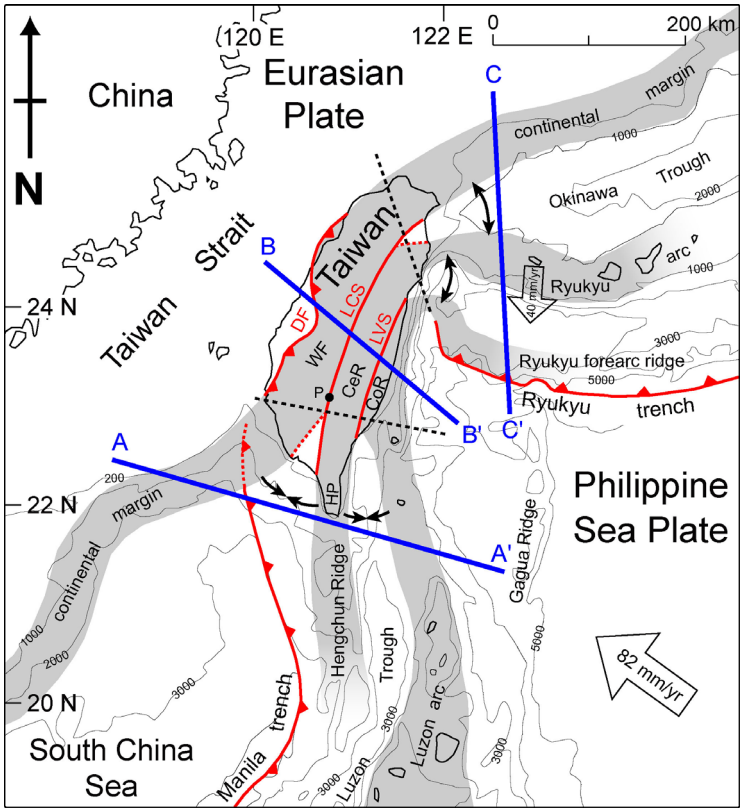

Figure 1.2. Taiwan is experiencing a tandem suturing of a volcanic arc and a sliver of continental crust to continental margin. In the south, the Luzon volcanic arc is converging on the Hengchun forearc ridge, which is, in turn, converging on the Chinese continental margin. Suturing of these three elements occurs in the middle of the island. In the north, both sutures are disarticulating, to form both the Okinawa Trough and troughs south of the Ryukyu island arc. Current velocity vector of the Philippine Sea plate is from [*Yu et al.*, 1997, 1999]. Current velocity vector of the Ryukyu arc adapted from [*Lallemand and Liu*, 1998]. Both are relative to the Penghu Islands in the Taiwan Strait. Black dashed lines are the northern and western limits of the Wadati-Benioff zone of the two subducting systems taken from the seismicity database of the Central Weather Bureau, Taiwan. Bold lines indicate cross sections of Figure 1.3. DF: deformation front; LCS: Lishan-Chaochou suture; LVS: Longitudinal Valley suture; WF: Western Foothills; CeR: Central Range; CoR: Coastal Range; HP: Hengchun Peninsula; P: Outcrops of pillow lava along the western suture.

appears to be no major structural break between the Central Range and the westernmost part of the arc (Figures 1.1 and 1.2). Supporting this idea is the fact that at the latitude of the Ryukyu arc the structural grain of the Central Range bends distinctly eastward, toward the arc [*Tan*, 1977; *Suppe*, 1984]. Thus it is plausible that the submarine Hengchun Ridge, the Central Range, and the substrate of the westernmost Ryukyu arc form a single, narrow but contiguous sliver of continental lithosphere, as suggested in Figure 1.2.

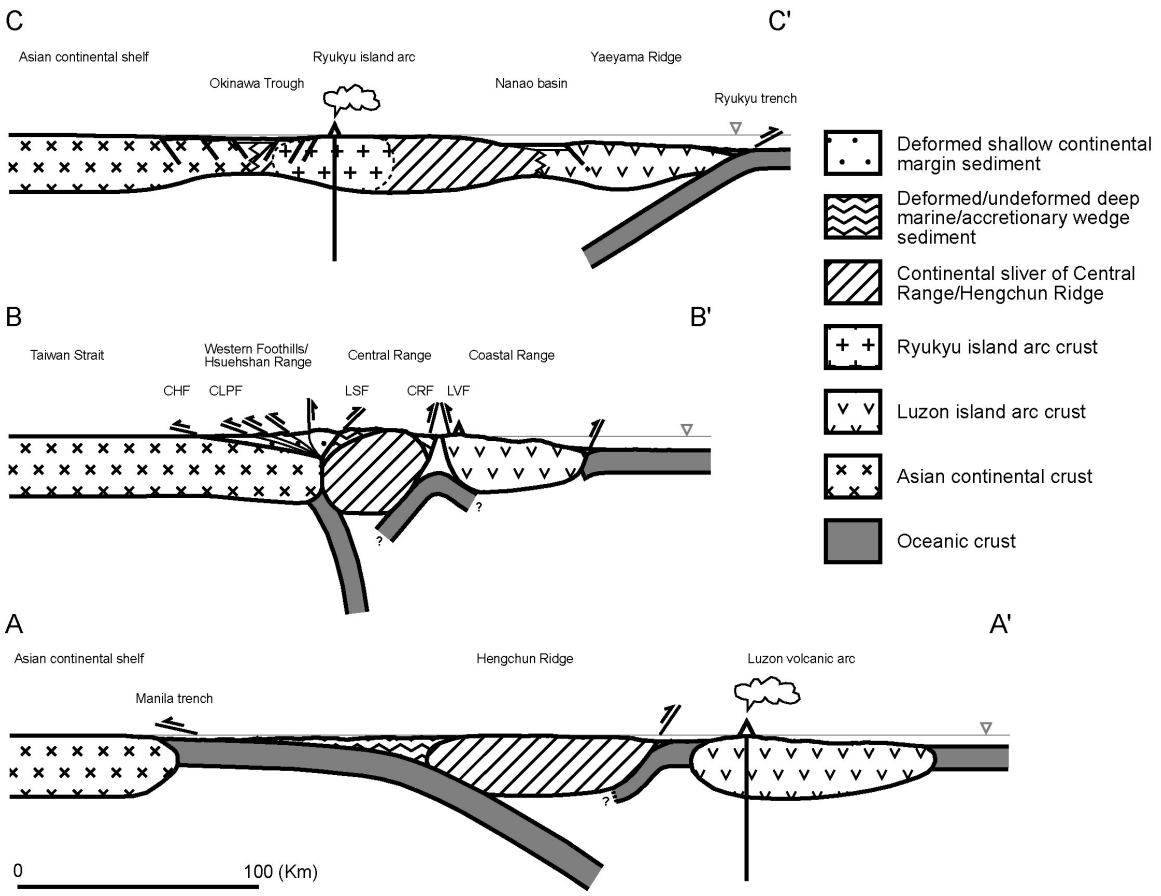

Figure 1.3. Three schematic crustal cross sections across Taiwan illustrate three stages in the process of tandem suturing and disengagement. A. Section just south of Taiwan shows the final stages of subduction and consumption of oceanic lithosphere between the three buoyant terranes. B. Section across central Taiwan shows relationship of the three terranes during suturing. C. Section north and east of Taiwan shows the subduction of the Philippine Sea plate and disengagement of the three terranes across the sutures. CHF: Changhua fault; CLPF: Chelungpu fault; LSF: Lishan fault; CRF: Central Range fault; LVF: Longitudinal Valley fault. No vertical exaggeration.

This hypothesis and the active structures of Taiwan lead us to propose that the Taiwan orogen is a twin suturing and parting of three lithospheric blocks. The Luzon volcanic arc and the Hengchun Ridge/Central Range/westernmost Ryukyu continental sliver join and separate along the eastern neotectonic belt. The western neotectonic belt results from the suturing and separation of this same continental sliver and the Eurasian continental margin (Figures 1.2 and 1.3).

Key to our tandem-suturing hypothesis is the claim that the Hengchun Ridge, Central Range, and substrate of the westernmost Ryukyu island arc are the same buoyant

lithospheric fragment. Many more observations than those mentioned above support this interpretation. The Hengchun Peninsula – an anticlinorial welt of deep marine rocks [*Chen et al.*, 1985; *Sung and Wang*, 1985, 1986] that is rising at a rate of several mm/yr [*Chen and Liu*, 1993, 2000] – extends southward toward the Philippines as the elongate submarine Hengchun Ridge. Though covered by deep marine rocks, distinctive gravity signals and P-wave velocity suggest that the underlying rocks of the ridge may have continental affinity [e.g., *Chi et al.*, 1998; *Nakamura et al.*, 1998]. The Hengchun anticlinorium continues to the north as the Central Range, Taiwan's mountainous backbone, where exhumation has been great enough to expose Paleozoic granites, marbles, and schists of the continental sliver [e.g., *Ho*, 1988]. Similar continental basement rocks may also exist beneath the marine rocks of the Hengchun anticlinorium, where the exhumation is just beginning. In the Central Range, the continental rocks are flanked by highly tectonized Cenozoic slates [e.g., *Ho*, 1988], which are likely the metamorphosed equivalent of the marine sedimentary cover of the Hengchun Peninsula and the Hengchun Ridge. Farther north, the similarity of basement rocks beneath the Ryukyu volcanoes to rocks of the Central Range [*Kizaki*, 1986] suggests the continuation of the continental sliver beneath the westernmost Ryukyu arc.

This continental sliver may have been split off the eastern margin of the Eurasian continent during the opening of the South China Sea, which occurred about 15 to 32 myr ago [e.g., *Briais et al.*, 1993; *Lee and Lawver*, 1995]. Several other continental blocks within the South China Sea were, in fact, split off the Eurasian margin during this period [e.g., *Lee and Lawver*, 1994; *Lin et al.*, 2003]. The recovery from wells of pre-Cenozoic rocks similar to the rocks of the Central Range at depths of several thousand meters beneath Taiwan's west coast [*Jahn et al.*, 1992] supports the idea that the Central Range is a sliver derived from the Asian continental margin.

Elimination of the oceanic lithosphere between the Eurasian continental margin, the continental sliver, and the Luzon volcanic arc culminates in southern Taiwan, on either

side of the Hengchun Ridge, where oblique convergence between the Luzon volcanic arc and the Eurasian continental margin is occurring at about 80 mm/yr [*Yu et al.*, 1999]. Half of this convergence occurs along the western belt, between the Hengchun Ridge and the continental margin, where oceanic lithosphere of the South China Sea is sliding eastward beneath the Hengchun Ridge continental sliver and the Philippine Sea plate (Figure 1.3a). Oceanic lithosphere is being consumed at a similar rate between the Hengchun Ridge and the Luzon volcanic arc. We propose that consumption of this oceanic lithosphere is being facilitated by westward underthrusting of the forearc basin, as suggested by clear bathymetric evidence [e.g., *Malavieille et al.*, 2002; *Shyu et al.*, 2005a]. Eastward subduction of forearc lithosphere beneath the Luzon arc has been proposed [e.g., *Chemenda et al.*, 1997; *Malavieille et al.*, 2002; *Tang et al.*, 2002], but our analysis of bathymetry suggests that this is happening only locally [*Shyu et al.*, 2005a].

Consumption of the oceanic fragments west and east of the Hengchun Peninsula is nearing completion at about 23°N, the northern limit of the Wadati-Benioff zone [*Kao et al.*, 2000] (dashed line in Figure 1.2). The presence of the subducting slab beneath the Pingtung Plain suggests that the rapid subsidence of the plain is related to foundering of subjacent oceanic lithosphere. The termination of the active faults bounding the Pingtung Plain at its northern end also suggests that subduction ends and collision begins at that latitude.

Consumption of forearc oceanic crust between the Hengchun Peninsula and the Luzon volcanic arc ends near Taitung, where the thrust faults and folds on the ocean floor disappear (Figure 1.1). Ultramafic blocks in the Lichi Formation along the southwestern margin of the Coastal Range [e.g., *Ho*, 1988] are likely the remnants of this forearc oceanic lithosphere [e.g., *Chang et al.*, 2001].

The Lishan fault (LSF), which runs through the center of the island from 23° to about 25°N, represents the western suture (Figures 1.2 and 1.3). Although the exact location and the geologic meaning of this fault have been disputed, this structure is

extremely obvious topographically and constitutes a major boundary between two very different sedimentary facies of Eocene-Miocene slate on either side of the fault: The slates west of the fault originated in shallow shelf to coastal environments, whereas the slates east of the fault, in the Central Range, formed in a much deeper basin [e.g., *Ho*, 1988]. Near the southern end of this structure, Early Miocene(?) pillow lavas that crop out along our proposed western suture [*Kuo*, 1984] (P in Figures 1.1 and 1.2) may well be a remnant of South China Sea oceanic crust.

The accretion of the continental sliver to the continental margin created a myriad of active structures in the fold-and-thrust belt of western Taiwan. Both the characteristics of the active structures and geodetically determined rates of shortening indicate that the accretion matures northward [e.g., *Yu et al.*, 1997]. These thin-skinned structures developed in the deformed sedimentary wedge above and west of the lithospheric suture, and the eastern boundary of the wedge is the Lishan fault (Figure 1.3b). This relationship of the thrusts to the Lishan fault would indicate that the western neotectonic belt of Taiwan has both a thick-skinned and a thin-skinned manifestation. The active faults of the Western Foothills are thin-skinned, but they root into a lithospheric suture.

Along the eastern neotectonic belt, suturing of the volcanic arc to the Central Range begins near Taitung in southeastern Taiwan. There the arc begins its collision with the lithosphere of the Central Range continental sliver as the intervening oceanic crust disappears beneath the thick accumulation of debris being shed off both terranes. The Longitudinal Valley (Figures 1.2 and 1.3b) is the subaerial manifestation of the suture. High slip rates on the Longitudinal Valley fault at the eastern side of the valley indicate that the final removal of the forearc oceanic lithosphere also involves eastward subduction. The Coastal Range, east of the Longitudinal Valley, consists of a dramatically telescoped assortment of late-Cenozoic arc-volcanic and marine sedimentary rocks [*Chen*, 1988; *Ho*, 1988], remnants of accreted arc volcanoes and cover sediments of the Luzon Trough [e.g., *Huang et al.*, 1992; *Chang et al.*, 2001]. As along the western

neotectonic belt, the degree of development of the structures and lessening of geodetic rates of convergence [e.g., *Yu et al.*, 1997] indicate that suturing matures northward.

Both sutures are disarticulating across northeastern Taiwan. Along the western suture, the continental sliver begins to tear away from the Asian continental margin in the Lanyang Plain, which is bounded by normal faults (Figure 1.1). The fact that the apex of the triangle-shaped plain is at the northern end of the Lishan fault indicates clearly that the parting is occurring along the old suture. The plain widens to the east into the westernmost part of the Okinawa Trough (Figures 1.2 and 1.3c).

It is noteworthy that the current arc volcanism in western Ryukyu is localized between the northern part of the Ryukyu arc and the center of the Okinawa Trough [e.g., *Sibuet et al.*, 1998; *Chung et al.*, 2000] (Figure 1.3c). Thus, the Okinawa Trough is not a conventional back-arc basin. Instead, its spreading may be better explained by the post-collisional disengagement of the continental sliver from the Asian continental margin [e.g., *Teng*, 1996; *Wang et al.*, 1999; *Chung et al.*, 2000].

In summary, the sliver approaches the continental margin in southern Taiwan, accretes to it in central Taiwan, and disengages from the continental margin across the Lanyang Plain in northeastern Taiwan. Normal faulting that created the Taipei Basin is therefore a minor manifestation of the disarticulation of the western suture, off on the western edge of the Western Foothills.

Along the eastern belt the Coastal Range dives below sea level at the northern end of the Longitudinal Valley to form a bathymetric high between the Ryukyu trench and Hoping basin (Figure 1.1). This odd, E-W trending Hsincheng Ridge provides the topographic link between the Coastal Range and the westernmost part of the Yaeyama forearc ridge, immediately north of the Ryukyu trench. We suggest that rocks with affinities to the Coastal Range might well be found in the basement of the fold-and-thrust belt of that part of the Yaeyama forearc ridge. The implication would be that after suturing to the Central Range lithosphere along the Longitudinal Valley, the lithosphere

of the Coastal Range disarticulates from the Central Range along the northeastern coast (Figures 1.2 and 1.3c). Normal faults and complex strike-slip faults surrounding the Hoping basin (Figure 1.1) would represent the initiation of this disengagement.

The accretion of pieces of continent and volcanic island arcs onto continental margins is one of the most common phenomena in the geologic record [e.g., *Saleeby*, 1983; *Şengör and Natal'in*, 1996]. The disarticulation of lithosphere in areas of former suture zones may also be commonplace in Earth's geologic history (e.g., the Aegean Sea). Taiwan is, however, one of the very few places on Earth that exhibit both phenomena in action in a single orogenic belt; suturing that begins in the south is coming undone in the north and east (Figures 1.2 and 1.3). This occurs in tandem, with a separate suture on each side of a narrow sliver of continental material that is caught between the volcanic arc and the continent.

In this example, it is clear that the disengagement of terranes occurs along the not-so-old sutures. This may well reflect a fundamental weakness in the lithospheric sutures. In this case, it appears that all that is needed to induce disengagement of the terranes is the subduction of the Philippine Sea plate along the Ryukyu subduction zone to a position below the upper crust. Once this buttress is removed, the two sutures disengage.

1.5 Implications for future earthquake sources

The tandem-suture model of the Taiwan orogen raises interesting questions with respect to the evaluation of seismic hazard in Taiwan. It is plausible that a large earthquake could be generated by slip on the subduction interface beneath Kaohsiung, Tainan, and the Pingtung Plain. In addition, a myriad of smaller potentially seismic sources lie within the hanging-wall block of the subduction interface there. Only the question is: Which of these are locked and potentially seismic, and which are slipping

aseismically?

Large thrust faults in the submarine realm south of Taitung may also generate large subduction-like earthquakes. High rates of suturing along the southern Longitudinal Valley should mean that large earthquakes are more common there than in the northern Longitudinal Valley, as has been the case during the century or so of recorded history.

One can reasonably expect the blind thrust faults of the western neotectonic belt (in the Chiayi and Miaoli Domains) to generate earthquakes at least as large as that generated in 1999 by the intervening Chelungpu thrust. The normal fault on the western side of the Taipei Basin half-graben should generate earthquakes less frequently than normal faults near the Lanyang Plain because strain rates are so much lower across the Taipei Basin. One can expect the western margin of the Ryukyu subduction zone to generate a bewildering variety of large earthquakes given the abundance of right-lateral tear faults and normal faults there.

Finally, rapid uplift of the Central Range may not imply loading of seismic sources within the Central Range lithosphere. Instead, pervasive ductile crustal thickening may produce the rapid uplift.

1.6 Concluding Remarks

The construction of this tandem-suture model of the Taiwan orogen was made possible by our comprehensive mapping of the neotectonic elements of Taiwan. Our descriptions of active structures, in combination with previously published structural, stratigraphic, and geophysical information necessitated a new tectonic framework for the orogen. This new tectonic framework involves three lithospheric elements, two continental and one island-arc, which first suture and then disengage.

The model could be tested with a number of new observations. For example, is the unexposed basement of the Hengchun Ridge actually similar to the metamorphic core of

the Central Range; are there island-arc rocks beneath the sediments of the westernmost Yaeyama forearc ridge; and is there still oceanic lithosphere beneath the thick clastic fill of the Longitudinal Valley? Some of these questions can be answered by well-designed ocean-drilling projects. More investigations should be able to verify the cross sections we proposed in Figure 1.3. We hope, in fact, that the tandem suturing and disarticulation model will be subjected to such tests.

1.7 Acknowledgments

We are grateful for valuable discussions with J.-P. Avouac, O. Beyssac, W.-C. Chi, C.-Y. Lu, Y. Ota, C. Rubin, J. Saleeby, L.S. Teng, and B. Wernicke. We have also benefited from stimulating discussions with students of two field classes in Taiwan and a neotectonic seminar at National Taiwan University. We appreciate valuable comments and suggestions of three anonymous reviewers of this manuscript and a previous version. Our neotectonic mapping would have been impossible had C.-T. Lee and C.-S. Liu not made high-quality digital topography and bathymetry available to us. Our mapping was facilitated by J. Giberson, manager of the Geographic Information Systems (GIS) laboratory of California Institute of Technology (Caltech). Our project in Taiwan was initially supported by private funds of Caltech's Division of Geological and Planetary Sciences and later by National Science Foundation (NSF) grant EAR-0208505. This research was also supported in part by the Gordon and Betty Moore Foundation. This is Caltech Tectonics Observatory Contribution #1.

1.8 References

Barrier, E., and J. Angelier (1986), Active collision in eastern Taiwan: the Coastal Range, *Mem. Geol. Soc. China*, *7*, 135-159.

Bonilla, M. G. (1975), A review of recently active faults in Taiwan, *Open File Rep. 75-41*, 58pp., U. S. Geol. Surv., Menlo Park, Calif.

Bonilla, M. G. (1977), Summary of Quaternary faulting and elevation changes in Taiwan, *Mem. Geol. Soc. China*, *2*, 43-55.

Briais, A., P. Patriat, and P. Tapponnier (1993), Updated interpretation of magnetic anomalies and seafloor spreading stages in the South China Sea: implications for the Tertiary tectonics of Southeast Asia, *J. Geophys. Res.*, *98*, 6,299-6,328.

Chang, C. P., J. Angelier, C. Y. Huang, and C. S. Liu (2001), Structural evolution and significance of a mélange in a collision belt: the Lichi Mélange and the Taiwan arc-continent collision, *Geol. Mag.*, *138*, 633-651.

Chemenda, A. I., R. K. Yang, C.-H. Hsieh, and A. L. Groholsky (1997), Evolutionary model for the Taiwan collision based on physical modelling, *Tectonophysics*, *274*, 253-274.

Chemenda, A. I., R.-K. Yang, J.-F. Stephan, E. A. Konstantinovskaya, and G. M. Ivanov (2001), New results from physical modelling of arc-continent collision in Taiwan: evolutionary model, *Tectonophysics*, *333*, 159-178.

Chen, H.-H., and R.-J. Rau (2002), Earthquake locations and style of faulting in an active arc-continent plate boundary: the Chihshang fault of eastern Taiwan, *EOS, Trans., Am. Geophys. Uni.*, *83*(47), Fall Meet. Suppl., Abstract T61B-1277.

Chen, W.-S. (1988), Tectonic evolution of sedimentary basins in Coastal Range, Taiwan (in Chinese), Ph.D. thesis, 304pp., Natl. Taiwan Univ., Taipei.

Chen, W.-S., Y.-M. Cheng, and C.-Y. Huang (1985), Geology of the Hengchun Peninsula, southern Taiwan (in Chinese with English abstract), *Ti-Chih*, *6*(2), 47-74.

Chen, Y.-G., and T.-K. Liu (1993), Holocene radiocarbon dates in Hengchun Peninsula and their neotectonic implications, *J. Geol. Soc. China*, *36*, 457-479.

Chen, Y.-G., and T.-K. Liu (2000), Holocene uplift and subsidence along an active tectonic margin southwestern Taiwan, *Quat. Sci. Rev.*, *19*, 923-930.

Chen, Y.-G., W.-S. Chen, J.-C. Lee, Y.-H. Lee, C.-T. Lee, H.-C. Chang, and C.-H. Lo (2001), Surface rupture of 1999 Chi-Chi earthquake yields insights on active tectonics of central Taiwan, *Bull. Seismol. Soc. Am.*, *91*, 977-985.

Cheng, S. N., and Y. T. Yeh (1989), *Catalog of the Earthquakes in Taiwan from 1604 to*

1988 (in Chinese), 255pp., Inst. Earth Sci., Acad. Sinica, Taipei, Taiwan.

Chi, W.-C., D. L. Reed, C.-S. Liu, and N. Lundberg (1998), Distribution of the bottom-simulating reflector in the offshore Taiwan collision zone, *Terr. Atmos. Oceanic Sci.*, *9*, 779-794.

Chung, S.-L., S.-L. Wang, R. Shinjo, C.-S. Lee, and C.-H. Chen (2000), Initiation of arc magmatism in an embryonic continental rifting zone of the southernmost part of Okinawa Trough, *Terra Nova*, *12*, 225-230.

Ho, C. S. (1986), A synthesis of the geologic evolution of Taiwan, *Tectonophysics*, *125*, 1-16.

Ho, C. S. (1988), *An Introduction to the Geology of Taiwan, Explanatory Text of the Geologic Map of Taiwan*, 2nd ed., 192pp., Cent. Geol. Surv., Ministry Econ. Affairs, Taipei, Taiwan.

Hovius, N., C. P. Stark, H.-T. Chu, and J.-C. Lin (2000), Supply and removal of sediment in a landslide-dominated mountain belt: Central Range, Taiwan, *J. Geol.*, *108*, 73-89.

Hsu, M.-T. (1980), *Earthquake Catalogues in Taiwan (from 1644 to 1979)* (in Chinese), 77pp., Natl. Taiwan Univ., Taipei.

Hsu, S.-K., and J.-C. Sibuet (1995), Is Taiwan the result of arc-continent or arc-arc collision?, *Earth Planet. Sci. Lett.*, *136*, 315-324.

Huang, C.-Y., C.-T. Shyu, S. B. Lin, T.-Q. Lee, and D. D. Sheu (1992), Marine geology in the arc-continent collision zone off southeastern Taiwan: Implications for Late Neogene evolution of the Coastal Range, *Mar. Geol.*, *107*, 183-212.

Huang, C.-Y., W.-Y. Wu, C.-P. Chang, S. Tsao, P. B. Yuan, C.-W. Lin, and K.-Y. Xia (1997), Tectonic evolution of accretionary prism in the arc-continent collision terrane of Taiwan, *Tectonophysics*, *281*, 31-51.

Jahn, B.-M., W.-R. Chi, and T.-F. Yui (1992), A late Permian formation of Taiwan (marbles from Chia-Li Well No.1): Pb-Pb isochron and Sr isotopic evidence, and its regional geological significance, *J. Geol. Soc. China*, *35*, 193-218.

Ji, C., D. V. Helmberger, T.-R. A. Song, K.-F. Ma, and D. J. Wald (2001), Slip distribution and tectonic implication of the 1999 Chi-Chi, Taiwan, Earthquake, *Geophys. Res. Lett.*, *28*, 4,379-4,382.

Johnson, K. M., Y.-J. Hsu, P. Segall, and S.-B. Yu (2001), Fault geometry and slip distribution of the 1999 Chi-Chi, Taiwan earthquake imaged from inversion of GPS data, *Geophys. Res. Lett.*, *28*, 2,285-2,288.

Kao, H., G.-C. Huang, and C.-S. Liu (2000), Transition from oblique subduction to collision in the northern Luzon arc-Taiwan region: Constraints from bathymetry and seismic observations, *J. Geophys. Res.*, *105*, 3,059-3,079.

Kelson, K. I., K.-H. Kang, W. D. Page, C.-T. Lee, and L. S. Cluff (2001), Representative styles of deformation along the Chelungpu fault from the 1999 Chi-Chi (Taiwan) earthquake: Geomorphic characteristics and responses of man-made structures, *Bull. Seismol. Soc. Am.*, *91*, 930-952.

Kizaki K. (1986), Geology and tectonic framework of the Ryukyu Islands, *Mem. Geol. Soc. China*, *7*, 1-14.

Kuo, C.-S. (1984), Geochemistry and isotopic analysis of spilite in the Paolai area (in Chinese), M.S. thesis, 96pp., Natl. Taiwan Univ., Taipei.

Lacombe, O., F. Mouthereau, J. Angelier, and B. Deffontaines (2001), Structural, geodetic and seismological evidence for tectonic escape in SW Taiwan, *Tectonophysics*, *333*, 323-345.

Lallemand, S., and C.-S. Liu (1998), Geodynamic implications of present-day kinematics in the southern Ryukyus, *J. Geol. Soc. China*, *41*, 551-564.

Lee, T.-Y., and L. A. Lawver (1994), Cenozoic plate reconstruction of the South China Sea region, *Tectonophysics*, *235*, 149-180.

Lee, T.-Y., and L. A. Lawver (1995), Cenozoic plate reconstruction of Southeast Asia, *Tectonophysics*, *251*, 85-138.

Lin, A. T., A. B. Watts, and S. P. Hesselbo (2003), Cenozoic stratigraphy and subsidence history of the South China Sea margin in the Taiwan region, *Basin Res.*, *15*, 453-478.

Lu, C.-Y., and K. J. Hsü (1992), Tectonic evolution of the Taiwan mountain belt, *Pet. Geol. Taiwan*, *27*, 21-46.

Lundberg, N., D. L. Reed, C.-S. Liu, and J. Lieske, Jr. (1997), Forearc-basin closure and arc accretion in the submarine suture zone south of Taiwan, *Tectonophysics*, *274*, 5-23.

Ma, K.-F., T.-R. A. Song, S.-J. Lee, and H.-I. Wu (2000), Spatial slip distribution of the September 20, 1999, Chi-Chi, Taiwan, earthquake (Mw7.6)—Inverted from teleseismic data, *Geophys. Res. Lett.*, *27*, 3,417-3,420.

Ma, K.-F., J. Mori, S.-J. Lee, and S. B. Yu (2001), Spatial and temporal distribution of slip for the 1999 Chi-Chi, Taiwan, earthquake, *Bull. Seismol. Soc. Am.*, *91*, 1,069-1,087.

Malavieille, J., S. E. Lallemand, S. Dominguez, A. Deschamps, C.-Y. Lu, C.-S. Liu, P. Schnürle, and the ACT Scientific Crew (2002), Arc-continent collision in Taiwan: new marine observations and tectonic evolution, *Geol. Soc. Am. Spec. Paper*, *358*, 187-211.

Nakamura, Y., K. McIntosh, and A. T. Chen (1998), Preliminary results of a large offset seismic survey west of Hengchun Peninsula, southern Taiwan, *Terr. Atmos. Oceanic Sci.*, *9*, 395-408.

Saleeby, J. B. (1983), Accretionary tectonics of the North American Cordillera, *Ann. Rev.*

Earth Planet. Sci., *15*, 45-73.

Şengör, A. M. C., and B. A. Natal'in (1996), Paleotectonics of Asia: fragments of a synthesis, in *The Tectonic Evolution of Asia*, edited by A. Yin, and M. Harrison, pp. 486-640, Cambridge Univ. Press, Cambridge, UK.

Shieh, Y.-T. (2000), The paleogeography of the ancient Taipei lakebed in the K'anghsi Period (in Chinese with English abstract), *J. Geogr. Sci.*, *27*, 85-95.

Shyu, J. B. H., K. Sieh, Y.-G. Chen, and C.-S. Liu (2005a), The neotectonic architecture of Taiwan and its implications for future large earthquakes, *J. Geophys. Res.*, *110*, B08402, doi:10.1029/2004JB003251.

Shyu, J. B. H., L.-H. Chung, Y.-G. Chen, J.-C. Lee, and K. Sieh (2005b), Re-evaluation of the surface ruptures of the November 1951 earthquake series in eastern Taiwan, and its neotectonic implications, *J. Asian Earth Sci.*, submitted for publication.

Sibuet, J.-C., and S.-K. Hsu (1997), Geodynamics of the Taiwan arc-arc collision, *Tectonophysics*, *274*, 221-251.

Sibuet, J.-C., B. Deffontaines, S.-K. Hsu, N. Thareau, J.-P. Le Formal, C.-S. Liu, and ACT party (1998), Okinawa trough backarc basin: Early tectonic and magmatic evolution, *J. Geophys. Res.*, *103*, 30,245-30,267.

Sung, Q.-C., and Y. Wang (1985), Petrofacies of Miocene sediments in the Hengchun Peninsula and its tectonic implication, *Proc. Geol. Soc. China*, *28*, 23-44.

Sung, Q., and Y. Wang (1986), Sedimentary environments of the Miocene sediments in the Hengchun Peninsula and their tectonic implication, *Mem. Geol. Soc. China*, *7*, 325-340.

Suppe, J. (1976), Décollement folding in southwestern Taiwan, *Pet. Geol. Taiwan*, *13*, 25-35.

Suppe, J. (1984), Kinematics of arc-continent collision, flipping of subduction, and back-arc spreading near Taiwan, *Mem. Geol. Soc. China*, *6*, 21-33.

Suppe, J. (1987), The active Taiwan mountain belt, in *Anatomy of Mountain Chains*, edited by J. P. Schaer, and J. Rodgers, pp. 277-293, Princeton Univ. Press, Princeton, N.J.

Suppe, J., and J. Namson (1979), Fault-bend origin of frontal folds of the western Taiwan fold-and-thrust belt, *Pet. Geol. Taiwan*, *16*, 1-18.

Tan, L. P. (1977), Pleistocene eastward bending of the Taiwan arc, *Mem. Geol. Soc. China*, *2*, 77-83.

Tang, J.-C., A. I. Chemenda, J. Chéry, S. Lallemand, and R. Hassani (2002), Compressional subduction regime and initial arc-continent collision: Numerical modeling, *Geol. Soc. Am. Spec. Paper*, *358*, 177-186.

Teng, L. S. (1987), Stratigraphic records of the late Cenozoic Penglai orogeny of Taiwan, *Acta Geol. Taiwanica*, *25*, 205-224.

Teng, L. S. (1990), Late Cenozoic arc-continent collision in Taiwan, *Tectonophysics*, *183*, 57-76.

Teng, L. S. (1996), Extensional collapse of the northern Taiwan mountain belt, *Geology*, *24*, 949-952.

Teng, L. S., C. T. Lee, C.-H. Peng, W.-F. Chen, and C.-J. Chu (2001), Origin and geological evolution of the Taipei Basin, northern Taiwan, *Western Pacific Earth Sci.*, *1*, 115-142.

Wang, K.-L., S.-L. Chung, C.-H. Chen, R. Shinjo, T. F. Yang, and C.-H. Chen (1999), Post-collisional magmatism around northern Taiwan and its relation with opening of the Okinawa Trough, *Tectonophysics*, *308*, 363-376.

Wu, F. T., R.-J. Rau, and D. Salzberg (1997), Taiwan orogeny: thin-skinned or lithospheric collision?, *Tectonophysics*, *274*, 191-220.

Yu, S.-B., H.-Y. Chen, and L.-C. Kuo (1997), Velocity field of GPS stations in the Taiwan area, *Tectonophysics*, *274*, 41-59.

Yu, S.-B., L.-C. Kuo, R. S. Punongbayan, and E. G. Ramos (1999), GPS observation of crustal deformation in the Taiwan-Luzon region, *Geophys. Res. Lett.*, *26*, 923-926.

Chapter 2

Neotectonic Architecture of Taiwan and Its Implications for Future Large Earthquakes

An edited version of this chapter has been published as:

Shyu, J.B.H., K. Sieh, Y.-G. Chen, and C.-S. Liu, 2005, *Journal of Geophysical Research*, 110, B08402, doi:10.1029/2004JB003251.

2.1 Abstract

The disastrous effects of the 1999 Chi-Chi earthquake in Taiwan demonstrated an urgent need for better knowledge of the island's potential earthquake sources. Toward this end, we have prepared a neotectonic map of Taiwan. The map and related cross sections are based upon structural and geomorphic expression of active faults and folds both in the field and on shaded-relief maps prepared from a 40-m resolution digital elevation model, augmented by geodetic and seismologic data. The active tandem suturing and tandem disengagement of a volcanic arc and a continental sliver to and from the Eurasian continental margin have created two neotectonic belts in Taiwan. In the southern part of the orogen, both belts are in the final stage of consuming oceanic crust. Collision and suturing occur in the middle part of both belts, and post-collisional collapse and extension dominate the island's northern and northeastern flanks. Both belts consist of several distinct neotectonic domains. Seven domains – Kaoping, Chiayi, Taichung, Miaoli, Hsinchu, Ilan, and Taipei – constitute the western belt, and four domains – Lutao-Lanyu, Taitung, Hualien, and Ryukyu – make up the eastern belt. Each domain is defined by a distinct suite of active structures. For example, the Chelungpu fault (source of the 1999 earthquake) and its western neighbor, the Changhua fault, are the principal components of the Taichung Domain, whereas both its neighboring domains – the Chiayi and Miaoli Domains – are dominated by major blind faults. In most of the domains, the size of the principal active fault is large enough to produce future earthquakes with magnitudes in the mid-7 values.

Keywords: Taiwan, earthquakes, neotectonics, seismic hazard, orogeny.

2.2 Introduction

Throughout its brief recorded history, Taiwan has experienced many strong and destructive earthquakes [e.g., *Bonilla*, 1975, 1977; *Hsu*, 1980; *Cheng and Yeh*, 1989]. These are the seismic manifestation of several million years of orogeny [e.g., *Ho*, 1986; *Teng*, 1987, 1990, 1996] (Figure 2.1). The human response to high seismicity has been building codes that anticipate high probabilities of future strong shaking on the island. Nonetheless, the disastrous effects of the M_w 7.6 Chi-Chi earthquake of 1999 show that many damaging effects were not anticipated. Meters of slip on the Chelungpu fault generated remarkable scarps that sliced through more than 80 km of urban, agricultural, and fluvial landscapes [*Central Geological Survey*, 1999a, 1999b; *Chen et al.*, 2002]. Folding produced impressive broad deformation of the ground surface and resultant large areas of damage [*Chen et al.*, 2001; *Kelson et al.*, 2001; *Lee et al.*, 2002]. Modeling of geodetic and seismic data showed that the specific geometries of the fault surfaces played an important role in the production of the patterns, durations, and levels of seismic shaking and surface deformation [*Ma et al.*, 2000, 2001; *Ji et al.*, 2001].

Many of these co-seismic phenomena could have been anticipated accurately if the earthquake source had been known in advance of the earthquake. For example, the trace of the principal fault that produced the 1999 earthquake was clear from its geomorphic expression well before its 1999 rupture, but had not been used to map prior ruptures systematically [*Chen et al.*, 2002]. The basic subsurface geometry of the fault had been known for nearly two decades [e.g., *Suppe*, 1976, 1980a, 1980b], but important details had not been investigated using the patterns of deformation of fluvial terraces along the fault. The same is true of several other destructive historical co-seismic ruptures in Taiwan, most notably those of 1935 and 1951. This demonstrates the practical need for better knowledge of the active structures of the island.

Our goal in this paper is both academic and practical. We wish to identify,

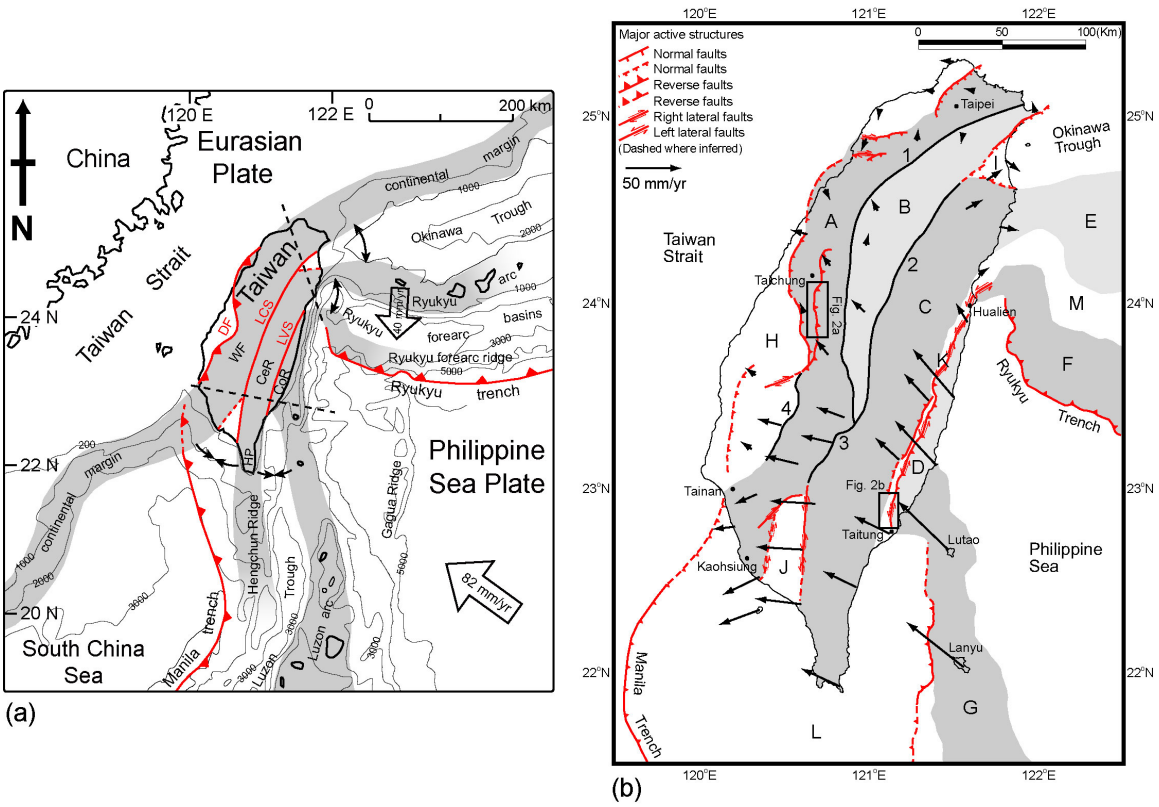

Figure 2.1. A neotectonic snapshot of Taiwan and adjacent regions. (a) Taiwan is currently experiencing a double suturing: In the south, the Luzon volcanic arc is colliding with the Hengchun forearc ridge, which is, in turn, colliding with the Eurasian continental margin. In the north, both sutures are unstitching. Their disengagement is forming both the Okinawa Trough and the forearc basins of the Ryukyu arc. Thus, in the course of passing through the island, the roles of the volcanic arc and forearc ridge flip along with the flipping of the polarity of subduction. The three gray strips represent the three lithospheric pieces of Taiwan's tandem suturing and disarticulation: the Eurasian continental margin, the continental sliver, and the Luzon arc. Black arrows indicate the suturing and disarticulation. This concept is discussed in detail in *Shyu et al.* [2005a]. Current velocity vector of the Philippine Sea plate relative to the Eurasian plate adapted from *Yu et al.* [1997, 1999]. Current velocity vector of the Ryukyu arc adapted from *Lallemand and Liu* [1998]. Black dashed lines are the northern and western limits of the Wadati-Benioff zone of the two subducting systems, taken from the seismicity database of the Central Weather Bureau, Taiwan. DF: deformation front; LCS: Lishan-Chaochou suture; LVS: Longitudinal Valley suture; WF: Western Foothills; CeR: Central Range; CoR: Coastal Range; HP: Hengchun Peninsula. (b) Major tectonic elements around Taiwan. Active structures identified in this study are shown in red. Major inactive faults that form the boundaries of tectonic elements are shown in black: 1: Chiuchih fault; 2: Lishan fault; 3: Laonung fault; 4: Chukou fault. Selected GPS vectors relative to the stable Eurasian continental shelf adapted from *Yu et al.* [1997]. A: Western Foothills; B: Hsueshan Range; C: Central Range and Hengchun Peninsula; D: Coastal Range; E: westernmost Ryukyu arc; F: Yaeyama forearc ridge; G: northernmost Luzon arc; H: western Taiwan coastal plains; I: Lanyang Plain; J: Pingtung Plain; K: Longitudinal Valley; L: submarine Hengchun Ridge; M: Ryukyu forearc basins.

describe, and interpret the principal active structural elements of Taiwan. For those interested in the evolution of the orogen over the past few million years, the current configuration of active structural elements is arguably the most accessible and complete

piece of the puzzle because so much of the older record has been eroded or buried [*Gilbert*, 1890, p.1]. On the more practical side, those interested in forecasting the effects of future fault ruptures must understand the locations, forms, and sense of slip of the active faults of the island. Realistic estimates of the magnitudes and patterns of future seismic shaking also require such knowledge. Moreover, reasonable interpretations of deformations now being recorded by an extensive geodetic network will be made best in the context of a firm structural, stratigraphic, and geomorphologic framework. And, finally, future land-use planning will be well served by maps of geologically recent surface faulting and folding in combination with maps of other geologic hazards.

Taiwan is well poised for the synoptic neotectonic evaluation we describe below. For decades, geographers have been mapping deformed fluvial and marine coastal terraces. More recently, radiometric dating of some of these surfaces has enabled determination of rates of the latest Pleistocene and Holocene deformation. Concurrent with these geomorphic efforts, stratigraphers and structural geologists have been mapping the surface and subsurface configurations of young sediments, faults, and folds, and employing these to interpret the Neogene history of the Taiwan orogen. For the most part, however, these geomorphologic, stratigraphic and structural studies have not been applied to interpreting the youngest active structures of the island, nor have they been systematically integrated into a synoptic neotectonic map.

A vigorous debate is currently underway in Taiwan regarding the appropriate means by which to construct neotectonic maps. The disparate results of several recent attempts illustrate the controversy. Some have relied upon stratigraphic relationships that demonstrate Quaternary activity, believing that this is a sufficient basis for considering a fault to be active [e.g., *Shih et al.*, 1986; *Yang*, 1986]. Use of this criterion alone, however, is inadequate, since many faults that were active earlier in the Quaternary Period have been demonstrably inactive during the late Pleistocene and Holocene Epochs.

At the other extreme are maps that depict as active only those faults that have ruptured historically [e.g., *H.-C. Chang et al.*, 1998; *Lin et al.*, 2000a]. These clearly are shutting the door after the horse has run out of the barn.

Our principal means for mapping the active structures of the island has been the use of fluvial and coastal landforms, which cover more than half of the surface of the island. Uplift and deformation of these features are readily apparent on shaded-relief maps. In many places we have also utilized more detailed mapping of landforms published by others.

The recent availability of a high-resolution national digital elevation model (DEM) makes the creation of a neotectonic map from landforms far easier than it would have been just a few years ago. Made from aerial photography of the island, the DEM has an elevation posting every 40 m. Although standard stereographic aerial photographs have higher resolution and include tonal information, they are not geo-referenced, so the data derived therefrom are more difficult to compile and view. The 40-m DEM displays all major and most minor topographic features necessary for interpreting broadly the tectonic geomorphology of the island. Furthermore, high-resolution bathymetric databases that have recently become available [e.g., *Lallemand et al.*, 1997; *Liu et al.*, 1998; *Malavieille et al.*, 2002] allow us to incorporate geomorphic information from the surrounding sea floor.

Two examples clearly demonstrate the ability to identify most structures using the 40-m DEM (Figure 2.2). Topographic features along most segments of the Chelungpu fault, the source of the 1999 earthquake, revealed the exact location of not only all of the major ruptures but also many of the secondary ones, even before the earthquake struck (Figure 2.2a). Another example in the eastern part of Taiwan shows that the topographic features visible in the DEM can be used to identify a major fault there, with its secondary folds and the different characteristics of the fault along several of its segments (Figure 2.2b). Due to space limitations, we can only include these two

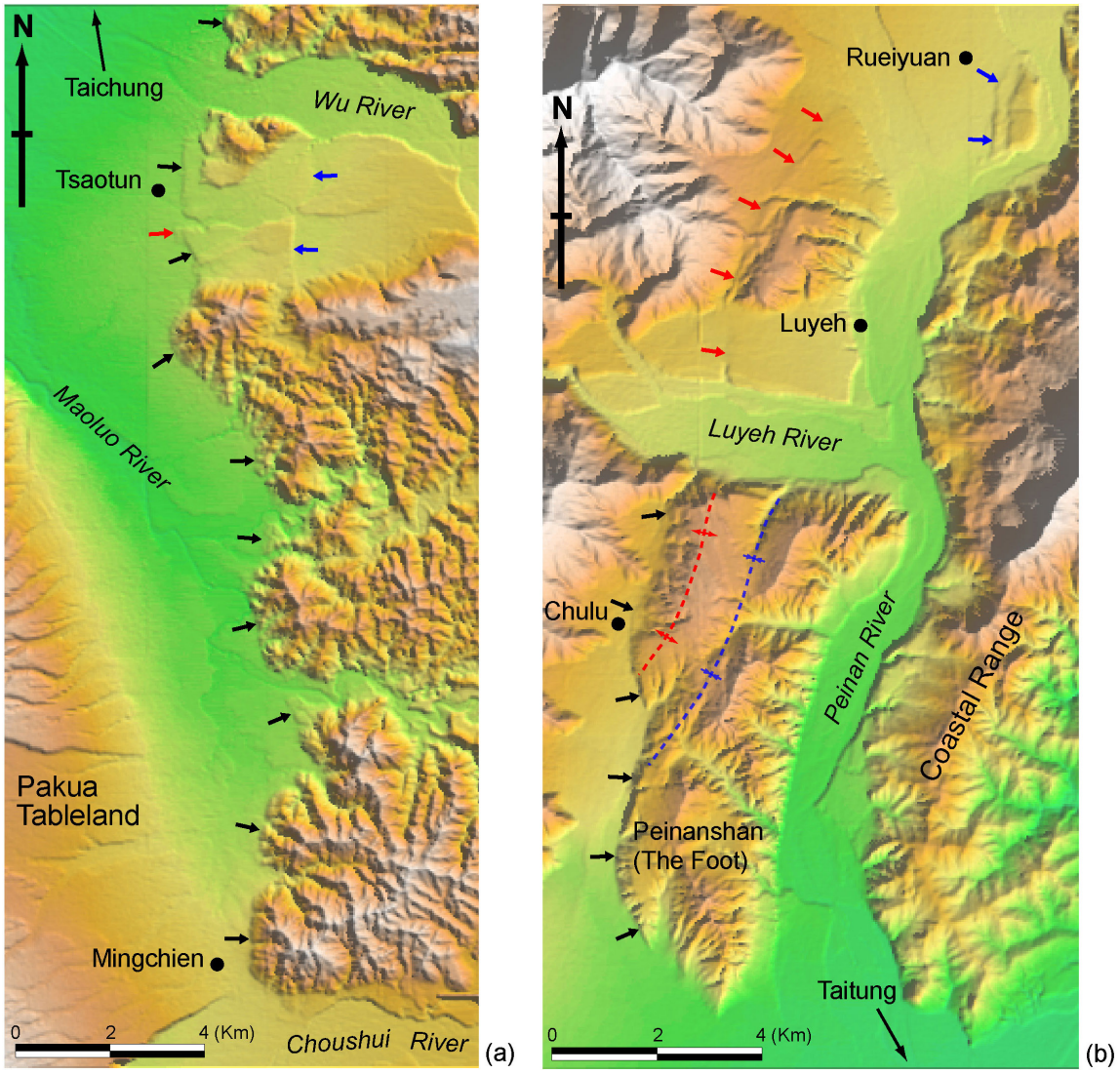

Figure 2.2. Two examples showing the geomorphic evidence for active structures visible in the 40-m DEM. Figures of similar resolution for other parts of Taiwan are available as electronic data supplements. Locations of the two are shown in Figure 2.1(b). (a) Along a southern segment of the Chelungpu fault, topographic features not only readily predict the locations of the 1999 major rupture (marked by black arrows), but also show a minor, secondary fault rupture (marked by a red arrow) and a monoclinal surface rupture on the hanging wall of the fault (marked by blue arrows). (b) Near the southern end of the Longitudinal Valley, eastern Taiwan, geomorphic features clearly show a thrust fault along the western edge of the Peinanshan (marked by black arrows). The same fault becomes a series of anticlinal folds north of the Luyeh River (marked by red arrows) and eventually steps eastward to the western base of the river terraces east of Rueiyuan (marked by blue arrows). Fluvial surfaces in northern part of the Peinanshan clearly warped into an anticline (in red) and a syncline (in blue).

examples of the usefulness and our interpretations of the DEM data. High-resolution figures of interpreted DEM data for other part of Taiwan are available as electronic data supplements, along with much more detailed discussion of our interpretations.

Our primary reliance on the geomorphic manifestation of active structures means, of course, that we have undoubtedly missed some important features. For example, in the coastal plains where sedimentation rates are as high as 20 mm/yr [e.g., *Shyu*, 1999], surfaces that are deforming slowly may well be buried beneath late Holocene deposits. We have attempted to minimize this deficiency by incorporating locally available subsurface data. We may also have neglected to identify faults with low rates of slip within the high mountains, where rates of erosion are more than 5 mm/yr [e.g., *Hovius et al.*, 2000]. Furthermore, small features, such as the scarps that formed on the coastal plain during the historical earthquakes of 1906, 1935 and 1946, have been obliterated by human activity. We have relied on published post-seismic investigations of these historical ruptures to ensure that our map is as complete as possible. But this, of course, means that we are likely to have missed similar structures on the coastal plains that ruptured prior to the 20th century.

We have augmented our geomorphic analysis with as much additional stratigraphic and structural data as was available to us to construct our map of the active tectonic features of the island. Even so, we do not claim to have made a complete description of the active structures of Taiwan. Decades of additional work would be required to accomplish that goal. Our intent has been simply to provide an up-to-date picture of the active neotectonic features of the island, compiled from sources of data currently available, and their implications for future large earthquakes.

2.3 Neotectonic overview of Taiwan

The island of Taiwan occupies a pivotal position along the boundary between the Eurasian and Philippine Sea plates. To the south, the young Eurasian oceanic lithosphere of the South China Sea is subducting eastward beneath lithosphere of the Philippine Sea plate at a rate of about 80 mm/yr at the Manila trench [*Yu et al.*, 1999]

(Figure 2.1a). To the north, by contrast, the polarity of subduction is the opposite, and extension is occurring at about 30-40 mm/yr in a back-arc region above the Ryukyu subduction zone [e.g., *Lallemand and Liu*, 1998].

The active Taiwan orogen embodies a tandem suturing and disarticulation [*Shyu et al.*, 2005a]. In southernmost Taiwan, consumption of the Eurasian oceanic lithosphere is nearly complete, and two collisions are beginning (Figure 2.1a). On the west is the collision of a forearc sliver embedded within the Philippine Sea plate and the Eurasian continental margin. On the east is the collision of the forearc sliver and the Luzon volcanic arc [e.g., *Biq*, 1972; *Barrier and Angelier*, 1986; *Suppe*, 1987; *Reed et al.*, 1992; *Lundberg et al.*, 1992; *Huang et al.*, 1992, 1997; *Malavieille et al.*, 2002]. Taiwan consists of the rocks of these three lithospheric elements. Clastic sedimentary rocks of the shallow marine continental shelf constitute the western half of the island. Basement rocks and deep marine sedimentary rocks of the forearc ridge form the island's high mountainous backbone. And volcanic rocks and associated marine sedimentary rocks underlie the central eastern coast.

The Taiwan orogen is collapsing in the north and east because of its transfer to the region of back-arc extension of the Ryukyu subduction zone [*Teng*, 1996; *Teng et al.*, 2000] (Figure 2.1a). The predominant feature of this back-arc region is the gaping Okinawa Trough, which has been opening to the south along the eastern flank of the island for the past few million years [e.g., *Suppe*, 1987; *Teng*, 1996]. This collapse in the north is chasing construction of the fold-and-thrust belt in the south and center. *Suppe* [1981, 1984, 1987] calculated that the leading edges of both construction (in the south) and collapse (in the north) are both proceeding southward at about 100 mm/yr. Thus, latitude is commonly considered to be grossly correlative to orogenic maturity in Taiwan. Conventional wisdom is that if one wishes to understand what was happening in the north several million years ago, one studies what is going on now in the ocean just south of the island.

The collapse of the orogen in the north is concentrated along the two sutures. The western suture is unstitching across the Okinawa Trough, which can be considered a reincarnation of the South China Sea. The eastern suture is tearing apart along the coastline a little farther south [*Shyu et al.*, 2005a] (Figure 2.1a). The disengagement of the western suture is clearly manifest in the oroclinal bending of the rocks of Taiwan's Central Range at the southern limit of current extension, where foliations of Central Range rocks bend eastward and strike out to sea, toward the Ryukyu island arc [e.g., *Tan*, 1977; *Suppe*, 1984]. Except for a right-lateral tear, no major structural break appears between the rocks of Taiwan's mountainous backbone and the westernmost part of the Ryukyu island arc. In fact, the oldest rocks of the southern Ryukyu Islands are metamorphic rocks that are similar to the Tananao Schists of the Central Range of Taiwan [e.g., *Kizaki*, 1986]. Thus, the Ryukyu arc next to Taiwan may well be the ancient forearc ridge of the Philippine Sea plate.

A similar disengagement of the eastern suture is apparent farther south, where the rocks of the Luzon arc in Taiwan's Coastal Range are pulling away from those of the forearc ridge (Central Range). Although we have no knowledge of the properties of the basement rocks between the Ryukyu arc and the trench, topography suggests that the old Luzon arc lithosphere overlies the more shallow parts of the Ryukyu subduction zone [*Shyu et al.*, 2005a].

Taiwan thus provides a particularly clear example of the weakness of lithospheric sutures. The two sutures that juxtaposed three diverse pieces of lithosphere during collision only a few million years ago are being preferentially ripped apart now in the back-arc region of a subduction zone. This basic neotectonic framework of Taiwan will be important in making sense of its active tectonic structures, below.

2.4 Neotectonic domains of Taiwan

The Taiwan orogen consists of two principal loci of active deformation (Figures 2.1 and 2.3). On the west is a fold-and-thrust belt, along which shallow marine rocks of the outer continental shelf are piling up onto the Eurasian continental shelf of the Taiwan Strait. On the east is a second collisional belt, where the Luzon volcanic arc of the Philippine Sea plate is slamming into forearc rocks of the Central Range. Along both the eastern and western systems, collision began in the north about 5 myr ago [*Ho*, 1986; *Suppe*, 1987; *Teng*, 1987, 1990], reached the middle of the island about 3 myr ago [*Teng*, 1987, 1990], and is just beginning near Taiwan's southern tip [*Huang et al.*, 1992, 1997, 2000; *Kao et al.*, 2000]. In the process of double collision, most of the 300-km-wide piece of oceanic lithosphere between the Manila trench and the Luzon volcanic island arc has disappeared. Only the 40-km-wide strip of forearc-ridge lithosphere remains as the backbone of the island. The result has been a southward-progressing orogen.

Our examination reveals that the manifestation of active deformation varies considerably and progressively from south to north. However, this progressive along-strike variation in deformation is not gradational. Instead, it occurs across discrete steps. Hence, both the western and the eastern belts divide naturally into several distinct structural domains. Seven discrete domains comprise the western belt, and four constitute the eastern belt. Distinct principal structures characterize each of these eleven domains. Some domains are dominated by relatively simple emergent thrust faults, whereas others are dominated by hidden, or "blind," thrusts. In some domains the principal structures traverse tens of kilometers and cross the entire domain. In other cases, a myriad of small active structures prevail. The transitions between domains are well defined, although in several cases they are 10 to 20 km wide and involve the interpenetration of principal structures from the adjacent domains.

We have divided our discussion into two sections below, one for each of the

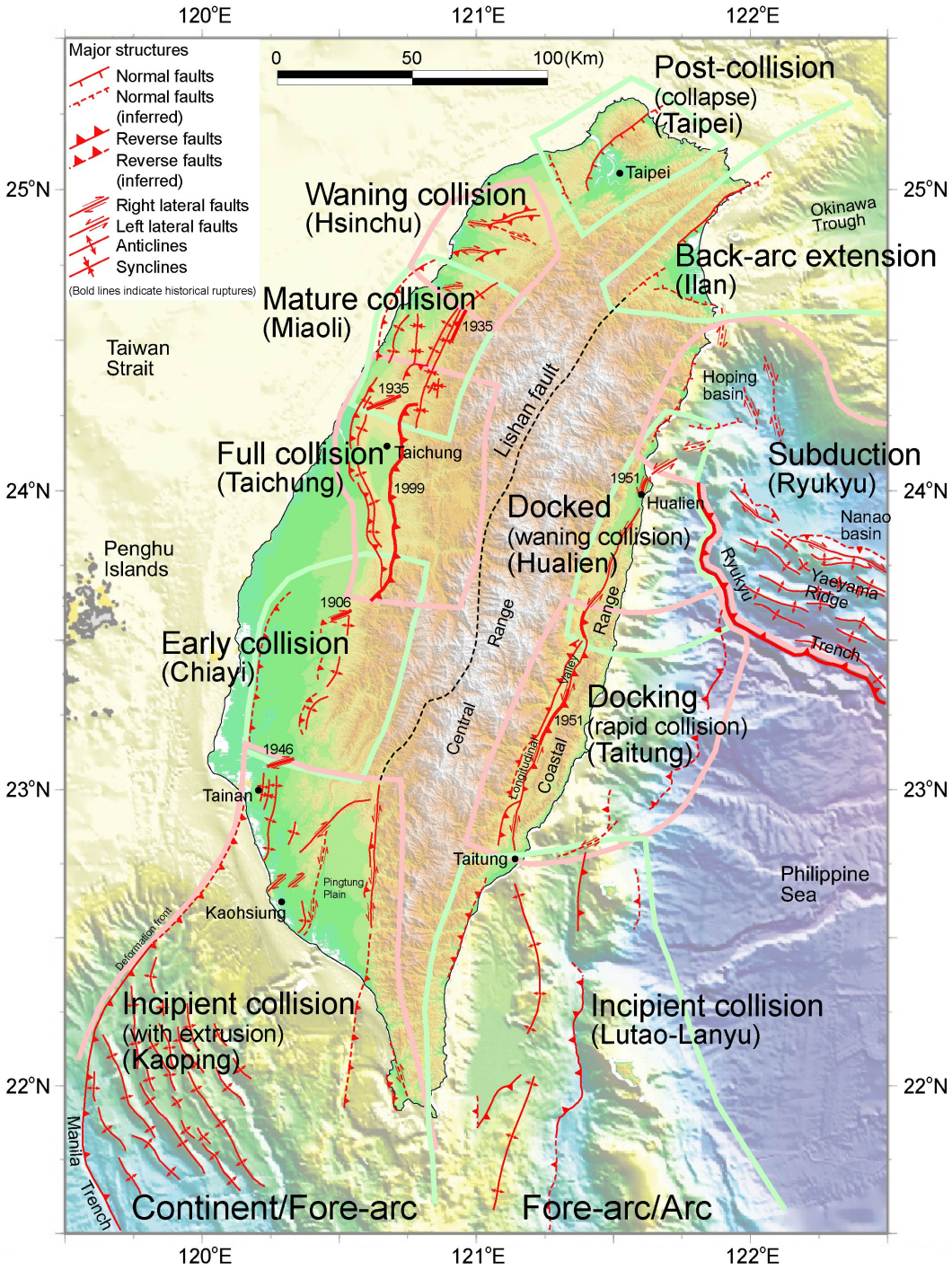

Figure 2.3. Map of major active faults and folds of Taiwan (in red) shows that the two sutures are producing separate western and eastern neotectonic belts. Each collision belt matures and then decays progressively from south to north. This occurs in discrete steps, manifested as seven distinct neotectonic domains along the western belt and four along the eastern. A distinctive assemblage of active structures defines each domain. For example, two principal structures dominate the Taichung Domain. Rupture in 1999 of one of these, the Chelungpu fault, caused the disastrous Chi-Chi earthquake. The Lishan fault (dashed black line) is the suture between forearc ridge and continental margin. Bold light green and pink lines are boundaries of domains.

neotectonic belts. In each section we discuss the general characteristics of each of the eleven active structure domains. Each domain derives its name from the most prominent city or other geographic feature of the region. Due to space limitations, we have made more detailed discussion of these neotectonic domains, together with higher-resolution interpreted DEM figures, available as electronic data supplements.

2.4.1 Eastern neotectonic belt

The progressive south-to-north accretion and disengagement of the volcanic arc occurs across four discrete domains in eastern Taiwan. From south to north, collision is proceeding from the Lutao-Lanyu to the Taitung and Hualien Domains (Figure 2.3). These correspond to three stages in the accretion of the island arc—incipient collision, docking, and docked. Farther east and north, the Ryukyu Domain encompasses the splitting of the Coastal Range away from the Central Range and the locked part of the Ryukyu subduction interface.

The Lutao-Lanyu Domain is in the early stages of collision. A wide submerged fragment of forearc-basin lithosphere remains between the volcanic arc and the southeastern coast of the main island [e.g., *Huang et al.*, 1992]. GPS measurements show that it is being shortened at about 40 mm/yr (Figure 2.1b). This strain accumulation is accommodated by active thrust faults beneath the sea. To the north, in the Taitung Domain, forearc lithosphere has sundered completely and, except for shallow crustal sediments, is no longer visible at the surface. The volcanic island arc is accreting to the metamorphic core of the island at the prodigious rate of about 30 mm/yr along a suture marked by the narrow, N-S trending Longitudinal Valley (Figure 2.1b). Meanwhile, not only the forearc ridge has emerged above sea level, but the metamorphic core of the ridge has also risen to the surface as the major component of the Central Range. Farther north, in the Hualien Domain, lower geodetic rates of convergence

suggest that accretion is nearing completion. Just north of the Hualien Domain, in the transition to the subduction of the Ryukyu Domain, the volcanic arc and forearc terranes are disengaging.

The bathymetry south of Taiwan is dominated by a prominent forearc ridge and forearc basin. This antiform/synform pair, the Hengchun Ridge and the Luzon Trough, trend roughly NNW-SSE, parallel to the trench and arc (Figure 2.1a). Bathymetric relief across these features is about 3 km, and together they span a forearc that is about 150 km wide. The Hengchun Ridge is the southward, submarine extension of the Hengchun Peninsula of southern Taiwan [e.g., *Huang et al.*, 1992; *Lundberg et al.*, 1997]. The Luzon Trough, between the ridge and the volcanic arc, does not extend onshore. Instead it truncates against the southeastern coast of Taiwan where volcanic arc rocks are first juxtaposed against the metamorphic rocks that form the basement core of the forearc. Thus, the oceanic lithosphere of the Luzon Trough must have been largely consumed in the course of southward progression of orogeny in Taiwan [e.g., *Chemenda et al.*, 1997].

Long ago, *Chen et al.* [1988] recognized that the submarine topography of the northern sector of the North Luzon Trough defines three N-S trending structural features. From east to west, these are the Taitung Trough, the Huatung Ridge, and the Southern Longitudinal Trough (Figure 2.4). The southern limit of the ridge and two troughs, at about 21.5°N, may demarcate the southern front of forearc shortening [e.g., *Huang et al.*, 1992, 1997, 2000]. The east-dipping Wadati-Benioff zone of the Manila trench, however, extends under these structures as far north as Taitung [*Huang*, 1997; *Kao et al.*, 2000]. This indicates that seismic deformation of the subducting Eurasian oceanic lithosphere continues beneath the entire Lutao-Lanyu Domain but does not extend farther north (dashed black line in Figure 2.1a).

A closer examination of the structures within the Lutao-Lanyu Domain enables a better definition of the active structures of the incipient collision (Figure 2.4). The Huatung Ridge is probably an anticline or an anticlinorium. Seismic reflection lines

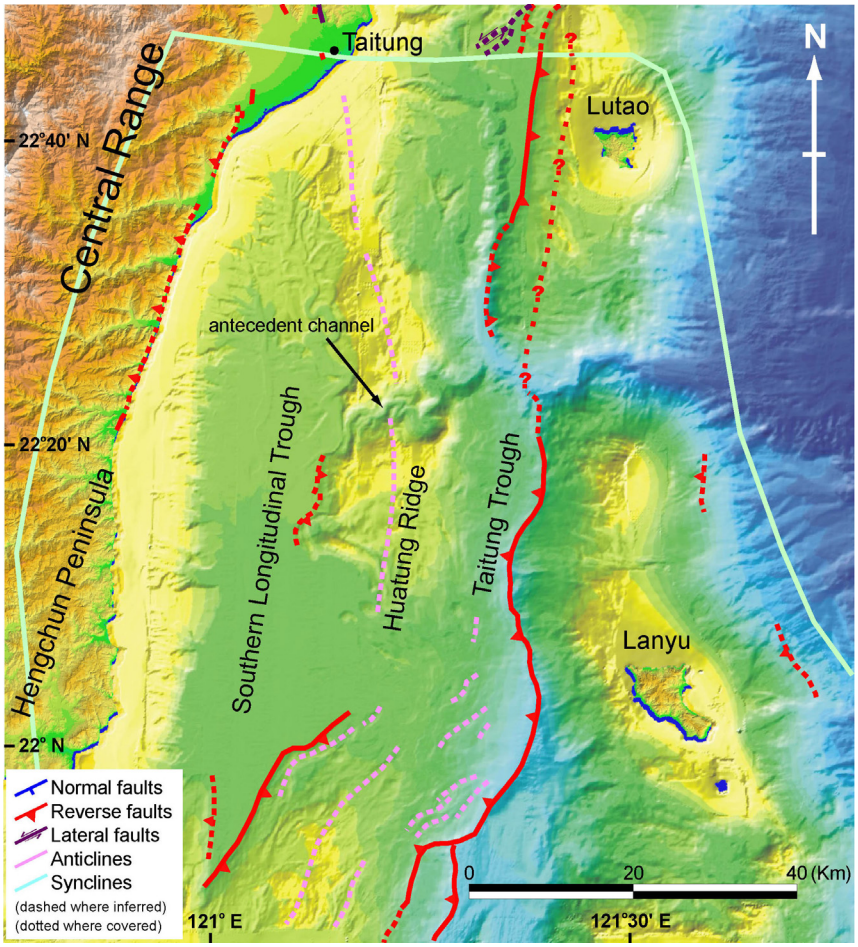

Figure 2.4. Active-tectonic map of the Lutao-Lanyu Domain. The Hengchun Peninsula, the Southern Longitudinal Trough, the Huatung Ridge, the Taitung Trough, and the Lutao and Lanyu volcanic islands are the major geomorphic elements of this domain. The Huatung Ridge is an anticline, produced by slip on a major west-dipping thrust fault. A backthrust crops out in the south along its western base. West of Lutao, an east-dipping thrust fault may be responsible for the fast uplift of the island. The irregular polygon that surrounds the active structures in Figure 2.4 to Figure 2.14 defines the perimeter of the domain.

show, in fact, that sediments on the western flank of the ridge at about 22°20'N tilt westward [*Huang et al.*, 1992]. Bathymetry and seismic reflection profiles clearly show a west-dipping thrust fault on the east flank of the ridge from about 21°40' to 22°20'N [*Lundberg et al.*, 1997; *Chang et al.*, 2001; *Malavieille et al.*, 2002]. In the vicinity of 22°N, a clear but lesser scarp exists on the west side of the ridge as well. North of about 22°20'N, however, no scarps are obvious on either side of the ridge, so either the underlying thrust faults are blind or currently inactive. These observations and the basic

symmetry of the Huatung Ridge suggest that it is the submarine expression of a fault-bend fold above a variably west-dipping thrust fault. Growth of the fold has been incremental, as evidenced by the presence of an antecedent meandering submarine channel cutting across the feature about halfway between the latitudes of Lanyu and Lutao islands (Figure 2.4).

High rates of uplift of the volcanic islands, about 3.4 mm/yr [*Chen and Liu*, 1992; *Chen*, 1993] since Late Pleistocene, suggest that the volcanic arc is also involved substantially in the incipient collision of the Lutao-Lanyu Domain. However, only one fault is obvious in the bathymetry: A 20-km long linear scarp west of Lutao (Figure 2.4) suggests that an east-dipping fault crops out there and dips under the island.

Recent geodetic measurements by GPS reveal that Lutao and Lanyu are converging northwestward toward the Hengchun Peninsula at about 40 mm/yr [*Yu et al.*, 1997, 1999]. We propose that slip on the major west-dipping thrust fault, on the east flank of the Huatung Ridge, accommodates most of this strain. The high uplift rates of Lutao and Lanyu islands suggest that thrust faults beneath them also are contributing significantly to the shortening. The high late Pleistocene uplift rates of these islands suggest that the component of horizontal shortening on the underlying thrusts is about 6 mm/yr, perpendicular to strike.

The northern edge of the Lutao-Lanyu Domain is abrupt. The Southern Longitudinal Trough, the Taitung Trough and the Huatung Ridge do not continue northward beyond the latitude of Taitung city (Figure 2.4). The submarine ridge of the volcanic arc disappears only a little farther north. The topography and bathymetry to the north is utterly different.

Figure 2.5 shows that the Taitung Domain is characterized by a long, narrow valley between the Central Range and the arc-volcanic rocks of the Coastal Range and a precipitous offshore escarpment. The active structures that have created these features are not contiguous with those of the Lutao-Lanyu Domain. In fact, the sense of

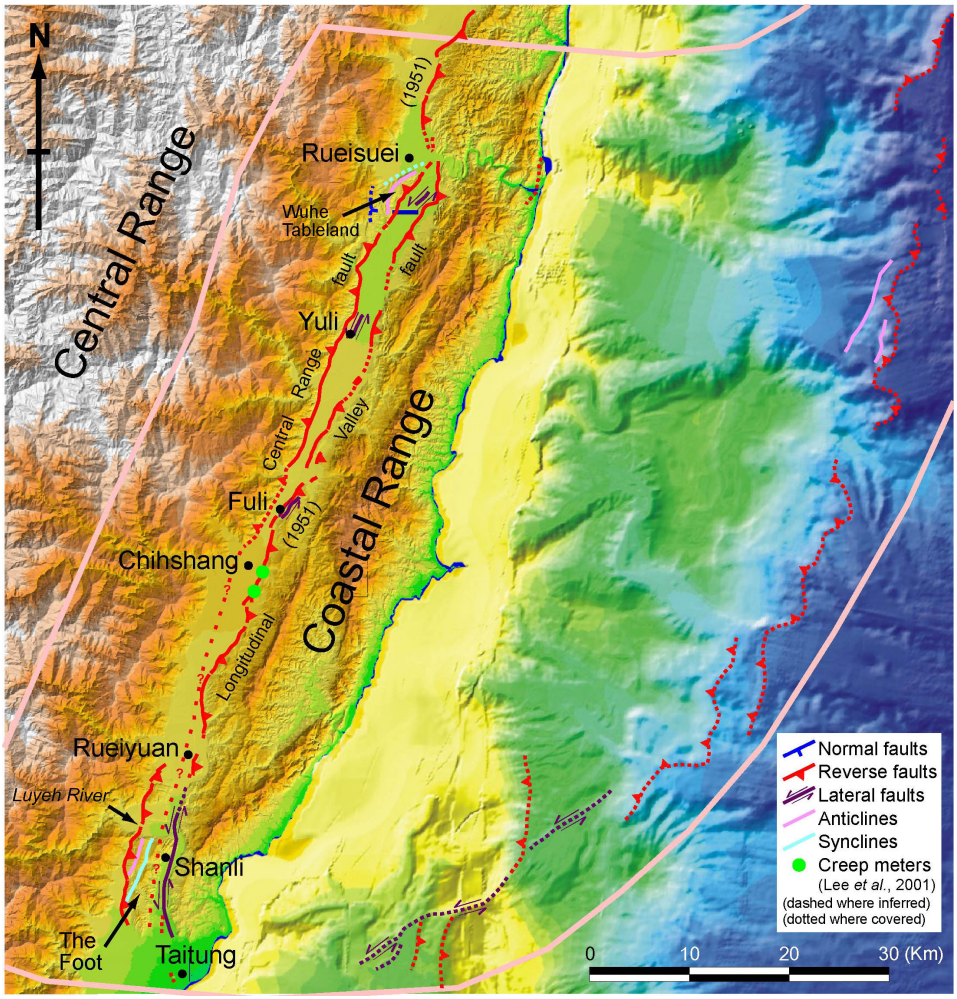

Figure 2.5. Active-tectonic map of the Taitung Domain. The east-dipping, oblique-slipping Longitudinal Valley fault along the eastern edge of the Longitudinal Valley and the west-dipping Central Range fault along its western edge are the two major structures. The Longitudinal Valley fault partitions into dip-slip and strike-slip strands near "The Foot," just north of Taitung. The Central Range fault may be blind south of Fuli. Minor, discontinuous left-lateral faults occur near Yuli and east of the Wuhe Tableland.

vergence of the dominant structure changes abruptly across the boundary between the two domains.

The dominant neotectonic element of the Taitung Domain is the east-dipping Longitudinal Valley fault, along the eastern edge of the valley (Figure 2.5). It is characterized by high rates of sinistral reverse motion. A clear example of slip partitioning between strike-slip and dip-slip faulting occurs in the southern 20 km of the Taitung Domain [*J.-C. Lee et al.*, 1998; *Hu et al.*, 2001; *Shyu et al.*, 2002]. Geodetic

measurements confirm that the Longitudinal Valley fault is active and slipping at a high rate. Across a segment of the Longitudinal Valley fault zone near Chihshang, creepmeters show that it is creeping obliquely at a high rate [*Angelier et al.*, 1997; *Lee et al.*, 2001]. Field measurements of deformed man-made structures indicate that the rate of horizontal shortening is about 22 mm/yr directed 323° [*Angelier et al.*, 1997], and leveling confirms a vertical dislocation rate of up to 20-24 mm/yr [*Yu and Liu*, 1989; *Yu and Kuo*, 2001].

Rupture of the Longitudinal Valley fault in the Taitung Domain produced two large earthquakes, three minutes apart, on 25 November 1951 — a M7.0 earthquake in the north, near Yuli, and a M6.2 earthquake in the south, near Chihshang [*Cheng et al.*, 1996]. The ruptures were not well documented, but there were sparse observations of fault rupture between about Chihshang and a point about 40 km north of Rueisuei [*Hsu*, 1962; *Cheng et al.*, 1996; *Shyu et al.*, 2005b] (Figure 2.5).

East-facing scarps on the seafloor about 50 km east of the Longitudinal Valley are evidence of active thrust faulting there. *Malavieille et al.* [2002] suggest that this fault is the principal fault of the Coastal Range block, and that the Longitudinal Valley fault is a backthrust that rises from it. We question the proposal that the Longitudinal Valley fault plays a subsidiary role, given its very high rate of slip. Such high rates suggest that the Longitudinal Valley fault is, in fact, the principal fault, and that the fault on the sea floor is subsidiary.

The existence of a reverse fault dipping westward beneath the eastern flank of the Central Range has long been suspected. *Biq* [1965], in fact, named this structure the Central Range fault. Several independent lines of evidence suggest its existence. First, the exposed slates of the Central Range formed at depths far below the land surface and, thus, must have been uplifted many kilometers. Second, the range's eastern flank is notably straighter than it is in the Hualien Domain to the north. Third, fluvial terraces are perched tens to hundreds of meters above modern streambeds along the eastern range

front of the Central Range. Fourth, a leveling line that extends 16 km into the Central Range near Chihshang shows tilt of the easternmost 16 km of the range at about 0.8 μradian/yr [*Liu and Yu*, 1990]. Similar eastward tilting of the eastern Central Range is also occurring west of the Yuli area [*Yu and Kuo*, 2001]. Furthermore, recent analysis of seismicity may support the presence of a west-dipping structure beneath the eastern Central Range [e.g., *Carena et al.*, 2001].

In summary, the principal structures of the Taitung Domain are accommodating about 40 mm/yr of obliquely convergent shortening (Figure 2.1b). Most of this is currently being taken up across the rapidly creeping (but occasionally seismic) Longitudinal Valley fault, which dips east beneath the Coastal Range. A subsidiary west-dipping reverse fault crops out about 40 km offshore, on the seafloor. The Central Range thrust, which dips under the eastern flank of the Central Range, also appears to be active.

At first glance, the northern half of the Longitudinal Valley does not appear to be all that different from the southern half (Figure 2.3). As to the south, the width of the valley is about 5 km (Figure 2.6) and the valley is filled with coarse clastic sediments derived predominantly from the Central Range on its western flank. Despite these similarities, the Hualien Domain (Figure 2.3) is fundamentally distinct from its neighbor to the south. The principal differences are that 1) the west-dipping Central Range thrust appears to be either inactive or much less active than it is to the south, 2) the east-dipping Longitudinal Valley fault has a higher ratio of sinistral to dip slip, and 3) rather than a west-dipping thrust fault offshore, the edge of the Ryukyu deformation front sits offshore.

Along the entire 65 km onland length of the Hualien Domain the Longitudinal Valley fault crops out at the base of the western edge of the Coastal Range. Along much of that length the fault has separate strike-slip and dip-slip strands. The strike-slip traces of the fault are much more prominent and continuous than they are in the Taitung Domain. The dominance of left-lateral movement on the northern Longitudinal Valley fault system

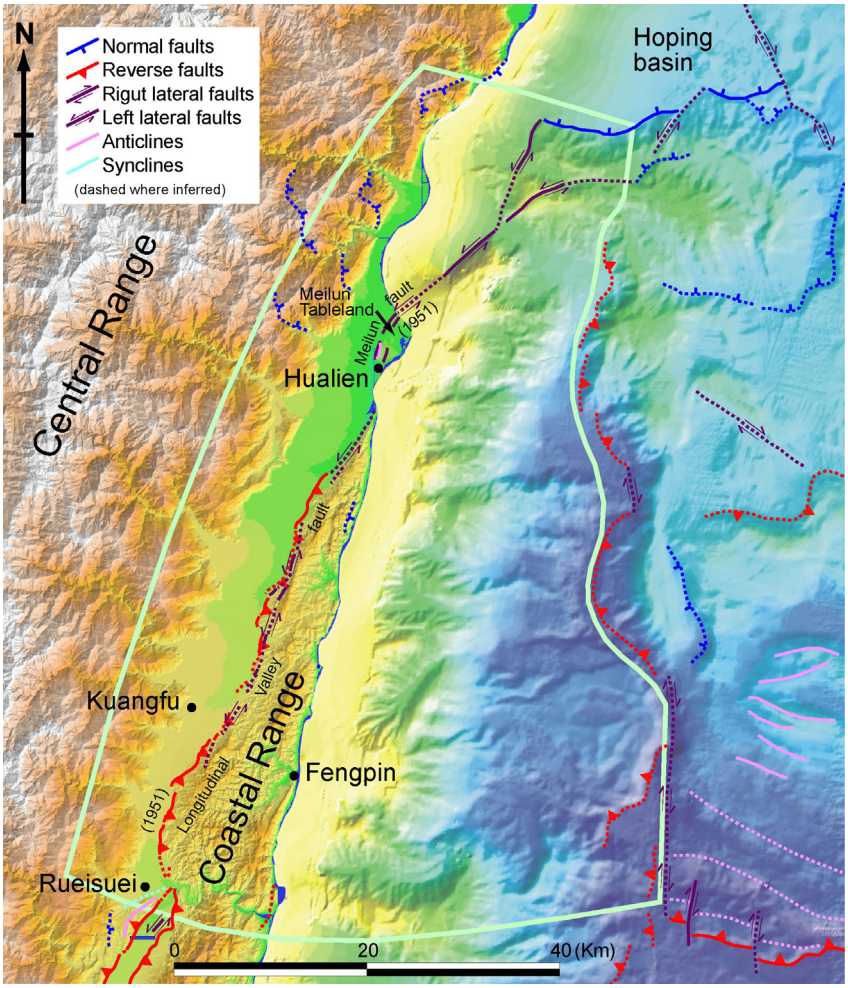

Figure 2.6. Active-tectonic map of the Hualien Domain. The Longitudinal Valley fault is the only major active structure in this domain. This fault commonly partitions into separate thrust and left-lateral strands. The faults around Hualien City and in the sea farther northeast are the northward extension of the Longitudinal Valley fault.

near Hualien is also clear in geodetic measurements [e.g., *Chen*, 1974; *Yang*, 1999]. Seismic rupture of a section of the Longitudinal Valley fault provides additional support for the predominance of strike slip over dip slip. Rupture of the Meilun strand, which runs along the western edge of the Meilun Tableland near Hualien City, produced a M7.3 earthquake in October 1951 [*Yang*, 1953; *Hsu*, 1962]. Vertical offsets across the rupture were about 1.2 m, and left-lateral offsets were about 2 m [*Hsu*, 1955; *Lin*, 1957; *Bonilla*, 1975, 1977; *Yu*, 1997].

A submarine ridge extends northeastward approximately 10 km from the Meilun

Tableland (Figure 2.6). Further northeast is another submarine ridge, which trends nearly E-W and seems to be unconnected to any onland topography. The abrupt and steep scarps at its northern flank separate the ridge from the much lower and smoother Hoping Basin. These scarps appear to represent the initiation of the eastward peeling off of the Coastal Range from the Taiwan orogen. As one would expect in a region of transition between suturing and unsuturing, many minor structures are present in this area.

We find scant evidence for activity of the Central Range thrust within the Hualien Domain. The rarity of high lateritic fluvial terraces in the river drainages of the eastern flank of the range [*Yang*, 1986; *Chang et al.*, 1992] suggests lower uplift rates than to the south. Moreover, the sinuosity of the eastern flank of the Central Range indicates that rates of alluvial deposition outpace rates of uplift of the range. Thus, it appears that the Longitudinal Valley fault is the only major active structure of the onshore part of the Hualien Domain.

The southern boundary of the Hualien Domain is well defined. It appears to be a 20-km-wide transition zone between Rueisuei and Kuangfu (Figure 2.6). At Rueisuei the northernmost clear evidence for activity of the Central Range thrust is present. Between Rueisuei and Kuangfu the geomorphology of the fault trace suggests that thrusting is dominant over sinistral slip, as in the Taitung Domain to the south, but we find no indication of activity of the Central Range thrust along this portion of the valley. Thus, this section of the valley is transitional between the two domains. Recent GPS measurements support this conclusion, showing that south of Kuangfu the convergence rate normal to the strike of the Longitudinal Valley fault is as high as 30 mm/yr [*Yu et al.*, 1997, 1999]. North of Kuangfu, however, the convergence rate is dramatically lower – just 5 mm/yr.

The eastern and northern boundaries of the Hualien Domain are the edge of the Ryukyu subduction system. North of Hualien, the Coastal Range and Longitudinal

Valley drop to sea level, and the sea laps against a precipitous eastern flank of the Central Range (Figure 2.3). This is the southern edge of the extension associated with the Ryukyu subduction system and the tearing apart of the forearc/volcanic arc suture.

The Ryukyu Domain encompasses that part of the Ryukyu subduction megathrust nearest Taiwan that is capable of producing large subduction earthquakes. We have drawn the boundaries of the domain with the intention of encompassing all active structures between the trench and the southern side of the back-arc Okinawa Trough. The dominant structure in this domain is, of course, the subduction interface, but accommodation structures on the western edge of the domain are also important.

Isobaths drawn on the top of the Wadati-Benioff zone show that the dip of the Ryukyu subduction interface averages about 40° to a depth of about 50 km and steepens downdip from there to more than 55°. The Wadati-Benioff zone defines the subducting slab to a depth of greater than 250 km [*Kao et al.*, 1998; *Kao and Rau*, 1999]. The termination of seismicity at the western edge of the Wadati-Benioff zone is abrupt. It trends nearly N-S, from the edge of the Ryukyu Domain to the western edge of the Taipei Domain (dashed black line in Figure 2.1a).

Secondary thrust faults in the hanging-wall block are also apparent. Immediately north of the Ryukyu trench is the Yaeyama forearc ridge [*Liu et al.*, 1998] (Figures 2.3 and 2.7), a 40-km-wide feature that consists of a series of E-W trending anticlinal ridges and synclinal valleys. Also, two major right-lateral faults in the northern portion of the ridge have been proposed to accommodate the oblique subduction direction [e.g., *Lallemand et al.*, 1999; *Chemenda et al.*, 2000; *Font et al.*, 2001]. North of this fold-and-thrust belt of the accretionary prism is an irregular 40-km-wide forearc trough that includes the Hoping and Nanao forearc basins [*Liu et al.*, 1998]. The southern flank of the trough is clearly faulted, with deformed and offset sediment layers in the seismic reflection profiles [e.g., *Schnürle et al.*, 1998; *Font et al.*, 2001].

The western margin of the Ryukyu Domain is a very complex transition zone

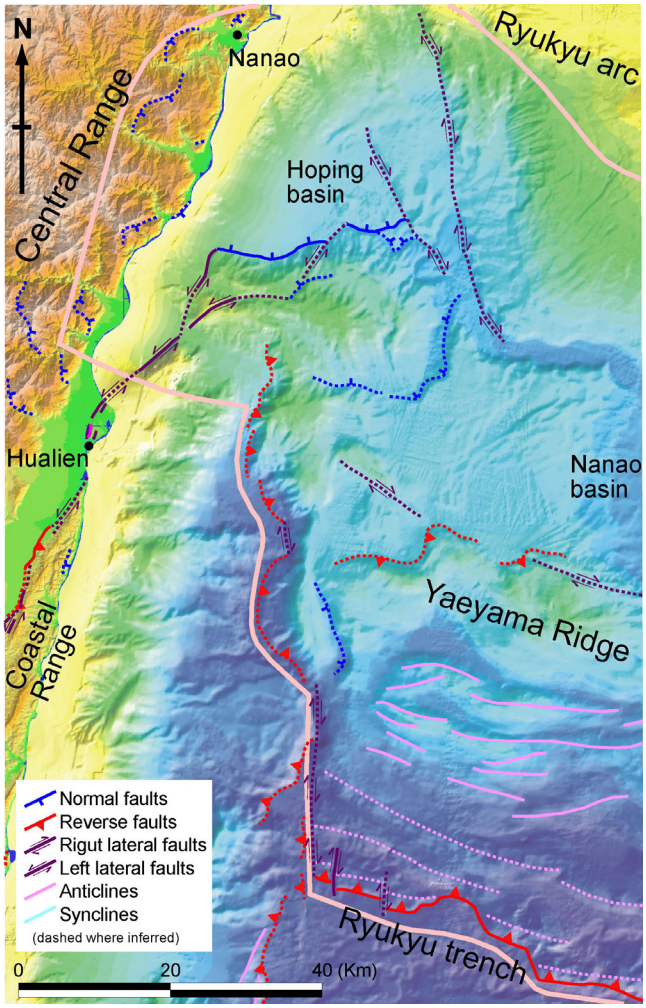

Figure 2.7. Active-tectonic map of the western part of the Ryukyu Domain. The Ryukyu trench is the major element of this domain. Numerous folds are present in its hanging wall. Its western margin includes major right-lateral faults and a complex of normal faults around the Hoping basin, a triangular-shaped graben.

between three domains: the Hualien, Ryukyu, and Ilan Domains. Thus, in this region one may expect to find numerous minor accommodation structures. In addition, bathymetry shows that the westernmost part of the Ryukyu deformation front swings abruptly northward (Figure 2.7). The linearity of the scarp along this N-S trending segment suggests a substantial component of right-lateral strike slip. Two more right-lateral faults are present in the eastern part of the Hoping basin. On 15 May 2002, a moderate earthquake (M_w 6.0) resulted from slip on a related right-lateral strike-slip fault. The epicenter of the earthquake was offshore, about 25 km north of Nanao, and

the fault plane solutions of the main shock and its aftershocks showed right-lateral movement on an approximately N-S striking plane. This structure is properly situated and oriented to serve as one of the structures that form the western boundary of the Ryukyu subduction zone.

2.4.2 Western neotectonic belt

Western Taiwan's active deformational belt divides naturally into seven distinct neotectonic domains. From south to north, these seven are the Kaoping, Chiayi, Taichung, Miaoli, Hsinchu, Ilan, and Taipei Domains (Figure 2.3). As in the Eastern neotectonic belt, all but the northernmost represent a northward maturation in the progress of collision. As in the east, the northernmost domains encompass the region that has switched from shortening to back-arc extension of the Ryukyu subduction system. Unlike the Eastern neotectonic belt, however, the Western belt is not the result of volcanic arc/forearc collision and separation. Rather, it is the product of collision and separation of the forearc and the continental margin.

Docking of the two terranes begins in the southernmost (Kaoping) domain, and disengagement occurs in the northern (Ilan and Taipei) domains. In the Kaoping Domain, deep marine, shallow marine, and terrestrial sediments are deforming very rapidly by contraction and lateral extrusion over the last remnants of oceanic Eurasian lithosphere. Eurasian oceanic lithosphere continues to subduct beneath the entirety of this domain.

Along the central four domains of the Western belt, the lithosphere of the forearc ridge has made contact with the edge of the continental shelf, and shallow marine and foredeep sedimentary rocks of the continental shelf are being pushed northwestward farther onto the Eurasian continental margin. Very rapid rates of shortening continue to prevail in the Chiayi Domain, but the style of deformation is quite different than in the

Kaoping Domain. There, a blind thrust fault system that extends out under the foothills and coastal plain predominates. Further north, in the Taichung Domain, rates of shortening are lower, but two major emergent thrust faults, including the one that ruptured to produce the 1999 earthquake, dominate the neotectonic picture. Still farther north, across the Miaoli Domain, shortening rates are also relatively low, but the style of deformation is more complex; tight and open folds lie above a master blind thrust that extends from beneath the foothills all the way to the western coast. Shortening is in the waning stages in Hsinchu, the next domain to the north. Its active reverse faults strike more easterly than the trend of the western deformation belt and are cut by active strike-slip tear faults. Extension and subsidence characterize the active tectonics of the Ilan and Taipei Domains, the northernmost domains of the western belt. The Ilan Domain belongs to the western belt because it embodies the unstitching of the suturing that is currently in progress in the Kaoping Domain. It encompasses most of the back-arc extension of the Okinawa Trough. The Taipei Domain is dominated by a geologically minor normal fault in the hinterland of the Okinawa Trough. This one active normal fault lies on the western margin of the Taipei Basin and splits the edifice of the large, dormant Quaternary volcano to the north.

The Kaoping Domain, the southernmost of the western domains, encompasses the final episode of subduction of oceanic lithosphere prior to collision of forearc ridge and continental margin. Its northern boundary coincides with the northern limit of the Wadati-Benioff zone of the Manila trench [e.g., *Huang et al.*, 1992; *Kao et al.*, 2000] (dashed black line in Figure 2.1a). It also coincides with the impingement of the Western Foothills and the Central Range, which we infer to reflect the elimination of oceanic lithosphere from between the edge of the Eurasian continental shelf and the forearc ridge. Unlike the more mature collisional domains farther north, the Kaoping Domain includes a rapidly subsiding basin between the Central Range and the Western Foothills. We interpret this to be analogous to the submarine part of the Lutao-Lanyu

Domain, its neighbor to the east: these are the last vestiges of oceanic lithosphere to be consumed prior to suturing (converging arrows in Figure 2.1a).

Both the submarine and subaerial sectors of the Kaoping Domain consist of three tracts. On the east is the forearc ridge, which continues onto land as the rapidly rising Hengchun Peninsula and Central Range (Figures 2.3 and 2.8). The peninsula and range consist of deep marine turbidites and mélange in the south and metamorphosed slate and continental basement rocks in the north [e.g., *Chen et al.*, 1985; *Sung and Wang*, 1985, 1986; *Ho*, 1988; *Lin*, 1998]. This south-to-north progression of lithology indicates the progressive uplift and unroofing of the basement of the forearc ridge across the Kaoping Domain. On the western margin of the domain is a 50-km-wide submarine fold-and-thrust belt above the shallowest part of the Manila trench. This appears to extend onto land as the subaerial belt of deformation between Tainan and the Western Foothills. Between these eastern and western structural elements is a structurally non-descript tract of what must be marine lithosphere overlain mostly by deep-sea sediments. This extends onshore to the Pingtung Plain, where subsidence is occurring at rates up to 13 mm/yr in the Holocene [e.g., *Lu et al.*, 1998; *Shyu*, 1999].

The Chaochou fault separates the Pingtung Plain from the Central Range (Figure 2.8). The presence of Miocene-age rocks in the mountains on the east and a thick section of Quaternary strata in the basin to the west demonstrates that the fault has a significant component of vertical slip, up on the east [e.g., *Ho*, 1988]. The linearity of this fault suggests that it also has a significant component of strike-slip motion (Figure 2.8). Some previous mapping [e.g., *Wu*, 1978; *Ho*, 1988] inferred that this fault continues southward along the western front of the Hengchun Peninsula and becomes the Hengchun fault [e.g., *Shih et al.*, 1985; *Yang*, 1986] near the southern tip of the peninsula. Alternatively, *Malavieille et al.* [2002] suggest that the Chaochou fault runs southward into a submarine canyon west of the Hengchun Peninsula (Figure 2.3). The western flank of the Pingtung Plain may also represent another active fault.

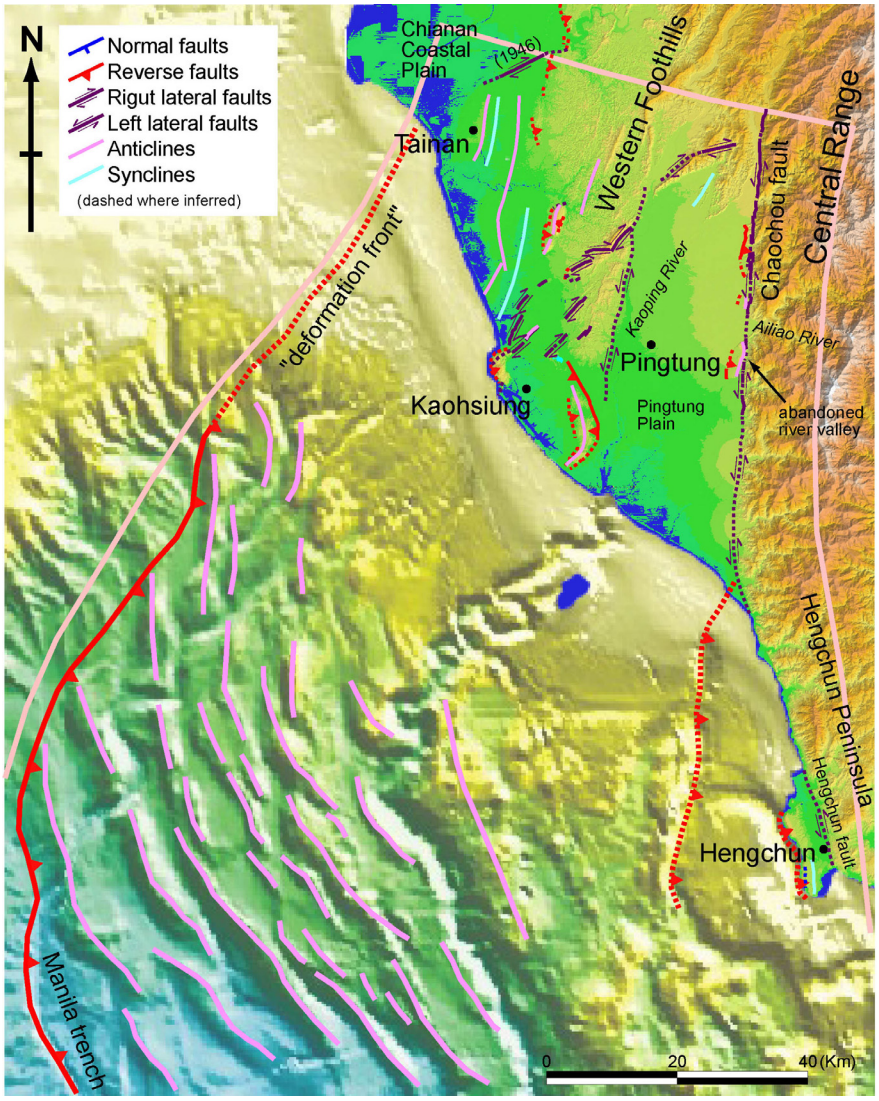

Figure 2.8. Active-tectonic map of the Kaoping Domain. Offshore, complexities of the Manila subduction interface are producing numerous active folds. On land, the left-lateral reverse Chaochou fault separates the Central Range and the Pingtung Plain. The west side of the Pingtung Plain is approximately coincident with another left-lateral fault. Deformation within and west of the Western Foothills includes a complex of numerous short folds and right-lateral faults which facilitate southwestward extrusion.

Offshore to the southwest are numerous anticlinal ridges and minor thrust faults on the seafloor [e.g., *Liu et al.*, 1997] (Figure 2.8). Several submarine canyons cut through a series of these ridges, clearly indicating their antecedence and the incremental growth of the folds. We interpret this submarine fold-and thrust belt to be the result of the shortening of the forearc between the continental margin and the forearc Hengchun Ridge and the embryonic form of Taiwan's Western Foothills.

On land, NE-SW striking right-lateral faults and N-S trending folds dominate the deformation of the Western Foothills (Figure 2.8). The orientations of these structures indicate an overall N-S stretching and E-W shortening of the shallow crust. The crust between these right-lateral structures and the two major left-lateral structures of the Pingtung Plain must be extruding southwestward [e.g., *Lacombe et al.*, 1999, 2001; *Chan et al.*, 2001, 2002].

In summary, deformation in the Kaoping Domain reflects E-W shortening and southward extrusion of sediments above a foundering oceanic lithosphere [e.g., *Lacombe et al.*, 1999, 2001]. This shortening reduces the width of the domain from more than 100 km in the south to less than 50 km in the north. With the shortening, a broad offshore fold-and-thrust belt in the south transforms into the nascent, narrow Western Foothills in the north, characterized by several prominent N-S trending folds and NE-SW striking right-lateral faults. Farther east, the rapidly-sinking Pingtung Plain is bounded by left-lateral structures that facilitate its southwestward extrusion and is likely to be above the last piece of sundering South China Sea oceanic lithosphere.

Farther north, in the Chiayi Domain, the collision of forearc ridge and continental shelf has begun. There is no intervening basin analogous to the Pingtung Plain between the Western Foothills and the Central Range (Figures 2.3 and 2.9). Instead these two ranges abut along a fault zone that displays no clear evidence of activity. Furthermore, the Kaoping Domain's complex of small active folds and strike-slip faults within the Western Foothills does not extend northward into the Chiayi Domain. Rather, the folds of the Western Foothills there display no clear evidence for activity. Instead, the most prominent geomorphic evidence of youthful deformation exists in the low Chiayi Hills, farther west. Young lateritic fluvial terraces and active streambeds display evidence of recent folding along axes that trend nearly N-S. The geometry of these folds is broadly consistent with the presence of a shallow-dipping blind thrust fault complex beneath the Chiayi Hills and the coastal plain.

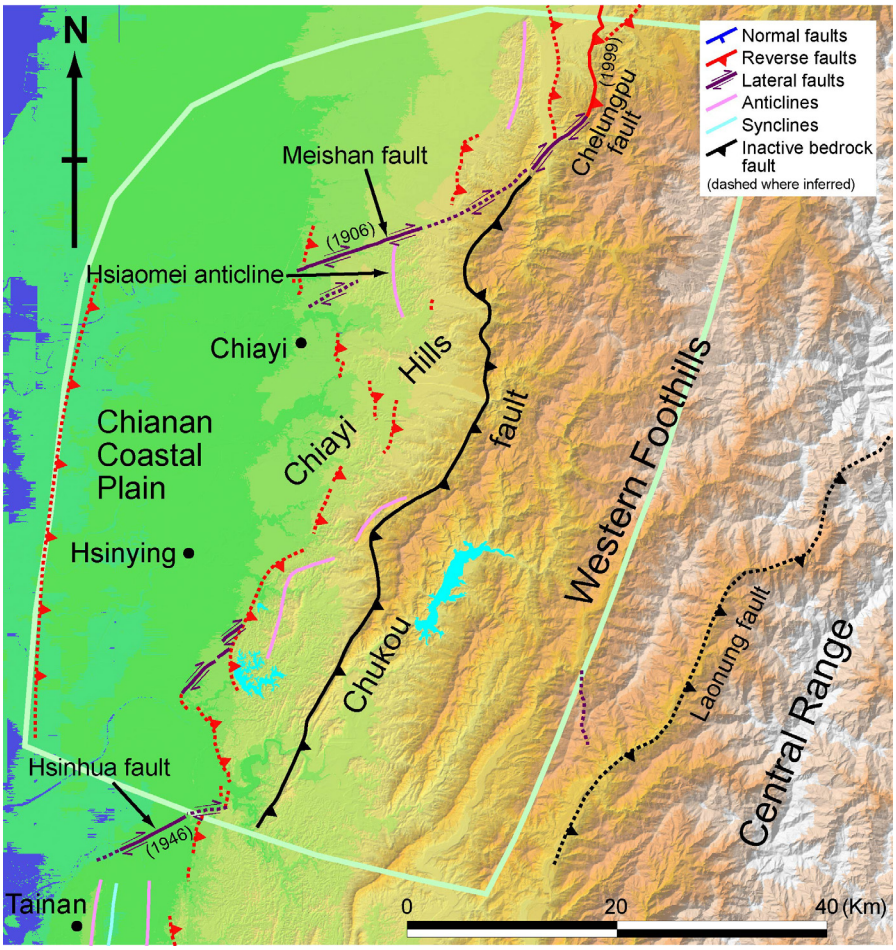

Figure 2.9. Active-tectonic map of the Chiayi Domain. Minor reverse faults and anticlines in the Chiayi Hills and incised streams across the Chianan Coastal Plain betray the presence of a blind thrust fault beneath the region. Geomorphic evidence shows that the Chukou fault, a major bedrock geologic structure in this area, is no longer active.

The low hills immediately west of the Western Foothills are commonly referred to as the Chiayi Hills. These hills are mantled with uplifted late-Quaternary lateritic fluvial terraces and consist of Quaternary fluvial sandstones and conglomerates. Between the Chiayi Hills and the west coast is the gently sloping Chianan Coastal Plain, the most important agricultural area in Taiwan. This basin is filled with Quaternary coastal and fluvial sediments up to 1500-2000 m thick [*Stach*, 1958; *Hsiao*, 1971, 1974; *Sun*, 1970, 1971, 1972; *Tong and Yang*, 1999; *Yeh et al.*, 1999].

Bedrock structures east of the Chiayi Hills do not exhibit evidence of recent activity. In contrast, evidence for youthful tectonic deformation is abundant in the Chiayi Hills

and the Chianan Coastal Plain (Figure 2.9). Uplifted fluvial terraces in the Chiayi Hills west of the Chukou fault clearly indicate deformation across several folds and minor faults [e.g., *Huang*, 1996; *Chen*, 1999]. Progressively tilted lateritic surfaces indicate ongoing deformation over the past few tens of thousands of years. Terraces along the major rivers of the Chianan Coastal Plain indicate regional uplift. This evidence belies the presence of a major active thrust fault below the Chiayi Hills and the Chianan Coastal Plain. This deeper structure has long been suspected [*Suppe*, 1980b; *Hung*, 1996; *Hung et al.*, 1999] and is likely to be the blind décollement of the western Taiwan fold-and-thrust belt. The deformation front associated with this blind structure just a few kilometers inland from the west coast is aligned with the deformation front of the Kaoping Domain, to the south. Small folds of the Chiayi Domain may be the result of irregularities in the underlying décollement and secondary structures above it [*Suppe*, 1976, 1980b]. Recent GPS measurements of the velocity field within the Chiayi Domain are consistent with the neotectonic evidence for a shallow blind master thrust fault [e.g., *Yu et al.*, 1997; *Yu and Chen*, 1998; *Hung et al.*, 1999; *Hsu et al.*, 2003].

The surface ruptures associated with two large destructive historical earthquakes provide important insights regarding the northern and southern boundaries of the Chiayi Domain. A M7.1 earthquake in 1906 occurred near the northern boundary of the domain and was accompanied by right-lateral ruptures along the ENE-WSW striking Meishan fault [e.g., *Omori*, 1907; *Bonilla*, 1975, 1977; *Hsu and Chang*, 1979; *Huang et al.*, 1985] (Figure 2.9). Likewise, the southern few kilometers of the 1999 Chi-Chi rupture was a strike-slip fault that appears to be collinear with the 1906 Meishan rupture [*Central Geological Survey*, 1999a, 1999b; *Lin et al.,* 2000b]. Therefore, the Meishan fault and the terminal right-lateral fault of the 1999 rupture serve as accommodation structures between the blind thrust décollement of the Chiayi Domain and the active thrust faults of the neighboring domain to the north.

Another historic fault rupture appears to have served a similar purpose at the

southern end of the Chiayi Domain. This N70°E rupture of the right-lateral Hsinhua fault produced the M6.8 earthquake in 1946 [*Chang et al.*, 1947; *Bonilla*, 1977] (Figure 2.9). Judging from its location, orientation, and sense of slip, this structure is also likely to be an accommodation structure in the transition zone between the Kaoping and Chiayi Domains (Figure 2.3).

In the center of the western Taiwan orogenic belt, imbricated thrust sheets with many kilometers of accumulated slip reveal that the collision is well-established. Two sub-parallel thrust faults, the Chelungpu in the east and the Changhua in the west, are the major active components (Figure 2.10) of the Taichung Domain. These structures merge and die out near the southern edge of the domain and through a complex 20-km-wide transition zone in the north.

The 1999 rupture of the Chelungpu fault provided the critical first clue that the active Taiwan orogeny segregates naturally into discrete structural domains. The principal clue was that the fault broke along nearly the entire length of the active mountain front. Only along the ~90-km length of the 1999 rupture does the flank of the Western Foothills sport such a sharp, youthful, pre-existing thrust scarp [*Chen et al.*, 2002] (Figure 2.10). The length of this young scarp also coincides with the lengths of the Taichung piggyback basin and the tablelands to the west of the basin. The northern termination of the 1999 rupture occurred in a region where the structural and geomorphic expression of the thrust belt changes markedly [*Chen et al.*, 2000; *Lee et al.*, 2000]. North of the 1999 rupture, the tablelands dramatically change character and the Taichung foreland basin ends. All these observations indicate that there are fundamental structural differences between the portion of the Western Foothills and foreland basin adjacent to the rupture of 1999 and the regions to the north.

The other major active fault of the Taichung Domain underlies the Taichung Basin and the tablelands to the west (Figure 2.10). This fault bears several names in the literature [e.g., *Shih et al.*, 1983, 1984a, 1984b; *Shih and Yang*, 1985; *Yang*, 1986], but is

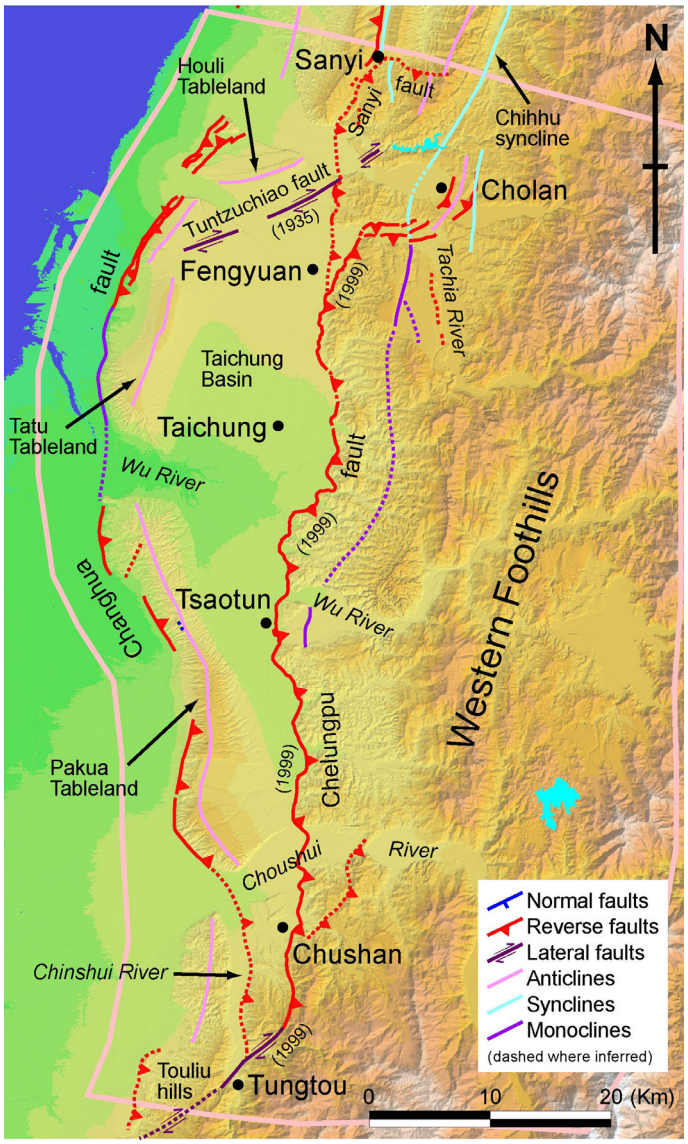

Figure 2.10. Active-tectonic map of the Taichung Domain. The Chelungpu fault ruptured along almost the entire length of the domain during the 1999 Chi-Chi earthquake. The Changhua fault is the other major structure. The Taichung Basin is a piggyback basin between these two major thrust faults.

commonly referred to as the Changhua fault.

The tablelands are the geomorphic expression of the Changhua fault (Figure 2.10). Their surfaces and underlying Quaternary deposits form an anticlinal welt separating the Taichung and coastal foreland basins. Small steep west-facing scarps along the western flank of the Houli and Tatu Tablelands suggest that the Changhua fault breaks the surface, at least locally [*Pan et al.*, 1983; *Shih et al.*, 1983, 1984a, 1984b; *Shih and Yang*, 1985;

Yang, 1986]. Despite these steep scarps, several recent seismic reflection lines suggest that the Changhua fault itself may be a fault-propagation fold that does not break cleanly to the surface [*Lee et al.*, 1997; *Shih et al.*, 2000, 2002; *Yang et al.*, 2000; *Hsu*, 2001], as was suggested by *Chen* [1978]. Nonetheless, the presence of steep scarps suggests that deformation on the western flank of the tablelands could be severe locally during ruptures of the Changhua fault.

The Changhua fault appears to represent the western limit of active deformation at the latitude of the Taichung Domain. Thus, the western limit of deformation in the Taichung Domain is substantially farther to the east than it is in the neighboring Chiayi and Miaoli Domains (Figure 2.3). Total reverse slip on the Changhua fault is merely a few hundred meters [*Chen*, 1978], far less than the many kilometers of slip on the Chelungpu fault. However, the long-term slip rate and the age of initiation of the Changhua fault are unknown currently, so that the fraction of strain across the Taichung Domain that is taken up by the Changhua fault is not known. Nor have paleoseismic studies shed any light on the recurrence characteristics of the fault.

Both ends of the 1999 rupture provide important information about the transitions of the Taichung Domain with its neighbors to the north and south. In the south, geomorphic features indicate that both the Chelungpu fault and the Changhua fault diminish in prominence south of the Choushui River and terminate in the dextral strike-slip fault mentioned earlier (Figure 2.10). The geomorphic expression of the Chelungpu and Changhua faults also diminishes in this region. The Changhua fault probably extends along scarps on the east side of the Chinshui River valley and diminishes southward along this tributary river valley and merges with the Chelungpu fault as shown in Figure 2.10 [*Ota et al.*, 2002]. This interpretation suggests an overlap in structures of the Taichung and Chiayi Domains. Structures underlying the Touliu and Chiayi hills are the northernmost expressions of the Chiayi Domain, and the dying southern strands of the Chelungpu and Changhua faults south of the Choushui River are

the southernmost expressions of the Taichung Domain. The overlap of these structures indicates that the transition between the two domains is about 20 km wide (Figure 2.3).

Complexities at the northern end of the Taichung Domain define a wide transition zone with its northern neighbor, the Miaoli Domain. The odd, E-W trending anticlinal welt and bounding thrust faults and kink bands that formed the ~10-km-long northern segment of the 1999 rupture [*Chen et al.*, 2001] form a small rabbit-ear-like anticline that cuts across regional bedding and into this syncline. Spectacular though this co-seismic welt was, it is not a large regional structure. The Chihhu syncline, across which this minor appendage of the 1999 rupture cut, is a major element of the Miaoli Domain to the north (Figures 2.10 and 2.11). This indicates that the northernmost rupture of the Chi-Chi earthquake is not really part of the Chelungpu fault; rather it is a surficial accommodation structure within the transition zone between the Taichung and Miaoli Domains.

A co-seismic fault rupture associated with a large earthquake in 1935 is also within the transition zone between these two domains. The predominantly right-lateral Tuntzuchiao fault extends southwestward across the northern edge of the Taichung Basin into the Houli and Tatu Tablelands. It cuts across the strike of the basin and tablelands at about a 45° angle, about the relationship one would expect for a strike-slip structure serving as an accommodation structure within a fold-and-thrust belt [e.g., *Yeats et al.*, 1997]. The fault separates the tablelands to the south from the broad open Tunghsiao anticline and associated folds of the Miaoli Domain to the north (Figures 2.10 and 2.11). The width of the transition zone between the Taichung and the Miaoli Domains, as measured by the distance between the southern end of the Tuntzuchiao fault and the northern end of the Sanyi fault, is about 20 km.

The active structures of the Miaoli Domain are roughly on trend but contrast sharply with those of the Taichung Domain (Figure 2.3). The active tectonic landforms on land

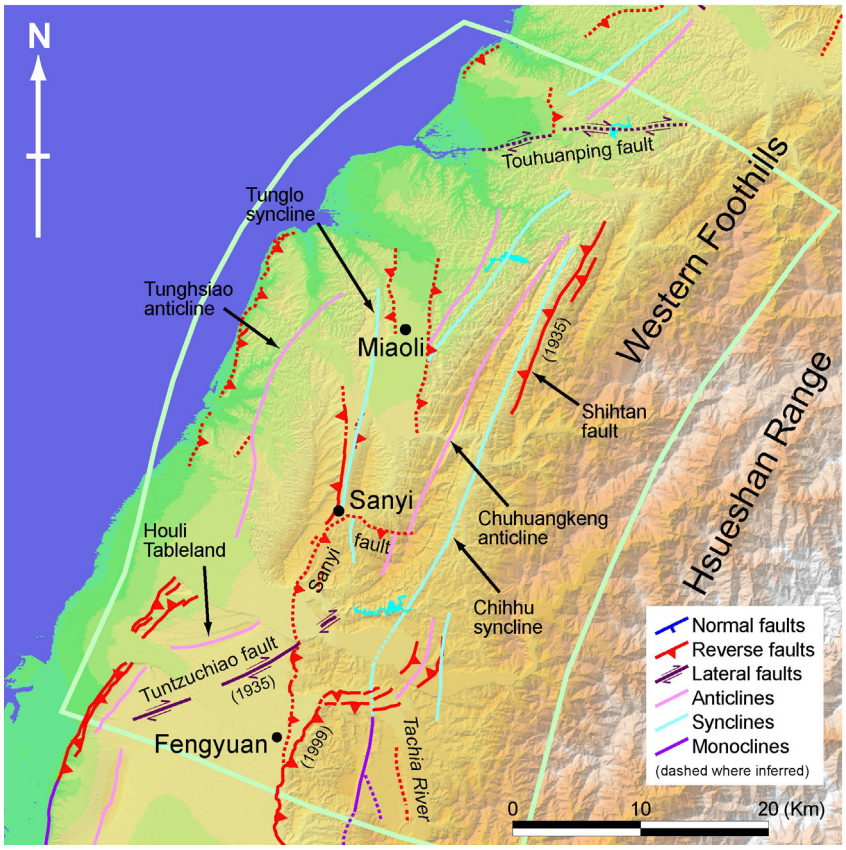

Figure 2.11. Active-tectonic map of the Miaoli Domain. Two major anticline-syncline pairs indicate that the major active thrust fault of the Miaoli Domain is blind. The Shihtan fault, which ruptured during the 1935 earthquake, is a minor bedding-plane backthrust within the eastern limb of the Chihhu syncline. The right-lateral Tuntzuchiao fault, which also ruptured during the 1935 event, is an accommodation structure between the Miaoli and Taichung Domains.

are broad coastal and narrower foothill anticline-syncline pairs (Figure 2.11). Reverse faults, including one that ruptured during an earthquake in 1935, are locally clear in the topography. The fact that active folding extends to the west coast suggests that a west-verging master thrust fault underlies the entire region between the Western Foothills and the coast. GPS geodetic measurements show that convergence across the domain is approximately N40°W at about 5 mm/yr [e.g., *Yu et al.*, 1997], similar in azimuth but far lower in magnitude than convergence across domains to the south.

The two major anticline-syncline pairs that dominate the landforms of the Miaoli Domain are along strike with the features of the Taichung Domain. The eastern pair, the Chuhuangkeng anticline and Chihhu syncline, forms the western flank of the Western

Foothills (Figure 2.11). The Shihtan fault, a bedding-plane backthrust on the steep eastern limb of the syncline, ruptured during the 1935 earthquake [*Hayasaka*, 1935; *Otuka*, 1936; *Wang et al.*, 1994]. The structural position of the Shihtan fault, on the limb of a syncline and parallel to bedding, indicates that it is not a major structure.

West of the Miaoli valley is the other pair of major folds, the Tunghsiao anticline and Tunglo syncline [e.g., *Chang*, 1974; *Chinese Petroleum Corporation*, 1994]. The geomorphic expression of this anticline is less clear than that of the Chuhuangkeng anticline because only gently dipping, less consolidated young beds are exposed in its eroded core. Tilted remnants of a lateritic terrace west of the town of Sanyi form a prominent cap to the eastern limb of this anticline [e.g., *J.-C. Chang et al.*, 1998].

In contrast to the Taichung Domain, no major thrust fault crops out on land within the Miaoli Domain. Nonetheless, the two major anticline and syncline pairs probably are the superficial manifestation of a major underlying detachment [e.g., *Elishewitz*, 1963; *Suppe and Namson*, 1979; *Namson*, 1981, 1983, 1984; *Hung and Wiltschko*, 1993]. This major detachment, if it were to crop out at the surface, would do so offshore and delimit the western edge of the Miaoli Domain. In fact, previous seismic reflection surveys have found folds offshore of the Miaoli area [*Wang*, 1967], indicating that the detachment does indeed continue beneath the offshore region.

The fact that the deformation front of the Miaoli Domain is much farther west than that of the Taichung Domain suggests a structural down-step from the Changhua and Chelungpu faults of the Taichung Domain to the décollement of the Miaoli Domain [e.g., *Chen et al.*, 2001]. This step is accommodated by many minor structures in the transition zone between the two domains.

The Hsinchu Domain contains the northernmost evidence for active crustal shortening in Taiwan. It is a transitional domain between the active shortening of the Miaoli Domain and active extension of the Taipei Domain (Figure 2.3). Its reverse and strike-slip faults bring the active deformation front of the Miaoli Domain back onto land.

N-S shortening across the domain is accommodated by two groups of reverse faults and folds. GPS measurements are not coherent across the Hsinchu Domain but do suggest that shortening rates are no more than a few mm/yr.

Two groups of active structures disrupt rocks of the foreland basin. The northern of the two groups of active structures disrupts the surfaces of the Taoyuan-Hukou Tableland as a series of ENE-WSW striking scarps and fold axes (Figure 2.12). The scarps have long been considered to be active fault or fold scarps [e.g., *Hanai*, 1930; *Ku*, 1963; *Sunlin*, 1982; *Yang*, 1986]. All of the scarps are related to two major structures, the Pingchen and Hukou anticlines [e.g., *Tang*, 1963; *Wang*, 1964]. The Hukou anticline is likely to be a fault-bend fold created by an underlying thrust ramp, and the higher scarp south of the valley is a manifestation of its forelimb. The Pingchen anticline appears to be the result of a wedge thrust, and the lower scarp north of the valley may be a fold scarp related to its forelimb [*Wang*, 2003]. A right-lateral fault zone that strikes WNW-ESE forms the southern boundary of the structures of the Taoyuan-Hukou Tableland [*Wang*, 2003]. The fact that this right-lateral fault zone heads offshore suggests that it is a tear fault between the structures of the Tableland and unidentified structures offshore.

The other group of active structures in the Hsinchu Domain is geomorphically apparent just south of the Touchien River (Figure 2.12). Scarps of the Hsincheng and Hsinchu faults and enigmatic intervening scarps cut and deform the narrow fluvial terraces south of the river. The overall trend of the fault system is E-W.

Both of the two groups of faults in the Hsinchu Domain accommodate shortening in a direction that is nearly N-S. NNE-SSW striking thrust faults dominate the domain, but right-lateral faults intersect these at angles of about 45° [e.g., *Yang et al.*, 1996, 1997]. The direction of shortening across these faults is NNW, nearly 80° clockwise from the direction of shortening across the Miaoli Domain.

This kinematic interpretation is consistent with the Hsinchu Domain being the

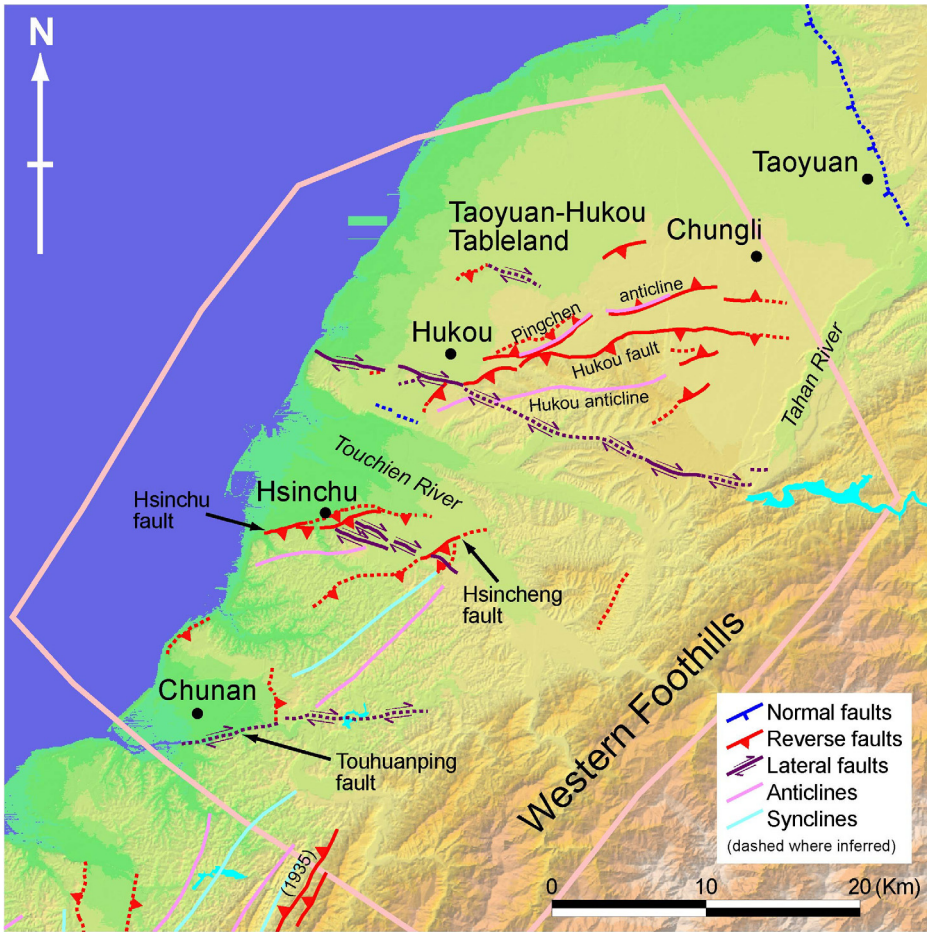

Figure 2.12. Active-tectonic map of the Hsinchu Domain. Two groups of active structures comprise this domain. On the Taoyuan-Hukou Tableland is a complex of reverse faults, folds, and a discontinuous right-lateral fault. South of the Touchien River is a group of active reverse and right-lateral strike-slip faults.

northernmost region of shortening in Taiwan. To the south, the Miaoli Domain continues to suffer WNW-ESE shortening as a result of the collision of the forearc sliver of the Central Range and the South China continental shelf. To the north, the Taipei Domain is experiencing post-collisional collapse in the region of back-arc extension above the Wadati-Benioff zone of the Ryukyu subduction system [*Teng*, 1996; *Teng et al.*, 2000] (Figure 2.3). The neutral plane separating these two regimes is immediately north of the Hsinchu Domain. In this context it is reasonable to conclude that the structures of the Hsinchu Domain are merely the northern end of the structures associated with the major detachment of the Miaoli Domain, as suggested by *Biq* [1992]. However,

bathymetric data offshore Hsinchu and Miaoli are insufficient to test this hypothesis [e.g., *Pan and Hu*, 1972].

Within the Taipei Domain, formerly active thrust faults are being buried by young fluvial, marine, and volcanic sediments and locally obliterated by the construction of a volcanic edifice. NW-SE extension across the domain is concentrated on one principal normal fault, across which the long-term rate of extension appears to be at least 1 mm/yr (Figure 2.13). Motion across this structure, the Shanchiao fault, has been producing the Taipei Basin half-graben for the past few hundred thousand years. Seismic slip on the fault may have produced a marine incursion into the Taipei Basin in 1694. Decadal rates of extension across the domain are poorly constrained by GPS measurements [*Yu et al.*, 1997], but the magnitude of extension could be consistent with the long-term rate of extension across the Shanchiao fault.

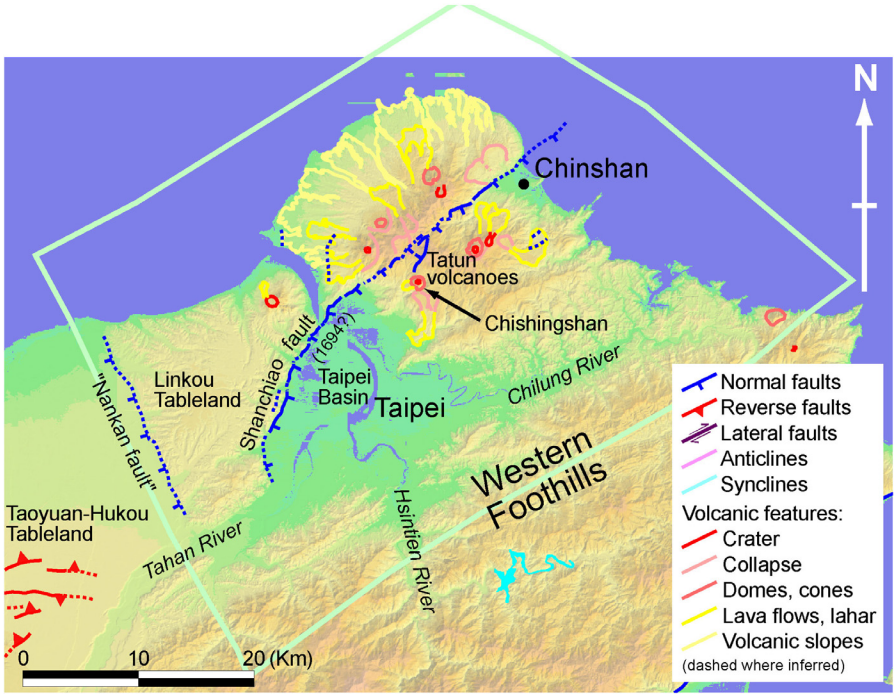

Figure 2.13. Active-tectonic map of the Taipei Domain. The Taipei Basin is a half-graben, formed by slip in the late Quaternary Period on the Shanchiao normal fault. The fault also extends northeastward and offsets the edifice of the Tatun volcanic edifice. The sudden appearance of a lake in the Taipei Basin in 1694 may have resulted from a large rupture of the Shanchiao fault.

The major active structure of the Taipei Domain is the Shanchiao fault, which separates the Taipei Basin and the Linkou Tableland (Figure 2.13). The observation of numerous triangular facets along the eastern foothills of the Linkou Tableland led to the discovery of the fault many decades ago [*Tan*, 1939; *Lin*, 1957]. In general, the surface trace of the Shanchiao fault lies slightly east of the inactive Hsinchuang fault [*Sun*, 1990], a thrust fault that probably represents the deformation front of northern Taiwan in the early Quaternary Period [*Ho*, 1988; *Wang-Lee et al.*, 1978; *Teng et al.*, 2001]. The parallel traces of the two faults suggest that the steeper normal fault and shallower thrust fault merge at depth and that the younger Shanchiao fault has reoccupied the older fault plane [e.g., *Wu*, 1965; *Hsieh et al.*, 1992]. The reoccupation by the Shanchiao fault of the Hsinchuang fault in the late Quaternary Period demonstrates that the Taipei Domain has changed recently from a regime of shortening to one of extension. This is consistent with the movement of the domain out of the influence of the Manila subduction system to that of the Ryukyu subduction system [e.g., *Suppe*, 1984, 1987; *Teng*, 1996; *Teng et al.*, 2000].

The Tatun volcanic edifice is clearly bisected by the northern extension of the Shanchiao fault (Figure 2.13). On the uplifted block, northwest of the fault, the semi-circular perimeter of about half the edifice is preserved. Southeast of the fault, the narrower width of the volcanic construct may well be due to burial of the flanks by sediments of the Taipei Basin. In detail, the scarp across the volcano is not as clear as it is between the Taipei Basin and Linkou Tableland. Nonetheless the overall trajectory of the fault zone over the volcano is clear, and numerous small scarps and other linear features form a clear fault zone.

History records a very interesting occurrence that is quite relevant to understanding the relevance of the Shanchiao fault to seismic hazard assessment. In 1694, historical documents indicate an abrupt subsidence in the Taipei region and the formation of a brackish-water lake that inundated at least a third of the basin [*Shieh*, 2000]. The lake

was deep enough to permit large ships to sail far into the basin. The formation of the lake is most easily explained by several meters of slip on the Shanchiao fault, since such a rupture would result in subsidence of a large portion of the Taipei Basin.

The Okinawa Trough is the back-arc basin of the Ryukyu subduction system (Figure 2.1). Its progressive westward propagation is splitting the country's mountainous backbone along the western suture, now occupied by the Lanyang Plain (Figure 2.14). This large, triangular basin reflects the current foundering of the western tip of the westward propagating Okinawa back-arc trough. On the northwestern flank of the Lanyang Plain is the Hsueshan Range, and on the southern flank of the plain is the northern tip of the Central Range. Two observations suggest that these flanking ranges are sinking as well. First, their crests are appreciably lower than range crests farther south. Second, their flanks are being buried by alluvium on the east coast and in the Taipei Basin.

If *Suppe*'s [1987] calculation is correct that the western edge of Ryukyu subduction is migrating southwestward at about 100 mm/yr, then one would anticipate that none of the extensional features nor the sinking of the onshore part of the Ilan Domain would be older than about 0.5 myr. This is supported by stratigraphic evidence that post-collisional collapse of northeastern Taiwan has occurred in just the past million years [*Teng*, 1996; *Teng et al.*, 2000].

Two systems of geomorphically expressed normal faults are apparent in the onland portion of the Ilan Domain. They bound the Lanyang Plain on the northwest and on the south. Normal faulting along the northwestern flank of the Lanyang Plain is complex. Instead of possessing the simple morphology of a simple normal fault, the Hsueshan Range front displays a complex family of triangular facets that step up slope from the base of the range [*C.-T. Lee et al.*, 1998] (Figure 2.14). The southern edge of the Lanyang Plain also appears to be controlled by normal faulting. The seaward extension of these two normal fault systems is not very clear, and the lack of high-resolution

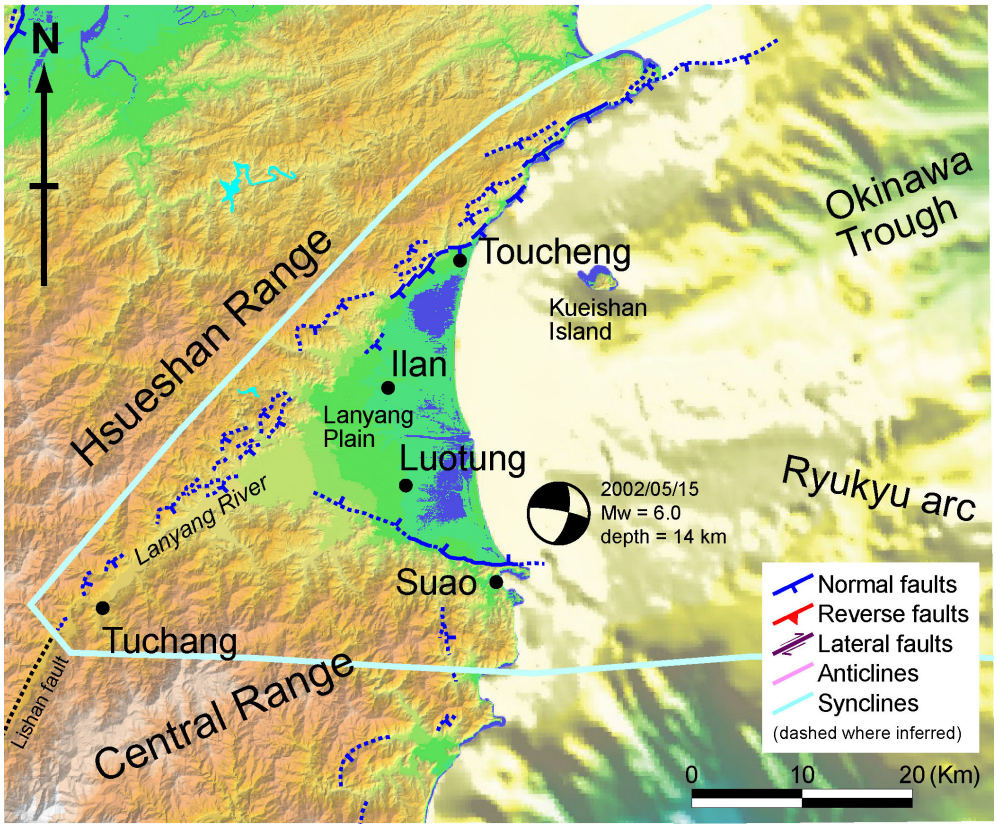

Figure 2.14. Active-tectonic map of the onland part of the Ilan Domain. Two major bounding normal faults facilitate the incipient opening of the Okinawa Trough across the Lanyang Plain. Other faults within the domain are poorly known because of rapid sedimentation rate and lack of high-resolution bathymetry. Focal mechanism and other parameters of the 15 May 2002 earthquake adapted from the BATS database.

bathymetry near the coast prohibits resolution of the issue. However, a submarine scarp along the northeastern extension of the northern normal fault system suggests that the northern structure continues for at least another 15 km. The presence of a submarine canyon just offshore Suao, on the other hand, indicates that the southern structure may not extend very far seaward.

The normal faults that bound the Lanyang Plain are generally considered to be the southwestward extension of normal faults bounding the Okinawa Trough. Bathymetry of the Okinawa Trough indicates that the most active opening area in the recent 2 myr is its southern part [*Hsu et al.*, 1996; *Wang et al.*, 1998], adjacent to the Lanyang Plain.

The Lishan fault, which runs along the Lanyang River valley, upstream from the

Lanyang Plain, is not likely to be an active structure despite its linear course. This fault is a major bedrock structure in Taiwan [e.g. *Ho*, 1986, 1988; *Yang*, 1986] (Figure 2.3), and it has a complicated structural history. Geomorphic evidence, however, indicates that the fault is not likely to be active.

2.5 Discussion and earthquake scenarios

A principal motive for our investigation of the active tectonics of Taiwan has been to develop a synoptic view of the island's earthquake potential. What we have found is that the island is divisible into eleven discrete active tectonic domains and that a unique suite of active structures defines each domain. The above descriptions of these active structures provide a basis for developing simple, preliminary characterizations of the predominant seismic sources for each of the eleven domains.

There are many other questions that our investigation of the island's active tectonics has raised, but digging deeply into these issues is outside the scope of this already lengthy paper. Some of the unresolved questions are: How will the Taiwan orogeny evolve over the next million or so years? Is it, for example, a valid hypothesis that latitude in Taiwan is a surrogate for maturity of the orogen? If so, we can speculate that progressively more southern parts of the outer-arc ridge and volcanic arc of the Philippine Sea plate will continue to dock with the continental margin in the south while the forearc and arc disengage from the continental margin in the north.

Figure 2.3 shows that the Central Range is not included in any of the domains. Why is there no separate Central Range Domain? Because we have found no clear geomorphic evidence for active faulting through the high mountains. Many of the active structures of the domains dip toward the Central Range, but we estimate that these structures pass through the brittle-ductile transition where we have drawn the mountain-ward edge of each domain. This may be at odds, however, with recent work

that shows minor seismicity continuing well below what we have assumed to be the brittle-ductile transition [e.g., *Wu et al.*, 1997; *Rau and Wu*, 1998; *Kao and Chen*, 2000; *Carena et al.*, 2002]. Farther into and beneath the mountains we assume any major structures behave aseismically. We have not resolved whether these extend through the brittle-ductile transition or if strain beneath the high mountains occurs by penetrative deformation. We suspect that, however, it is the pervasive ductile crustal thickening that produces the rapid uplift of the Central Range. Any deeper ductile detachment(s) must interact somehow with the presumably steep contact that separates the lithosphere of the continental shelf (i.e., Western Foothills and Hsueshan Range) and that of the forearc ridge (i.e., Central Range).

Why is the active architecture of Taiwan divisible into discrete domains? One possibility is that the geometry of currently active structures is controlled by pre-existing faults. It is well known that some of the currently active structures have re-occupied older structures. For example, the Shanchiao fault, the principal active fault of the Taipei Domain, occupies much of the plane of the inactive Hsinchuang thrust fault. Many inactivated normal faults of the continental margin are now also partially reactivated by active thrust faults of the Hsinchu and Taichung Domains. Perhaps the lengths of the currently active faults are influenced by the lengths of these older faults. Another plausible reason for the discreteness of the domains may have to do with the efficiency of breaking crustal rocks. The fact that fault planes re-rupture is an indication that less energy is expended by the re-rupture of a favorably oriented pre-existing fault plane than by fresh rupture of unfaulted rock. This should be true even in an evolving orogen, in which a pre-existing fault will re-rupture until creation of a new fault becomes more efficient energetically. The discreteness of the faults and their transition zones may be a reflection of this basic principle. It may be only at rare critical junctures in the history of a fault that the fault becomes inactive and that new structures are born.

The transition zone between the Taichung and Miaoli Domains provides a possible

example of this. The 1999 mountain-front rupture from about Fengyuan northward lies farther east than an older trace of the Chelungpu fault (Figure 2.10). The anticlinal welt that ruptured eastward in 1999 from the younger trace of the Chelungpu into the Tachia River also appears to represent a very young feature, perhaps with only a few earlier paleoseismic events. The hook-like map pattern of the new branch of the Chelungpu fault and the anticlinal welt is geometrically very similar to the hook-like pattern of the old Chelungpu and Sanyi faults about 10 km farther north (Figure 2.10). The old hook may well represent a recently abandoned, more northern end of the Chelungpu fault zone. If so, the northern end of the fault zone has jumped recently about 10 km southward from the northern hook to the southern one. Resolution of this question about the discreteness of the domains will come only with more detailed geochronologic, stratigraphic, and geomorphic work.

What seismic events can Taiwan expect in the next century or two? To begin to answer this question, we must know the geometries and slip characteristics of the active faults in each domain. These characteristics are not known well or uniformly for all the domains. Nonetheless, we can estimate major source shapes and locations well enough to give a preliminary notion of the major earthquakes that should be expected. This will be the main focus of the discussion below.

Seismic moment (M_o) is a parameter that we can estimate from structural data:

$$Mo = \mu WLD, \tag{2.1}$$

where μ is the shear modulus, commonly about 3×10^{11} dyne/cm^2 in the crust; W is the down-dip width of the rupture; L is the along-strike length of the rupture; and D is the average slip across the rupture plane. Furthermore, these structural parameters are directly related via seismic moment to earthquake moment magnitude (M_w), by another formula:

$$M_w = 2/3 \text{ Log } M_o - 10.73. \tag{2.2}$$

Furthermore, moment magnitude has the following relationship to rupture area (A,

in km^2) based upon published regression results [e.g., *Wells and Coppersmith*, 1994]:

$$M_w = 3.98 + 1.02 \times \log A \text{ for strike-slip faults,} \quad (2.3)$$

$$M_w = 3.93 + 1.02 \times \log A \text{ for normal faults, and,} \quad (2.4)$$

$$M_w = 4.33 + 0.90 \times \log A \text{ for reverse faults.} \quad (2.5)$$

Since rupture area equals rupture length (L) times down-dip rupture width (W), we can estimate the magnitudes of future earthquakes in Taiwan's eleven domains from the data we have presented in this paper and figure out a reasonable average slip in a typical earthquake event for a given structure.

In each domain we have identified the surface manifestations of the one or more predominant structures. Thus we can estimate the length of future seismic ruptures. This presumes, of course, that like the 1999 Chelungpu rupture, the entire length of the fault is involved, and the rupture does not spill over significantly onto other faults. Since this is not always the case, our estimates of magnitude using the entire length (L) of a fault will be maximum values for individual faults. We would have overestimated, for example, the size of the earthquakes in the Longitudinal Valley in 1951, since only portions of the fault broke during those events. On the other hand, since ruptures sometimes break across structural complexities [e.g., *Matsuda*, 1974; *Sieh et al.*, 1993; *Eberhart-Phillips et al.*, 2003], using just the length of one major fault can significantly underestimate the magnitude of complex earthquakes. With these caveats in mind, however, we use fault length for rupture length in the calculations below because it provides a simple starting point for future discussions.

Our estimates of down-dip width derive from estimates of the dips of the faults and the depth of the brittle-ductile transition. For the depth of the brittle-ductile transition, we would use the depth of greatest upper-crustal seismicity, if it were not for the fact that in Taiwan this presents a confusing picture. Numerous deep crustal earthquakes beneath the island, especially in its eastern part, have in fact inspired *Wu et al.* [1997] to propose that the Taiwan orogeny results from lithospheric collision as distinct from thin-skinned

tectonics. Therefore, in most cases, we make the simple assumption that the brittle-ductile transition beneath the island is everywhere at a depth of 15 km. The brittle-plastic transition of quartz occurs at approximately 300°C [e.g., *Kerrich et al.*, 1977; *Tullis and Yund*, 1977] and that of feldspar occurs at approximately 500°C [e.g., *White*, 1975; *Tullis and Yund*, 1977]. The average geothermal gradient of Taiwan is approximately 30°C/km [e.g., *Huang*, 1990]. Given the fact that most of the rocks in the upper crust of Taiwan are quartz-rich sedimentary rocks, a 15 km brittle-ductile transition is therefore a reasonable and conservative estimation. In fact, few earthquakes occur at a depth greater than 15 km in western Taiwan [e.g., *Carena et al.*, 2002].

Certainly, this estimate is only a first-cut attempt and we have ignored many possible variations in seismogenic depth [e.g., *Scholz*, 2002; *Nazareth and Hauksson*, 2004]. In a few cases we use better information. For example, for the Chelungpu fault, model inversions of co-seismic geodetic displacements and seismograms provide excellent constraints on the depth of the co-seismic rupture plane.

For fault dips we use published structural analyses, where available and credible. Elsewhere we use conventional dips of 30°, 60°, and 90° for thrust, normal, and strike-slip faults, respectively, with steeper dips for thrust faults if there is a component of slip along strike. Figure 2.15 displays these interpretations, drawn from a variety of sources. Several are from published sources, but others are our own sketches.

Figure 2.16 is a map of the major seismic structures that we propose. Table 2.1 accompanies this graphical representation of the same data. It includes the values of length (L), width (W), average slip (D), as well as other parameters that we have used in estimating the magnitude of earthquake associated with each source. On the map each source appears as a polygon, with surface traces solid and the surface projections of subsurface edges dashed. For most of the domains, the dashed lines closest to the Central Range represent our estimate of the down-dip limit of seismic rupture, based

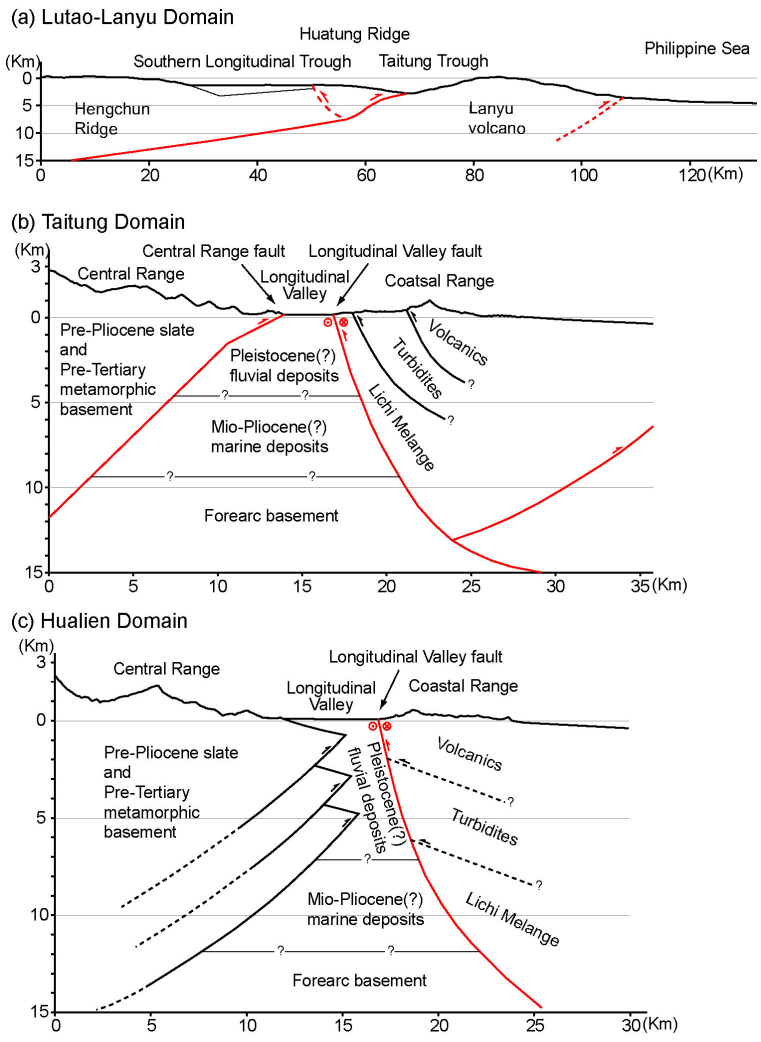

Figure 2.15. Simple cross sections proposed for each of the eleven tectonic domains. Each crude, unbalanced cross section provides tentative geometries of the major active faults, based upon geomorphic, geodetic, structural, and seismic data. Red: active structures; black: inactive structures.

upon a 15-km depth for the brittle-ductile transition.

The Lutao-Lanyu Domain is dominated by a major fault that crops out along the eastern base of the Huatung Ridge (Figure 2.16). Based upon published seismic reflection and topographic data, we believe that the Huatung Ridge thrust crops out south of about 22°20'N but may be blind farther north. We assume a dip of about 30° west for the fault [e.g., *Lundberg et al.*, 1997; *Chang et al.*, 2001; *Malavieille et al.*, 2002]. The resulting moment magnitudes (M_w) would be about 7.6 for the fault (Figure 2.16). Average slip across the fault would be about 2.4 m based upon the seismic moment that

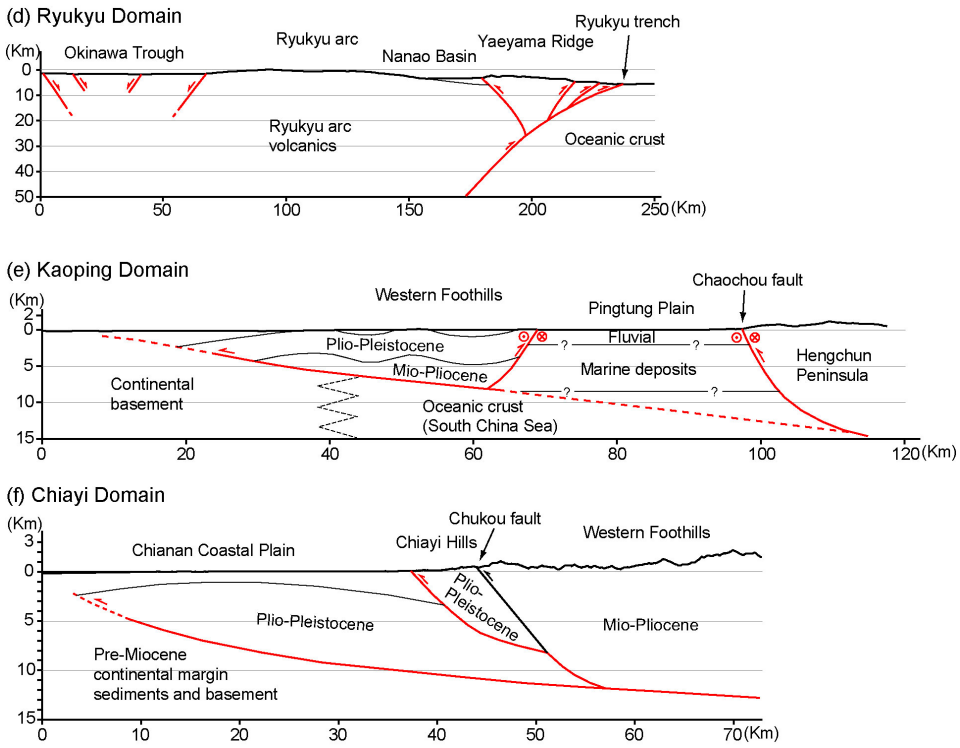

Figure 2.15. (continued)

we have calculated.

The east-dipping fault that we propose beneath the island of Lutao appears to be significantly shorter, perhaps only 40 km long. The length and width of this fault suggest a maximum magnitude of 7.0. The lesser thrust fault that dips southeast beneath the southern part of the Huatung Ridge at about 22°N (Figure 2.4) is only about 30 km long, so the largest magnitude we would expect from it is in the high 6s.

The Taitung Domain has two and probably three principal seismic sources (Figure 2.16). The clearest is the steeply east-dipping Longitudinal Valley fault, which has significant components of both thrust and left-lateral strike-slip motion. If the entire length of the fault in the Longitudinal Valley were to rupture in a single event, the magnitude could well be 7.4 (Table 2.1). We have also argued for activity of the west-dipping Central Range fault within the Taitung Domain, but we have no reliable estimate of its dip. Its 80-km length and an assumed dip of 45° yields a maximum

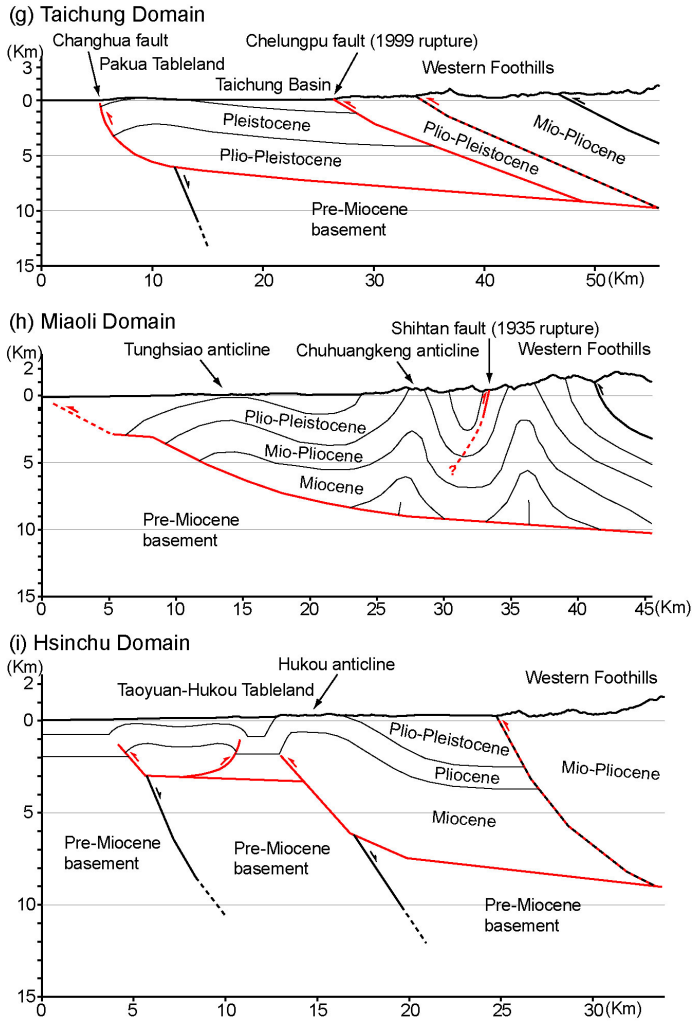

Figure 2.15. (continued)

magnitude of 7.2. Evidence for activity of the west-dipping thrust fault that appears to daylight 20 km offshore is sparser still. If this is indeed an active, 120-km long structure, we would predict a maximum magnitude of about 7.4. Of these three, only the Longitudinal Valley fault has ruptured historically: in the M7.0 and M6.2 earthquakes of 1951 [*Shyu et al.*, 2005b] and during smaller events in 1995 and 2003 [*Chen and Rau*, 2002; *R.-J. Rau*, unpublished data]. Creep at rapid rates is well known along parts of this fault, but geodetic measurements are too sparse to allow determination of the full extent of the creep, either along strike or down dip. Furthermore, the temporal stability of the current pattern of creep is unknown. More work will be necessary to better define

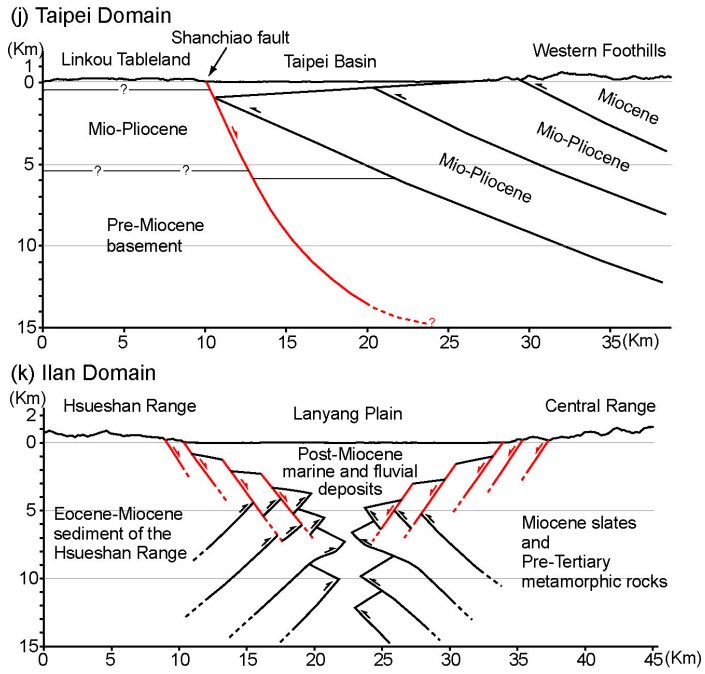

Figure 2.15. (continued)

the extent to which creep of the fault reduces the threat of seismic rupture.

Within the Hualien Domain, the Longitudinal Valley fault appears to be the only active structure. Earthquakes produced by this fault in 1951 were magnitude 7.3 and 7.1, and the surface rupture involved only approximately 6% of the total subaerial extent of the fault. The length of the fault within the Hualien Domain yields a hypothetical largest event of M_w 7.2.

The Ryukyu Domain encompasses the seismic Ryukyu subduction zone, the largest seismogenic source of Taiwan. The seismic portion of the subduction interface in the westernmost part of the Ryukyu trench is limited approximately to that portion above a depth of about 35 km [*Kao et al.*, 1998]. Thus, only that ~50-km wide strip between the trench and the Ryukyu Islands is likely to generate great subduction earthquakes. The eastern limit of the interface is hard to specify. At about 123°E, however, the Gagua Ridge collides with the Ryukyu trench and creates a major geometric irregularity in the Ryukyu subduction interface [e.g., *Sibuet and Hsu*, 1997; *Schnürle et al.*, 1998] (Figure 2.1a). The dip angle of the Wadati-Benioff zone changes dramatically across the

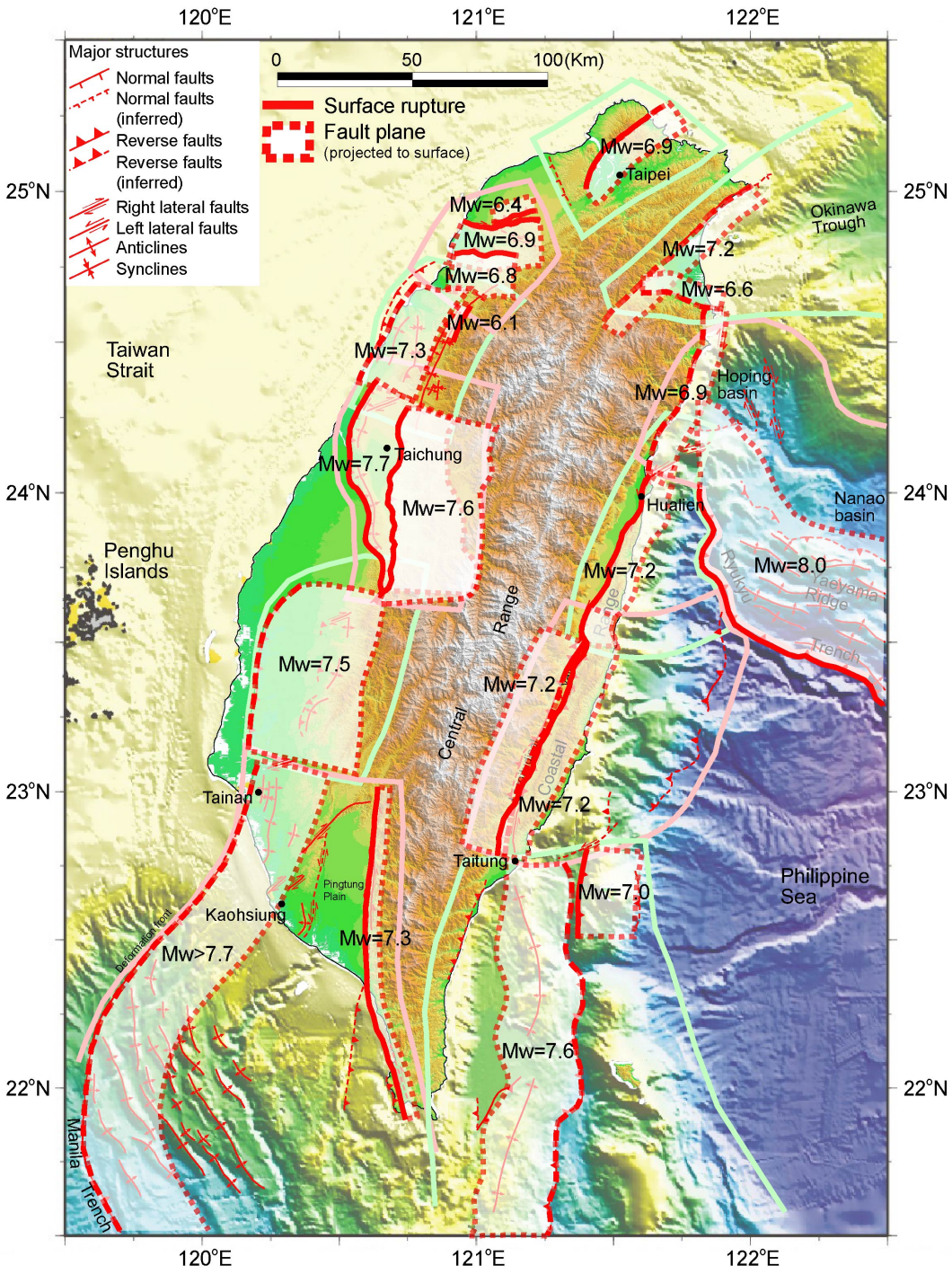

Figure 2.16. Proposed major sources for future large earthquakes in and around Taiwan. Bold red lines are proposed future ruptures, and the white patches are rupture planes projected to the surface. Here we have selected only a few representative scenarios from Table 2.1 to show in this figure. Earthquake magnitude of each scenario is predicted value from our calculation.

longitude of the Gagua Ridge, from 65° on the west to 50° on the east [e.g., *Deschamps*

et al., 2000]. We assume that this geometric break about 150 km east of Taiwan's east coast is a barrier to rupture propagation. This leads to calculation of a magnitude 8.0 as the largest plausible event on the subduction interface near Taiwan. Two large events with magnitudes greater than 8.0 in 1910 and 1920 [*Hsu*, 1980; *Cheng and Yeh*, 1989] most plausibly originated on this strip of the subduction interface.

The normal fault system along the coast between the Longitudinal Valley and the Lanyang Plain is about 50 km long. We therefore calculate a maximum magnitude of 6.9 and an average slip of about 1.2 m for this zone (Table 2.1 and Figure 2.16).

In the Kaoping Domain three active structures appear to dominate (Figures 2.15 and 2.16). One of these is the Chaochou fault zone. As discussed previously, this fault may extend southeastward to connect with the strike-slip Hengchun fault. Alternatively, it may also extend southward along a submarine canyon to about the latitude of the southern tip of Taiwan (Figure 2.8). In either scenario, this possibly high-angle fault has a total length of about 120 km and is capable of producing an earthquake of about M_w 7.3 (Table 2.1). Rupture of only the onland portion of the Chaochou fault could also produce a M_w 7.2 earthquake. Another major structure in the Kaoping Domain is the strike-slip fault along the western margin of the Pingtung Plain. Its length yields a maximum magnitude of 6.9. The other structure is the deformation front, which is likely to be a reverse fault that runs all the way to the Manila trench in the south. Between the latitudes of Tainan and Kaohsiung there is no topographic evidence for the existence of this reverse fault. To the south, however, numerous folds and minor faults on the seafloor are likely to be the result of irregularities in the underlying deformation front and secondary structures above it. This huge reverse fault system has a length of at least 200 km in Figure 2.3 and might produce an earthquake event of at least M_w 7.7.

We have discussed four main constraints on the nature of the principal active structures in the Chiayi Domain: the young deformation of the coastal plain and the Chiayi Hills, abundant small to moderate earthquakes between the coast and the Western

Table 2.1. Proposed major seismic structures of Taiwan. In this table we include rupture length (L), width (W), and average slip (D), as well as other perimeters used in estimating the magnitude of earthquakes associated with each source. Note: not to be used for site specific studies.

Fault name	Fault type*	L (km)	Fault dip (degree)	Down-dip limit (km)	W (km)**	A (km2)#	M_w##	M_o (1025 dyne-cm)+	D (m)++
Lutao-Lanyu Domain									
Huatung Ridge fault	R	140	30	15	30.00	4200.00	7.59	302.96	2.40
SW Taitung fault	R	40	45	15	21.21	848.53	6.97	34.97	1.37
West Lutao fault	R	40	45	15	21.21	848.53	6.97	34.97	1.37
West Huatung Ridge fault	R	30	45	15	21.21	636.40	6.85	23.72	1.24
Taitung Domain									
Longitudinal Valley fault, total	R/SS	160	60	15	17.32	2771.28	7.43	172.83	2.08
Longitudinal Valley fault, Taitung Domain only	R/SS	96	60	15	17.32	1662.77	7.23	86.72	1.74
Central Range fault, total	R	80	45	15	21.21	1697.06	7.24	89.14	1.75
Central Range fault, emerged part only	R	40	45	15	21.21	848.53	6.97	34.97	1.37
Taitung offshore fault	R	120	45	15	21.21	2545.58	7.40	154.10	2.02
Hualien Domain									
Longitudinal Valley fault, Hualien Domain only	SS	90	60	15	17.32	1558.85	7.24	89.12	1.91
Ryukyu Domain									
Ryukyu trench	R	~180	30	35	70.00	12600.00	8.02	1335.06	3.53
The major right-lateral accommodation structure	SS	50	90	15	15.00	750.00	6.91	29.10	1.29
Nanao normal fault system	N	50	60	15	17.32	866.03	6.93	30.51	1.17
Kaoping Domain									
Chaochou fault connecting Hengchun fault	SS/R	120	75	15	15.53	1863.50	7.32	117.11	2.09
Chaochou fault connecting the offshore fault	R/SS	120	75	15	15.53	1863.50	7.27	101.15	1.81
Onland Chaochou fault only	SS/R	75	75	15	15.53	1164.69	7.11	57.06	1.63

West Pingtung Plain fault (Kaoping River fault)	SS	50	90	15	15.00	750.00	6.91	29.10	1.29
The deformation front	R	>200	30	15	30.00	>6000.00	>7.73	>490.34	>2.72
Chiayi Domain									
Main detachment	R	60	15	15	57.96	3477.33	7.52	234.79	2.25
Meishan fault	SS	15	90	15	15.00	225.00	6.38	4.61	0.68
Hsinhua fault	SS	12	90	15	15.00	180.00	6.28	3.28	0.61
Taichung Domain									
Chelungpu fault	R	90	15	12	46.36	4172.80	7.59	300.32	2.40
Changhua fault	R	85	10	12	69.11	5874.35	7.72	476.54	2.70
Miaoli Domain									
Shihtan fault	R	20	75	5	5.18	103.53	6.14	2.04	0.66
Tuntzuchiao fault	SS	20	90	12	12.00	240.00	6.41	5.09	0.71
Shihtan and Tuntzuchiao faults[$]	Complex	--	--	--	--	343.53	6.51	7.13	0.69
Main detachment, only in Miaoli Domain	R	60	30	15	30.00	1800.00	7.26	96.52	1.79
Main detachment, extended to Hsinchu Domain	R	110	30	15	30.00	3300.00	7.50	218.77	2.21
Touhuanping fault	SS	25	90	15	15.00	375.00	6.61	10.08	0.90
Hsinchu Domain									
The northern fault on the Taoyuan-Hukou Tableland	R	20	30	5	10.00	200.00	6.40	4.97	0.83
The southern fault on the tableland (Hukou fault)	R	25	30	15	30.00	750.00	6.92	29.60	1.32
The major strike-slip fault on the tableland	SS	30	90	15	15.00	450.00	6.69	13.32	0.99
Fault system on the tableland, total[$]	Complex	--	--	--	--	1400.00	7.06	47.89	1.14
Hsinchu fault	R	12	45	15	21.21	254.56	6.50	6.88	0.90
Hsincheng fault	R	10	30	15	30.00	300.00	6.56	8.59	0.95
Other accommodation structures	SS	10	90	15	15.00	150.00	6.20	2.48	0.55
The southern system total[$]	Complex	--	--	--	--	704.56	6.77	17.96	0.85

Ilan Domain									
The northern Ilan fault system	N	90	60	15	17.32	1558.85	7.19	74.99	1.60
The southern Ilan fault system	N	25	60	15	17.32	433.01	6.62	10.56	0.81
Taipei Domain									
Shanchiao fault, only in the west of Taipei Basin	N	20	60	15	17.32	346.41	6.52	7.51	0.72
Shanchiao fault, extended to Chinshan	N	45	60	15	17.32	779.42	6.88	25.97	1.11

*R: reverse fault; SS: strike-slip fault; N: normal fault.
**W equals to down-dip limit divided by the sine value of fault dip.
#A equals to L times W.
##The moment magnitudes were calculated using the following equations: for reverse faults, $M_w = 4.33 + 0.90 \times \log A$; for strike-slip faults, $M_w = 3.98 + 1.02 \times \log A$; for normal faults, $M_w = 3.93 + 1.02 \times \log A$ [*Wells and Coppersmith*, 1994].
+The seismic moments were calculated using the following equation: $M_w = 2/3 \text{ Log } M_o - 10.73$.
++The average displacement per event was calculated using the equation $M_o = \mu AD$, where μ equals 3×10^{11} dyne/cm^2.
$For complex events resulted from ruptures of multiple faults, the calculations are as followed: first, calculate the seismic moment by adding up the moments of each fault; second, calculate the moment magnitude using the seismic moment calculated above; then, calculate the average displacement using the seismic moment and the sum of the rupture areas.

Foothills, structural interpretations based upon well data and surface outcrops, and interpretations of geodetic data. Several secondary features, such as the Hsiaomei anticline and the minor thrust faults in the Chiayi Hills, the duplexes and backthrusts of structural models, and the source faults of the 1906, 1946, 1999, and other earthquakes complicate the neotectonic picture. The historical fault ruptures demonstrate that many secondary structures exist within the domain and that some are capable of producing earthquakes in the upper 6s. The 1906 and 1946 events represent earthquakes produced by faults in the transition zones with neighboring domains. The M6.4 earthquake in October 1999 may represent events within crystalline bedrock of the continental shelf, well below the principal detachment that *Suppe* [1976, 1980b] proposed to exist within the Neogene shelf strata.

Having acknowledged these complications, let us focus here on the potential for

rupture of the principal structure within the Chiayi Domain. If we adopt the interpretations of *Hsu et al.* [2003] regarding the large horizontal gradient in GPS vectors, we can plot a rapidly creeping detachment approximately as shown on Figure 2.15. In their model, the creeping detachment dips about 15° eastward and extends up-dip as far as the eastern edge of our definition of the Chiayi Domain. A reasonable initial interpretation would be that a locked detachment extends westward from this edge to a position beneath the western edge of deformation, near the coast. This is our basis for proposing the source depicted beneath the Chiayi Domain in Figures 2.15 and 2.16. Judging from its width and length, the size of the resultant earthquake would be about M_w 7.5, with an average slip of approximately 2.3 m (Table 2.1). A M6.5 earthquake in 1930 and a M7.2 earthquake in 1941 [*Hsu*, 1980; *Cheng and Yeh*, 1989] could have been produced by partial rupture of this structure, although rupture of two secondary structures within the domain could also have produced these earthquakes.

The Chelungpu and the Changhua faults are the two major seismogenic structures of the Taichung Domain (Figures 2.15 and 2.16). Rupture of the entire Chelungpu fault and the accommodation structure on its north end in 1999 resulted in the M_w 7.6 Chi-Chi earthquake. The Changhua fault has a length similar to that of the Chelungpu, but the dip of the fault may be shallower than the Chelungpu fault in its deeper part (Figure 2.15). This suggests that rupture of the entire Changhua fault could produce an earthquake of even greater magnitude than the Chi-Chi event (Table 2.1).

As we have seen, the major active fault or faults of the Miaoli Domain are not as well defined as those in the Taichung Domain. The largest historical earthquake produced within the domain was the M7.1 event of 1935. Two disparate surface ruptures are associated with this earthquake – a right-lateral accommodation structure and a bedding-plane fault on the eastern limb of a tightly folded syncline. No modern inversion of the seismograms of this earthquake has been attempted, so we do not know if these two ruptures were accompanied by rupture of the underlying detachment.

However, the size of the earthquake indicates it might have involved rupture of more than just the two known secondary structures (Table 2.1).

The active folds and faults of the Miaoli Domain are probably subordinate to a major active detachment that underlies the domain (Figures 2.15 and 2.16). In calculating the length of the detachment, we assume that it extends southward beneath the transition zone with the Taichung Domain. We do not know whether or not to include the faults of the Hsinchu Domain, since these could be the northern wrap-around of the Miaoli Domain. If we terminate the detachment at the border with the Hsinchu Domain, we calculate a maximum magnitude of 7.3 for earthquakes produced by the detachment (Table 2.1). If, however, we extend the detachment through the entire the Hsinchu Domain, we derive a maximum magnitude of 7.5. By comparison, separate rupture of the Shihtan backthrust yields only a M_w 6.1 earthquake (Figure 2.16).

The Touhuanping fault in the transition zone between the Hsinchu and Miaoli Domains is a major strike-slip fault with a length up to 25 km. Rupture of this major accommodation structure is capable of producing an earthquake with a maximum magnitude of 6.6 (Table 2.1).

The Hsinchu Domain encompasses the densely populated regions of Hsinchu and Taoyuan. The principal emergent seismic sources include those of the Taoyuan-Hukou Tableland and of the Hsinchu-Hsincheng system (Figure 2.16). If they were to rupture together, the thrust faults and right-lateral faults of the Taoyuan-Hukou Tableland are large enough to produce a complex earthquake of about M_w 7.1 (Table 2.1). Separate failure of the largest of these structures, the Hukou fault, would produce about a M_w 6.9 event. Similarly, if all the thrust and strike-slip faults of the Hsinchu-Hsincheng system failed in unison, an earthquake of about M_w 6.8 would result. But if just the Hsinchu or Hsincheng fault failed separately, events of about M_w 6.5 and 6.6 would result.

The two major active structures in the Ilan Domain, the normal fault zones along the northwestern and southern flanks of the Lanyang Plain, are the bounding structures of the

disengagement of the continental and forearc lithospheres of the Hsueshan and Central Ranges. These structures have onland lengths of 75 and 25 km, but it is not clear how far seaward they extend. The northern structure may extend at least 15 km offshore, and the southern one is likely to end near the coastline. The resultant lengths for these two normal fault systems then yield maximum magnitudes of 7.2 and 6.6, respectively (Table 2.1 and Figure 2.16). The thick and rapidly accumulating sediments of the Lanyang Plain may well obscure other active normal faults between the two bounding faults within the back-arc basin. These would be additional potential sources of future earthquakes.

A seismic scenario for the Taipei Domain is one of the easiest to estimate because there is only one principal active fault, the Shanchiao fault (Figures 2.15 and 2.16). The threat posed by this active normal fault may be the greatest of any in Taiwan because the fault dips beneath the metropolitan region of Taipei, the capital and most populous city of the island. If we assume that a single rupture of the Shanchiao fault would extend only along the western edge of the Taipei basin, the resultant earthquake would have a magnitude of about M_w 6.5, with an average fault slip of about 0.7 m (Table 2.1). If, however, we postulate that a single rupture could continue from the edge of the basin over the volcanic edifice to the north, the rupture length becomes about 45 km and we calculate a M_w 6.9 with about 1.1 m of dip slip. Paleoseismic investigations may be able to resolve the rupture lengths of past earthquakes and provide some insight into which of these scenarios is more probable. One recent analysis, in fact, shows that two possible ruptures between 8 and 10 kyr ago may have involved as much as 3 to 4 m of slip [*Huang et al.*, 2005]. Such large slips imply even longer ruptures than we have proposed.

Vertical offsets of 1 to 3 m are common along active normal faults with lengths as great as the Shanchiao fault. Offsets of this size would have particularly serious consequences for Taipei because large portions of the Taipei basin are less than 3 m above sea level. The submergence event of AD 1694 may thus be related to rupture of

the fault.

Now that we have presented plausible seismic sources for all of Taiwan's neotectonic domains, we are tempted to calculate the frequency with which large earthquakes from these sources might visit each domain. This could be done using modern geodetic rates of horizontal shortening to estimate the average amount of time necessary to accumulate the strain relieved by each scenario event. These calculations would be simplest for the domains dominated by single faults, such as the Chiayi and Taipei Domains. For example, elastic strain accumulation equal to that relieved by 2.3 m of offset on the Chiayi detachment (our scenario event) would accumulate in only about 65 yr if the detachment is the only structure to release the strain. However, for the Taipei Domain the rate of strain accumulation is so low that the errors in GPS vectors are too large to allow such a calculation. In complex domains such as Kaoping, Lutao-Lanyu, Hsinchu, and Ilan, the long-term partitioning of deformation across the faults is so poorly known that calculations of average recurrence intervals using modern geodetically determined strain rates would not be very meaningful.

In some cases it would be more reliable to divide the cumulative slip on the principal faults over the past million or so years by the amount of slip that we anticipate in future events. For the Shanchiao fault in the Taipei Domain, for example, this yields an average interval of approximately 500 to 600 yr. In other cases, short paleoseismic records are beginning to provide direct evidence of recurrence intervals. For example, *Streig et al.* [2005] have shown that the previous rupture of the central part of the Chelungpu fault was similar to the 1999 rupture in slip magnitude and occurred about 640-740 yr ago. However, in most domains, geochronologic, stratigraphic, and structural controls on late Quaternary strata are still too poor to constrain recurrence intervals meaningfully.

Another complication in estimating average return periods for large earthquakes is the degree to which the major faults are creeping in the upper crust. Some, such as the

Chihshang fault in the Taitung Domain, are known to be creeping rapidly at the surface [*Angelier et al.*, 1997; *Lee et al.*, 2001] and probably at depth [*Chen and Rau*, 2002]. Complicating this is the fact that the rupture of 1951 earthquake extended into this creeping sector [*Hsu*, 1962; *Shyu et al.*, 2005b]. More detailed narrow-aperture geodetic experiments similar to those of *Angelier et al.* [1997] and *Lee et al.* [2001], as well as broad-aperture experiments are needed to resolve the importance of creep in diminishing the rate of production of large earthquakes in Taiwan.

In conclusion, then, the current state of structural, stratigraphic, rheological, and geodetic knowledge precludes us from offering meaningful calculations of average return times for seismic rupture of the large faults within each domain. Instead, we suggest that rigorous, multi-disciplinary programs be established to constrain average and actual recurrence intervals.

2.6 Conclusions

Using a 40-m resolution DEM, augmented by structural, geodetic, and seismologic data, we have prepared a neotectonic map and cross sections of Taiwan. The active structures we have identified suggest that the Taiwan orogen is due to a tandem suturing and tandem disengagement of a volcanic arc and a continental sliver to and from the Eurasian continental margin. Moreover, the island of Taiwan is divided naturally into distinct neotectonic domains, each with distinct principal structures. Four domains are present along the eastern suture, and seven domains comprise the western suture. These domains and their principal structures provide a basis for understanding future earthquakes around Taiwan. Using simple regression models, we have also proposed possible earthquake scenarios for each of the domains. These results should assist the many ongoing geodetic, geophysical, paleoseismic, and other attempts to understand future seismic hazard of the island.

2.7 Acknowledgments

We are grateful for valuable discussions with J.-P. Avouac, O. Beyssac, Y.-C. Chan, W.-C. Chi, H.-T. Chu, M.-L. Hsieh, J.-C. Hu, J.-C. Lee, C.-H. Lo, C.-Y. Lu, Y. Ota, C. Rubin, M. Simons, Q. Sung, L.S. Teng, B. Wernicke, and S.-B. Yu. We have also benefited from stimulating discussions with students of two field classes in Taiwan and a neotectonic seminar at National Taiwan University. The comments and suggestions of reviewers I. Manighetti and R.S. Yeats greatly helped us improve this manuscript. Our mapping would have been impossible had C.-T. Lee not made us aware that high-quality digital topography of the island existed. J. Giberson, manager of the Geographic Information Systems (GIS) laboratory of California Institute of Technology (Caltech), helped with the technical aspects of mapping. Our project in Taiwan was initially supported by private funds of Caltech's Division of Geological and Planetary Sciences and later by National Science Foundation (NSF) grant EAR-0208505. This research was also supported in part by the Gordon and Betty Moore Foundation. This is Caltech Tectonics Observatory Contribution #3.

2.8 References

Angelier, J., H.-T. Chu, and J.-C. Lee (1997), Shear concentration in a collision zone: kinematics of the Chihshang Fault as revealed by outcrop-scale quantification of active faulting, Longitudinal Valley, eastern Taiwan, *Tectonophysics*, *274*, 117-143.

Barrier, E., and J. Angelier (1986), Active collision in eastern Taiwan: the Coastal Range, *Mem. Geol. Soc. China*, *7*, 135-159.

Biq, C. (1965), The East Taiwan Rift, *Pet. Geol. Taiwan*, *4*, 93-106.

Biq, C. (1972), Dual-trench structure in the Taiwan-Luzon region, *Proc. Geol. Soc. China*, *15*, 65-75.

Biq, C. (1992), Another Coastal Range on Taiwan (in Chinese with English summary), *Ti-Chih*, *12*, 1-12.

Bonilla, M. G. (1975), A review of recently active faults in Taiwan, *Open File Rep. 75-41*, 58pp., U. S. Geol. Surv., Menlo Park, Calif.

Bonilla, M. G. (1977), Summary of Quaternary faulting and elevation changes in Taiwan, *Mem. Geol. Soc. China*, *2*, 43-55.

Carena, S., J. Suppe, and H. Kao (2001), Imaging the main detachment under Taiwan: implications for the critical-taper mechanics and large-scale topography, *EOS, Trans., Am. Geophys. Uni.*, *82*(47), Fall Meet. Suppl., Abstract T32A-0863.

Carena, S., J. Suppe, and H. Kao (2002), Active detachment of Taiwan illuminated by small earthquakes and its control of first-order topography, *Geology*, *30*, 935-938.

Central Geologic Survey (1999a), Map of surface ruptures along the Chelungpu fault during the Chi-Chi earthquake, Taiwan, scale 1:25,000, Cent. Geol. Surv., Ministry Econ. Affairs, Taipei, Taiwan.

Central Geologic Survey (1999b), Report of the geological survey of the 1999 Chi-Chi earthquake (in Chinese), 314pp., Cent. Geol. Surv., Ministry Econ. Affairs, Taipei, Taiwan.

Chan, Y.-C., J.-C. Lee, C.-Y. Lu, and H.-T. Chu (2001), Transtensional tectonics along a major north-south trending fault in the active convergent Taiwan mountain belt, *EOS, Trans., Am. Geophys. Uni.*, *82*(47), Fall Meet. Suppl., Abstract T32A-0880.

Chan, Y. C., J. C. Lee, C. Y. Lu, J. C. Hu, H. T. Chu, C. S. Hou, R. J. Rau, and K. E. Ching (2002), Neotectonic and structural characteristics along the Chaochou fault system in SW Taiwan: implications for tectonic escape during oblique plate convergence, *EOS, Trans., Am. Geophys. Uni.*, *83*(47), Fall Meet. Suppl., Abstract T62D-12.

Chang, C. P., J. Angelier, C. Y. Huang, and C. S. Liu (2001), Structural evolution and significance of a mélange in a collision belt: the Lichi Mélange and the Taiwan arc-continent collision, *Geol. Mag.*, *138*, 633-651.

Chang, H.-C., C.-W. Lin, M.-M. Chen, and S.-T. Lu (1998), *An Introduction to the Active Faults of Taiwan, Explanatory Text of the Active Fault Map of Taiwan* (in Chinese with English abstract), *Spec. Pub. Cent. Geol. Surv.*, *10*, 103pp., Cent. Geol. Surv., Ministry Econ. Affairs, Taipei, Taiwan.

Chang, J.-C., T.-T. Shih, S.-M. Shen, and C.-L. Chang (1992), A geomorphological study of river terrace in northern Huatung Longitudinal Valley (in Chinese with English abstract), *Geogr. Res.*, *18*, 1-51.

Chang, J.-C., K.-H. Teng, and M.-C. Liu (1998), A geomorphological study on river terraces in Miaoli Hills (in Chinese with English abstract), *Geogr. Res.*, *29*, 97-112.

Chang, L.-S., M. Chow, and P.-Y. Chen (1947), The Tainan earthquake of December 5, 1946 (in Chinese with English summary), *Bull. Geol. Surv. Taiwan*, *1*, 11-18 (Chinese), and 17-20 (English).

Chang, S. S. L. (1974), Subsurface geologic study of the Miaoli area, Taiwan, *Pet. Geol. Taiwan*, *11*, 1-25.

Chemenda, A. I., R. K. Yang, C.-H. Hsieh, and A. L. Groholsky (1997), Evolutionary model for the Taiwan collision based on physical modelling, *Tectonophysics*, *274*, 253-274.

Chemenda, A., S. Lallemand, and A. Bokun (2000), Strain partitioning and interplate friction in oblique subduction zones: Constraints provided by experimental modeling, *J. Geophys. Res.*, *105*, 5,567-5,581.

Chen, C.-Y. (1974), Verification of the north-northeastward movement of the Coastal Range, eastern Taiwan, by re-triangulation (in Chinese with English abstract), *Bull. Geol. Surv. Taiwan*, *24*, 119-123.

Chen, H.-H., and R.-J. Rau (2002), Earthquake locations and style of faulting in an active arc-continent plate boundary: the Chihshang fault of eastern Taiwan, *EOS, Trans., Am. Geophys. Uni.*, *83*(47), Fall Meet. Suppl., Abstract T61B-1277.

Chen, J.-S. (1978), A comparative study of the refraction and reflection seismic data obtained on the Changhua plain to the Peikang Shelf, Taiwan, *Pet. Geol. Taiwan*, *15*, 199-217.

Chen, M.-P., Y.-T. Shieh, and C.-S. Shyr (1988), Seafloor physiography and surface sediments off southeastern Taiwan, *Acta Geol. Taiwanica*, *26*, 333-353.

Chen, R.-F. (1999), Geomorphic index study of active structures in Chiayi-Tainan area, southwestern Taiwan (in Chinese with English abstract), M.S. thesis, 146pp., Natl.

Cheng Kung Univ., Tainan, Taiwan.

Chen, W.-S., Y.-M. Cheng, and C.-Y. Huang (1985), Geology of the Hengchun Peninsula, southern Taiwan (in Chinese with English abstract), *Ti-Chih*, *6*(2), 47-74.

Chen, W.-S., Y.-G. Chen, T.-K. Liu, N.-W. Huang, C.-C. Lin, S.-H. Sung, and K.-J. Lee (2000), Characteristics of the Chi-Chi earthquake ruptures (in Chinese with English abstract), *Spec. Pub. Cent. Geol. Surv.*, *12*, 139-154.

Chen, Y.-G. (1993), Sea-level change and neotectonics in southern part of Taiwan region since Late Pleistocene (in Chinese), Ph.D. thesis, 158pp., Natl. Taiwan Univ., Taipei.

Chen, Y.-G., and T.-K. Liu (1992), Vertical crustal movement of a tectonic uplifting volcanic island – Lutao, *J. Geol. Soc. China*, *35*, 231-246.

Chen, Y.-G., W.-S. Chen, J.-C. Lee, Y.-H. Lee, C.-T. Lee, H.-C. Chang, and C.-H. Lo (2001), Surface rupture of 1999 Chi-Chi earthquake yields insights on active tectonics of central Taiwan, *Bull. Seismol. Soc. Am.*, *91*, 977-985.

Chen, Y.-G., W.-S. Chen, Y. Wang, P.-W. Lo, T.-K. Liu, and J.-C. Lee (2002), Geomorphic evidence for prior earthquakes: Lessons from the 1999 Chichi earthquake in central Taiwan, *Geology*, *30*, 171-174.

Cheng, S. N., and Y. T. Yeh (1989), *Catalog of the Earthquakes in Taiwan from 1604 to 1988* (in Chinese), 255pp., Inst. Earth Sci., Acad. Sinica, Taipei, Taiwan.

Cheng, S.-N., Y. T. Yeh, and M.-S. Yu (1996), The 1951 Taitung earthquake in Taiwan, *J. Geol. Soc. China*, *39*, 267-285.

Chinese Petroleum Corporation (1994), The geologic map of Miaoli, scale 1:100,000, *No. 3*, Taiwan Pet. Exploration Div., Chinese Pet. Corp., Miaoli, Taiwan.

Deschamps, A., P. Monié, S. Lallemand, S.-K. Hsu, and K. Y. Yeh (2000), Evidence for Early Cretaceous oceanic crust trapped in the Philippine Sea Plate, *Earth Planet. Sci. Lett.*, *179*, 503-516.

Eberhart-Phillips, D., et al. (2003), The 2002 Denali fault earthquake, Alaska: a large magnitude, slip-partitioned event, *Science*, *300*, 1,113-1,118.

Elishewitz, B. (1963), A new interpretation of the structure of the Miaoli area in the light of the décollement tectonics of northwest Taiwan, *Pet. Geol. Taiwan*, *2*, 21-45.

Font, Y., C.-S. Liu, P. Schnurle, and S. Lallemand (2001), Constraints on backstop geometry of the southwest Ryukyu subduction based on reflection seismic data, *Tectonophysics*, *333*, 135-158.

Gilbert, G. K. (1890), *Lake Bonneville*, *U. S. Geol. Surv. Monograph I.*, 438pp., U. S. Geol. Surv., Washington, D. C.

Hanai, S. (1930), Active faults in the Toen Hill, Formosa (in Japanese), *Geogr. Rev. Japan*, *6*(7), 778-789.

Hayasaka, I. (1935), On the earthquake of April, 21, 1935 in Sintiku and Taityû Prefectures (in Japanese), *Taiwan Tigaku Kizi*, *6*(6), 58-78.

Ho, C. S. (1986), A synthesis of the geologic evolution of Taiwan, *Tectonophysics*, *125*, 1-16.

Ho, C. S. (1988), *An Introduction to the Geology of Taiwan, Explanatory Text of the Geologic Map of Taiwan*, 2nd ed., 192pp., Cent. Geol. Surv., Ministry Econ. Affairs, Taipei, Taiwan.

Hovius, N., C. P. Stark, H.-T. Chu, and J.-C. Lin (2000), Supply and removal of sediment in a landslide-dominated mountain belt: Central Range, Taiwan, *J. Geol.*, *108*, 73-89.

Hsiao, P. T. (1971), Seismic study of the area between the coastal plain and the foothills, Yunlin, Taiwan, *Pet. Geol. Taiwan*, *8*, 249-263.

Hsiao, P. T. (1974), Subsurface geologic study of the Hsinying coastal plain area, Taiwan, *Pet. Geol. Taiwan*, *11*, 27-39.

Hsieh, C.-H., Y.-F. Chang, and R.-H. Sun (1992), Seismic investigate Hsin-Chuan fault on the west of Taipei Basin (in Chinese with English abstract), *Ti-Chih*, *12*(1), 13-26.

Hsu, M.-T. (1980), *Earthquake Catalogues in Taiwan (from 1644 to 1979)* (in Chinese), 77pp., Natl. Taiwan Univ., Taipei.

Hsu, S.-K., J.-C. Sibuet, S. Monti, C.-T. Shyu, and C.-S. Liu (1996), Transition between the Okinawa Trough backarc extension and the Taiwan collision: new insights on the southernmost Ryukyu subduction zone, *Mar. Geophys. Res.*, *18*, 163-187.

Hsu, T. L. (1955), Earthquakes in Taiwan (in Chinese), *Quart. J. Bank Taiwan*, *7*(2), 148-164.

Hsu, T. L. (1962), Recent faulting in the Longitudinal Valley of eastern Taiwan, *Mem. Geol. Soc. China*, *1*, 95-102.

Hsu, T. L., and H. C. Chang (1979), Quaternary faulting in Taiwan, *Mem. Geol. Soc. China*, *3*, 155-165.

Hsu, W.-L. (2001), Detecting the Changhua fault and its neighboring structures (in Chinese with English abstract), M.S. thesis, 94pp., Natl. Cent. Univ., Chungli, Taiwan.

Hsu, Y.-J., M. Simons, S.-B. Yu, L.-C. Kuo, and H.-Y. Chen (2003), A two-dimensional dislocation model for interseismic deformation of the Taiwan mountain belt, *Earth Planet. Sci. Lett.*, *211*, 287-294.

Hu, J.-C., J. Angelier, C. Homberg, J.-C. Lee, and H.-T. Chu (2001), Three-dimensional modeling of the behavior of the oblique convergent boundary of southeast Taiwan: friction and strain partitioning, *Tectonophysics*, *333*, 261-276.

Huang, C.-Y., C.-T. Shyu, S. B. Lin, T.-Q. Lee, and D. D. Sheu (1992), Marine geology in the arc-continent collision zone off southeastern Taiwan: Implications for Late

Neogene evolution of the Coastal Range, *Mar. Geol.*, *107*, 183-212.

Huang, C.-Y., W.-Y. Wu, C.-P. Chang, S. Tsao, P. B. Yuan, C.-W. Lin, and K.-Y. Xia (1997), Tectonic evolution of accretionary prism in the arc-continent collision terrane of Taiwan, *Tectonophysics*, *281*, 31-51.

Huang, C.-Y., P. B. Yuan, C.-W. Lin, T. K. Wang, and C.-P. Chang (2000), Geodynamic processes of Taiwan arc-continent collision and comparison with analogs in Timor, Papua New Guinea, Urals and Corsica, *Tectonophysics*, *325*, 1-21.

Huang, G.-C. (1997), The structural characteristics of the subducting slab between the Luzon Arc and the Taiwan collision belt revealed by focal mechanisms (in Chinese), M.S. thesis, 160pp., Natl. Taiwan Univ., Taipei.

Huang, G.-T. (1996), Preliminary study on the tectonic geomorphology in the southwestern Foothills, Taiwan (in Chinese), M.S. thesis, 114pp., Natl. Cent. Univ., Chungli, Taiwan.

Huang, L. S. (1990), Preliminary study on the subsurface temperature and geothermal gradients of the late Cenozoic basin in western Taiwan (in Chinese with English abstract), *Bull. Cent. Geol. Surv.*, *6*, 117-144.

Huang, M.-T., W.-L. Wang, K.-L. Pan, and T. P. Yen (1985), Photogeologic study of active fault II: The Meishan surface fault (in Chinese with English abstract), *Hazard Mitigation Res. Rep. 73-29*, 42pp., Natl. Sci. Council, Taipei, Taiwan.

Huang, S.-Y., C. M. Rubin, Y.-G. Chen, and H.-C. Liu (2005), Prehistoric earthquakes along the Shanchiao Fault, Taipei Basin, Northern Taiwan, *J. Asian Earth Sci.*, submitted for publication.

Hung, J.-H. (1996), Structure of Western Foothills and crustal deformation in southwestern Taiwan (in Chinese with English abstract), *Program with Abstracts, 1996 Ann. Meet. Geol. Soc. China*, 436-440, Taipei, Taiwan.

Hung, J.-H., and D. V. Wiltschko (1993), Structure and kinematics of arcuate thrust faults in the Miaoli-Cholan area of western Taiwan, *Pet. Geol. Taiwan*, *28*, 59-96.

Hung, J.-H., D. V. Wiltschko, H.-C. Lin, J. B. Hickman, P. Fang, and Y. Bock (1999), Structure and motion of the southwestern Taiwan Fold and Thrust Belt, *Terr. Atmos. Oceanic Sci.*, *10*, 543-568.

Ji, C., D. V. Helmberger, T.-R. A. Song, K.-F. Ma, and D. J. Wald (2001), Slip distribution and tectonic implication of the 1999 Chi-Chi, Taiwan, Earthquake, *Geophys. Res. Lett.*, *28*, 4,379-4,382.

Kao, H., and W.-P. Chen (2000), The Chi-Chi earthquake sequence: active, out-of-sequence thrust faulting in Taiwan, *Science*, *288*, 2,346-2,349.

Kao, H., and R.-J. Rau (1999), Detailed structures of the subducted Philippine Sea plate

beneath northeast Taiwan: A new type of double seismic zone, *J. Geophys. Res.*, *104*, 1,015-1,033.

Kao, H., S.-s. J. Shen, and K.-F. Ma (1998), Transition from oblique subduction to collision: Earthquakes in the southernmost Ryukyu arc-Taiwan region, *J. Geophys. Res.*, *103*, 7,211-7,229.

Kao, H., G.-C. Huang, and C.-S. Liu (2000), Transition from oblique subduction to collision in the northern Luzon arc-Taiwan region: Constraints from bathymetry and seismic observations, *J. Geophys. Res.*, *105*, 3,059-3,079.

Kelson, K. I., K.-H. Kang, W. D. Page, C.-T. Lee, and L. S. Cluff (2001), Representative styles of deformation along the Chelungpu fault from the 1999 Chi-Chi (Taiwan) earthquake: Geomorphic characteristics and responses of man-made structures, *Bull. Seismol. Soc. Am.*, *91*, 930-952.

Kerrich, R., R. D. Beckinsale, and J. J. Durham (1977), The transition between deformation regimes dominated by intercrystalline diffusion and intracrystalline creep evaluated by oxygen isotope thermometry, *Tectonophysics*, *38*, 241-257.

Kizaki, K. (1986), Geology and tectonic framework of the Ryukyu Islands, *Mem. Geol. Soc. China*, *7*, 1-14.

Ku, C.-C. (1963), Photogeologic study of terraces in northwestern Taiwan, *Proc. Geol. Soc. China*, *6*, 51-60.

Lacombe, O., F. Mouthereau, B. Deffontaines, J. Angelier, H. T. Chu, and C. T. Lee (1999), Geometry and Quaternary kinematics of fold-and-thrust units of southwestern Taiwan, *Tectonics*, *18*, 1,198-1,223.

Lacombe, O., F. Mouthereau, J. Angelier, and B. Deffontaines (2001), Structural, geodetic and seismological evidence for tectonic escape in SW Taiwan, *Tectonophysics*, *333*, 323-345.

Lallemand, S., and C.-S. Liu (1998), Geodynamic implications of present-day kinematics in the southern Ryukyus, *J. Geol. Soc. China*, *41*, 551-564.

Lallemand, S. E., C.-S. Liu, and ACT cruise scientific team (1997), Swath bathymetry reveals active arc-continent collision near Taiwan, *EOS, Trans., Am. Geophys. Uni.*, *78*(17), 173-175.

Lallemand, S., C.-S. Liu, S. Domingues, P. Schnürle, J. Malavieille, and the ACT Scientific Crew (1999), Trench-parallel stretching and folding of forearc basins and lateral migration of the accretionary wedge in the southern Ryukyus: A case of strain partition caused by oblique convergence, *Tectonics*, *18*, 231-247.

Lee, C.-T., C.-T. Cheng, C.-W. Liaw, and Y.-B. Chang (1998), Active fault map of Taiwan, Inst. Applied Geology, Natl. Cent. Univ., Chungli, Taiwan.

Lee, J.-C., H.-T. Chu, C.-Y. Lu, B. Deffontaines, O. Lacombe, F. Mouthereau, J. Angelier, and B. Delcaillau (1997), Structural characteristics of the Changhua thrust zone, western Taiwan (in Chinese), *Program and Expanded Abstracts, 1997 Ann. Meet. Geol. Soc. China*, 313-314, Tainan, Taiwan.

Lee, J.-C., J. Angelier, H.-T. Chu, S.-B. Yu, and J.-C. Hu (1998), Plate-boundary strain partitioning along the sinistral collision suture of the Philippine and Eurasian plates: Analysis of geodetic data and geological observation in southeastern Taiwan, *Tectonics*, *17*, 859-871.

Lee, J.-C., J. Angelier, H.-T. Chu, J.-C. Hu, and F.-S. Jeng (2001), Continuous monitoring of an active fault in a plate suture zone: a creepmeter study of the Chihshang Fault, eastern Taiwan, *Tectonophysics*, *333*, 219-240.

Lee, J.-C., H.-T. Chu, J. Angelier, Y.-C. Chan, J.-C. Hu, C.-Y. Lu, and R.-J. Rau (2002), Geometry and structure of northern surface ruptures of the 1999 Mw = 7.6 Chi-Chi Taiwan earthquake: influence from inherited fold belt structures, *J. Struct. Geol.*, *24*, 173-192.

Lee, Y.-H., W.-Y. Wu, T.-S. Shih, S.-T. Lu, M.-L. Hsieh, and H.-C. Chang (2000), Deformation characteristics of surface ruptures of the Chi-Chi earthquake, east of the Pifeng Bridge (in Chinese with English abstract), *Spec. Pub. Cent. Geol. Surv.*, *12*, 19-40.

Lin, C.-C. (1957), *Geomorphology of Taiwan* (in Chinese), 424pp., Taiwan Prov. Literature Comm., Taipei, Taiwan.

Lin, C.-W., H.-C. Chang, S.-T. Lu, T.-S. Shih, and W.-J. Huang (2000a), *An Introduction to the Active Faults of Taiwan, 2nd ed., Explanatory Text of the Active Fault Map of Taiwan* (in Chinese with English abstract), *Spec. Pub. Cent. Geol. Surv.*, *13*, 122pp., Taipei, Taiwan.

Lin, C.-W., S.-T. Lu, W.-J. Huang, T.-S. Shih, and H.-C. Chang (2000b), The Chi-Chi earthquake fault and structural analysis of the area south of Choshuihsi, central Taiwan (in Chinese with English abstract), *Spec. Pub. Cent. Geol. Surv.*, *12*, 89-111.

Lin, H.-Y. (1998), Depositional system of the Maanshan Formation, Hengchun Peninsula (in Chinese), M.S. thesis, 74pp., Natl. Sun Yat-sen Univ., Kaohsiung, Taiwan.

Liu, C.-C., and S.-B. Yu (1990), Vertical crustal movements in eastern Taiwan and their tectonic implications, *Tectonophysics*, *183*, 111-119.

Liu, C.-S., I. L. Huang, and L. S. Teng (1997), Structural features off southwestern Taiwan, *Mar. Geol.*, *137*, 305-319.

Liu, C.-S., S.-Y. Liu, S. E. Lallemand, N. Lundberg, and D. L. Reed (1998), Digital elevation model offshore Taiwan and its tectonic implications, *Terr. Atmos. Oceanic*

Sci., *9*, 705-738.

Lu, S., T.-H. Lai, and C.-J. Chiang (1998), Long-term subsidence rates of the Pingtung Plain (in Chinese with English abstract), *Proceedings of the Symposium on Groundwater and Hydrogeology of the Pingtung Plain*, 153-163, Taipei, Taiwan.

Lundberg, N., D. L. Reed, C.-S. Liu, and J. Lieske, Jr. (1992), Structural controls on orogenic sedimentation, submarine Taiwan collision, *Acta Geol. Taiwanica*, *30*, 131-140.

Lundberg, N., D. L. Reed, C.-S. Liu, and J. Lieske, Jr. (1997), Forearc-basin closure and arc accretion in the submarine suture zone south of Taiwan, *Tectonophysics*, *274*, 5-23.

Ma, K.-F., T.-R. A. Song, S.-J. Lee, and H.-I. Wu (2000), Spatial slip distribution of the September 20, 1999, Chi-Chi, Taiwan, earthquake (Mw7.6)—Inverted from teleseismic data, *Geophys. Res. Lett.*, *27*, 3,417-3,420.

Ma, K.-F., J. Mori, S.-J. Lee, and S. B. Yu (2001), Spatial and temporal distribution of slip for the 1999 Chi-Chi, Taiwan, earthquake, *Bull. Seismol. Soc. Am.*, *91*, 1,069-1,087.

Malavieille, J., S. E. Lallemand, S. Dominguez, A. Deschamps, C.-Y. Lu, C.-S. Liu, P. Schnürle, and the ACT Scientific Crew (2002), Arc-continent collision in Taiwan: new marine observations and tectonic evolution, *Geol. Soc. Am. Spec. Paper*, *358*, 187-211.

Matsuda, T. (1974), Surface faults associated with Nobi (Mino-Owari) earthquake of 1891, Japan (in Japanese with English abstract), *Spec. Bull. Earthquake Res. Inst., Univ. Tokyo*, *13*, 85-126.

Namson, J. (1981), Structure of the Western Foothills belt, Miaoli-Hsinchu area, Taiwan: (I) Southern part, *Pet. Geol. Taiwan*, *18*, 31-51.

Namson, J. (1983), Structure of the Western Foothills belt, Miaoli-Hsinchu area, Taiwan: (II) Central part, *Pet. Geol. Taiwan*, *19*, 51-76.

Namson, J. (1984), Structure of the Western Foothills belt, Miaoli-Hsinchu area, Taiwan: (III) Northern part, *Pet. Geol. Taiwan*, *20*, 35-52.

Nazareth, J. J., and E. Hauksson (2004), The seismogenic thickness of the southern California crust, *Bull. Seismol. Soc. Am.*, *94*, 940-960.

Omori, F. (1907), Preliminary note on the Formosa earthquake of March 17, 1906, *Bull. Imp. Earthquake Invest. Comm.*, *1*(2), 53-69.

Ota, Y., J. B. H. Shyu, Y.-G. Chen, and M.-L. Hsieh (2002), Deformation and age of fluvial terraces south of the Choushui River, central Taiwan, and their tectonic implications, *Western Pacific Earth Sci.*, *2*, 251-260.

Otuka, Y. (1936), The earthquake of central Taiwan (Formosa), April 21, 1935, and earthquake faults (in Japanese with English résumé), *Bull. Earthquake Res. Inst., Tokyo*

Imp. Univ., *Suppl. 3*, 22-74.

Pan, K.-L., W.-N. Wang, K.-H. Hu, and T.-P. Yen (1983), Photogeologic investigations of the earthquake fault of 1935, central Taiwan (in Chinese), *Hazard Mitigation Res. Rep. 72-20*, 48pp., Natl. Sci. Council, Taipei, Taiwan.

Pan, Y. S., and C.-C. Hu (1972), An analysis on the sea bottom topography of the offshore area west of Hsinchu and Miaoli, Taiwan, *Pet. Geol. Taiwan*, *10*, 339-349.

Rau, R.-J., and F. T. Wu (1998), Active tectonics of Taiwan orogeny from focal mechanisms of small-to-moderate-sized earthquakes, *Terr. Atmos. Oceanic Sci.*, *9*, 755-778.

Reed, D. L., N. Lundberg, C.-S. Liu, and B.-Y. Kuo (1992), Structural relations along the margins of the offshore Taiwan accretionary wedge: implications for accretion and crustal kinematics, *Acta Geol. Taiwanica*, *30*, 105-122.

Schnürle, P., C.-S. Liu, S. E. Lallemand, and D. L. Reed (1998), Structural insight into the south Ryukyu margin: effects of the subducting Gagua Ridge, *Tectonophysics*, *288*, 237-250.

Scholz, C. H. (2002), *The Mechanics of Earthquakes and Faulting*, 2nd ed., 471pp., Cambridge Univ. Press, Cambridge, UK.

Shieh, Y.-T. (2000), The paleogeography of the ancient Taipei lakebed in the K'anghsi Period (in Chinese with English abstract), *J. Geogr. Sci.*, *27*, 85-95.

Shih, R.-C., P.-H. Chen, H.-Y. Yen, and C.-H. Lin (2000), Geophysical investigations on active faults in the central part of Taiwan and Taitung area (in Chinese), *2000 Ann. Rep., Geophysical Investigation Projects on Active Faults*, 126pp., Cent. Geol. Surv., Ministry Econ. Affairs, Taipei, Taiwan.

Shih, R.-C., P.-H. Chen, M.-T. Lu, and W.-S. Chen (2002), Earthquake geology investigation and the construction of the active faults database (in Chinese), *2002 Ann. Rep., Geophysical Investigation Projects on Active Faults*, 166pp., Cent. Geol. Surv., Ministry Econ. Affairs, Taipei, Taiwan.

Shih, T.-T., and G.-S. Yang (1985), The active faults and geomorphic surfaces of Pakua Tableland in Taiwan (in Chinese with English abstract), *Geogr. Res.*, *11*, 173-186.

Shih, T.-T., J.-C. Chang, and G.-S. Yang (1983), The active faults and geomorphic surfaces of Houli Tableland in Taiwan (in Chinese), *Bull. Geogr. Soc. China*, *11*, 46-55.

Shih, T.-T., K.-H. Teng, J.-C. Chang, C.-D. Shih, G.-S. Yang, and M.-Y. Hsu (1984a), A geomorphological study of active fault in western and southern Taiwan (in Chinese with English abstract), *Geogr. Res.*, *10*, 49-94.

Shih, T.-T., K.-H. Teng, and G.-S. Yang (1984b), The active faults and geomorphic surfaces of Tatu Tableland in Taiwan (in Chinese), *Bull. Geogr. Soc. China*, *12*, 9-21.

Shih, T.-T., K.-H. Teng, J.-C. Chang, and G.-S. Yang (1985), The active faults and geomorphic surfaces of Hengchun area in Taiwan (in Chinese with English abstract), *Geogr. Education*, *11*, 1-14.

Shih, T.-T., K.-H. Teng, J.-C. Chang, C.-D. Shih, and G.-S. Yang (1986), A geomorphological study of active fault in Taiwan (in Chinese with English abstract), *Geogr. Res.*, *12*, 1-44.

Shyu, J. B. H. (1999), The sedimentary environment of southern Pingdong Plain since the Last Glacial (in Chinese with English abstract), M.S. thesis, 212pp., Natl. Taiwan Univ., Taipei, Taiwan.

Shyu, J. B. H., K. Sieh, L.-H. Chung, Y.-G. Chen, and Y. Wang (2002), The active tectonics of eastern Taiwan—new insights from the two geomorphic tablelands ("the Feet") in the Longitudinal Valley, *EOS, Trans., Am. Geophys. Uni.*, *83*(47), Fall Meet. Suppl., Abstract T61B-1278.

Shyu, J. B. H., K. Sieh, and Y.-G. Chen (2005), Tandem suturing and disarticulation of the Taiwan orogen revealed by its neotectonic elements, *Earth Planet. Sci. Lett.*, *233*, 167-177.

Shyu, J. B. H., L.-H. Chung, Y.-G. Chen, J.-C. Lee, and K. Sieh (2005b), Re-evaluation of the surface ruptures of the November 1951 earthquake series in eastern Taiwan, and its neotectonic implications, *J. Asian Earth Sci.*, submitted for publication.

Sibuet, J.-C., and S.-K. Hsu (1997), Geodynamics of the Taiwan arc-arc collision, *Tectonophysics*, *274*, 221-251.

Sieh, K., et al. (1993), Near field investigations of the Landers earthquake sequence, April to July 1992, *Science*, *260*, 171-176.

Stach, L. W. (1958), Subsurface exploration and geology of the coastal plain region of western Taiwan, *Proc. Geol. Soc. China*, *1*, 55-96.

Streig, A. R., C. M. Rubin, W.-S. Chen, Y.-G. Chen, L.-S. Lee, S.-T. Lu, S. Thompson, and S.-Y. Huang (2005), Evidence for prehistoric coseismic folding along the Tsaotun segment of the Chelungpu fault near Nan-Tou, Taiwan: Seismic hazard along active fold scarps, *J. Geophys. Res.*, submitted for publication.

Sun, R.-H. (1990), The seismic survey on the subsurface structures in the western edge (Wuku-Taishan) area of Taipei Basin (in Chinese), M.S. thesis, 61pp., Natl. Cent. Univ., Chungli, Taiwan.

Sun, S. C. (1970), Photogeologic study of the Tainan-Hsinying coastal plain, Taiwan, *Pet. Geol. Taiwan*, *7*, 133-144.

Sun, S. C. (1971), Photogeologic study of the Hsinying-Chiayi coastal plain, Taiwan, *Pet. Geol. Taiwan*, *8*, 65-75.

Sun, S. C. (1972), Photogeologic study of the Peikang-Choshuichi coastal plain, Taiwan, *Pet. Geol. Taiwan*, *10*, 187-199.

Sung, Q.-C., and Y. Wang (1985), Petrofacies of Miocene sediments in the Hengchun Peninsula and its tectonic implication, *Proc. Geol. Soc. China*, *28*, 23-44.

Sung, Q., and Y. Wang (1986), Sedimentary environments of the Miocene sediments in the Hengchun Peninsula and their tectonic implication, *Mem. Geol. Soc. China*, *7*, 325-340.

Sunlin, Y.-M. (1982), A geomorphological study on active faults on the Taoyuan Tablelands (in Chinese), M.S. thesis, 53pp., Natl. Taiwan Normal Univ., Taipei.

Suppe, J. (1976), Décollement folding in southwestern Taiwan, *Pet. Geol. Taiwan*, *13*, 25-35.

Suppe, J. (1980a), A retrodeformable cross section of northern Taiwan, *Proc. Geol. Soc. China*, *23*, 46-55.

Suppe, J. (1980b), Imbricated structure of western foothills belt, southcentral Taiwan, *Pet. Geol. Taiwan*, *17*, 1-16.

Suppe, J. (1981), Mechanics of mountain building and metamorphism in Taiwan, *Mem. Geol. Soc. China*, *4*, 67-89.

Suppe, J. (1984), Kinematics of arc-continent collision, flipping of subduction, and back-arc spreading near Taiwan, *Mem. Geol. Soc. China*, *6*, 21-33.

Suppe, J. (1987), The active Taiwan mountain belt, in *Anatomy of Mountain Chains*, edited by J. P. Schaer, and J. Rodgers, pp. 277-293, Princeton Univ. Press, Princeton, N.J.

Suppe, J., and J. Namson (1979), Fault-bend origin of frontal folds of the western Taiwan fold-and-thrust belt, *Pet. Geol. Taiwan*, *16*, 1-18.

Tan, K. (1939), Geological consideration on the Taihoku Basin (in Japanese with English abstract), *Jubilee Pub. Commemoration Prof. H. Yabe, M. I. A., 60th Birthday*, *1*, 371-380.

Tan, L. P. (1977), Pleistocene eastward bending of the Taiwan arc, *Mem. Geol. Soc. China*, *2*, 77-83.

Tang, C. H. (1963), Geology and oil potentialities of the Hukou anticline, Hsinchu, *Pet. Geol. Taiwan*, *2*, 241-252.

Teng, L. S. (1987), Stratigraphic records of the late Cenozoic Penglai orogeny of Taiwan, *Acta Geol. Taiwanica*, *25*, 205-224.

Teng, L. S. (1990), Late Cenozoic arc-continent collision in Taiwan, *Tectonophysics*, *183*, 57-76.

Teng, L. S. (1996), Extensional collapse of the northern Taiwan mountain belt, *Geology*,

24, 949-952.

Teng, L. S., C. T. Lee, Y. B. Tsai, and L.-Y. Hsiao (2000), Slab breakoff as a mechanism for flipping of subduction polarity in Taiwan, *Geology*, *28*, 155-158.

Teng, L. S., C. T. Lee, C.-H. Peng, W.-F. Chen, and C.-J. Chu (2001), Origin and geological evolution of the Taipei Basin, northern Taiwan, *Western Pacific Earth Sci.*, *1*, 115-142.

Tong, L.-T., and C.-H. Yang (1999), Geophysical survey and stratigraphic correlations of the Chianan Plain (in Chinese), *Cent. Geol. Surv. Rep. 88-017*, 122pp., Cent. Geol. Surv., Ministry Econ. Affairs, Taipei, Taiwan.

Tullis, J., and R. A. Yund (1977), Experimental deformation of dry Westerly granite, *J. Geophys. Res.*, *82*, 5,705-5,718.

Wang, C., M.-L. Yung, C.-S. Lee, and C.-P. Chou (1998), Morphology and seismicity distribution of the Okinawa Trough: western extension to the island of Taiwan (in Chinese), *Program and Abstracts, 1998 Ann. Meet. Geol. Soc. China*, 115, Chungli, Taiwan.

Wang, C.-Y., G.-P. Chen, and D.-T. Jong (1994), The detection of active faults on Taiwan using shallow reflection seismics, *Terr. Atmos. Oceanic Sci.*, *5*, 277-293.

Wang, P. C. M. (1964), Reflection seismic survey conducted on the Hukou-Yangmei structure, Taiwan, *Pet. Geol. Taiwan*, *3*, 185-191.

Wang, P. C. M. (1967), Subsurface geology and oil possibilities of the Taoyuan-Miaoli offshore region, Taiwan, *Pet. Geol. Taiwan*, *5*, 81-98.

Wang, Y. (2003), Morphotectonics in Taoyuan-Hsinchu area, northwestern Taiwan (in Chinese with English abstract), M.S. thesis, 105pp., Natl. Taiwan Univ., Taipei.

Wang-Lee, C. M., Y. M. Cheng, and Y. Wang (1978), Geology of the Taipei Basin (in Chinese), *Taiwan Mining Industry*, *30*(4), 350-380.

Wells, D. L., and K. J. Coppersmith (1994), New empirical relationships among magnitude, rupture length, rupture width, rupture area, and surface displacement, *Bull. Seismol. Soc. Am.*, *84*, 974-1,002.

White, S. (1975), Tectonic deformation and recrystallisation of oligoclase, *Contrib. Mineral. Petrol.*, *50*, 287-304.

Wu, F.-T. (1965), Subsurface geology of the Hsinchuang structure in the Taipei Basin, *Pet. Geol. Taiwan*, *4*, 271-282.

Wu, F. T. (1978), Recent tectonics of Taiwan, *J. Phys. Earth*, *26*, Suppl., S265-S299.

Wu, F. T., R.-J. Rau, and D. Salzberg (1997), Taiwan orogeny: thin-skinned or lithospheric collision?, *Tectonophysics*, *274*, 191-220.

Yang, G.-S. (1986), A geomorphological study of active faults in Taiwan – especially on

the relation between active faults and geomorphic surfaces (in Chinese), Ph.D. thesis, 178pp., Chinese Culture Univ., Taipei, Taiwan.

Yang, K.-M., J.-C. Wu, J. S. Wickham, H.-H. Ting, J.-B. Wang, and W.-R. Chi (1996), Transverse structures in Hsinchu and Miaoli areas: structural mode and evolution in foothills belt, northwestern Taiwan, *Pet. Geol. Taiwan*, *30*, 111-150.

Yang, K.-M., H.-H. Ting, J.-C. Wu, and W.-R. Chi (1997), Geological model for complex structures and its implications for hydrocarbon exploration in northwestern Taiwan, *Pet. Geol. Taiwan*, *31*, 1-42.

Yang, K.-M., M.-G. Yeh, J.-C. Wu, and Z.-F. Sun (2000), Geometry, characteristics and evolution of Changhua fault and its associated structures (in Chinese with English abstract), *Program and Abstracts, 2000 Ann. Meet. Geol. Soc. China*, 103-105, Taipei, Taiwan.

Yang, S.-H. (1999), Determination of the fault locations using surface movement – examples from the Hualien area (in Chinese), M.S. thesis, 92pp., Natl. Cent. Univ., Chungli, Taiwan.

Yang, Y.-C. (1953), Earthquakes in Hualien in the latest 41 years (in Chinese), *Hualien Literatures*, *1*, 67-71.

Yeats, R. S., K. Sieh, and C. R. Allen (1997), *The Geology of Earthquakes*, 568pp., Oxford Univ. Press, New York.

Yeh, M.-G., W.-S. Chen, and W.-C. Shyr (1999), Seismic study of the Pliocene to Pleistocene Series in the southwest plain, Taiwan (in Chinese with English abstract), *Pet. Geol. Taiwan*, *33*, 199-215.

Yu, M.-S. (1997), Active faults in the Taitung Longitudinal Valley (in Chinese), Ph.D. thesis, 141pp., Natl. Taiwan Univ., Taipei.

Yu, S.-B., and H.-Y. Chen (1998), Strain accumulation in southwestern Taiwan, *Terr. Atmos. Oceanic Sci.*, *9*, 31-50.

Yu, S.-B., and L.-C. Kuo (2001), Present-day crustal motion along the Longitudinal Valley Fault, eastern Taiwan, *Tectonophysics*, *333*, 199-217.

Yu, S.-B., and C.-C. Liu (1989), Fault creep on the central segment of the Longitudinal Valley fault, eastern Taiwan, *Proc. Geol. Soc. China*, *32*, 209-231.

Yu, S.-B., H.-Y. Chen, and L.-C. Kuo (1997), Velocity field of GPS stations in the Taiwan area, *Tectonophysics*, *274*, 41-59.

Yu, S.-B., L.-C. Kuo, R. S. Punongbayan, and E. G. Ramos (1999), GPS observation of crustal deformation in the Taiwan-Luzon region, *Geophys. Res. Lett.*, *26*, 923-926.

Chapter 3

Re-evaluation of the Surface Ruptures of the November 1951 Earthquake Series in Eastern Taiwan and Their Neotectonic Implications

An earlier version of this chapter has been submitted as:

Shyu, J.B.H., L.-H. Chung, Y.-G. Chen, J.-C. Lee, and K. Sieh, 2005, *Journal of Asian Earth Sciences*, submitted for publication.

3.1 Abstract

The earthquakes of November 1951 constitute the most destructive seismic episode in the recorded history of the Longitudinal Valley, eastern Taiwan. However, information about their source parameters is sparse. To understand the relationship between the 1951 ruptures and new interpretations of the regional neotectonic architecture of the Longitudinal Valley, we re-evaluated the November 1951 ruptures by analyzing old documents, reports, and photographs, and by interviewing local residents who experienced the earthquake. As a result, we have revised significantly the rupture map previously published. We divide the surface ruptures into the Chihshang, Yuli, and Rueisuei sections. The first shock of the 1951 series probably resulted from the Chihshang rupture, and the second shock probably resulted from the Yuli and Rueisuei ruptures. The lengths of these ruptures indicate that the two shocks had similar magnitudes. The Chihshang and Rueisuei ruptures are along segments of the Longitudinal Valley fault, a left-lateral oblique fault along which the Coastal Range thrusts westward over the Longitudinal Valley. The Yuli rupture, on the other hand, appears to be part of a separate, left-lateral strike-slip Yuli fault, which traverses the middle of the Longitudinal Valley. The complex behavior of these structures and interaction between them are important in understanding the future seismic hazard of the area.

Keywords: Taiwan, Longitudinal Valley fault, earthquake, surface ruptures, seismic hazard.

3.2 Introduction

The island of Taiwan occupies a unique position along the boundary between the Eurasian and Philippine Sea plates, where subduction and collision are progressively consuming oceanic fragments of both the Eurasian and the Philippine Sea lithosphere (Figure 3.1). In the century or so of recorded history, Taiwan has experienced several strong and destructive earthquakes [e.g., *Bonilla*, 1975, 1977; *Hsu*, 1980; *Cheng and Yeh*, 1989], the most recent of which was the disastrous 1999 Chi-Chi earthquake [e.g., *Chen et al.*, 2001]. These are the seismic manifestation of an orogeny that has been in progress for the past several million years [e.g., *Ho*, 1986; *Teng*, 1987, 1990, 1996]. Along the narrow, N-S Longitudinal Valley suture in eastern Taiwan, the Luzon volcanic island arc is actively accreting to the metamorphic core of the island [e.g., *Shyu et al.*, 2005a] (Figure 3.1). Almost half a century before the 1999 earthquake, an earthquake series there dramatized the important role the valley plays in the overall neotectonics of Taiwan. This series included three magnitude 7 earthquakes centered near the northern end of the valley on 22 October 1951, and two events on 25 November 1951 which shook the middle part of the valley most severely. Onland surface ruptures approximately 15 km long at the northern end of the valley accompanied the October earthquakes, and more than 60 km of surface rupture in the central part of the Longitudinal Valley accompanied the November earthquakes [e.g., *Hsu*, 1962; *Yu*, 1997]. Together, the five earthquakes killed more than 80 people and destroyed thousands of houses [*Hsu*, 1980; *Cheng and Yeh*, 1989], thus constituting the most disastrous seismic event in eastern Taiwan in recorded history.

Despite their pre-eminence in Taiwan's seismic history, we know little about these earthquakes. The November doublet and its surface ruptures are particularly obscure. Although casualties were not as large as those from the October earthquakes, principally because the November ones occurred in a rural part of the countryside, the surface

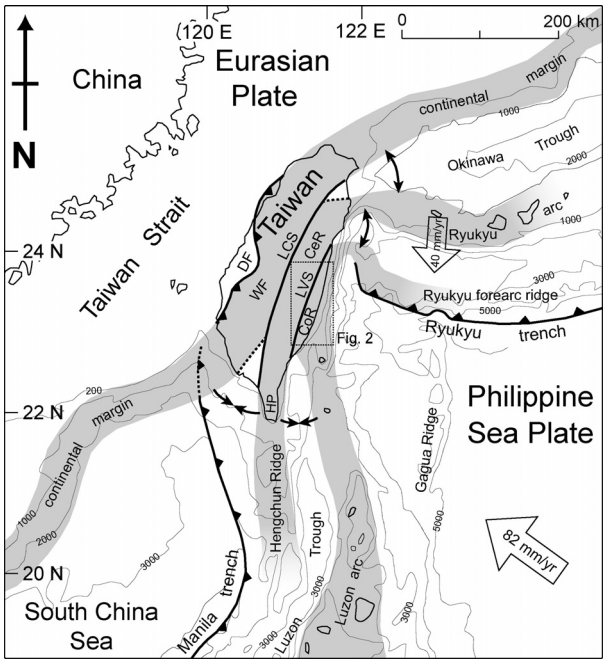

Figure 3.1. Taiwan is experiencing a transitory tandem suturing of a volcanic arc and a sliver of continental crust to the Asian continental margin. The 1951 earthquakes resulted from failure of faults along the Longitudinal Valley suture (LVS), the eastern of the two sutures. This suture is developing by the oblique collision of the Luzon volcanic arc into a narrow strip of continental crust. Adapted from *Shyu et al.* [2005a]. Current velocity vector of the Philippine Sea plate relative to the Eurasian plate adapted from *Yu et al.* [1997, 1999]. Current velocity vector of the Ryukyu arc adapted from *Lallemand and Liu* [1998]. DF: deformation front; LCS: Lishan-Chaochou suture; WF: Western Foothills; CeR: Central Range; CoR: Coastal Range; HP: Hengchun Peninsula.

ruptures of the November earthquakes were longer. However, the remoteness of the locality at that time hampered immediate investigation and detailed mapping of the ruptures. Thus, the only map of the November 1951 surface ruptures has been an approximately 1:2,000,000-scale figure published more than 10 yr after the earthquake [*Hsu*, 1962]. There have been several subsequent attempts to investigate active faults in the Longitudinal Valley [e.g., *Hsu and Chang*, 1979; *Shih et al.*, 1983; *Yang*, 1986; *Chu and Yu*, 1997; *Chang et al.*, 1998; *Lin et al.*, 2000]. Nonetheless, most of these efforts either confused the 1951 ruptures with fault scarps that did not rupture in 1951, mapped only short segments of the 1951 rupture, or used erroneous information in compiling rupture locations. For example, some of these compilers considered the collapse of houses and bridges to indicate ground ruptures through these structures. On other maps,

landslides reported by local witnesses or visible in photographs taken after the earthquake appear as tectonic ruptures.

More detailed maps of the active structures of the Longitudinal Valley have been produced recently [e.g., *Shyu et al.*, 2002; 2005b]. These new efforts have stimulated us to attempt compilation of a more detailed and accurate map of the 1951 ruptures in order to gain a better understanding of their relationship to the active faults of the valley and their neotectonic roles. The most important question we attempt to address is whether the 1951 events were caused by the major structures of the Longitudinal Valley. If so, did the rupture involve all or just a subset of these structures? The answer to this question has important implications for the evaluation of seismic hazard in the area.

In our attempt to re-evaluate the surface ruptures, our principal sources have been the published literature, vintage photographs, and interviews of local residents. We have examined all available scientific and non-scientific reports on the earthquake, including a number of newspaper reports written after the earthquake. We have also examined many old photographs taken after the earthquake, searching for evidence of surface rupture. Some, but not all, of these photographs appeared in earlier reports [*Taiwan Weather Bureau*, 1952; *Chu and Yu*, 1997; *Yu*, 1997]. These photographs were taken by several different investigators in locations wherever surface deformation was noticed. Fortunately, although the Longitudinal Valley was not heavily populated, there had already been many small villages along most part of it. Thus these photographs should reveal most of the surface ruptures. We have made a considerable effort to determine the exact locations of the features in these photographs, particularly by checking in the field for the topographic features and evidence of the rupture shown in the photographs. Moreover, we interviewed more than 40 local residents who experienced the earthquake and had information about the location of surface ruptures and other aspects of the earthquakes. A complete compilation of these data appears in *Chung* [2003]. In this brief paper we present only a few examples of these data.

Although we have attempted to ensure the reliability of all of this information, some uncertainties remain. Many reports in the literature are, for example, too vague for us to determine whether or not they are reliable. Some photographs cannot be assigned a certain location because of agricultural modifications in the 50 yr after the earthquake or lack of distinctive landmarks. Also, some of the information we acquired in the interviews was vague, uncertain, or even contradictory. Nonetheless, by sifting all of the information, we have been able to improve significantly our understanding of the ruptures associated with the earthquake.

3.3 Tectonic background of the Longitudinal Valley

The Longitudinal Valley in eastern Taiwan is located between two major tectonic blocks. To the east is the Coastal Range, an assemblage of Miocene through early Pliocene volcanic arc rocks and associated turbidite deposits, mélange, and fringing-reef limestones [*Chen*, 1988; *Ho*, 1988]. These rocks are similar to rocks that constitute the remnant of the Luzon island arc immediately to the south and the sediments of the adjacent sea floor. Thus, the rocks of the Coastal Range appear to represent a highly shortened forearc basin and volcanic arc [e.g., *Chang et al.*, 2001]. On the western side of the Longitudinal Valley is the eastern flank of the Central Range, composed of Mesozoic to Paleogene low-grade metamorphic rocks, predominantly schists and slates [*Ho*, 1988]. The contrast in the composition of the two ranges demonstrates that the intervening long, linear Longitudinal Valley occupies a major tectonic suture [e.g., *York*, 1976; *Teng*, 1990]. Coarse late Quaternary clastic fluvial sediments fill the valley. The thickness of these sediments is unknown, but is likely more than 1 km [e.g., *Chen et al.*, 1974; *Chen*, 1976].

The dominant neotectonic element of this part of the island is the east-dipping Longitudinal Valley fault, which traverses the eastern edge of the valley (Figure 3.2). It

is characterized by high rates of sinistral reverse motion along its southern two-thirds and mostly sinistral motion along its northern one-third [*Shyu et al.*, 2005b]. The geomorphic manifestation of this fault is clear along most of the valley but is rather complex, especially along its southern two-thirds. Distinctive tectonic landforms include discontinuous scarps that range up to several meters high along the range front and are lobate and irregular in plan view. These are associated commonly with east-tilted surfaces on the hanging-wall block. Along most of the valley, these thrust-fault scarps are also accompanied by numerous secondary anticlines and synclines in the hanging-wall block.

Another major active structure along the southern two-thirds of the valley is a reverse fault that dips westward beneath the eastern flank of the Central Range (Figure 3.2). This fault, named the Central Range fault by *Biq* [1965], may be the major structure along which rapid uplift of the eastern flank of the Central Range is occurring [e.g., *Shyu et al.*, 2005b]. Geomorphic evidence of this active fault includes a straight eastern flank of the Central Range along the southern two-thirds of the Longitudinal Valley and fluvial terraces that are perched tens to hundreds of meters above modern streambeds along a long segment of the range front. The most prominent feature among these is the Wuhe Tableland near Rueisuei in the middle of the valley [*Shyu et al.*, 2002; 2005b] (Figure 3.2).

Recent geodetic measurements show that the Longitudinal Valley is narrowing at a rate of about 40 mm/yr [e.g., *Yu et al.*, 1997]. Creepmeter measurements show that the Longitudinal Valley fault zone near the town of Chihshang (Figure 3.2) is creeping at a rate of about 20 mm/yr [*Angelier et al.*, 1997; *Lee et al.*, 2001]. Inversions of GPS data across southern Taiwan also indicate that the Longitudinal Valley fault is a major active structure [e.g., *Hsu et al.*, 2003]. Contributions to strain accumulation by the Central Range fault, however, are not yet clear.

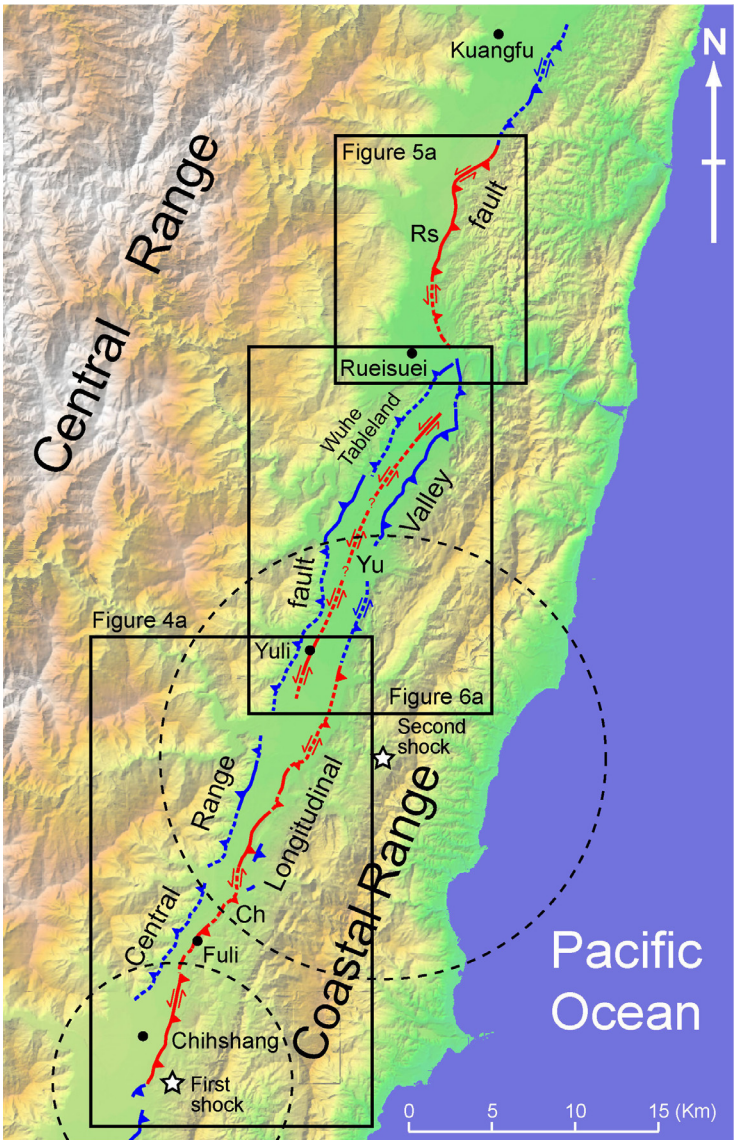

Figure 3.2. Shaded relief map showing the active structures in the middle part of the Longitudinal Valley, between the Central and Coastal Ranges. Our estimate of the extent of the November 1951 ruptures is shown in red. Major active reverse faults and flexures that did not rupture in 1951 are shown in blue. Modified from *Shyu et al.* [2002, 2005b] and unpublished results of J.B.H. Shyu and L.-H. Chung. Ch: Chihshang rupture; Yu: Yuli rupture; Rs: Rueisuei rupture. Dashed faults are inferred. White stars are relocated epicenters of the November 1951 earthquakes, after *Cheng et al.* [1996], with their uncertainties shown as dashed circles.

3.4 The November 1951 earthquake series

The major shocks of November 25th occurred at 02:47 and 02:50, local time [*Taiwan Weather Bureau*, 1952]. Because they occurred just 3 minutes apart and only

ten seismic stations were operating in Taiwan at that time, widely disparate source parameters have been calculated and reported for the earthquakes [e.g., *Taiwan Weather Bureau*, 1952; *Gutenberg and Richter*, 1954; *Lee et al.*, 1978; *Hsu*, 1980; *Abe*, 1981]. The analyses by the *Taiwan Weather Bureau* [1952] and *Hsu* [1980] indicate the first one was the larger of the two, whereas the catalog of *Lee et al.* [1978] indicates the opposite. In the catalogs of *Gutenberg and Richter* [1954] and *Abe* [1981] the two events appear as a single earthquake. Epicentral locations vary widely among these reports and are commonly very far from known faults of the Longitudinal Valley.

Recently *Cheng et al.* [1996] tried to use the limited information of S-P times reported by the *Taiwan Weather Bureau* [1952], a Monte Carlo algorithm, and information about the surface faults and maximum ground motion amplitudes to relocate the epicenters and calculate the magnitudes of the two events. They placed the hypocenter of the first shock at 23.1°N and 121.225°E at a depth of 16 km (Figure 3.2). Their hypocenter for the second shock was at 23.275°N and 121.35°E at a depth of 36 km. They also found that the magnitude of the second shock was larger than that of the first shock (M_w 7.0 vs. M_w 6.2). Although their results still have large uncertainties, they are much better than the previous reports, and their results clearly show that the two earthquakes are related to mapped faults of the Longitudinal Valley. Moreover, they derived focal mechanisms using the first motions reported by the *Taiwan Weather Bureau* [1952] and *Hsu*'s [1962] map of the surface ruptures. They concluded that the first shock was generated by a thrust fault with a subordinate left-lateral component, striking N32°E and dipping 70°S. From more limited first-motion information, they concluded that the second shock originated on a left-lateral strike-slip fault with a subordinate thrust component.

The surface ruptures of the earthquakes have never been mapped in detail. The most widely accepted version is depicted in Figure 3.3, after *Hsu* [1962]. In this representation the fault extends approximately 40 km from about 10 km south of

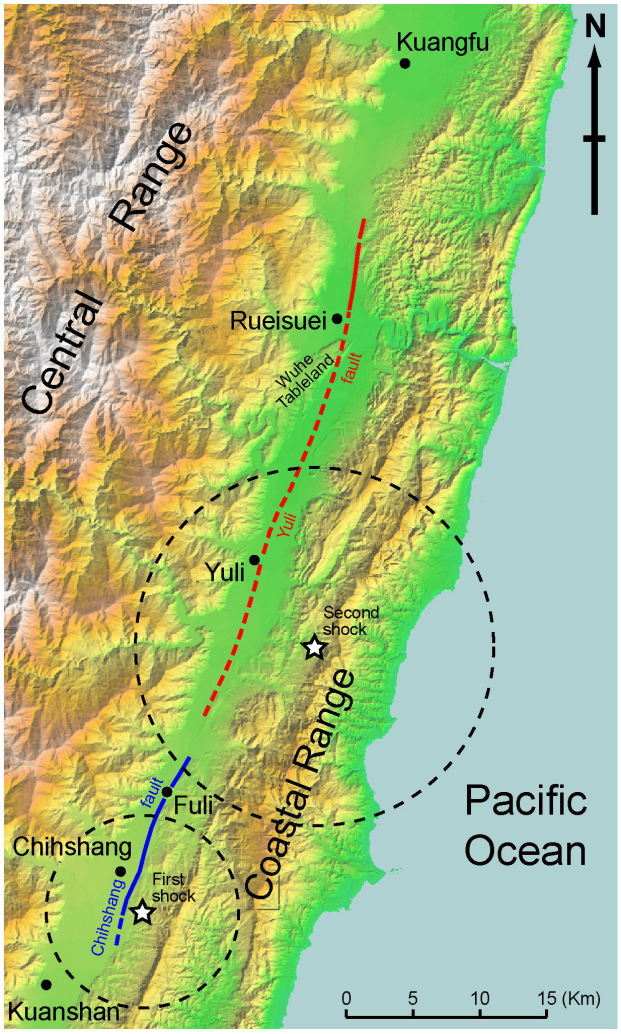

Figure 3.3. Map of published surface ruptures of the November 1951 earthquakes, after *Hsu* [1962]. *Hsu* [1962] concluded that the Yuli fault (in red) is the source of the 1951 earthquakes and that the Chihshang fault (in blue) is an active fault that did not rupture in 1951. *Cheng et al.* [1996], on the other hand, suggested that sinistral reverse slip on the Chihshang fault produced the first of the two earthquakes and that similar slip on the Yuli fault produced the second earthquake. White stars are relocated epicenters of the November 1951 earthquakes, after *Cheng et al.* [1996], with their uncertainties shown as dashed circles.

Kuangfu to just north of Fuli (Figure 3.3). Since this line runs through the town of Yuli, Hsu named it the Yuli fault and considered it to be the rupture that caused both of the November 1951 earthquakes. On the same map he also drew another line just south of the Yuli fault, extending about 20 km from around Fuli to near Kuanshan. He named this the Chihshang fault and believed it to be an active fault by virtue of its clear and young topographic appearance. However, *Cheng et al.* [1996] suggested that Hsu's

Chihshang fault also ruptured in 1951, suggesting that the Chihshang fault ruptured during the first shock and that the Yuli fault ruptured during the second shock.

Several important questions arise from these earlier efforts. Did the Chihshang fault rupture during the earthquake as proposed by *Cheng et al.* [1996]? If so, how far north did the rupture extend? And was the Chihshang rupture contiguous with the Yuli rupture? If both structures ruptured, are they parts of the same fault? If not, what is the relationship between them? And finally, what are the relationships between the Yuli and Chihshang ruptures and the Longitudinal Valley fault? Are they along two segments of the Longitudinal Valley fault? Or, are they ruptures of faults that are distinct from the Longitudinal Valley fault? What is the implication of the fact that the Yuli fault runs through the town of Yuli, very far from the western mountain front of the Coastal Range? In our attempt to re-evaluate the November 1951 ruptures, our main goal has been to answer these questions.

3.5 Re-evaluation of the November 1951 ruptures

We have been able to determine the location of the November 1951 ruptures in many places. Our re-evaluation leads us to divide the ruptures into three separate strands (Figure 3.2), which we call the Chihshang, Yuli, and Rueisuei ruptures. The Chihshang rupture is similar to the Chihshang fault first noted by *Hsu* [1962]. The Yuli and Rueisuei ruptures are roughly coincident with his Yuli fault, but constitute two entirely different structures.

3.5.1 The Chihshang rupture

The southern end of the Chihshang rupture is approximately 4 km south of the town of Chihshang [*Chung*, 2003] (Figure 3.4a). The rupture extends northward from there

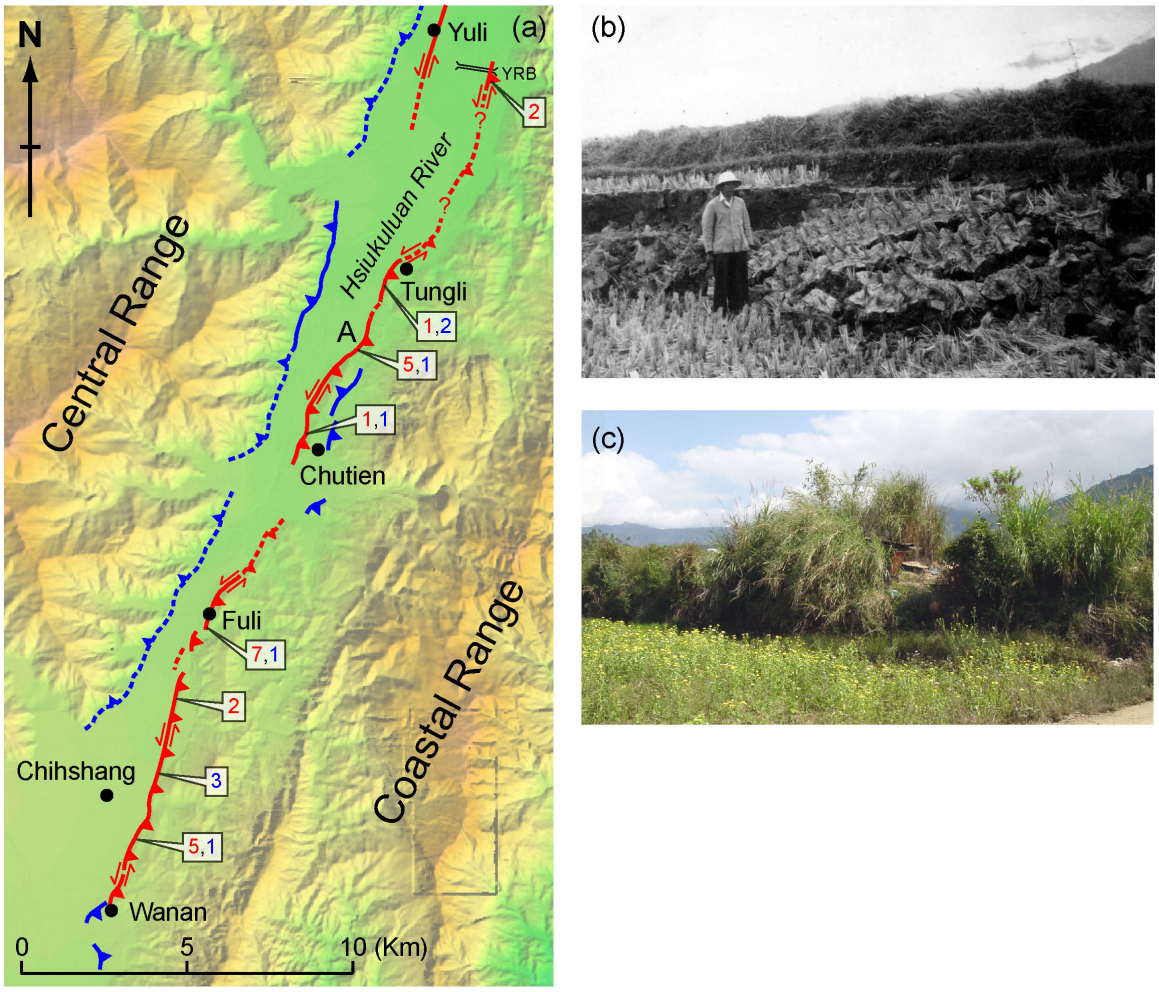

Figure 3.4. (a) Map of the Chihshang rupture (in red). Blue lines are active structures that did not rupture in 1951. Modified from *Shyu et al.* [2005b] and unpublished results of J.B.H. Shyu and L.-H. Chung. YRB: Yuli railroad bridge. For each section of the rupture a few km long, numbers of photographs showing ruptures or cracks (in red) and interview results of actual surface break (in blue) are also shown. (b) An old photograph of the rupture at point A, between Chutien and Tungli, shows approximately 1.5 m vertical offset that occurred during the earthquake. The photograph was taken by T. L. Hsu, looking toward the east, and was provided by M.-S. Lin. (c) A recent photograph taken at the same location, also looking toward the east. The scarp is only 1 m high at present due to modifications associated with agriculture.

along the western foothills of the Coastal Range for about 20 km to a point near the village of Tungli. It is difficult to determine confidently whether the rupture extended north of Tungli because the evidence is very scattered. We suggest, however, that it may have reached the Yuli railroad bridge just east of Yuli. If this is the case, the total rupture length of the Chihshang rupture is close to 30 km.

Although *Hsu* [1962] did not document surface rupture near Chihshang during the November 1951 earthquakes, we believe that surface rupture did occur there because many local residents in villages around Chihshang we interviewed did witness surface rupture there, along the western foothills of the Coastal Range. This is consistent with the reports of damage and destruction around Chihshang in many local newspapers after the earthquake [*Yang*, 1953; *Chung*, 2003]. Moreover, this makes a lot more sense because the southernmost point of the rupture mapped by *Hsu* [1962] lies very far northeastward from the relocated epicenter of the first shock in the November 1951 series, even after the large uncertainty of the relocation was taken into consideration (Figure 3.3). Many recent large strike-slip earthquakes, such as the 1992 Landers, 1999 Izmit, and 1999 Hector Mine earthquakes, have epicenters on or very close to surface ruptures [e.g., *Sieh et al.*, 1993; *Barka*, 1999; *Treiman et al.*, 2002]. Thus it is reasonable to find surface rupture near Chihshang, much closer to the epicenter of the first shock, for an earthquake with a significant strike-slip component.

Our interviews indicate that the southern end of the Chihshang rupture was near the small village of Wanan (Figure 3.4a). Local witnesses told us that the surface rupture stopped and did not extend onto mapped structures south of Wanan. From Wanan north to near Fuli, more than ten photographs and the results of our interviews suggest almost continuous rupture along the eastern edge of the Longitudinal Valley. Our interviews indicate that the largest vertical offset along this segment was about 0.5 m with smaller left-lateral offset. Around Fuli several photographs suggest that the surface ruptures were characterized by *en echelon* cracking and that vertical displacements were smaller, less than 0.2 m, with the eastern side moving upward. Left-lateral offset appears to be more obvious according to newspaper reports collected by *Yu* [1997]. Farther north, between Chutien and Tungli, vertical displacement was much larger, approximately 1 to 1.5 m, and with seven photographs showing the rupture it appears to be continuous again. We found an old photograph of a locality near the Yuli Convalescent Hospital in which

the rupture exhibits a scarp about 1.5 m high (Figure 3.4b). This scarp is only 1 m high now due to agricultural modifications (Figure 3.4c).

We did not find undisputable evidence for rupture in 1951 north of Tungli. Based upon newspaper reports published shortly after the earthquake which indicated that the Yuli railroad bridge was offset and broken by the earthquake, *Yu* [1997] suggested that the rupture ran through the bridge about 200 m west of the bridge's eastern end (Figure 3.4a), with offsets about 0.1-0.3 m vertically and 0.3-0.4 m left-laterally. However, no other document confirms the existence of the rupture there. *Yang* [1953] mentioned that there were cracks in the Hsiukuluan River bed, but without photographs or eyewitness accounts we are uncertain whether the cracks were in fact fault ruptures. The bridge did break during the earthquake, but this may have been due to seismic shaking rather than surface rupture. Because *Yu* [1997] was confident about this location and provided detailed information about the offset, we favor his suggestion.

Our interviews indicate that the rupture did not extend north of the Yuli railroad bridge (Figure 3.4a). Although *Cheng et al.* [1996] maintained that their photograph on Plate I-3, which shows rupture with ~0.6 m vertical offset, was from a point north of the Yuli railroad bridge, the location of the photograph has been strongly questioned [e.g., *Yu*, 1997; *Chung*, 2003].

It is quite clear that the Chihshang rupture occurred on a segment of the Longitudinal Valley fault. The fault has long been known to be an oblique-slip fault with a significant component of vertical movement [e.g., *Hsu*, 1962; *Ho*, 1986, 1988; *Chen*, 1988]. The Chihshang rupture had a similar sense of oblique slip. Based upon geomorphic evidence, *Shyu et al.* [2005b] mapped the major strand of the Longitudinal Valley fault along the eastern edge of the Longitudinal Valley. East of Chihshang, this strand follows a clear, almost linear scarp about 20 m high. This is exactly coincident with surface ruptures of 1951. The fault has been rapidly creeping along this reach at rates up to 20 mm/yr for at least 20 yr [e.g., *Yu and Liu*, 1989; *Chu et al.*, 1994; *Angelier*

et al., 1997; *Chow et al.*, 2001; *Lee et al.*, 2001]. Our discovery of 1951 ruptures here demonstrates that the fault fails by both creep and by seismic rupture.

North of Fuli, the hanging-wall block of the Longitudinal Valley fault exhibits a series of anticlinal hills and backthrusts [*Yang*, 1986; *Chung*, 2003; *Shyu et al.*, 2005b]. Although the 1951 ruptures were coincident with the Longitudinal Valley fault there, along the westernmost edge of these hills, we have no evidence that the folds and backthrusts in the hanging-wall block of the fault moved during the earthquakes.

In summary, the Chihshang rupture of 1951 occurred along an up to 30 km length of the Longitudinal Valley fault. The ruptures were characterized by oblique offset, similar to the sense of slip along the fault depicted on geologic maps [e.g., *Chen*, 1988; *Ho*, 1988] and monitored during the past 20 yr. Along most of its length, the vertical offset along the rupture was less than 0.5 m, but along the Tungli-Chutien section it was as much as 1.5 m. We are uncertain about the total length of this rupture, but it was at least 20 km and no longer than 30 km.

3.5.2 The Rueisuei rupture

The southern end of the Rueisuei rupture of 1951 is about 2 km east of the town of Rueisuei (Figure 3.5a). From there the rupture extended about 15 km north along the western foothills of the Coastal Range to the Tzu-Chiang Prison, about 10 km south of the town of Kuangfu. We have found abundant evidence that rupture was almost continuous along this reach [*Chung*, 2003].

Like the Chihshang rupture, the Rueisuei rupture followed the western edge of the Coastal Range, along the eastern side of the Longitudinal Valley. Sense of slip on the rupture appears to be oblique, with significant amounts of vertical offset. For example, *Hsu* [1962] reported that at one location the slickensides on the fault plane showed 1.63 m of left-lateral offset and 1.3 m of vertical offset. However, in most of the photographs

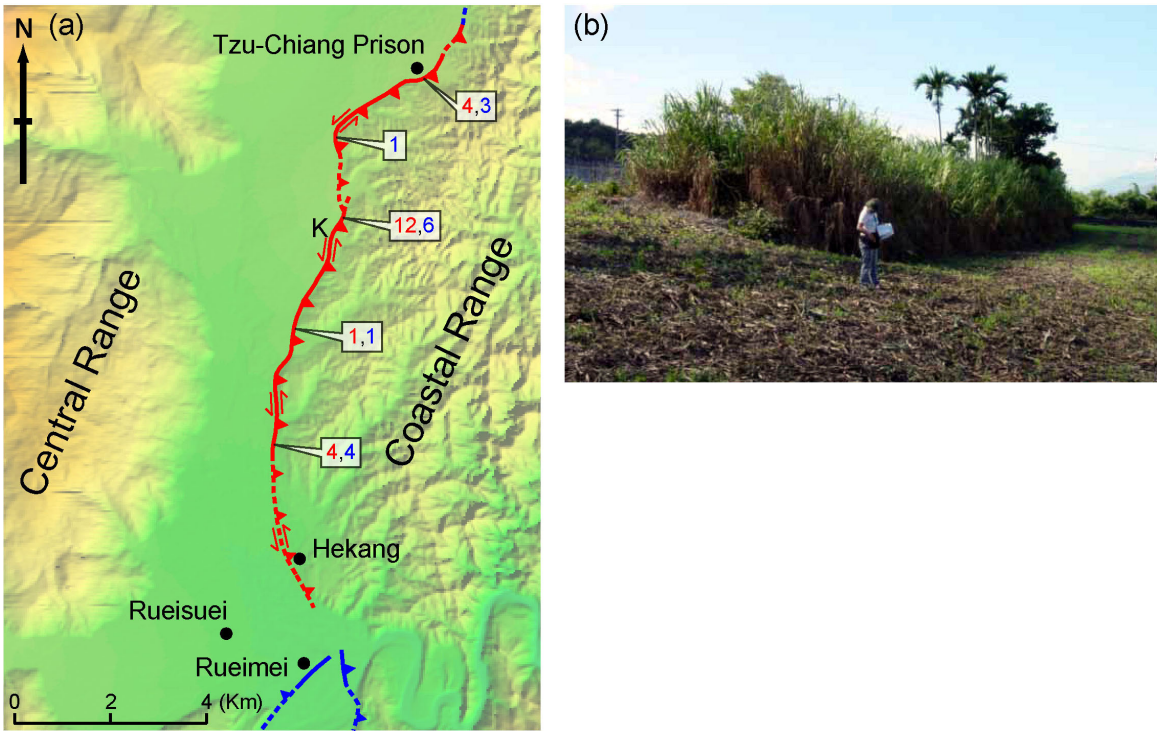

Figure 3.5. (a) Map of the Rueisuei rupture (in red). Blue lines are active structures that did not rupture in 1951. Modified from *Shyu et al.* [2002, 2005b] and unpublished results of J.B.H. Shyu and L.-H. Chung. For each section of the rupture a few km long, numbers of photographs showing ruptures or cracks (in red) and interview results of actual surface break (in blue) are also shown. (b) A photograph taken at point K in Figure 3.5a, showing the scarp produced in 1951. View is toward the south. A recent trench opened at this location revealed 0.75 m of vertical offset during the 1951 event [*Chen et al.*, 2004].

we have found, there is no way to resolve a left-lateral component. Vertical offset, on the other hand, is usually clear and greater than 1 m, with a maximum of 2.1 m. Most of the rupture scarps are still visible, and a recent trench across one of them (Figure 3.5b) revealed 0.75 m of vertical offset during the 1951 earthquake [*Chen et al.*, 2004].

Our investigation indicates that the northern end of the Rueisuei rupture is near the Tzu-Chiang Prison, but its southern end is more difficult to determine. The southernmost location where we have found evidence for the rupture is near the village of Hekang (Figure 3.5a). Although the village of Rueimei was heavily damaged during the earthquake with many collapses of houses, none of the local residents we interviewed recalled any surface rupture in or near the village. There were also widespread landslides south of Rueimei during the earthquake, but none are clearly related to fault

rupture. Thus, it appears that the southern end of the Rueisuei rupture was approximately at Hekang.

The Rueisuei rupture was coincident with a topographic break at the western base of the Coastal Range, where, based upon geomorphic evidence, *Shyu et al.* [2005b] mapped the active strand of the Longitudinal Valley fault. Thus, as with the 1951 Chihshang rupture, the Rueisuei rupture of 1951 occurred along a segment of the Longitudinal Valley fault. The oblique sense of offset along the Rueisuei rupture was similar to the sense of offset along the Chihshang rupture, and in both cases, the 1951 rupture had the same sense of slip as is indicated on geologic maps of the Longitudinal Valley fault [e.g., *Chen*, 1988; *Ho*, 1988].

3.5.3 The Yuli rupture

The Yuli rupture of 1951 was best documented near the town center of Yuli. Since Yuli was already a medium-sized town when the earthquake struck, we have found more than five photographs showing the ruptures and earthquake damage. Farther from the town center, the evidence is far more scattered [*Chung*, 2003].

Unlike the Chihshang and Rueisuei ruptures, which followed mostly the eastern edge of the Longitudinal Valley, the Yuli rupture lay on the valley floor, in places only 1 km or so from the Central Range (Figure 3.6a). The southern end of the rupture was just south of Yuli. It ran through the town center and destroyed many buildings, including the former Yuli Elementary School [e.g., *Hsu*, 1962; *Bonilla*, 1975; *Yu*, 1997]. North of the town center, the rupture probably extended along the Hsiukuluan River bed. Based upon local witnesses and old photographs, we suggest that it extended to a point about 4 km southeast of Rueisuei (Figure 3.6a). The total length of the Yuli rupture is about 20 km. Near Yuli, the Yuli rupture was nearly parallel to the Chihshang rupture and stepped about 1.5 km to the west of the Chihshang rupture.

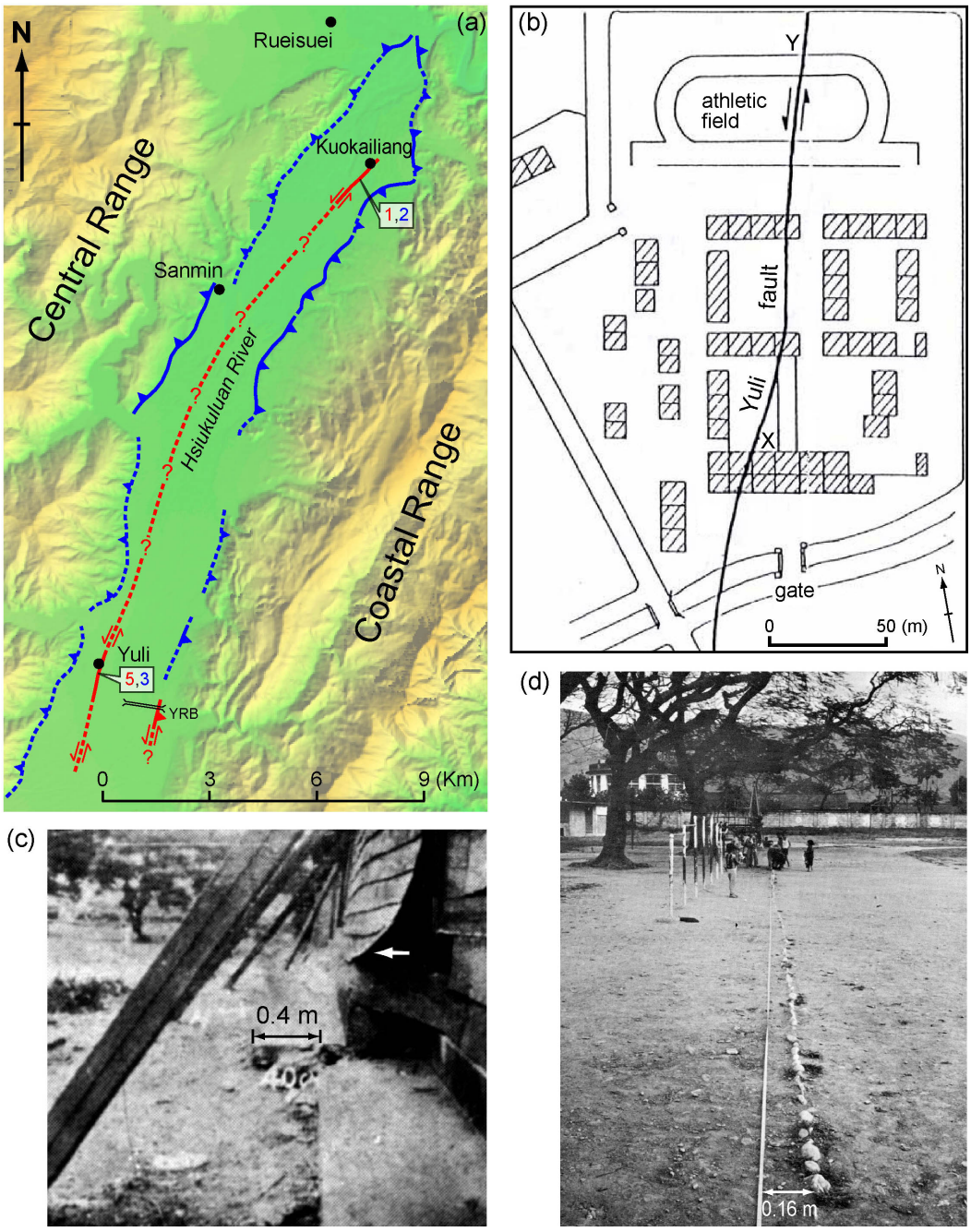

Figure 3.6. (a) Map of the Yuli rupture (in red). Blue lines are active structures that did not rupture in 1951. Modified from *Shyu et al.* [2005b] and unpublished results of J.B.H. Shyu and L.-H. Chung. Note that near Yuli, the Yuli and Chihshang ruptures were sub-parallel and about 1.5 km apart. YRB: Yuli railroad bridge. For the sections of the rupture near Yuli and Kuokailiang ridge, numbers of photographs showing ruptures or cracks (in red) and interview results of actual surface break (in blue) are also shown. (b) Detailed map showing the Yuli rupture at the Yuli Elementary School, modified from *Bonilla* [1975] and *Yu* [1997]. (c) Offset in 1951 of about 0.4 m near the classrooms in the Yuli Elementary School, at point X in Figure 3.6b. View is toward the east. Modified from *Taiwan Weather Bureau* [1952]. (d) Offset in 1951 of about 0.16 m at the edge of the athletic field in the Yuli Elementary School, at point Y in Figure 3.6b. View is toward the east. Modified from *Bonilla* [1975].

In the town center of Yuli, all of the photographs we have found indicate that the rupture was almost purely left-lateral strike slip. Although some reports suggested a small vertical component of slip [e.g., *Yu*, 1997], no vertical offsets are visible in the photographs. One of the most thoroughly documented locations of the rupture was the former Yuli Elementary School (Figure 3.6b). The classroom building at the school was offset left-laterally about 0.4 m (Figure 3.6c). However, a row of pebbles at the northern edge of the athletic field of the school was offset only about 0.16 m [*Bonilla*, 1975] (Figure 3.6d). The amount of offset therefore varied significantly in a very short distance within the school grounds [*Bonilla*, 1975], typical for strike-slip faults.

While no document reported the extension of the rupture north from the town center of Yuli, we believe that it extended along the Hsiukuluan River bed to Kuokailiang, approximately 4 km southeast of Rueisuei (Figure 3.6a) where there is a linear ridge about 200 m long, rising more than 10 m above a river terrace east of the Hsiukuluan River (Figure 3.7a). The landowner, who lives right next to the ridge, recalled ruptures along the eastern side of the ridge during the 1951 earthquake which may have also extended southward more than 500 m past the ridge [*Yang*, 1986]. Since the long axis of the ridge trends toward the ruptures in Yuli, we wonder whether or not the surface ruptures were continuous between these two locations. In fact, we have found a couple of photographs of ruptures in the riverbed between Yuli and Kuokailiang, near the village of Sanmin [*Yu*, 1997] (Figures 3.7b and 3.7c). We therefore believe the Yuli rupture may well have traversed the riverbed from Yuli to Kuokailiang ridge, a distance of about 16 km.

There is no evidence for the Yuli rupture north of Kuokailiang. Although the Yuli and Rueisuei ruptures were originally mapped by *Hsu* [1962] as a single Yuli fault, with most of the later investigations [e.g., *Yu*, 1997; *Cheng et al.*, 1996; *Lin et al.*, 2000] followed this interpretation, we found no evidence that the Yuli rupture was continuous with the Rueisuei rupture. In fact, our mapping of tectonic landforms [*Shyu et al.*,

Figure 3.7. Proposed extrapolation of the Yuli rupture of 1951 north of Yuli. (a) Kuokailiang ridge, about 4 km southeast of Rueisuei, is a linear ridge about 200 m long and more than 10 m high above a river terrace. The 1951 ruptures ran along the near (eastern) side of the ridge. (b) Ruptures in the riverbed, perhaps near the village of Sanmin. View is toward northeast. From *Yu* [1997]. (c) Another photograph of ruptures in the riverbed north of Yuli. The photograph was taken by T. L. Hsu and provided by M.-S. Lin.

2005b] shows that the two ruptures occurred on two distinct faults. First, the Yuli rupture traversed the Longitudinal Valley floor, whereas the Rueisuei rupture ran along the eastern edge of the valley. More importantly, the style of offset on the two ruptures differed markedly. Offsets along the Yuli rupture were almost pure left-lateral strike slip, while offsets on the Rueisuei rupture were oblique-slip with a distinct vertical component. This difference in style of offset may well be the reason why documentation was more sparse along the Yuli rupture; the moletracks and *en echelon* cracks of strike-slip ruptures are generally more subtle to the untrained eye than the scarps of dip-slip faults.

3.5.4 The Yuli rupture and the Longitudinal Valley fault

We believe that the Yuli rupture, unlike the Chihshang and Rueisuei ruptures, is not part of the Longitudinal Valley fault. Co-seismic offsets along both the Chihshang and Rueisuei ruptures were oblique-slip, as is the long-term movement along the Longitudinal Valley fault [e.g., *Chen*, 1988; *Ho*, 1988], whereas the Yuli rupture had predominantly left-lateral offset. Moreover, there was a 1.5 km left step between the Chihshang and Yuli ruptures.

Based upon geomorphic evidence, *Shyu et al.* [2005b] have mapped the major active strand of the Longitudinal Valley fault between Yuli and Rueisuei (Figure 3.6a). This active strand runs approximately along the eastern side of the Longitudinal Valley, about 1.5 km east of the Yuli rupture. Although this active fault strand is obvious geomorphically, it did not break during the 1951 earthquake. We have found neither documents nor photographs showing rupture along any of the topographic scarps along this strand, and none of the residents we interviewed recalled any surface ruptures on this side of the Longitudinal Valley between Yuli and Rueisuei. Although the area was not as heavily populated as Yuli in 1951, there were many small villages on the eastern side of the Longitudinal Valley, most of them along the mapped strand of the Longitudinal Valley fault. It is therefore unlikely that any surface rupture would have gone unnoticed, even if the offset had been small. By contrast, there are many photographs showing very subtle surface deformation from even more sparsely-populated areas along the Chihshang, Rueisuei, and Yuli ruptures. Thus, we believe that the lack of photographs showing surface rupture along this strand indeed indicates that there was no surface rupture along this part of the Longitudinal Valley fault.

Of course, this segment of the Longitudinal Valley fault might have ruptured at depth during the November 1951 earthquakes but the rupture might not have reached the surface. No reliable seismologic information such as relocated aftershocks is available

to verify or disprove this. However, since the well-documented part of the Yuli rupture within the town center of Yuli was clearly separate from and sub-parallel to the mapped strand of the Longitudinal Valley fault, any attempt to connect the Yuli rupture back to the fault would be geometrically difficult. Thus we believe that the Yuli rupture is wholly separate from this part of the Longitudinal Valley fault.

Instead, the Yuli rupture appears to traverse the Hsiukuluan River bed to Kuokailiang ridge. When mapping the active structures in the Longitudinal Valley, *Shyu et al.* [2005b] interpreted the ridge to be the product of a strike-slip fault west of the Longitudinal Valley fault. The mapped strand of the Longitudinal Valley fault, with obvious reverse fault landforms such as secondary folds in its hanging-wall block, lies about 1.5 km east of the ridge. We believe that the ridge is not formed by another strand of the fault because it is symmetrical: both its western and eastern slopes above the river terrace are steep and similar in height. This is distinct from the secondary folds found along the Longitudinal Valley fault. Rather, it resembles a "pressure" ridge, like those typically found along strike-slip faults. Moreover, the November 1951 rupture ran along the eastern side of the ridge. If the ridge is indeed formed by movements along an east-dipping strand of the Longitudinal Valley fault, the rupture would have been along its western side.

A small outcrop in Kuokailiang ridge reveals that the top of fluvial gravels underlying the ridge surface is currently higher than the surrounding terraces [*Chung*, 2003; *L.-H. Chung and J.B.H. Shyu*, unpublished data]. This indicates at least several meters of vertical separation between the ridge and the surrounding terraces. For a fault that is dominantly strike-slip, this amount of total vertical offset suggests at least several tens of meters of cumulative left-lateral offset. Thus the Yuli rupture appears to break along a pre-existing strike-slip fault, with clear evidence for prior strike slip.

One may argue that our interpolation of the Yuli rupture from Yuli to Kuokailiang is rather speculative and that the surface deformation shown in Figure 3.7 may be merely

secondary effects caused by the shaking of the earthquake. In fact, there are several photographs showing secondary effects such as sandblows or other liquefaction features. We did not use those photographs because they do not indicate the location of surface ruptures. However, because the ruptures were well-documented both at Yuli and Kuokailiang, it seems more likely than not that surface rupture extended between the two locations. Thus the fissures shown in Figure 3.7, with their NNE-SSW orientation, may indeed be primary surface ruptures within the riverbed.

3.6 Discussion

3.6.1 The November 1951 earthquake series: a complex rupture event

The November 1951 earthquakes in the Longitudinal Valley constitute one of the most disastrous seismic episodes in the recorded history of eastern Taiwan. Although many kilometers of surface rupture were reported after the earthquake, no detailed map of the ruptures was produced. Most maps depicted the ruptures as occurring along a nearly straight line, with a discontinuity between Fuli and Yuli in some renditions [e.g., *Hsu*, 1962; *Hsu and Chang*, 1979; *Cheng et al.*, 1996; *Chu and Yu*, 1997] (Figure 3.2). Our re-evaluation reveals that, in fact, the ruptures were more complicated than this. We divide the surface breaks into three separate ruptures — the Chihshang, Yuli, and Rueisuei ruptures, each with its own distinct characteristics. The Chihshang and Rueisuei ruptures occupied separate 30- and 15-km-long segments of the sinistral reverse Longitudinal Valley fault. The Yuli rupture occurred along a left-lateral fault that traverses the valley floor more than 1 km west of the Longitudinal Valley fault.

The recent relocation and parameterization of the sources of the two earthquakes by *Cheng et al.* [1996] are consistent with these rupture patterns. Their hypocenter for the first shock, at 02:47, is approximately at the southern end of the Chihshang rupture

(Figure 3.2). The focal mechanism of this earthquake shows that the earthquake was generated by a thrust fault with a left-lateral component, striking similarly to the Chihshang rupture. Taking into account the uncertainty, the hypocenter may well be on the east-dipping plane of the Longitudinal Valley fault. Their hypocenter for the second shock, at 02:50, is near the northern end of the Chihshang rupture and the southern end of the Yuli rupture. The large uncertainty of the hypocenter means that it could be consistent with rupture along a primarily sinistral Yuli fault. The focal mechanism of this earthquake is poorly constrained, but *Cheng et al.* [1996] believed that there was a significant left-lateral strike-slip component of the rupture.

We believe that the Chihshang rupture produced the first shock and induced the Yuli and Rueisuei ruptures, producing the second, larger shock. The lengths of the ruptures help us calculate the moment magnitudes (M_w) of the two shocks based upon published regressions of length against magnitude [e.g., *Wells and Coppersmith*, 1994]. The first shock would have a moment magnitude (M_w) of 6.8, whereas the moment magnitude of the second shock would have been about 6.9. The similarity in magnitude of these two shocks is significantly different from that calculated by *Cheng et al.* [1996], because the calculation of *Cheng et al.* [1996] was based on the map of *Hsu* [1962] which shows a much greater difference in the lengths of the Chihshang and combined Yuli/Rueisuei ruptures. Similarity in magnitude of the two quakes is supported by the original earthquake report of the *Taiwan Weather Bureau* [1952], in which the intensity maps for the two shocks have similar peak intensities and areas.

It is well known that earthquakes can be triggered by changes in Coulomb failure stress that result from an earlier earthquake [e.g., *Harris*, 1998; *Stein*, 2003]. This mechanism has been invoked, for example, to explain the progressive failure of the North Anatolian fault between 1939 and 1999 [e.g., *Stein et al.*, 1997] and to calculate future seismic hazards along the fault [e.g., *Hubert-Ferrari et al.*, 2000; *Parsons et al.*, 2000]. In general, after a major earthquake, areas where shear stress has increased on optimally

oriented planes are favored areas for aftershocks and/or subsequent mainshocks to occur [*Harris*, 1998]. In many cases, the areas where stress increases significantly are near the ends of the ruptures [e.g., *Hubert-Ferrari et al.*, 2000; *Anderson and Ji*, 2003]. Since the epicenter of the second shock of the 1951 earthquakes was near the northern end of the first rupture, it might well be in an area where the local stress field changed to promote ruptures. Moreover, the Yuli rupture of the second shock lay about 1.5 km west of the Chihshang rupture, which broke during the first shock. The reverse component of slip on the east-dipping Chihshang rupture might have also decreased the normal stress around the Yuli rupture, thus promoting the left-lateral rupture to occur. Such induced rupture events, with different modes of slip due to local stress field change, are exemplified by the Rainbow Mountain-Fairview Peak-Dixie Valley earthquake of 1954 [e.g., *Hodgkinson et al.*, 1996]. There, a M7.2 oblique-slip event triggered failure of an adjacent normal fault in a M6.7 earthquake.

The relationship between the Yuli and Rueisuei ruptures is also complex. There is a gap of approximately 5 km between these two ruptures (Figure 3.2). It is noteworthy, however, that the northern end of the Yuli rupture at Kuokailiang is very close to the unruptured strand of the Longitudinal Valley fault and may well extend beneath the Longitudinal Valley fault further north (Figures 3.2 and 3.6a). Thus it is plausible that the Yuli rupture triggered the Rueisuei rupture. This would be reminiscent of what happened during the Enggano, Sumatra, earthquake, which occurred on 4 June 2000. About 65% of this earthquake's moment was produced by strike-slip rupture on a fault in the downgoing oceanic slab. This was followed by failure of a patch of the overlying subduction interface [*Abercrombie et al.*, 2003].

Another important result of this documentation of the 1951 rupture is that the Longitudinal Valley fault, a fault that is currently creeping at a rate up to 20 mm/yr, previously failed seismically. The Chihshang rupture was along a portion of the fault that is well known for its rapid creep behavior [e.g., *Yu and Liu*, 1989; *Angelier et al.*,

1997; *Chow et al.*, 2001; *Lee et al.*, 2001]. Since the fault ruptured during the 1951 earthquake, one might well suspect that, if currently observed creep is not merely the afterslip from the 1951 earthquakes, creep is not releasing all strain accumulating in the blocks adjacent to the fault and that creep should be viewed as retarding rather than eliminating the prospect of future seismic ruptures there. At this moment we do not have enough information to determine whether or not this dual behavior also characterizes strands of the Longitudinal Valley fault further to the north or to the south. Preliminary geodetic measurements near Rueisuei indicate the fault may creep there, but much more slowly [*Yu and Liu*, 1989]. Further investigation is needed to resolve these details of strain accumulation and release along the Longitudinal Valley fault.

3.6.2 What is the Yuli fault?

The Yuli fault was originally proposed by *Hsu* [1962] in describing the 1951 earthquake ruptures. *Hsu*'s [1962] definition encompasses both our Yuli and Rueisuei ruptures. His idea was that since the Yuli fault ruptured in 1951, it is probably the main fault of the Longitudinal Valley. Later studies of the Longitudinal Valley, such as those by *Chu and Yu* [1997], *Yu* [1997], and *Lin et al.* [2000], all adopted this point of view, mapping the Longitudinal Valley fault through the town of Yuli. This, however, creates geometric problems. The town of Yuli is far from the western foothills of the Coastal Range, where the Longitudinal Valley fault runs. As a result, previous maps show either a significant bend or *en echelon* step over of the fault south of Yuli. These maps ignore the continuous geomorphic evidence showing that the Longitudinal Valley fault lies along the western Coastal Range front.

In fact, there are three principal faults in the valley, and portions of two of these ruptured in 1951. No geomorphic or structural evidence supports the geometries of the earlier workers. The sinistral reverse Longitudinal Valley fault is clearly continuous

along the entire eastern side of the valley between Taitung and Hualien [*Shyu et al.*, 2005b]. It does not bend or step over toward the west except at Rueisuei, where the Coastal Range front itself bends.

Therefore, the "Yuli fault" of *Hsu* [1962] clearly encompasses two different structures. Its northern part, defined by the Rueisuei rupture, is actually a portion of the sinistral reverse Longitudinal Valley fault that is bringing Coastal Range rocks over the Longitudinal Valley. The southern part of *Hsu*'s [1962] Yuli fault is the predominantly left-lateral Yuli rupture. Since the northern part of *Hsu*'s [1962] Yuli fault is part of the Longitudinal Valley fault, we propose to retain Hsu's name only for the fault that broke along the Yuli rupture. Thus, we suggest that the term "Yuli fault" hereinafter only be used in reference to the Yuli rupture of the 1951 earthquakes. This fault is a sinistral fault that traverses the Longitudinal Valley with negligible vertical movement.

We are unsure whether or not the Yuli fault dips eastward at depth. If so, it could be an integral part of the obliquely slipping Longitudinal Valley fault zone. However, its location, west of the east-dipping Longitudinal Valley fault, and its predominance of strike-slip movement make such a geometry quite unlikely. We believe the alternative — that it is a separate, steeply dipping, strike-slip fault that has developed within the sediments of the valley, structurally separate from the Longitudinal Valley fault system (Figure 3.8).

Why is there a Yuli fault? During the oblique collision between the Luzon volcanic arc and the Central Range of Taiwan, the Longitudinal Valley suture is absorbing both the convergence between the two and the northward movement of the docked volcanic rocks of the Coastal Range [e.g., *Shyu et al.*, 2005a, 2005b]. Thus the Longitudinal Valley fault is characterized by high rates of both reverse and left-lateral motions. Along the middle part of the Longitudinal Valley, the existence of the predominantly sinistral Yuli fault may indicate that the Longitudinal Valley fault there has a smaller left-lateral component than elsewhere. Topographic features of the Longitudinal Valley fault, in

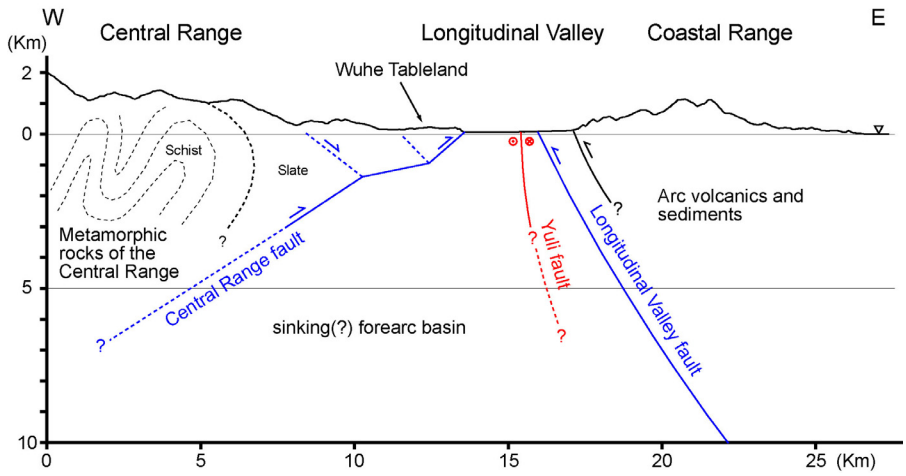

Figure 3.8. A schematic tectonic E-W cross section of the Longitudinal Valley at the latitude of the Wuhe Tableland. The west-dipping Central Range fault crops out along the eastern edge of the Central Range and the Wuhe Tableland, but did not rupture during the 1951 earthquakes. The steeply dipping(?) Yuli fault and sections of the east-dipping Longitudinal Valley fault, on the other hand, ruptured. The Longitudinal Valley fault crops out along the eastern side of the Longitudinal Valley and accommodates uplift and deformation of the terraces along the western flank of the Coastal Range. The Yuli fault is a separate, discontinuous strike-slip fault developed in the sediments of the valley, structurally separate from the Longitudinal Valley fault system. The Longitudinal Valley fault may have a smaller left-lateral component in this segment than elsewhere, and the sinistral Yuli fault appears to accommodate the northward motion of the Coastal Range. Black: inactive fault in basement rocks; Blue: active fault not ruptured in 1951; Red: ruptures of 1951.

fact, suggest that this may be the case. The extreme linearity of the Chihshang segment of the fault probably indicates a large component of strike-slip motion, whereas north of Yuli the fault trace is more irregular with many secondary anticlines and synclines in its hanging-wall block, typical for structures with larger components of reverse motion [*Shyu et al.*, 2005b]. Along-strike difference in behavior has also been suggested for the Longitudinal Valley fault based upon the significantly different pattern and numbers of relocated small earthquakes along the fault [e.g., *Kuochen et al.*, 2004]. We therefore suggest that the Yuli fault appears where oblique slip across the Longitudinal Valley has been more effectively partitioned onto two separate faults.

3.6.3 Implications for seismic hazard assessment

Our re-evaluation of the November 1951 ruptures raises many important questions

relevant to seismic hazard assessment in the Longitudinal Valley. For example, it is clear that between Yuli and Rueisuei the Longitudinal Valley fault did not rupture during the 1951 earthquakes. Why did this happen? We have proposed that the stress loading on the Yuli fault by the failure of the Chihshang segment of the Longitudinal Valley fault promoted the failure on the Yuli fault. The stress loading should, in fact, have been even higher for the unruptured segment of the Longitudinal Valley fault between Yuli and Rueisuei and have brought it closer to failure. A pre-1951 rupture along this segment may have shed so much stress from the adjacent crust that this segment could not be loaded to the point of failure by the rupture of adjoining segments to the north and south in 1951. Alternatively, it is conceivable that this segment fails entirely by creep. More detailed paleoseismic and geodetic investigations along this segment are needed to resolve this question.

The Chihshang and Rueisuei ruptures clearly represent seismic failure along segments of the Longitudinal Valley fault. However, the two segments are behaving quite differently at present. The Chihshang segment is creeping rapidly, whereas the Rueisuei segment is not. What does this imply about future seismic activity along these two segments? Does the Chihshang segment have a longer average recurrence interval than the Rueisuei segment, or does it just have smaller amounts of offset per earthquake? Again, paleoseismological and geodetic studies along these two segments could address these questions.

The Yuli fault may be the most poorly understood structure in the middle Longitudinal Valley. For example, we don't know at this moment whether or not this fault extends further northward, beneath the Longitudinal Valley fault, or further southward, beneath the Central Range fault. Although the Yuli fault appears to have moved previously, there is no constraint on its long-term slip rate. Furthermore, *Bonilla* [1975] suggested that the Yuli fault might be creeping, but more recent investigations suggest that it is not [e.g., *Chung*, 2003]. A short-aperture geodetic array across this

fault should reveal which is the case. Paleoseismic studies could reveal its seismic behavior.

3.7 Conclusions

In our attempt to re-evaluate the ruptures of the November 1951 earthquake series in the Longitudinal Valley, eastern Taiwan, we have analyzed all published documents, relevant reports, and photographs and have interviewed more than 40 elderly local residents who experienced the earthquake. We divide the surface breaks into three separate ruptures from south to north — the Chihshang, Yuli, and Rueisuei ruptures. The Chihshang rupture was approximately 30 km long and probably ruptured during the first shock of the 1951 earthquake series. The length of the Yuli rupture was about 20 km, and the Rueisuei rupture was about 15 km long. Consideration of epicentral locations and focal mechanisms suggests that the Yuli and Rueisuei ruptures produced the second shock of the November 1951 series. The Chihshang and Rueisuei ruptures occurred along widely separate lengths of the Longitudinal Valley fault, and both experienced oblique-slip movement during the earthquake. The sense of slip along the Yuli rupture, on the other hand, was left-lateral, and the rupture occurred on a fault that traverses the middle of the valley floor and is distinct from the Longitudinal Valley fault. The failure of the Chihshang rupture, which produced the first shock of the November 1951 earthquakes, probably triggered the subsequent failure of the Yuli and Rueisuei ruptures. The active structures in this middle section of Taiwan's Longitudinal Valley are complex — mountain ranges to the east and west are converging on the valley on two opposing reverse faults. The 1951 earthquakes involved partial rupture of just one of these and a strike-slip fault broke the valley sediments in between.

3.8 Acknowledgments

We thank T.-C. Lin and Y. Wang for their assistance with the field work. We are also grateful for valuable discussions with J.-P. Avouac, W.-S. Chen, J.-C. Hu, J.-C. Lin, and M.-S. Lin. The comments and suggestions of reviewers H.-T. Chu and T.E. Fumal helped us improve this manuscript significantly. Many old photographs and documents were kindly provided by T.L. Hsu, M.-S. Lin, and S.-N. Cheng. The help of many local residents in eastern Taiwan, especially S.-H. Chang, K.-C. Chiang, L.-P. Tseng, and C.-S. Chang, is greatly appreciated. This work was supported by both the National Science Foundation and the National Science Council. This research was also supported in part by the Gordon and Betty Moore Foundation. This is California Institute of Technology (Caltech) Tectonics Observatory Contribution #2.

3.9 References

Abe, K. (1981), Magnitudes of large shallow earthquakes from 1904 to 1980, *Phys. Earth Planet. Int.*, *27*, 72-92.

Abercrombie, R. E., M. Antolik, and G. Ekström (2003), The June 2000 M_w 7.9 earthquakes south of Sumatra: Deformation in the India-Australia Plate, *J. Geophys. Res.*, *108*, 2018, doi:10.1029/2001JB000674.

Anderson, G., and C. Ji (2003), Static stress transfer during the 2002 Nenana Mountain-Denali Fault, Alaska, earthquake sequence, *Geophys. Res. Lett.*, *30*, 1310, doi:10.1029/2002GL016724.

Angelier, J., H.-T. Chu, and J.-C. Lee (1997), Shear concentration in a collision zone: kinematics of the Chihshang Fault as revealed by outcrop-scale quantification of active faulting, Longitudinal Valley, eastern Taiwan, *Tectonophysics*, *274*, 117-143.

Barka, A. (1999), The 17 August 1999 Izmit earthquake, *Science*, *285*, 1,858-1,859.

Biq, C. (1965), The East Taiwan Rift, *Pet. Geol. Taiwan*, *4*, 93-106.

Bonilla, M. G. (1975), A review of recently active faults in Taiwan, *Open File Rep. 75-41*, 58pp., U. S. Geol. Surv., Menlo Park, Calif.

Bonilla, M. G. (1977), Summary of Quaternary faulting and elevation changes in Taiwan, *Mem. Geol. Soc. China*, *2*, 43-55.

Chang, C. P., J. Angelier, C. Y. Huang, and C. S. Liu (2001), Structural evolution and significance of a mélange in a collision belt: the Lichi Mélange and the Taiwan arc-continent collision, *Geol. Mag.*, *138*, 633-651.

Chang, H.-C., C.-W. Lin, M.-M. Chen, and S.-T. Lu (1998), *An Introduction to the Active Faults of Taiwan, Explanatory Text of the Active Fault Map of Taiwan* (in Chinese with English abstract), *Spec. Pub. Cent. Geol. Surv.*, *10*, 103pp., Cent. Geol. Surv., Ministry Econ. Affairs, Taipei, Taiwan.

Chen, J.-S. (1976), The analysis and design of refraction and reflection seismic survey of the Taitung area, *Pet. Geol. Taiwan*, *13*, 225-246.

Chen, J.-S., J.-N. Chou, Y.-C. Lee, and Y.-S. Chou (1974), Seismic survey conducted in eastern Taiwan (in Chinese with English Abstract), *Pet. Geol. Taiwan*, *11*, 147-163.

Chen, W.-S. (1988), Tectonic evolution of sedimentary basins in Coastal Range, Taiwan (in Chinese), Ph.D. thesis, 304pp., Natl. Taiwan Univ., Taipei.

Chen, W.-S., et al. (2004), Paleoseismologic studies of the 1951 earthquake rupture, Eastern Taiwan (in Chinese with English abstract), *Spec. Pub. Cent. Geol. Surv.*, *15*, 137-145.

Chen, Y.-G., W.-S. Chen, J.-C. Lee, Y.-H. Lee, C.-T. Lee, H.-C. Chang, and C.-H. Lo (2001), Surface rupture of 1999 Chi-Chi earthquake yields insights on active tectonics of central Taiwan, *Bull. Seismol. Soc. Am.*, *91*, 977-985.

Cheng, S. N., and Y. T. Yeh (1989), *Catalog of the Earthquakes in Taiwan from 1604 to 1988* (in Chinese), 255pp., Inst. Earth Sci., Acad. Sinica, Taipei, Taiwan.

Cheng, S.-N., Y. T. Yeh, and M.-S. Yu (1996), The 1951 Taitung earthquake in Taiwan, *J. Geol. Soc. China*, *39*, 267-285.

Chow, J., J. Angelier, J.-J. Hua, J.-C. Lee, and R. Sun (2001), Paleoseismic event and active faulting: from ground penetrating radar and high-resolution seismic reflection profiles across the Chihshang Fault, eastern Taiwan, *Tectonophysics*, *333*, 241-259.

Chu, H.-T., and M.-S. Yu (1997), The relationships between earthquakes and faults in the Taitung Longitudinal Valley (in Chinese), *Natl. Sci. Council Project Rep., No. NSC-86-2116-M-047-002*, 133pp., Natl. Sci. Council, Taipei, Taiwan.

Chu, H.-T., J.-C. Lee, and J. Angelier (1994), Non-seismic rupture of the Tapo and the Chinyuan area on the southern segment of the Huatung Longitudinal Valley Fault, Eastern Taiwan (in Chinese with English abstract), *Program with Abstracts, 1994 Ann. Meet. Geol. Soc. China*, 156-160, Taipei, Taiwan.

Chung, L.-H. (2003), Surface Rupture Reevaluation of the 1951 Earthquake Sequence in the Middle Longitudinal Valley and Neotectonic Implications (in Chinese with English Abstract), M.S. thesis, 138pp., Natl. Taiwan Univ., Taipei.

Gutenberg, B., and C. F. Richter (1954), *Seismicity of the Earth and Associated Phenomena*, 2nd ed., 310pp., Princeton Univ. Press, Princeton, N.J.

Harris, R. A. (1998), Stress triggers, stress shadows, and implications for seismic hazard, *J. Geophys. Res.*, *103*, 24,347-24,358.

Ho, C. S. (1986), A synthesis of the geologic evolution of Taiwan, *Tectonophysics*, *125*, 1-16.

Ho, C. S. (1988), *An Introduction to the Geology of Taiwan, Explanatory Text of the Geologic Map of Taiwan*, 2nd ed., 192pp., Cent. Geol. Surv., Ministry Econ. Affairs, Taipei, Taiwan.

Hodgkinson, K. M., R. S. Stein, and G. C. P. King (1996), The 1954 Rainbow Mountain-Fairview Peak-Dixie Valley earthquakes: A triggered normal faulting sequence, *J. Geophys. Res.*, *101*, 25,459-25,471.

Hsu, M.-T. (1980), *Earthquake Catalogues in Taiwan (from 1644 to 1979)* (in Chinese), 77pp., Natl. Taiwan Univ., Taipei.

Hsu, T. L. (1962), Recent faulting in the Longitudinal Valley of eastern Taiwan, *Mem. Geol. Soc. China*, *1*, 95-102.

Hsu, T. L., and H. C. Chang (1979), Quaternary faulting in Taiwan, *Mem. Geol. Soc. China*, *3*, 155-165.

Hsu, Y.-J., M. Simons, S.-B. Yu, L.-C. Kuo, and H.-Y. Chen (2003), A two-dimensional dislocation model for interseismic deformation of the Taiwan mountain belt, *Earth Planet. Sci. Lett.*, *211*, 287-294.

Hubert-Ferrari, A., A. Barka, E. Jacques, S. S. Nalbant, B. Meyer, R. Armijo, P. Tapponnier, and G. C. P. King (2000), Seismic hazard in the Marmara Sea region following the 17 August 1999 Izmit earthquake, *Nature*, *404*, 269-273.

Kuochen, H., Y.-M. Wu, C.-H. Chang, J.-C. Hu, and W.-S. Chen (2004), Relocation of the eastern Taiwan earthquakes and its tectonic implications, *Terr. Atmos. Oceanic Sci.*, *15*, 647-666.

Lallemand, S., and C.-S. Liu (1998), Geodynamic implications of present-day kinematics in the southern Ryukyus, *J. Geol. Soc. China*, *41*, 551-564.

Lee, J.-C., J. Angelier, H.-T. Chu, J.-C. Hu, and F.-S. Jeng (2001), Continuous monitoring of an active fault in a plate suture zone: a creepmeter study of the Chihshang Fault, eastern Taiwan, *Tectonophysics*, *333*, 219-240.

Lee, W. H. K., F. T. Wu, and S. C. Wang (1978), A catalog of instrumentally determined earthquakes in China (magnitude ≥ 6) compiled from various sources, *Bull. Seismol. Soc. Am.*, *68*, 383-398.

Lin, C.-W., H.-C. Chang, S.-T. Lu, T.-S. Shih, and W.-J. Huang (2000), *An Introduction to the Active Faults of Taiwan, 2nd ed., Explanatory Text of the Active Fault Map of Taiwan* (in Chinese with English abstract), *Spec. Pub. Cent. Geol. Surv.*, *13*, 122pp., Taipei, Taiwan.

Parsons, T., S. Toda, R. S. Stein, A. Barka, and J. H. Dieterich (2000), Heightened odds of large earthquakes near Istanbul: an interaction-based probability calculation, *Science*, *288*, 661-665.

Shih, T.-T., J.-C. Chang, C.-E. Hwang, C.-D. Shih, G.-S. Yang, and Y.-M. Sunlin (1983a), A geomorphological study of active fault in northern and eastern Taiwan (in Chinese with English abstract), *Geogr. Res.*, *9*, 20-72.

Shyu, J. B. H., K. Sieh, L.-H. Chung, Y.-G. Chen, and Y. Wang (2002), The active tectonics of eastern Taiwan—new insights from the two geomorphic tablelands (“the Feet”) in the Longitudinal Valley, *EOS, Trans., Am. Geophys. Uni.*, *83*(47), Fall Meet. Suppl., Abstract T61B-1278.

Shyu, J. B. H., K. Sieh, and Y.-G. Chen (2005a), Tandem suturing and disarticulation of the Taiwan orogen revealed by its neotectonic elements, *Earth Planet. Sci. Lett.*, *233*, 167-177.

Shyu, J. B. H., K. Sieh, Y.-G. Chen, and C.-S. Liu (2005b), The neotectonic architecture of Taiwan and its implications for future large earthquakes, *J. Geophys. Res.*, *110*, B08402, doi:10.1029/2004JB003251.

Sieh, K., et al. (1993), Near field investigations of the Landers earthquake sequence, April to July 1992, *Science*, *260*, 171-176.

Stein, R. S. (2003), Earthquake conversations, *Sci. Am.*, *288*(1), 72-79.

Stein, R. S., A. A. Barka, and J. H. Dieterich (1997), Progressive failure on the North Anatolian fault since 1939 by earthquake stress triggering, *Geophys. J. Int.*, *128*, 594-604.

Taiwan Weather Bureau (1952), The 1951 Earthquake Report (in Chinese), 83pp., Taiwan Weather Bureau, Taipei.

Teng, L. S. (1987), Stratigraphic records of the late Cenozoic Penglai orogeny of Taiwan, *Acta Geol. Taiwanica*, *25*, 205-224.

Teng, L. S. (1990), Late Cenozoic arc-continent collision in Taiwan, *Tectonophysics*, *183*, 57-76.

Teng, L. S. (1996), Extensional collapse of the northern Taiwan mountain belt, *Geology*, *24*, 949-952.

Treiman J. A., K. J. Kendrick, W. A. Bryant, T. K. Rockwell, and S. F. McGill (2002), Primary surface rupture associated with the M_w 7.1 16 October 1999 Hector Mine earthquake, San Bernardino County, California, *Bull. Seismol. Soc. Am.*, *92*, 1,171-1,191.

Wells, D. L., and K. J. Coppersmith (1994), New empirical relationships among magnitude, rupture length, rupture width, rupture area, and surface displacement, *Bull. Seismol. Soc. Am.*, *84*, 974-1,002.

Yang, G.-S. (1986), A geomorphological study of active faults in Taiwan – especially on the relation between active faults and geomorphic surfaces (in Chinese), Ph.D. thesis, 178pp., Chinese Culture Univ., Taipei, Taiwan.

Yang, Y.-C. (1953), Earthquakes in Hualien in the latest 41 years (in Chinese), *Hualien Literatures*, *1*, 67-71.

York, J. E. (1976), Quaternary faulting in eastern Taiwan, *Bull. Geol. Surv. Taiwan*, *25*, 63-75.

Yu, M.-S. (1997), Active faults in the Taitung Longitudinal Valley (in Chinese), Ph.D. thesis, 141pp., Natl. Taiwan Univ., Taipei.

Yu, S.-B., and C.-C. Liu (1989), Fault creep on the central segment of the Longitudinal Valley fault, eastern Taiwan, *Proc. Geol. Soc. China*, *32*, 209-231.

Yu, S.-B., H.-Y. Chen, and L.-C. Kuo (1997), Velocity field of GPS stations in the Taiwan

area, *Tectonophysics*, *274*, 41-59.

Yu, S.-B., L.-C. Kuo, R. S. Punongbayan, and E. G. Ramos (1999), GPS observation of crustal deformation in the Taiwan-Luzon region, *Geophys. Res. Lett.*, *26*, 923-926.

Chapter 4

Millennial Slip Rate of the Longitudinal Valley Fault from River Terraces: Implications for Convergence across the Active Suture of Eastern Taiwan

An earlier version of this chapter has been submitted as:

Shyu, J.B.H., K. Sieh, J.-P. Avouac, W.-S. Chen, and Y.-G. Chen, 2005, *Journal of Geophysical Research*, submitted for publication.

4.1 Abstract

The east-dipping Longitudinal Valley fault is a key element in the active tectonics of Taiwan. It is the principal structure accommodating convergence across one of the two active sutures of the Taiwan orogeny. To understand more precisely its role in the suturing process, we analyzed fluvial terraces along the Hsiukuluan River, the only river that cuts across the Coastal Range in eastern Taiwan in the fault's hanging-wall block. This allowed us to determine both its subsurface geometry and its millennial slip rate. The uplift pattern of the terraces is consistent with a fault-bend fold model. Our analysis yields a listric geometry, with dips decreasing downdip from about 50° to about 30° in the shallowest 2.5 km. The Holocene slip rate of the fault is about 23 mm/yr. This rate is far less than the 40 mm/yr rate of shortening across the Longitudinal Valley derived from GPS measurements. The discrepancy may reflect an actual difference in millennial and decadal rates of convergence. An alternative explanation is that the discrepancy is accommodated by a combination of subsidence of the Longitudinal Valley and slip on the Central Range fault. The shallow, listric geometry of the Longitudinal Valley fault at the Hsiukuluan River valley differs markedly from the deep listric geometry illuminated by earthquake hypocenters near Chihshang, 45 km to the south. We propose a model whereby this fundamental along-strike difference in geometry of the fault is a manifestation of the northward maturation of the suturing of the Luzon volcanic arc to the Central Range continental sliver.

Keywords: Taiwan, river terraces, Longitudinal Valley fault, neotectonics, suture.

4.2 Introduction

The Taiwan orogen is the product of ongoing collision between the Eurasian and Philippine Sea plates [e.g., *Ho*, 1986; *Teng*, 1987, 1990, 1996; and references therein] (Figure 4.1). This collision, which started a few million years ago, has created two belts of active structures on and around the island [*Malavieille et al.*, 2002; *Shyu et al.*, 2005a]. Frequent ruptures of these active faults have made Taiwan one of the most seismically active places on Earth [e.g., *Bonilla*, 1975, 1977; *Hsu*, 1980; *Cheng and Yeh*, 1989]. The most notable recent earthquake, the disastrous Chi-Chi earthquake of 1999, was produced by rupture of the Chelungpu fault, one of the many major active faults constituting Taiwan's western neotectonic belt [e.g., *Chen et al.*, 2001; *Kelson et al.*, 2001].

Along the eastern flank of the island, the linear, N-S trending Longitudinal Valley, which separates the Central and Coastal Ranges, marks the suture between an accreted volcanic island arc and a continental sliver. The Longitudinal Valley fault, one of the most active structures on the island, dominates this eastern neotectonic belt [e.g., *Angelier et al.*, 1997; *Shyu et al.*, 2005a] (Figure 4.2). This east-dipping thrust fault accommodates rapid uplift of the Coastal Range on its hanging-wall block [e.g., *Yu and Liu*, 1989; *Hsu et al.*, 2003]. Several large seismic ruptures of this fault have occurred in the past century [*Hsu*, 1962; *Bonilla*, 1975, 1977; *Cheng et al.*, 1996]. Part of the fault is also creeping aseismically at a high rate [e.g., *Angelier et al.*, 1997; *Lee et al.*, 2001, 2003]. Hypocenters of small earthquakes illuminate the fault plane and show that it has a listric geometry near the town of Chihshang [*Chen and Rau*, 2002; *Kuochen et al.*, 2004]. Elsewhere, however, the geometry of the fault remains poorly known.

According to GPS results, about 30-40 mm/yr of shortening is currently taken up between the Central Range block and the Coastal Range block [e.g., *Yu et al.*, 1997; *Hsu et al.*, 2003] (Figure 4.3). Whereas most of this shortening may be absorbed by

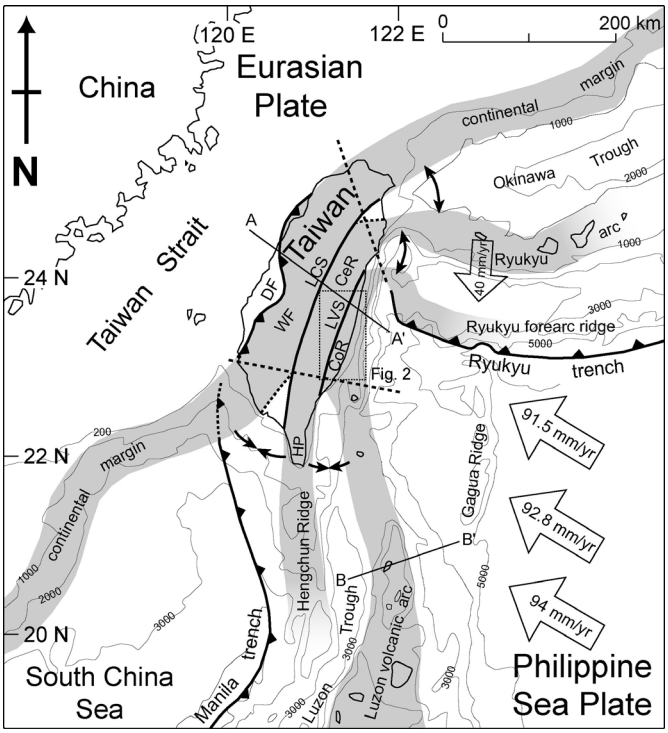

Figure 4.1. The Taiwan orogen is being created by a tandem suturing of the Luzon volcanic arc and a sliver of continental crust to the Chinese continental margin. The Longitudinal Valley suture (LVS) in eastern Taiwan represents the eastern of the two sutures, joining the Coastal Range (CoR) and the Central Range (CeR) blocks. Current velocity vectors of the Philippine Sea plate relative to South China, at 124°E and 20°, 21°, and 22°N, are calculated using the Recent plate velocity model (REVEL) of *Sella et al.* [2002]. Current velocity vector of the Ryukyu arc is adapted from *Lallemand and Liu* [1998]. Black dashed lines are the northern and western limits of the Wadati-Benioff zone of the two subduction zones, taken from the seismicity database of the Central Weather Bureau, Taiwan. DF: deformation front; LCS: Lishan-Chaochou suture; WF: Western Foothills; HP: Hengchun Peninsula. Adapted from *Shyu et al.* [2005b].

left-lateral reverse slip along the Longitudinal Valley fault, the Coastal Range, in the hanging-wall block of the fault, is not a large mountain range: Its maximum elevation is only about 1.6 km, significantly lower than the 4-km-high peaks of the Central Range. Therefore, one may suspect that other mechanisms, such as possible underthrusting of the Longitudinal Valley floor, may absorb at least part of the shortening, or the Longitudinal Valley fault is a relatively young feature of the Taiwan orogen.

Near the middle of the Longitudinal Valley the Hsiukuluan River cuts through the Coastal Range and flows eastward to the Philippine Sea. Along this segment of the river (hereafter referred to as Hsiukuluan canyon) are many levels of fluvial terrace [e.g.,

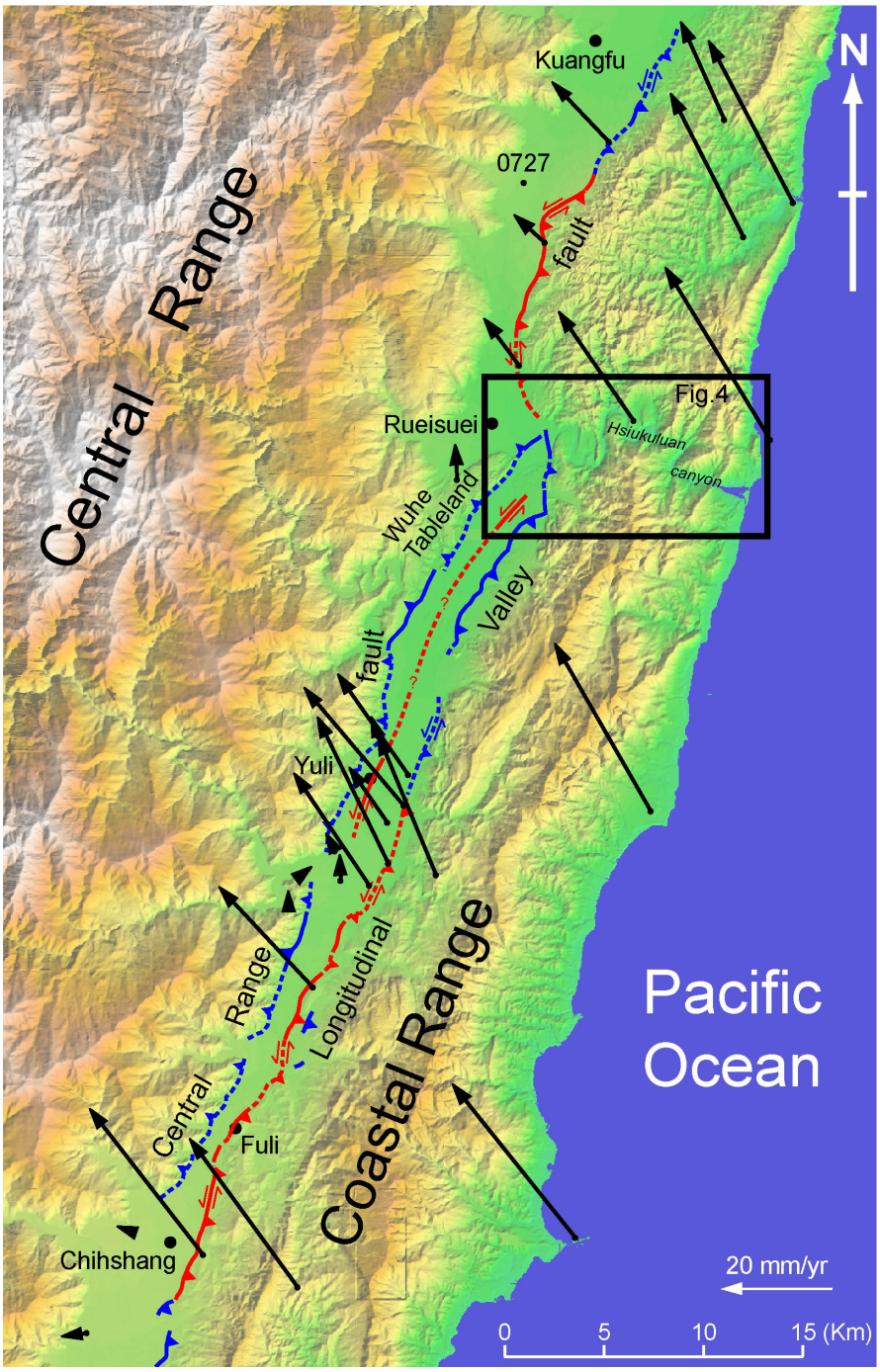

Figure 4.2. Map of major structures in the middle part of the Longitudinal Valley. The Longitudinal Valley fault is an east-dipping, obliquely slipping reverse fault, along which the Coastal Range is rising rapidly and moving toward the Central Range. The less prominent Central Range fault is a west-dipping reverse fault, above which many fluvial terraces and the Wuhe Tableland are rising slowly. Faults that ruptured during the 1951 earthquakes are colored red. Major faults and flexures that did not rupture in 1951 but are known to be active are colored blue. Adapted from *Shyu et al.* [2005c]. Black arrows are GPS vectors for the period 1993 to 1999 [*Hsu et al.*, 2003]. Motions are relative to station 0727, about 7 km southwest of Kuangfu. The differences between vectors indicate shortening across the valley of about 40 mm/yr.

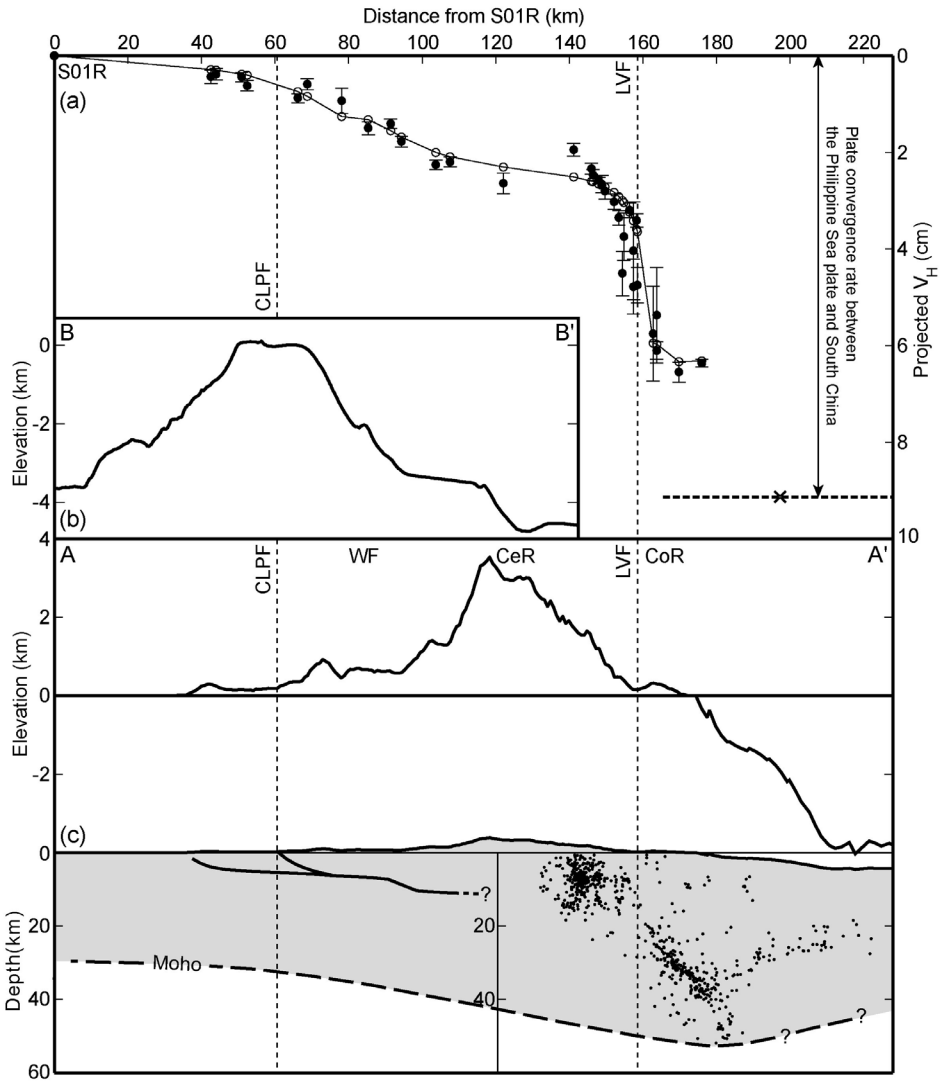

Figure 4.3. (a) A GPS transect across the Taiwan orogen (adapted from *Hsu et al.* [2003]). The transect trends 306° and includes measurements within a swath about 60 km wide, approximately along line A-A′ in Figure 4.1. About 40 mm/yr of horizontal shortening is currently absorbed across this section of the Longitudinal Valley. The western Taiwan neotectonic belt, which includes the Chelungpu fault (CLPF), absorbs the remaining ~20 mm/yr of horizontal shortening. Solid points are the observed velocities along 306°, and circles are the predicted points using a two-dimensional interseismic dislocation model. All points are relative to station S01R in the Penghu Islands, which can be considered to be on the stable South China continental block [e.g., *Sella et al.*, 2002]. The plate convergence rate between the Philippine Sea plate and South China, calculated using the Recent plate velocity model (REVEL) of *Sella et al.* [2002], is also along 306° and about 20 mm/yr greater than the convergence rate across the transect. LVF: Longitudinal Valley fault. (b) Topographic profiles across Taiwan along line A-A′, and for comparison, across an undeformed volcanic island of the Luzon arc along line B-B′ in Figure 4.1. Vertical exaggeration is 10 times. WF: Western Foothills; CeR: Central Range; CoR: Coastal Range. (c) Several major crustal structural features along the A-A′ profile across Taiwan. A shorter profile of seismicity across eastern Taiwan, at the same location but with about half the width, shows two notable planes of seismicity [*Kuochen et al.*, 2004]. A simplified structural cross section of the Western Foothills shows a décollement at a depth of about 6-10 km (modified from *Yue et al.* [2005]). The Moho across Taiwan, compiled from *Kim et al.* [2004], *Lin* [2005], and *McIntosh et al.* [2005], appears to be deepest beneath the Coastal Range, at about 50 km, and shallows to the west. No vertical exaggeration in (c).

Chang et al., 1992] (Figure 4.4), which provide a record of fluvial incision. Since the Hsiukuluan River is the only river that flows through the Coastal Range, these fluvial terraces provide a unique opportunity to assess long-term patterns and rates of uplift of the range. The deformational pattern and rates thus derived may then be translated into a geometry and slip rate for the Longitudinal Valley fault.

In this paper we first review the geologic setting of the Coastal Range and the Longitudinal Valley. We then describe the characteristics of the fluvial terraces along Hsiukuluan canyon, especially along the western half of the river valley where the terraces are more prominent. Age determinations of various terrace levels allow us to calculate incision rates along the river, which we can relate to uplift rates of the Coastal Range. These uplift rates and their spatial relationships provide information about the geometry and long-term slip rate of the Longitudinal Valley fault.

4.3 General geologic setting

Taiwan is located at the plate boundary of the Philippine Sea plate and the South China block of the Eurasian plate. South of Taiwan the convergence between these two blocks, currently at about 90 mm/yr (Figure 4.1), is absorbed by subduction of the South China Sea along the Manila trench. At the latitude of Taiwan, the continental margin of the South China Sea has impinged upon the trench so the convergence is absorbed by deformation of the continental margin, resulting in the formation of the mountainous island of Taiwan.

The Taiwan orogen is the product of a tandem suturing and tandem disengagement of the Asian continental margin, the Luzon volcanic island arc, and a thin intervening continental sliver [*Shyu et al.*, 2005b] (Figure 4.1). Both collisions mature northward, creating the main body of the island and its numerous active and inactive thrust faults and folds. A tandem disengagement occurs in the northeastern quarter of the island, where

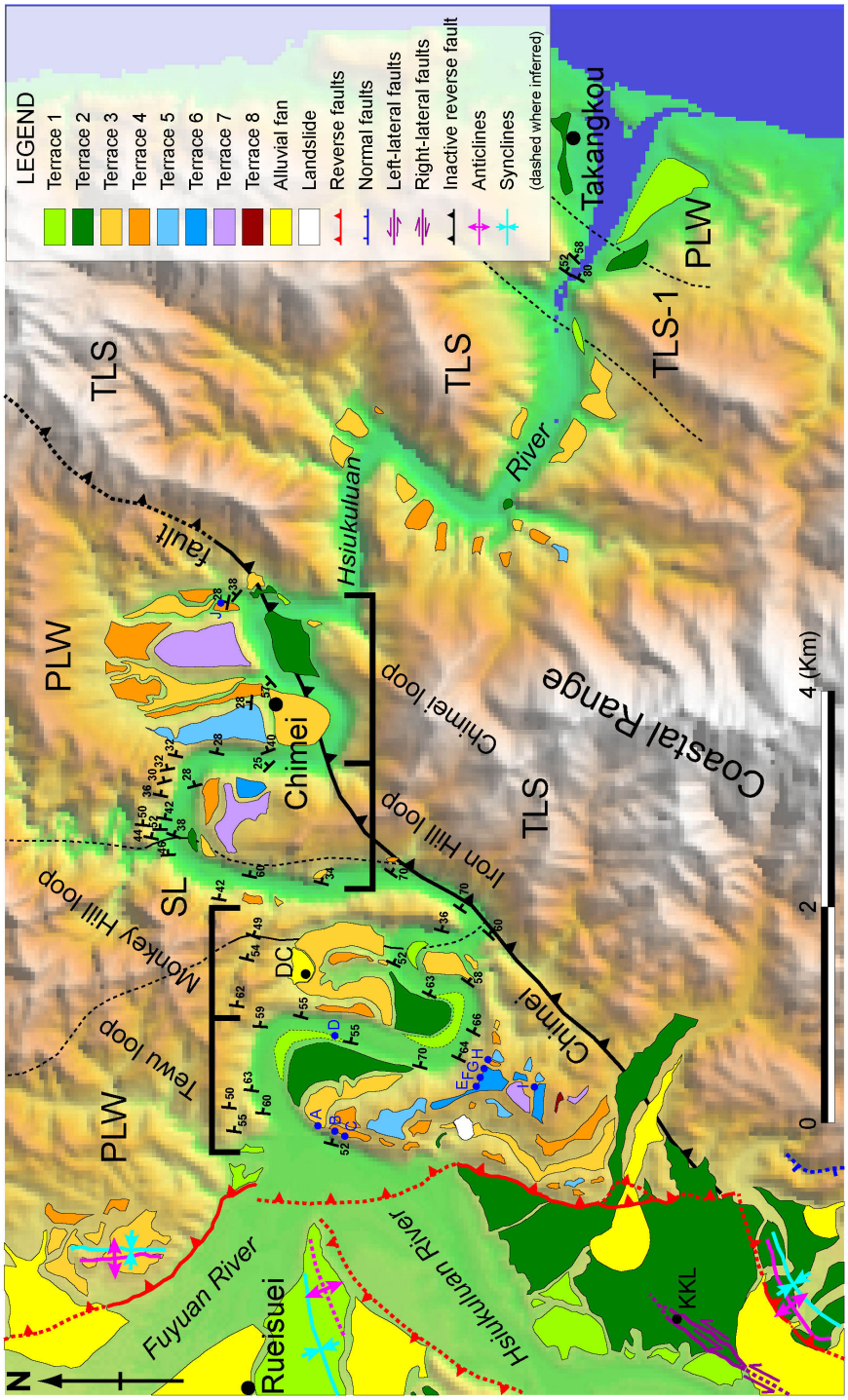

Figure 4.4. Since the Hsiukuluan River is the only river that flows across the Coastal Range, it provides a unique opportunity to determine the long-term rates of uplift of the range. Along the western part of its course across the range, the river has formed the deeply incised Tewu, Monkey Hill, Iron Hill, and Chimei meander loops. As many as eight levels of fluvial terraces exist on both sides of the river valley. PLW: sedimentary Paliwan Formation; SL: Shuilien Conglomerate Member of the Paliwan Formation; TLS: volcanic rocks of the Tuluanshan Formation; TLS-1: a thick layer of volcanic breccia within the Tuluanshan Formation. Dark blue dots indicate where the thickness of the fluvial terrace deposit was directly measured.

normal faulting is dominant above the Ryukyu subduction zone. The Central Range, Taiwan's mountainous backbone, is the exhumed portion of a sliver of continental lithosphere flanked on the east by the Coastal Range, the attached part of the Luzon volcanic arc. Between these two linear mountain ranges is the Longitudinal Valley, the locus of the suture between the continental sliver and the collided volcanic arc.

Two major structures dominate the Longitudinal Valley. On the eastern side of the valley, the east-dipping Longitudinal Valley fault has long been considered one of the most important and active faults in Taiwan [e.g., *Angelier et al.*, 1997; *Shyu et al.*, 2005a]. It is characterized by high rates of sinistral reverse motion. Near the town of Chihshang (Figure 4.2), this fault is creeping aseismically [e.g., *Angelier et al.*, 1997]. A creepmeter measurement reveals a one-dimensional shortening rate of about 20 mm/yr [*Lee et al.*, 2001, 2003]. The most recent surface rupture occurred along the Longitudinal Valley fault during an earthquake couplet in 1951 [*Shyu et al.*, 2005c]. This seismic rupture extended into the rapid creeping segment. Thus the Chihshang segment of the Longitudinal Valley fault exhibits both aseismic and seismic strain relief, and its long-term slip rate is likely to be higher than the 20 mm/yr measured by creepmeter.

The other major fault of the Longitudinal Valley is the Central Range fault, which crops out along the western flank of the valley [*Biq*, 1965; *Shyu et al.*, 2005a, 2005d]. This fault is a west-dipping thrust fault, above which the eastern flank of the Central Range is rising above the valley.

The Coastal Range is the shortened and accreted part of the Luzon volcanic arc and its forearc basin [e.g., *Huang et al.*, 1997; *Chang et al.*, 2001]. It is composed of an assemblage of young (Miocene through early Pliocene) volcanic arc rocks and associated turbidite deposits, mélange, and fringing-reef limestones [e.g., *W.-S. Chen*, 1988; *Ho*, 1988] (Figure 4.5). The major geologic unit of the range is the Tuluanshan Formation, comprised mostly of andesitic volcanic sedimentary rocks, such as breccias and tuffs. It

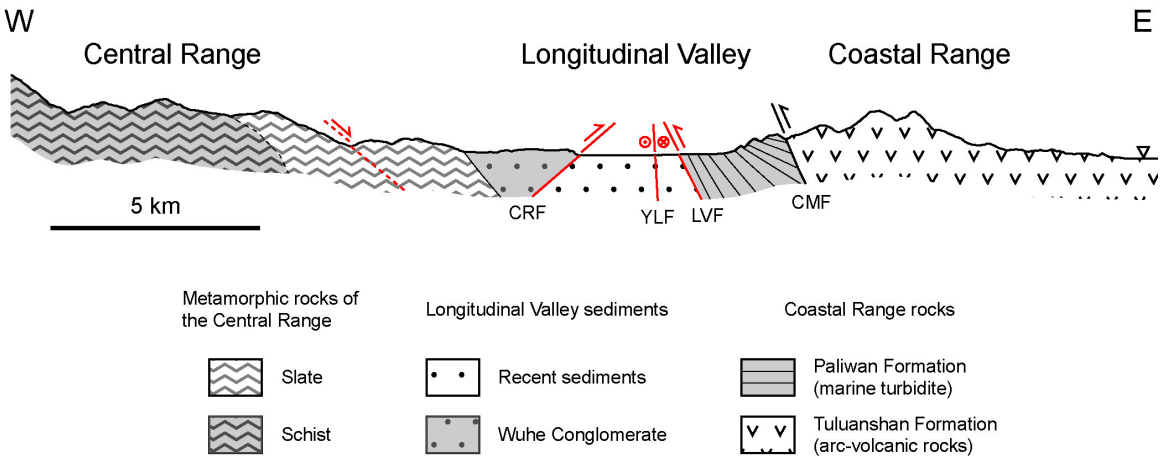

Figure 4.5. A schematic geologic cross section across the Longitudinal Valley near Hsiukuluan canyon shows the principal active structures of the suture and major rock units in the vicinity. The Coastal Range consists of the arc-volcanic Tuluanshan Formation and the marine turbidite of the Paliwan Formation. The Central Range, in the west, is composed of metamorphosed slates and schists. Between the east-dipping Longitudinal Valley fault (LVF) and the west-dipping Central Range fault (CRF) are fluvial sediments of the valley. One objective of this paper is to determine how convergence across the Longitudinal Valley suture is partitioned between these two faults. CMF: Chimei fault; YLF: Yuli fault.

forms the highest peaks and ridges of the range. Bordering the volcanic sedimentary rocks are deep-marine turbidites, including the Fanshuliao and Paliwan Formations [*Teng*, 1980; *Teng et al.*, 1988]. The latter has abundant metamorphic rock fragments derived from the Central Range, which indicate the exposure and proximity of the Central Range during its deposition in a forearc basin [*Teng*, 1982]. In the southern part of the Coastal Range, the Lichi Formation, with its highly sheared clays and severely fragmented sedimentary sequences, is likely to be a highly shortened section of the forearc basin. Pieces of mafic and ultramafic rocks within the Lichi Formation may be remnants of the forearc oceanic crust [e.g., *Chang et al.*, 2001].

In the middle part of the Coastal Range, the Chimei fault forms a major boundary between the volcanic Tuluanshan Formation and the sedimentary Paliwan Formation (Figures 4.4 and 4.5). Since the deep marine Paliwan Formation was deposited at a water depth of several thousand meters, more than 1000 m of reverse movement along the Chimei fault created the current juxtaposition of the two formations [e.g., *Chen et al.*, 1991]. Based upon recent GPS surveys and other evidence, many consider this fault to

be active. However, the recent activity of the Chimei fault remains highly controversial, since much of the evidence can be explained otherwise.

4.4 River terraces of Hsiukuluan canyon

4.4.1 Distribution and characteristics

The Hsiukuluan River is the largest river in the Longitudinal Valley. Most of its larger tributaries drain the eastern flank of the Central Range south of Rueisuei, but several smaller ones drain the western flank of the Coastal Range. East of Rueisuei, the Hsiukuluan River is joined by the Fuyuan River, its only tributary north of Rueisuei. At this juncture the river turns 90° to the east and enters the Coastal Range (Figure 4.4). Between the confluence and the village of Chimei, approximately 4 km downstream, the river flows in deeply incised meanders, characterized by many levels of river terraces, commonly sequestered in older, abandoned meander loops.

Four major meander loops exist in Hsiukuluan canyon. We call these the Tewu, Monkey Hill, Iron Hill, and Chimei loops, named after local village names (Figure 4.4). Only the Tewu and Iron Hill meanders are active today. Most of the Monkey Hill and Chimei loops are abandoned.

The Tewu loop is the farthest upstream, constituting the first reach of the river as it flows into the Coastal Range. Eight preserved terrace levels rise above the modern riverbed on the inside, southern bank of the meander loop (Figure 4.4). Since the horizontal distance from the highest terrace to the modern riverbed is much greater than the vertical separation of the two, northward lateral migration is clearly occurring at a higher rate than incision [*Hovius and Stark*, 2001].

Multiple terrace levels are also present within the Chimei loop, along the northern bank of the modern river (Figure 4.4). A large abandoned meander channel is present

immediately downstream of the village of Chimei. Including the abandoned channel, there are five terrace levels above the modern riverbed.

Fewer terrace levels are present within the Monkey Hill and Iron Hill loops. At Monkey Hill, the major terrace is the abandoned meander channel (Terrace 3 in Figure 4.4). About four levels of terraces are present at the Iron Hill loop. Two of them, however, are quite small.

In fluvial geomorphology, terraces are generally divided into two types: strath terraces are those underlain by no more than a few meters of fluvial sediments atop a bedrock erosional surface, or strath; alluvial (or fill) terraces sit atop tens or even hundreds of meters of fluvial sediments [e.g., *Bull*, 1990; *Bull and Knuepfer*, 1987]. The formation of strath terraces generally indicates rock uplift, but most alluvial terraces document aggradation and incision of rivers associated with other hydrological processes such as base level change and change in sediment supply, both commonly associated with climatic fluctuations [e.g., *Bull*, 1990; *Bull and Knuepfer*, 1987].

Although alluvial terraces are common in Taiwan [e.g., *Hsieh et al.*, 1994, *Liew and Hsieh*, 2000], Hsiukuluan canyon is dominated by strath terraces (Figure 4.6). For example, numerous outcrops within the Tewu loop reveal sediment thicknesses of less than 10 m above the terrace straths (Table 4.1). Only the abandoned meander loop near Monkey Hill may have thicker sediment cover. A drill core on that terrace (DC in Figure 4.4) reveals 28 m of sediments above the terrace strath [*Hsieh et al.*, 2003]. However, since the location of the core is on a small alluvial fan, some of this must be fan sediments deposited after abandonment of the paleochannel.

A layer of fine-grained overbank sediments caps the fluvial gravels of all river terrace sequences (Figure 4.6). The thickness of this fine-grained layer appears to be greater on the older terraces, but thicknesses commonly range between 2 and 4 m. On some of the Tewu terraces, a fining upward sequence above the fluvial gravels is consistent with a point-bar origin.

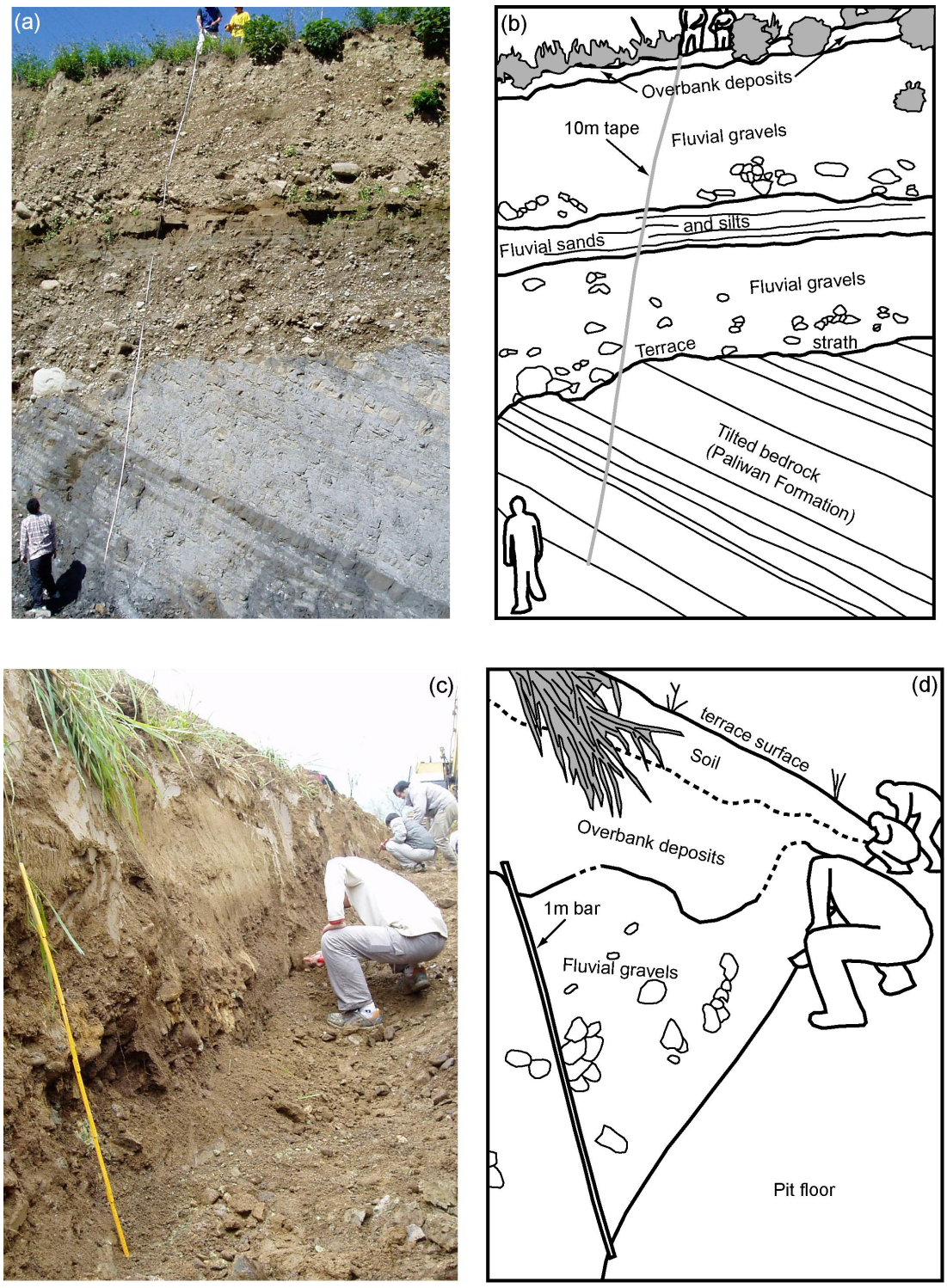

Figure 4.6. Typical exposures of the river terrace deposits along the western Hsiukuluan canyon. (a) Photograph and (b) sketch of an outcrop at site CYC (terrace 4). Typical terrace sediments include several meters of fluvial sand and gravels overlying the bedrock strath. The length of the white tape is 10 m. (c) Photograph and (d) sketch of the pit wall at site TW4 (terrace 4). A layer of fine-grained overbank deposits, locally as much as a couple of meters in thickness, exists at the top of most terraces. The length of the yellow bar is 1 m.

Table 4.1. Measurements of the river terrace sediment thickness above straths along Hsiukuluan canyon. Sites of measurement are shown in Figure 4.4.

Site (see figure 4.4)	Terrace level*	Sediment thickness (m)
A	3 (TW)	6.4
B	4 (TW)	6.5
C	4 (TW)	4.1
D	1 (TW)	3.8
E	6 (TW)	7.0
F	6 (TW)	5.5
G	6 (TW)	9.8
H	4 (TW)	0.3
I	6 (TW)	4.0
J	4 (CM)	6.9

* TW: Tewu loop; CM: Chimei loop.

Several meters of gravels underlie the overbank deposits (Figure 4.6). Except for the highest three terraces of the Tewu loop, all of the gravel layers consist predominantly of sub-rounded metamorphic clasts derived from the Central Range. A small portion of the gravels is derived locally from volcanic breccia of the Tuluanshan Formation. The gravels of the higher Tewu terraces are virtually all volcanic, indicating either that a thick tributary alluvial fan overlies the gravels of the main river or that the small terraces are entirely produced by a tributary originating in the Coastal Range.

Downstream from the Chimei Fault, where the river incises the volcanic Tuluanshan Formation, river terraces are much more poorly developed (Figure 4.4). Only scattered terraces with very thick sediment cover are present. The clasts of these thick cover beds are predominantly very large and angular boulders. Thus, these terraces are likely to be eroded remnants of tributary alluvial fans that covered the main channel of the river. If so, they do not provide as adequate a constraint for determining uplift rates as those strath terraces in the western half of the canyon. Fluvial terraces merge with well-developed marine terraces at the easternmost part of Hsiukuluan canyon near the small village of Takangkou.

4.4.2 Age of terraces

None of the river terraces in Hsiukuluan canyon is capped by a lateritic soil. Elsewhere in Taiwan, a lack of lateritic soil indicates that the terraces are less than about 50 kyr old [*Y.-G. Chen*, 1988]. Therefore, the Hsiukuluan terraces should be within the range of radiocarbon dating. Since wood samples are scarce in terrace outcrops, we dug small, shallow pits into the terrace surfaces, hoping to expose datable organic material.

In all, we have dug more than a dozen pits on terraces of all four loops (Figure 4.7). Several pits yielded charcoal samples. Most of these samples came from terraces that have a thick layer of fine-grained overbank deposits. Rarely, we were able to collect multiple samples from different depths. The ages of these samples help us constrain the duration of overbank deposition.

Figure 4.8 shows all of the stratigraphic columns constructed from exposures in the walls of the pits. The analytical results for all of the samples we collected are listed in Table 4.2. Our colleagues at Lawrence Livermore National Laboratory (LLNL) performed all age determinations by accelerator mass spectrometry (AMS). The multiple samples from sites CM1 and CM3 show that the fine-grained overbank deposits overlying the gravels have a depositional history that spans more than a couple thousand years. Since Hsiukuluan canyon is very narrow, we suspect that this long history may reflect slack water caused by occasional landslides that obstructed the course of the river and forced it to deposit overbank sediments on terraces high above the active channel. In fact, even without landslide damming, the water level during the most severe typhoons can rise more than 20 m above normal according to local witnesses. This would explain the unusually young ages we have found at sites such as CM1 and CM3.

Therefore, ages obtained from samples below the top of the gravels are generally considered more reliable [e.g., *Lavé and Avouac*, 2000, 2001]. For the same reason we chose not to use the age obtained from the IH1 site because it has an unusually young age

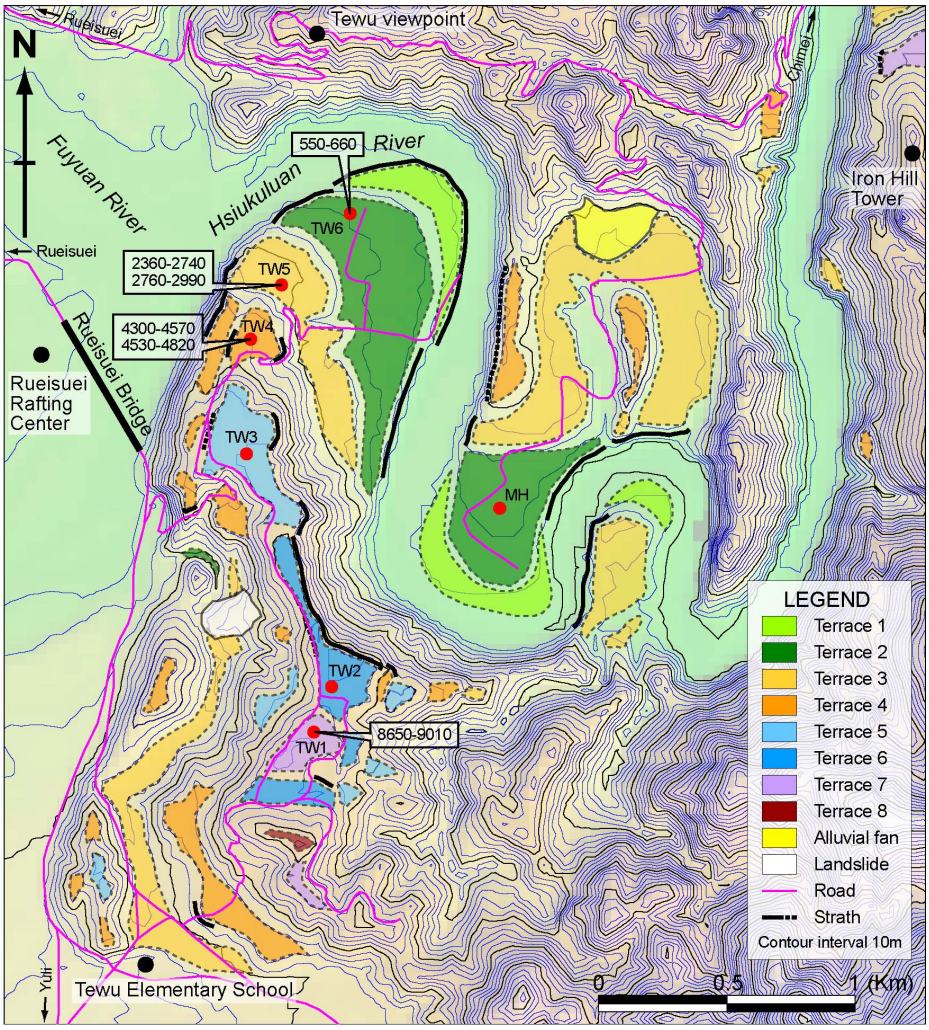

Figure 4.7. Detailed maps of the fluvial terraces of western Hsiukuluan canyon showing sampling sites and the strath contacts. Ages of terraces are calibrated ages (2σ) in cal BP. (a) Map of terraces of the Tewu and Monkey Hill loops.

for such a high terrace. Also, we did not use the ages from the MH site, because one of the samples there indicates a recent age, probably indicating flood deposition during a large typhoon.

The ages we obtained for the terraces along Hsiukuluan canyon show that the higher terraces of the Tewu loop are a little more than 10 kyr old (Table 4.2). The highest terrace of the Chimei loop (site CM1) has a similar age, but its elevation above the modern riverbed is much lower. The paleochannel of the major meander loop of Chimei was abandoned between 3 and 4 kyr ago.

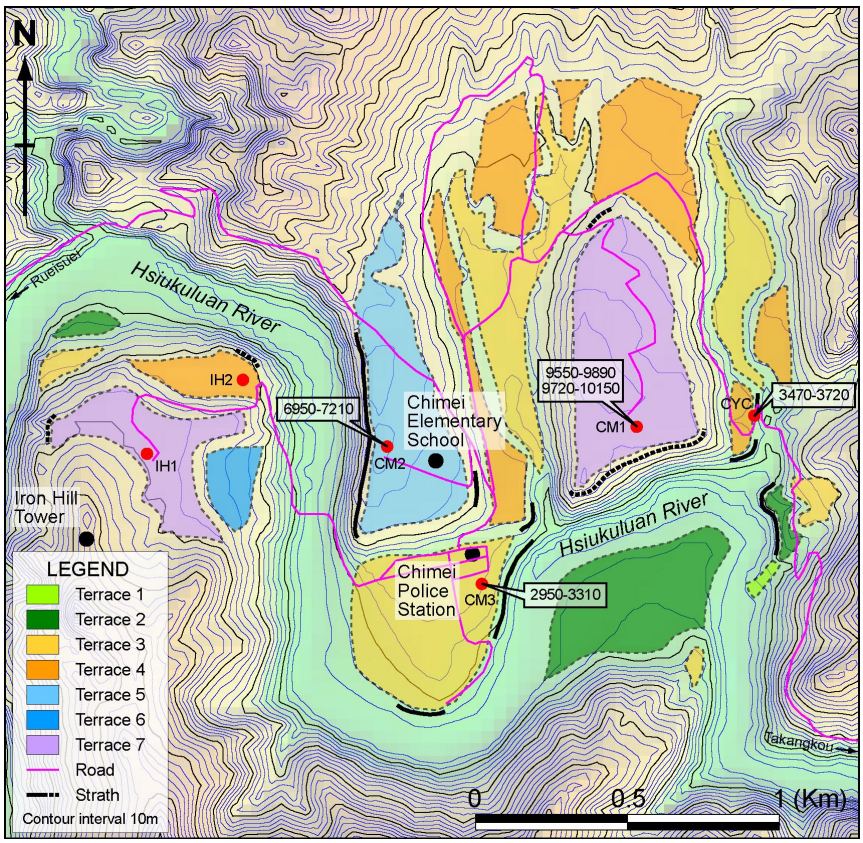

Figure 4.7. (continued) (b) Map of terraces of the Iron Hill and Chimei loops.

4.4.3 Reconstructions of river patterns in the past

Using the ages of terraces we obtained from the charcoal samples, we attempted to reconstruct the river courses at several points in the past. This enabled us to visualize the development of the meander loops and to see if there are any inconsistencies in the terrace ages. For each reconstruction we have tested the validity of the reconstruction by making longitudinal profiles of the river and calculating the approximate sinuosity of the river course at that time. The current river course within Hsiukuluan canyon has a sinuosity of approximately 2.5. If we assume that most of the variables along the river such as climate and bedrock type are basically invariant, the sinuosity and slope of the river should also stay similar.

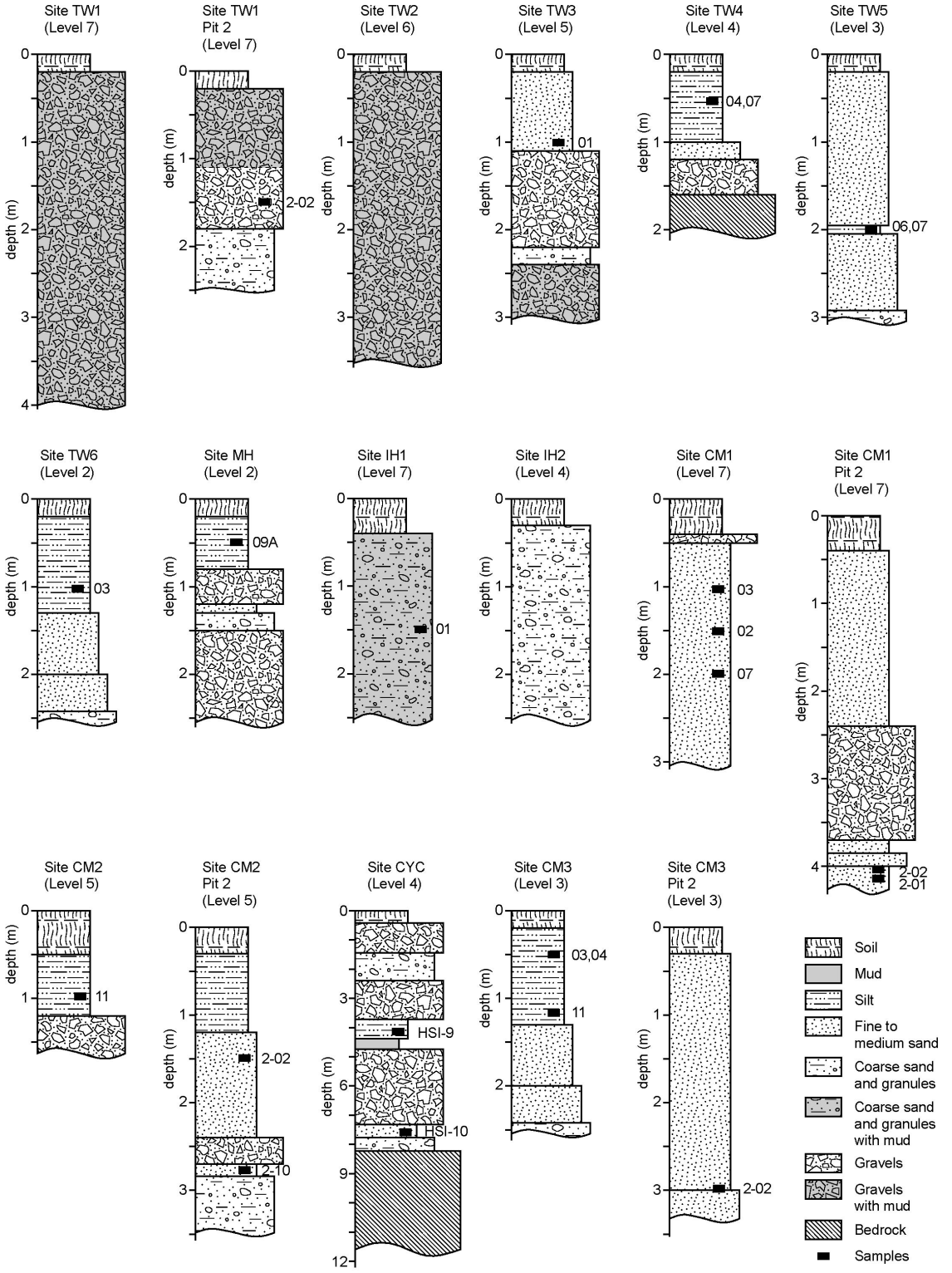

Figure 4.8. Stratigraphic columns of all sampling sites. Site CYC is an outcrop of terrace 4 exposed during a road construction. All other sites are sediment pits dug on terraces surfaces in this research. Locations of charcoal samples dated in this research are also shown with sample numbers next to them. Except for site CYC, where full sample numbers are shown, all other sample numbers are shown without site names.

Table 4.2. Analytical results of all of the samples dated in this research.

Sample number	Site name	GPS location of site		Terrace level	Age (yrBP)*	Calibrated age (2σ)(cal BP)#	Strath elevation above current riverbed(m)	Incision rate (mm/yr)
		X	Y					
TW1-2-02	TW1	291223	2597094	7	7980±45	8650-9010	>158	>17.5-18.3
TW3-01	TW3	290950	2598159	5	700±40	560-710	~128	##
TW4-04	TW4	290989	2598597	4	4135±40	4530-4820	~83	~17.2-18.3
TW4-07					3985±40	4300-4570		~18.2-19.3
TW5-06	TW5	291110	2598826	3	2495±30	2360-2740	~45	~16.4-19.1
TW5-07					2765±55	2760-2990		~15.1-16.3
TW6-03	TW6	291369	2599098	2	630±40	550-660	~15	~22.7-27.3
MH-09A	MH	291948	2597949	2	125±30	0-270	~12	##
IH1-01	IH1	293750	2599608	7	3720±40	3930-4220	~110	##
CM1-02	CM1	295341	2599806	7	3765±30	3990-4240	>102	##
CM1-03					3665±35	3870-4090		##
CM1-07					1570±40	1350-1540		##
CM1-2-01					8720±50	9550-9890		>10.3-10.7
CM1-2-02					8845±40	9720-10150		>10.0-10.5
CM2-11	CM2	294546	2599635	5	85±30	0-260	~90	##
CM2-2-02					165±30	0-290		##
CM2-2-10					6170±35	6950-7210		~12.3-12.9
HSI-9	CYC	295756	2599722	4	3145±70	3080-3550	43	##
HSI-10					3360±50	3470-3720		11.6-12.4
CM3-03	CM3	294857	2599213	3	1015±40	790-1050	~37	##
CM3-04					1055±30	930-1050		##
CM3-11					1625±30	1420-1610		##
CM3-2-02					2945±45	2950-3310		~11.2-12.5

* All samples were dated in LLNL using AMS with $\delta^{13}C$ corrected.
# Calibrated using the CALIB program [*Stuiver and Reimer*, 1993].
These samples appear to be collected from the overbank deposits and have younger ages than the ages of the terraces. Thus they were not used to calculate the incision rate.

Figure 4.9 shows our reconstructions of the paleo-Hsiukuluan River courses. According to these reconstructions, the Chimei meander loop was active until around 3.5 kyr ago, and was abandoned when the Monkey Hill loop was active. The Monkey Hill loop was abandoned after about 2.5 kyr ago, and the sinuosity of the river stayed relatively constant after that due to the development of the Tewu loop. Although it seems that the river sinuosity was a little lower in more ancient times, this is more likely

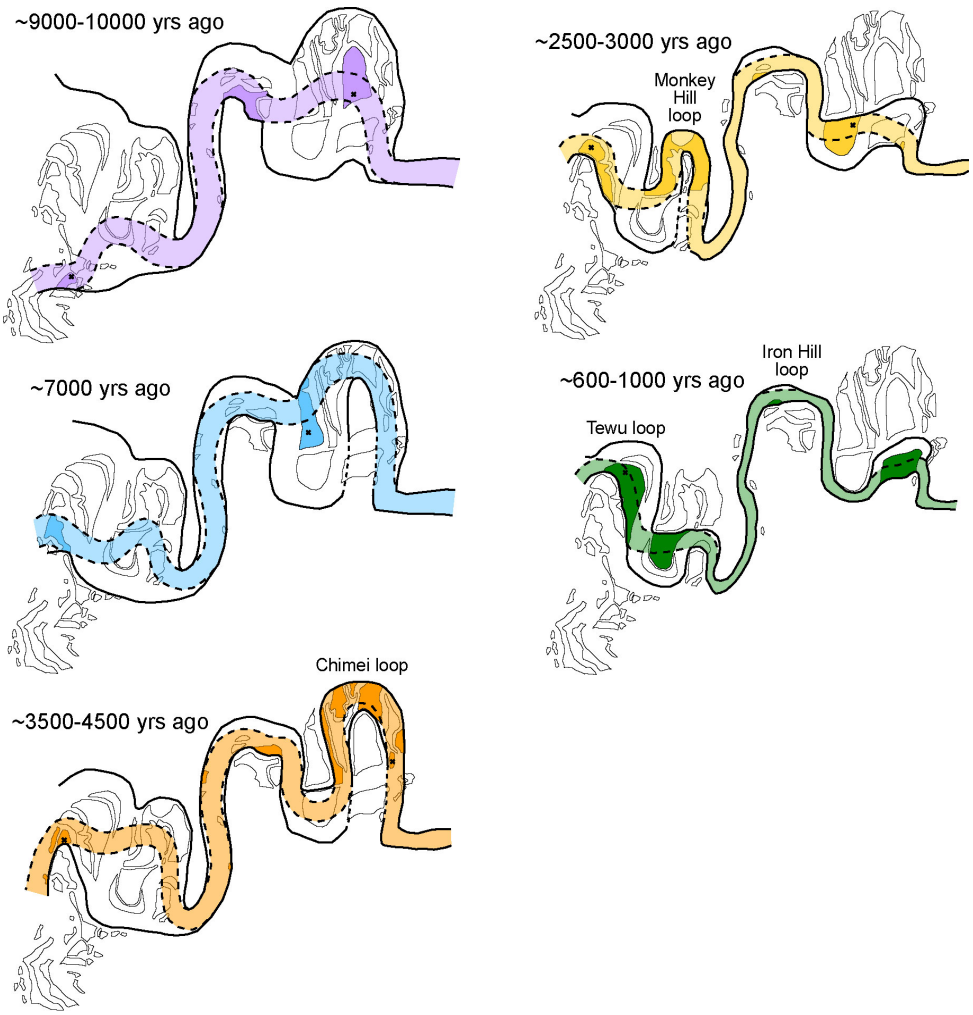

Figure 4.9. Reconstruction of river channels at about 9-10 kyr, 7 kyr, 3.5-4.5 kyr, 2.5-3 kyr, and 0.6-1 kyr ago along the western Hsiukuluan canyon. In each reconstruction the active fluvial channel at that time has the same color as the corresponding river terraces in Figure 4.7. At any given time, the paleochannels must lie within the confines of the valley sides, defined by the valley walls rising above the corresponding terraces (bold solid lines). Terraces that might have formed along tributary channels do not appear in the reconstructions.

to be the result of the lack of constraints on both the Monkey Hill and Chimei loops.

4.5 Incision and uplift rates along Hsiukuluan canyon

Since all of the Hsiukuluan terraces we have dated are strath terraces, their ages and the straths elevation above current riverbed allow calculation of the average bedrock incision rate since the abandonment of the terraces. The results of such calculations are

listed in Table 4.2.

The cumulative uplift $U(x, t)$ at point x since the formation of the terraces at time t, with respect to the Longitudinal Valley, can be written as [*Lavé and Avouac*, 2000]:

$$U(x, t) = I(x, t) + D(x, t) + P(x, t), \quad (4.1)$$

where $I(x, t)$ is the incision deduced from the terrace, $D(x, t)$ is the change in local base level, and $P(x, t)$ is the change in elevation at point x due to possible geomorphic contributions of the river, such as changes in river gradient and sinuosity. It has been shown that the geomorphic contribution is dominated by changes in river sinuosity, since the gradient of rivers tends to stay relatively constant (see discussion in *Lavé and Avouac* [2000]).

Therefore, the rock uplift rate would be approximately equal to the bedrock incision rate if the following three assumptions are true: 1) There is no change in climate, or the changes did not create significant river pattern change such as aggradation or incision. 2) There is no significant change in river base level, or the change did not create major changes in accommodation space. 3) The sinuosity of the river stayed relatively constant so that there is no local aggradation or incision.

Periods of climatic fluctuation have been documented for the Holocene in many places of Taiwan [e.g., *Kuo and Liew*, 2000]. In fact, many small but locally extensive aggradational terraces are present among several small drainages along the eastern slope of the Coastal Range [*Hsieh et al.*, 1994]. These terraces are considered to be the results of three particularly wet periods in eastern Taiwan, about 6 kyr, 4kyr, and 1 kyr ago [*M.-L. Hsieh*, unpublished data]. However, such a record is not present in Hsiukuluan canyon. Not only are there no major aggradational terraces, but also there is no extensive terrace development in any of these periods. We believe that the large drainage area and the long segment of the river upstream from the canyon, in the Longitudinal Valley, damped out any effects of climate change.

The late Quaternary sea level history around Taiwan has been studied intensively

[*Chen*, 1993; *Chen and Liu*, 1996, 2000]. According to the ages of emerged corals on the island of Penghu, a stable island in the Taiwan Strait, sea level rose to its highest Holocene level at about 4.7 kyr ago, about 2.4 m above the modern sea level [*Chen and Liu*, 1996]. The sea level has subsequently dropped slowly to its current position. Therefore there is no significant base level change for Hsiukuluan canyon in the past 4.7 kyr. Although there were base level changes before 4.7 kyr ago, if the slope of the river valley was similar to the slope of the ocean floor right after the river enters the sea, the changes might not have created much difference in accommodation space [e.g., *Miall*, 1991; *Schumm*, 1993]. The similarity of the incision rates before and after 4 kyr ago in Hsiukuluan canyon suggests that this may be the case.

Since our paleo-Hsiukuluan reconstructions show that there have been no significant sinuosity changes of the river course, and since there appear to have been no changes in base level, we are confident that the bedrock incision rates we have obtained for Hsiukuluan canyon are similar to the local rock uplift rates. Because the rock uplift of the Coastal Range should be the result of the upthrusting of the Longitudinal Valley fault, we will, therefore, use these rates to figure out the characteristics of the fault and its Holocene slip rate.

Figure 4.10 shows the terrace surfaces and straths of all river terraces of the western part of Hsiukuluan canyon along with the ages we obtained that were projected to the plane perpendicular to the general trend of the Longitudinal Valley fault. Upon first inspection, it appears that among the terraces that have similar ages, those further upstream are higher above the current riverbed than those farther to the east and closer to the coast. This indicates that the incision rate is higher closer to the Longitudinal Valley fault and decreases to the east. However, because the terraces are not continuous, these ages only provide us local incision rates. Thus, we decided to use two different methods to obtain a continuous incision rate profile along the entire river valley.

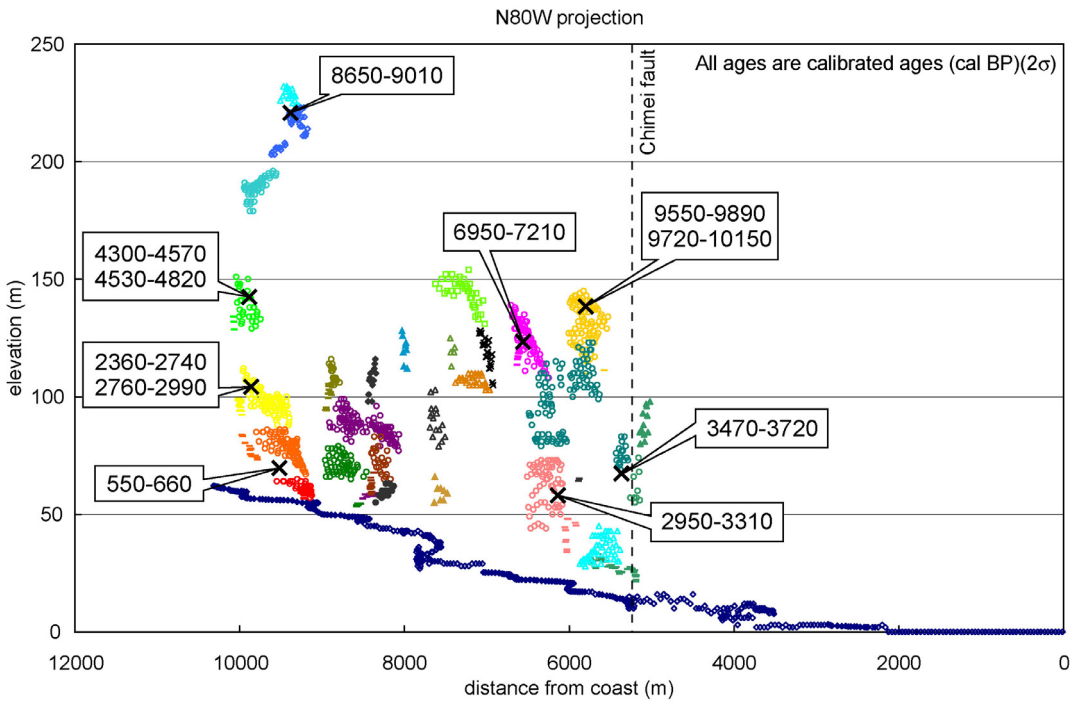

Figure 4.10. All of the river terraces, together with the sampling sites and the current Hsiukuluan riverbed, projected along a N80°W direction. Each color represents a single terrace. Solid dots represent terrace surface measurements from the DEM, and short bars represent terraces straths measured by laser range finder. All ages are calibrated ages (2σ) in cal BP.

4.5.1 Shear stress profile along Hsiukuluan canyon

The first method we employed uses the geometry of the Hsiukuluan River to calculate the river bed shear stress, which is related to the incision rate. Although many hydrologic parameters are highly simplified in this method, it generally yields a reasonably accurate result for regular rivers. A detailed discussion of the following calculations can be found in *Lavé and Avouac* [2001].

The incision rate (i) along a river is related to the shear stress (τ) at the base of the river channel:

$$i = K\,(\tau - \tau_b), \tag{4.2}$$

where τ_b is the critical shear stress above which bedrock incision starts to occur and K is an erodability constant, related to factors such as bedrock lithology. Most of the

bedrock incision occurs during major floods, such as those that occur in the typhoon season of Taiwan. For the Hsiukuluan River, we can assume that the width of the river is much larger than the depth of the river even during that period of time. Therefore, the shear stress can be simplified as

$$\tau = \rho g h S, \tag{4.3}$$

where ρ is the density of water, h is the depth of the river during floods, and S is the gradient of the river.

On the other hand, the river flux (Q) of a river can be calculated as

$$Q = v h W, \tag{4.4}$$

where v is the velocity of the flow and W is the width of the channel. Most of the Hsiukuluan drainage basin lies in eastern Central Range, and no large tributary joins this segment of the river. As a result, the river flux Q is approximately a constant along the entire segment.

Furthermore, the flow velocity is related to the geometry and slope of the channel, as shown in many hydrologic equations. Again, since we assume that the width of the river is much larger than the depth of the river, this equation can be simplified as

$$v = 1/N \times h^{2/3} \times S^{1/2}, \tag{4.5}$$

where N is the roughness coefficient [e.g., *Chang*, 1988], related to the grain size of the bed load. Combining equations (4.4) and (4.5), we get

$$h = (N \times Q/W \times S^{-1/2})^{3/5}. \tag{4.6}$$

Putting equation (4.6) back into equation (4.3), we can get the shear stress as

$$\tau = \rho g (NQ)^{0.6} \times S^{0.7} \times W^{-0.6} = \alpha \times S^{0.7} \times W^{-0.6}, \tag{4.7}$$

where α is a new constant. We can further put equation (4.7) back into equation (4.2) and find that the incision rate along the river is now simplified as

$$i = K (\alpha \times S^{0.7} \times W^{-0.6} - \tau_b). \tag{4.8}$$

If we assume that τ_b is very small comparing to the shear stress during floods, then

$$i = K\alpha \times S^{0.7} \times W^{-0.6} = K' \tau^*, \tag{4.9}$$

where K' is yet another constant and τ^* is a simple variable that is only related to the width and slope of the river channel.

Equation (4.9) indicates that, if all of our simplifications are true, the incision rate along the river is a function of only the width and the slope of the river. Therefore, using profiles of river slope and width, we can calculate a profile of τ^* and then use the incision rate we have obtained from the terrace ages to calculate the constant K', thus getting the incision rate profile for the entire river.

Figure 4.11 shows the results of our calculation. For the long profile of the Hsiukuluan River we have used real-time kinematic (RTK) GPS to measure the slope of the river wherever possible and utilized the 40-m digital elevation model (DEM) of Taiwan for locations that we were unable to reach (Figure 4.11a). It appears that there is only one major slope change along Hsiukuluan canyon. This is where the river flows out of the Paliwan Formation and into the Tuluanshan Formation, where the slope of the river changes from about 3.4 m/km to about 1.9 m/km.

The width of the river channel is more difficult to obtain correctly than the river slope. We used laser range finder as well as the DEM to get the river width profile (Figure 4.11b). It appears that along Hsiukuluan canyon, the river channel is most narrow in its middle part, near the Chimei fault, and becomes wider both upstream and downstream. However, since the river is meandering, laterally aggrading point bars are very well developed, making it very difficult to determine the correct channel width. This implies that some of the simplifications embedded in the hydrologic equations above, such as rectangular channel cross section [e.g., *Lavé and Avouac*, 2001], may not be true.

A profile of our calculated τ^* is shown as Figure 4.11c. Theoretically, the pattern of the τ^* profile should be similar to the pattern of the incision rates we obtained from the terrace ages. However, this is not the case. The τ^* profile clearly shows that the

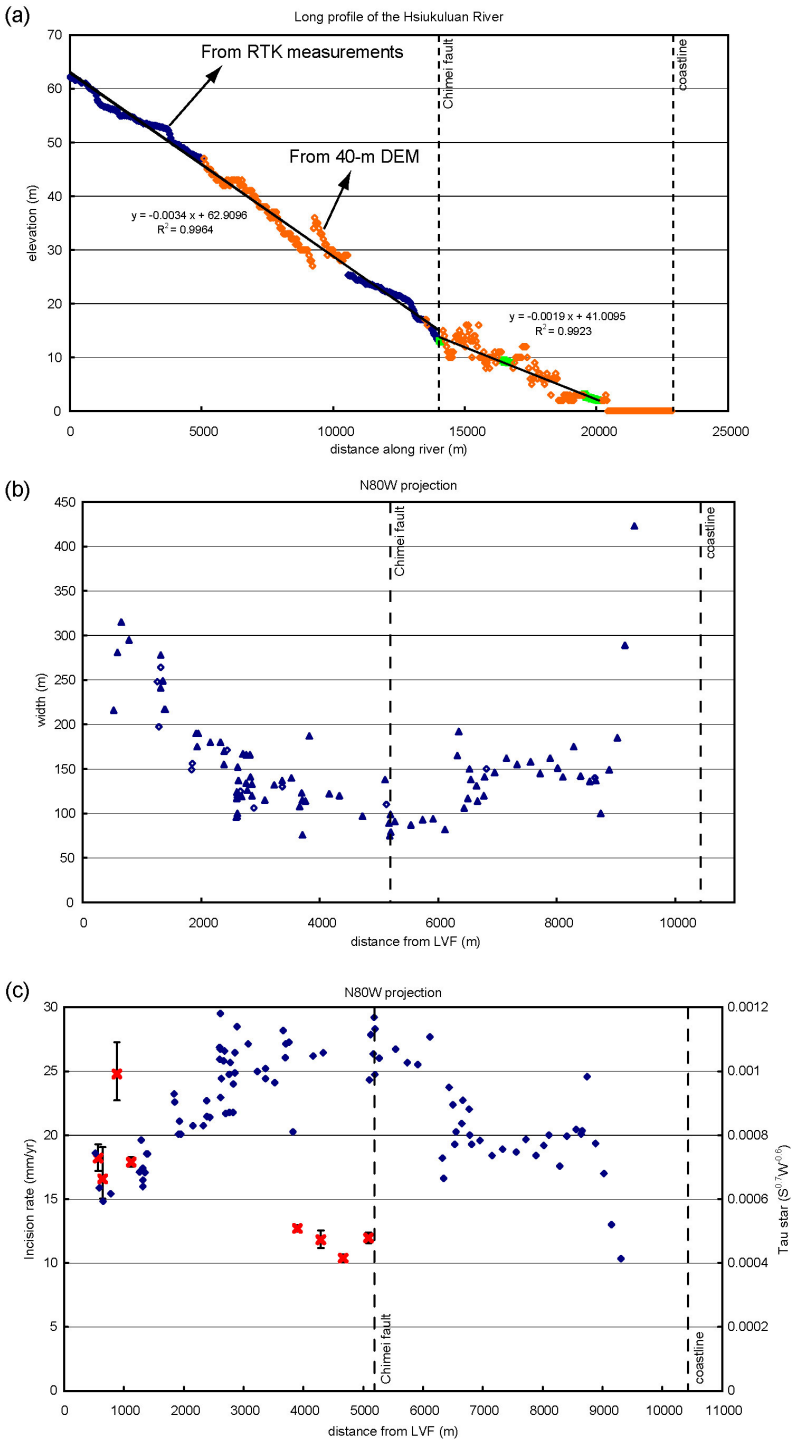

Figure 4.11. Shear stress calculations along Hsiukuluan canyon. (a) Long profile of the Hsiukuluan River. Only one major slope change appears along the canyon, where the river crosses the Chimei fault, the contact between Paliwan Formation and Tuluanshan volcanic rocks. (b) Width of current river channel along Hsiukuluan canyon. The current river channel is narrowest near the Chimei fault. (c) A profile of the calculated τ^* along Hsiukuluan canyon (in dark blue). The τ^* peaks in the central reach of the valley. This trend is different from the trend of the incision rates obtained from the ages of the river terraces (in red).

incision rate along the river should increase from the Longitudinal Valley fault to somewhere near the Chimei fault. This is opposite of what we have obtained from the uplift of river terraces, which shows that the incision rate is highest near the Longitudinal Valley fault and decreases to the east.

Such discrepancy may have resulted in several ways. For example, the incision of the river may have been controlled by lithologic differences along the river and thus differs from the shear stress patterns. It is more likely that because the Hsiukuluan River across the Coastal Range is highly sinuous, lateral erosion may have consumed much of the energy at the base of the channel, especially at active cut-banks. Therefore the shear stress profile we have calculated will have a different pattern from the pattern of the incision rate, which only considers vertical erosion by the river. Moreover, for a highly meandering river the channel shape is likely to be far from uniform, and many of the hydrologic calculations cannot be simplified as we did above.

4.5.2 Fault-bend fold model

Another way to get a continuous profile of uplift rates is to assume that deformation on the hanging-wall block of the Longitudinal Valley fault is consistent with a fault-bend fold model. Upon casual inspection, it appears that variations in the pattern of the bedding dip angle mimic the pattern of uplift rate along Hsiukuluan canyon (Figure 4.4). This is consistent with fault-bend folding [e.g., *Lavé and Avouac*, 2000]. Fault-bend fold models assume that deformation is accommodated by slip along the bedding planes, with no change of bed thickness. At a given point, the local uplift rate (U) relative to a fixed and rigid footwall is simply proportional to the sine of the apparent dip angle of the beds at the direction of fault slip (θ') with this relationship:

$$U = d \times \sin \theta', \tag{4.10}$$

where d is the slip rate along the fault. If the fault eventually turns into a horizontal

décollement, *d* will simply be the horizontal shortening rate [*Lavé and Avouac*, 2000].

Along Hsiukuluan canyon, θ′ is close to the true dip (θ) of the beds because most of the bedding attitudes have bedding strike directions similar to the strike direction of the Longitudinal Valley fault (Figure 4.4). Thus, their true dip should be approximately the same as the apparent dip in the direction of fault slip. Nonetheless, several points that are very close to the Chimei fault show anomalous strike directions. Because we have found evidence for drag folding of the beds by the Chimei fault, we decided to discard these dip measurements from our calculations. For the other points we will apply their true dip as θ′.

Since the pattern of bedding dip angle variation is similar to the pattern of the uplift rate, we believe the fault-bend fold model is valid for the Longitudinal Valley fault beneath Hsiukuluan canyon. Continuing with our analysis, we can fit the variation of the sine of bedding dip angles very well with a polynomial function (Figure 4.12a). Together with the curve of this polynomial function, we can also plot the uplift rates we obtained from the ages of the terraces along Hsiukuluan canyon using different values of *d* until the two data sets show a good match (Figure 4.12b). The optimal value of *d* is about 23 mm/yr.

We can also utilize the fault-bend fold model to reconstruct the subsurface geometry of the fault (Figure 4.13). In the model of the fault so constructed, the fault steepens downdip slightly about 1 km below the surface and then becomes gradually shallower farther downdip. At a depth of about 2.5 km the fault dips about 30°. If the dip angle continues to greater depth at this angle, the 23 mm/yr slip rate yields a horizontal shortening rate of about 19.9 mm/yr. If the fault becomes shallower at depth, however, the horizontal shortening rate will increase, to a limit of 23 mm/yr in the case of a flat dip.

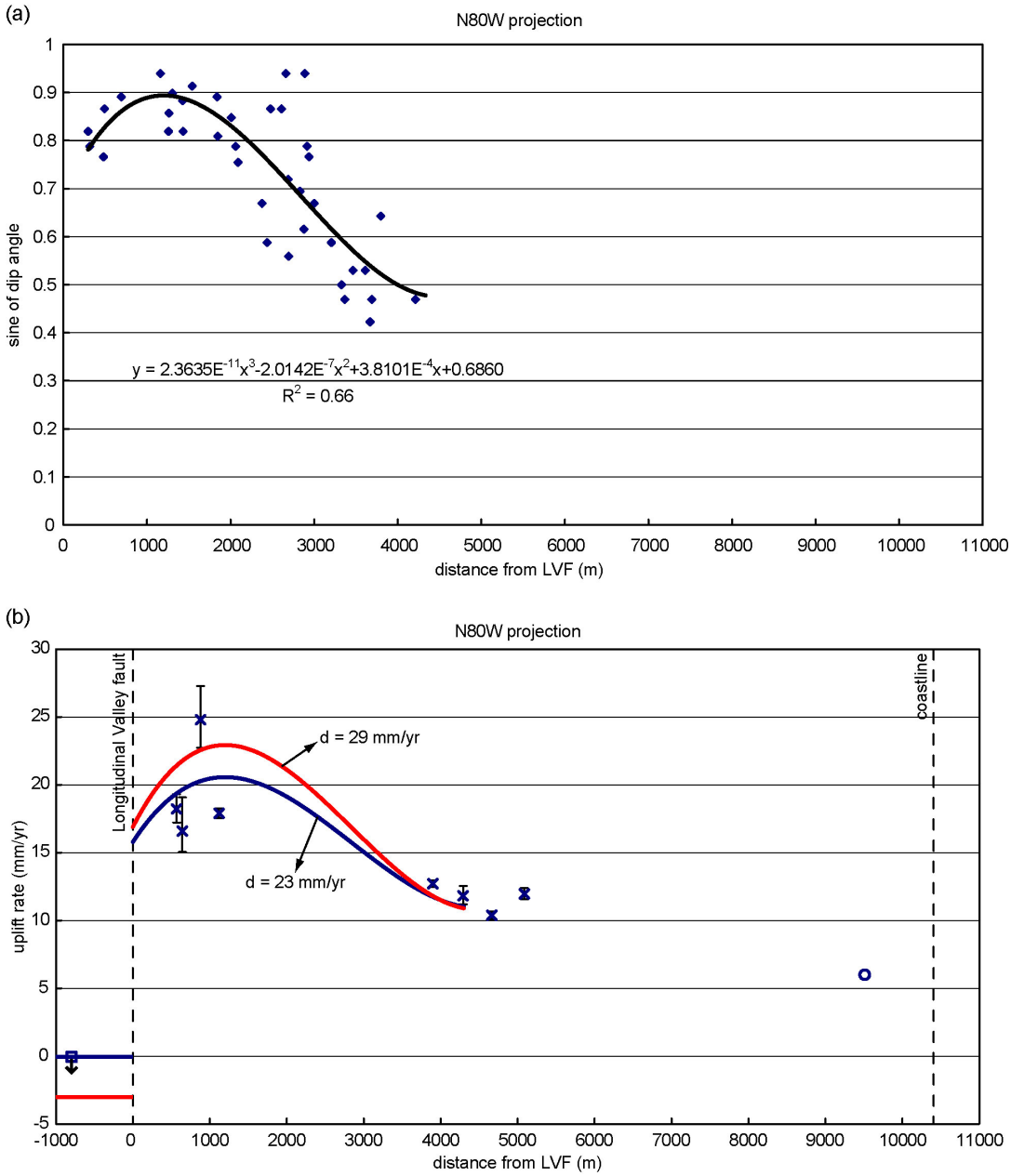

Figure 4.12. Fault-bend fold model of the Longitudinal Valley fault along Hsiukuluan canyon. (a) A polynomial function fits the variation of the sine of the bedding dip angles of the Paliwan Formation along Hsiukuluan canyon very well. Bedding dip angle measurements very close to the Chimei fault are not included because they reflect local deformation associated with slip on the Chimei fault. (b) Using different values of slip rate on the Longitudinal Valley fault (*d*), we can match the polynomial function from (a) with the uplift rates obtained from the river terraces (shown as crosses). The blue line is calculated without footwall subsidence (*d* = 23 mm/yr). The red line reflects 3 mm/yr of footwall subsidence (*d* = 29 mm/yr). The circle is the uplift rate obtained from a Hsiukuluan terrace near the river mouth by *Hsieh et al.* [2003]. The square is the minimum subsidence rate of the Longitudinal Valley footwall obtained from site KKL [*W.-S. Chen*, unpublished data]. See text for discussion.

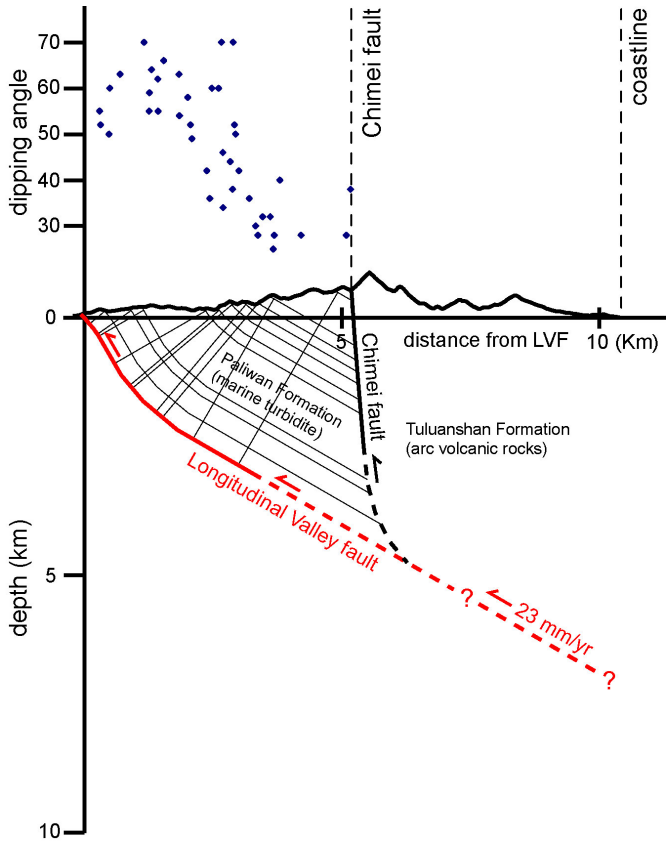

Figure 4.13. Reconstruction of the subsurface geometry of the Longitudinal Valley fault near Hsiukuluan canyon from bedrock dip angles. The azimuth of the section is approximately N80°W. This model indicates that the slip rate on the fault is about 23 mm/yr and that all of the deformation is accommodated by the slip along the fault plane, with no internal deformation of the beds.

4.6 Discussion

4.6.1 Shortening across the Longitudinal Valley suture

Our analysis of incision and uplift rates across the hanging-wall block of the Longitudinal Valley fault at Hsiukuluan canyon has many interesting implications. Our calculation, based on the rock uplift in the hanging-wall block of the Longitudinal Valley fault, indicates that the rock uplift corresponds to a shortening rate of no more than about 23 mm/yr along the N80°W azimuth if the footwall block (the floor of the Longitudinal Valley) is fixed. This equals about 25.6 mm/yr at 306°, the direction of relative plate

motion. This value is significantly smaller than the current shortening rate of about 40 mm/yr across eastern Taiwan, shown in Figure 4.3 [*Hsu et al.*, 2003]. There are several possible explanations for the discrepancy.

First, one could speculate that current GPS measurements reveal only decadal but not millennial shortening rates across the Taiwan orogen. Supporting this is a preliminary structural analysis across western Taiwan, which shows that the average shortening rate over the past million years there may be higher than 40 mm/yr [*Simoes and Avouac*, in preparation], much greater than the rates modeled from the GPS measurements shown in Figure 4.3. If this is the case, the long-term shortening rates from western and eastern Taiwan will add up to about 70-80 mm/yr. Based upon the plate convergence rate, there is still about 10-20 mm/yr of shortening that is not accounted for between the easternmost Taiwan and the Philippine Sea plate, similar to the pattern shown in the GPS measurement (Figure 4.3). A structure offshore eastern Taiwan, as proposed by *Malavieille et al.* [2002], might absorb the difference. Although topographic manifestation of such a structure is rather ambiguous [*Shyu et al.*, 2005a], thick sediments offshore eastern Taiwan [e.g., *Schnürle et al.*, 1998] may have obscured the topographic features.

However, if the current decadal rate of shortening is indeed the same as the long-term rate, we need to account for about 14 mm/yr across the Longitudinal Valley suture that is not accounted for by slip on the Longitudinal Valley fault. This amount can be provided in many ways. Surely, for example, slip on the Central Range fault must absorb some of the shortening. This amount, however, is not likely to be enough. The Wuhe Tableland (Figure 4.2) near Rueisuei provides a basis for calculating a maximum slip rate along the Central Range fault. The tableland is the result of uplift of the hanging-wall block above the fault [*Shyu et al.*, 2002, 2005a, 2005d], and the tableland surface, once the Hsiukuluan River bed, is now at about 170 m above the current river. Wood samples from the river sediments below the tableland surface are

older than 14-C dating limit, which is about 50 kyr. Thus, the maximum uplift rate of the tableland is about 3.4 mm/yr. Unless the dip of the Central Range fault is anomalously shallow for a thrust fault, this yields a maximum shortening rate of a few mm/yr. This likely still leaves a deficit of several mm/yr in the long-term shortening rate relative to the decadal rate.

The simplest way to accommodate the remainder of the deficit is to allow the footwall block of both the Longitudinal Valley and Central Range thrusts to founder. In other words, the Longitudinal Valley basement may be underthrusting beneath both the Coastal Range and the Central Range. This would result in higher slip rates on both faults. For example, if the both faults dip at 30° at depth, an underthrusting rate of about 6 mm/yr on both sides could easily absorb some 10.4 mm/yr shortening across eastern Taiwan.

Such an underthrusting would produce about 3 mm/yr of subsidence of the Longitudinal Valley floor. If we take such subsidence into account, the total uplift rate of the Coastal Range with respect to the footwall would be higher. For such a case we can use a higher slip rate on the Longitudinal Valley fault (*d*) to fit the uplift rate (Figures 4.12b and 4.14). However, the underthrusting of a rigid footwall is going to create geometric change of the fault plane over time, which is very difficult to quantify given the information we currently have.

This footwall subsidence, if it exists, may be balanced by sedimentation in the valley since the major rivers in the valley appear to have sedimentation rates higher than 5 mm/yr [*Hovius et al.*, 2000; *Dadson et al.*, 2003; *Fuller et al.*, 2003] (Figure 4.14). Some detailed information on the sedimentation rate in the valley and a well-designed leveling profile could test this hypothesis. There is, in fact, a data point at site KKL, a "pressure" ridge along a left-lateral fault in the valley (Figure 4.4). There a thick layer of mud, which contains numerous tree trunks older than 50 kyr, is present at a depth of about 3 m [*W.-S. Chen*, unpublished data]. This yields a subsidence rate of about 0.06

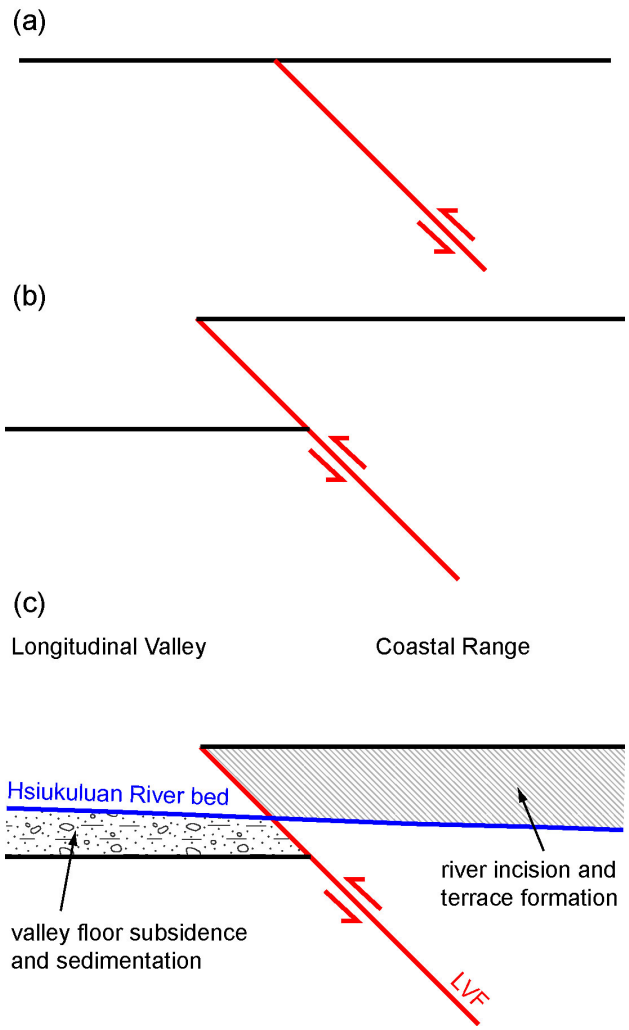

Figure 4.14. Cartoon showing the effect of footwall subsidence on the calculation of the Longitudinal Valley fault (LVF) slip rate. (a) Black line represents an original surface. In this case, it is an old Hsiukuluan River bed. (b) Slip along the fault produced offset of the original surface. (c) In the footwall block, the subsiding Longitudinal Valley floor is filled by fluvial sedimentation of the Hsiukuluan River. The river also incises the hanging-wall bock and produces river terraces. Thus the slip rate calculated from the incision rate is only a partial slip rate of the Longitudinal Valley fault. Blue line represents current Hsiukuluan River bed.

mm/yr (Figure 4.12b). Since this site is on a pressure ridge and is currently higher than the surrounding valley floor, the subsidence rate of the valley floor must be higher. Further to the south, however, a 3-yr-period leveling measurement, tied to tide gauge measurements at the coast southeast of Chihshang, does not show the valley floor to be subsiding [*Liu and Yu*, 1990]. More information is needed to solve this controversy.

Alternatively, the underthrusting footwall block may even be non-rigid. The

rigid-footwall assumption may be true for a continental foreland basin, where a fold-and-thrust belt forms over a non-deforming, rigid continental basement. However, in eastern Taiwan, the footwall of the Longitudinal Valley fault includes thick sediments and possible underlying forearc oceanic crust [*Shyu et al.*, 2005a]. These materials are not likely to behave rigidly. Therefore, the Longitudinal Valley fault may have a non-rigid, deforming footwall block. In such cases, the Longitudinal Valley floor will just underthrust and deform along the fault plane, providing the missing shortening rate. Since the footwall can deform, its underthrusting may have little or no effect on the uplift pattern of the hanging-wall block; thus the effect on the fault-bend fold calculation can be minimal. Therefore, the subsidence of the valley floor resulting from such underthrusting cannot be calculated from the uplift of the Coastal Range, and direct measurements of the valley floor subsidence rate are needed.

With the current inadequacy of information and the multiple possibilities in mind, we believe that the underthrusting of the Longitudinal Valley floor is responsible for at least part of the horizontal shortening. South of Taiwan, forearc oceanic lithosphere up to 40 km wide is being consumed between the Luzon volcanic arc and the submarine Hengchun Ridge [*Shyu et al.*, 2005b] (Figure 4.1). In order to create the current geographic pattern where the Coastal Range is attached to the Central Range, this forearc basement needs to be subducted beneath either the Central Range or the Coastal Range. Although the initial subduction may be in either direction [e.g., *Chemenda et al.*, 1997; *Malavieille et al.*, 2002; *Tang et al.*, 2002; *Shyu et al.*, 2005a], eastward underthrusting is likely to be the major mechanism for the final stage of the forearc oceanic lithosphere removal [*Shyu et al.*, 2005b]. Crustal thickening beneath eastern Taiwan, especially beneath the Coastal Range, has been observed in several seismic investigations [e.g., *Kim et al.*, 2004; *Lin*, 2005; *McIntosh et al.*, 2005]. Such observations are consistent with the hypothesis that the forearc oceanic lithosphere west of the Luzon volcanic arc is still subducting eastward at the latitude of Hsiukuluan canyon during the final phase of

collision.

4.6.2 Subsurface geometry of the Longitudinal Valley fault: The evolution of lithospheric sutures

The fault-bend fold model of the Longitudinal Valley fault has enabled us to construct its subsurface geometry beneath Hsiukuluan canyon using our measurements of bedding dip angles along the canyon. Figure 4.13 shows that the fault dips steeply initially, and the dip of the fault shallows at about 2.5 km below the surface to about 30°. This geometry, however, is very different from the geometry of the fault further to the south, near the town of Chihshang, where numerous small earthquake hypocenters define a listric shape with steep dips to much greater depths [*Chen and Rau*, 2002; *Kuochen et al.*, 2004].

It is possible that the Longitudinal Valley fault behaves differently along strike. In fact, although the listric band of seismicity is very obvious around Chihshang, it becomes less apparent both to the north and to the south [*Kuochen et al.*, 2004]. At the latitude of Hsiukuluan canyon there is a cluster of earthquake hypocenters between 20 and 40 km deep, much deeper than what was suggested by *Kuochen et al.* [2004] to be the Longitudinal Valley fault (Figure 4.3). There are, on the other hand, several small earthquakes at a shallower depth. More to the north, whereas many earthquakes are present, it becomes very difficult to visualize any cluster of earthquakes.

Why does the Longitudinal Valley fault behave significantly different along strike? We believe that this is the manifestation of the evolution of the Longitudinal Valley suture between the Luzon volcanic arc and the Central Range continental sliver. The collision, which began several million years ago, is progressing southward at a rate of about 90 mm/yr [*Suppe*, 1984, 1987]. During the collision, the Luzon volcanic arc and its forearc basins have shortened considerably to become the current Coastal Range and

Longitudinal Valley [e.g., *Chang et al.*, 2001; *Shyu et al.*, 2005b]. The transition area between the Taitung and Hualien Domains, near Hsiukuluan canyon, is where this shortening approaches its maximum [*Shyu et al.*, 2005a]. Therefore, at Hsiukuluan canyon the Longitudinal Valley fault should be close to its final, most mature form, whereas what is happening concurrently offshore, south of the Longitudinal Valley, should reveal what was occurring at Hsiukuluan canyon several million years ago. The along-strike difference of the Longitudinal Valley fault is thus reflecting the ongoing maturation of the suture.

We therefore propose the schematic model for the evolution of the Longitudinal Valley suture shown in Figure 4.15. Before the collision, the forearc oceanic lithosphere appears to subduct beneath the Central Range continental sliver, as is happening near the southern tip of Taiwan at about 22°N (Figure 4.15a). Bathymetric evidence suggests that the major structure there is a west-dipping thrust fault at the eastern edge of the forearc basin [*Shyu et al.*, 2005a]. When the two non-oceanic lithospheric blocks start to collide, an east-dipping reverse fault appears, along which the forearc oceanic crust begins to subduct eastward (Figure 4.15b). This would be the first generation of the Longitudinal Valley fault, and such geometry can be observed now at the southern end of the valley between about 22°40'N and 22°50'N.

As the two blocks continues to impinge upon each other, thickening of the two blocks next to the suture should occur. We believe this is facilitated by the evolution of multiple reverse-fault wedges, with younger ones at shallower depths (Figure 4.15). This is likely to be a very efficient way to thicken the margins of the two crustal blocks as the suture develops. At the latitude of Chihshang, about 23°10'N (Figure 4.15c), many earthquake hypocenters illuminate the listric-shaped Longitudinal Valley fault, but deeper seismicity appears to indicate an older, deeper reverse-fault wedge.

As the suture matures northward (Figure 4.15d), the shallow Longitudinal Valley fault, reconstructed from the fault-bend fold model for the latitude of Hsiukuluan canyon,

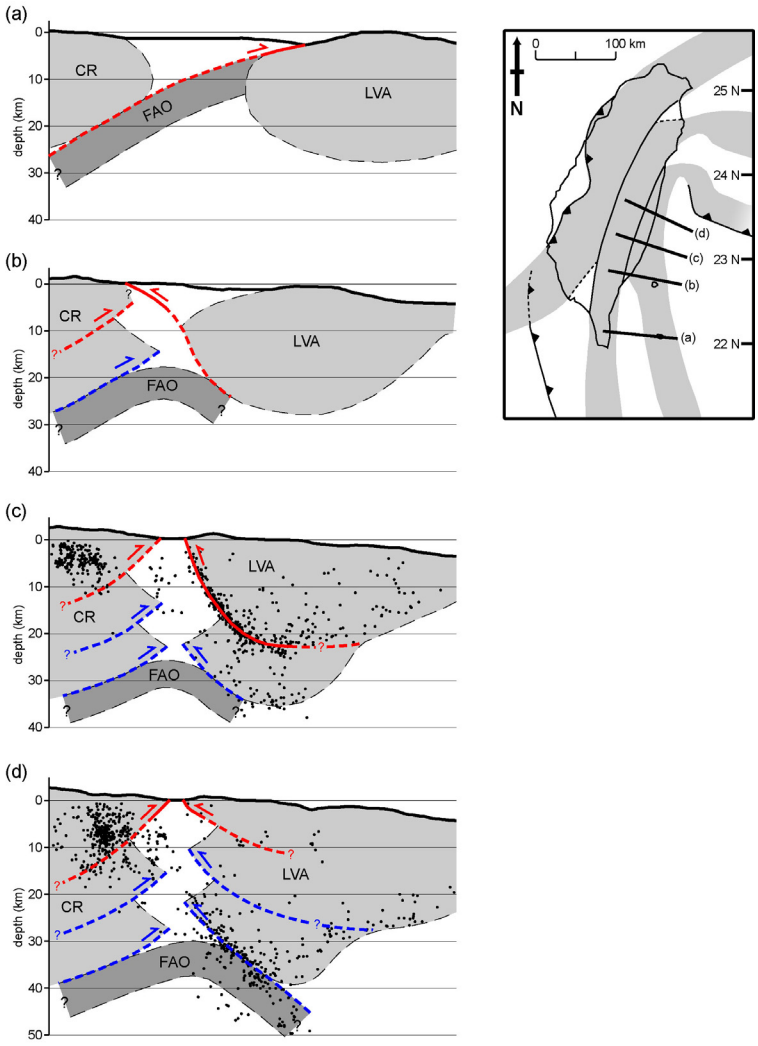

Figure 4.15. Schematic crustal cross sections show the evolution of the Longitudinal Valley suture. Each section is drawn using current topography and observations along the lines specified on the index map. (a) Before suturing, the Luzon forearc oceanic lithosphere (FAO) subducts beneath the Central Range continental sliver (CR). This is currently occurring at about the latitude of the southern tip of Taiwan at about 22°N. (b) As the Luzon volcanic arc lithosphere (LVA) approaches the Central Range, an east-dipping thrust fault appears, allowing the FAO to also subduct underneath the LVA. This is the first Longitudinal Valley fault. Contemporaneously on the west side of the Valley, the proximity of the LVA to the CR produces a newer, shallower west-dipping thrust fault above the original one. This is the current structural geometry near the southern end of the Longitudinal Valley between about 22°40'N and 22°50'N. (c) As the suture matures, the two non-oceanic lithospheric blocks both start to thicken by evolving multiple reverse-fault wedges, with the younger ones at shallower depth. Here the listric-shaped Longitudinal Valley fault is the second generation of the east-dipping fault. This is the current structural geometry at the latitude of Chihshang, about 23°10'N. (d) At the latitude of Hsiukuluan canyon, about 23°30'N, the suture is nearing maturity. The shallower dipping Longitudinal Valley fault, reconstructed using the fault-bend fold model, is the youngest and shallowest of the family of faults dipping under the Coastal Range. In all, the suture has evolved into a "Christmas tree" shape, with a thick pile of sediments between the two non-oceanic lithospheric blocks and underlain by the subducted forearc oceanic lithosphere. Red indicates the youngest and currently active faults at each time frame, and blue indicates older faults that may still be active. Faults are dashed where inferred. Relocated earthquake hypocenters in (c) and (d) were adapted from *Kuochen et al.* [2004].

about 23°30'N, appears to be the shallowest, youngest generation of the fault. There may be several deeper and older reverse-fault wedges, one of which should connect with the current, listric-shaped fault at the latitude of Chihshang. The deepest seismicity cluster under Hsiukuluan canyon (Figure 4.15d) may reflect the very late-stage of subduction of the oceanic forearc crust beneath the Coastal Range.

In all, the evolution of multiple reverse-fault wedges facilitates the thickening of the margins of both non-oceanic crust at the suture and creates a "Christmas tree" shape for the Longitudinal Valley suture. Between the two non-oceanic blocks of lithosphere, the Longitudinal Valley itself would be a thick pile of sediments underlain by the subducted forearc oceanic lithosphere. This "Christmas tree" geometry also explains the relatively uniform width of the Longitudinal Valley from south to north despite the orogeny being much more mature in the north [e.g., *Shyu et al.*, 2005a].

This geometry, however, requires accommodation structures between Chihshang and Hsiukuluan canyon in order to connect faults at different depths. Geomorphic manifestation of such accommodation structures is scarce, but there are, in fact, many other mapped faults present in the bedrock of the Coastal Range. Although the current activity and mechanisms of these structures are not well understood, some of them may be functioning currently as accommodation structures. Further analysis is needed in order to characterize such secondary structures.

We believe that the complex, "Christmas tree" pattern of indentation suggested in Figure 4.15 might be characteristic of the way suture zones form in general. Based upon seismic reflection profiles, structures that show indentations at crustal scale have been interpreted for several suture zones such as the Pyrenees [e.g., *Seguret and Daignieres*, 1986; *Roure et al.*, 1989; *Muñoz*, 1992] and the Urals [e.g., *Juhlin et al.*, 1998; *Steer et al.*, 1998; *Friberg et al.*, 2002]. Nonetheless, these interpretations, based on current observations of old, developed sutures, do not provide good insight into their early evolution. In other words, suture zones are nearly vertical structures that have to

evolve from the impingement of continental margins where crust is initially thinner, and little is known about the processes that are responsible for converting the thin continental margin into the thickened crust adjacent to a mature suture. The actively suturing Taiwan orogen may thus provide an insight about how to interpret old suture zones. In particular, the forearc oceanic crust has been removed and the suture between the Luzon arc and the Central Range continental sliver keeps a near vertical geometry due to the complex "Christmas tree" indentation pattern.

4.6.3 Long-term uplift rates of the Coastal Range

The exceptionally high rate of the Longitudinal Valley fault also implies that the current fault is a fairly new structure. One of the major questions raised by such a high rate is the different sizes of the two mountain ranges on both sides of the Longitudinal Valley. The Coastal Range, on the hanging-wall block of the Longitudinal Valley fault, is much lower than the Central Range, west of the valley. This is odd considering the fault's high rate: If we assume that the erosion rates around the Central and Coastal Ranges are similar, the Longitudinal Valley fault cannot be slipping at such a high rate for very long.

The rocks adjacent to the Longitudinal Valley fault belong to the Paliwan Formation, a Plio-Pleistocene deep marine turbidite unit [e.g., *Chi et al.*, 1981; *Teng et al.*, 1988]. Their original depositional environments are the forearc and intra-arc basins around the Luzon volcanic arc at water depths of about 3-4 km [e.g., *Chen and Wang*, 1988; *Teng et al.*, 1988]. These rocks currently have a maximum elevation of about 1 km in the Coastal Range. Therefore, the million-year uplift rate of these rocks since their deposition is only about a couple of mm/yr. Furthermore, since these rocks are not metamorphosed, they have not been buried much deeper than several kilometers. This also yields a long-term exhumation rate much less than 5 mm/yr.

This very low long-term rock uplift rate and the high recent slip rate of the Longitudinal Valley fault implies that the current rapid uplift of the Coastal Range, produced by the slip on the Longitudinal Valley fault, is a rather young phenomenon. At an uplift rate of 20 mm/yr, the uplift may have started only a couple hundred thousand years ago. This implication is consistent with the fact that there is no Longitudinal Valley fault equivalent further south, in the Lutao-Lanyu Domain of the Taiwan orogen [*Shyu et al.*, 2005a] (Figure 4.15a). In fact, very clear bathymetric evidence suggests that the major structure in the Lutao-Lanyu Domain is a west-dipping thrust fault at the eastern edge of the forearc basin [*Shyu et al.*, 2005a] and that the westward underthrusting is the major mechanism for the consumption of the forearc oceanic lithosphere there [*Shyu et al.*, 2005b].

The Longitudinal Valley fault is therefore the product of the final episode of the evolution of Taiwan's eastern suture. This structure appeared when most of the forearc lithosphere had been consumed and the volcanic arc started to impinge upon the Central Range continental sliver [*Shyu et al.*, 2005b] (Figure 4.15b). At the latitude of Hsiukuluan canyon this is likely to have begun a few hundred thousand years ago. After its appearance, this structure absorbed most of the shortening by the deformation of the forearc sediments, and several generations of this structure evolved into a series of reverse-fault wedges (Figure 4.15), creating the "Christmas tree" shape of the Longitudinal Valley suture. Further to the north, where the volcanic arc has fully docked to the continental sliver of the Central Range, the Longitudinal Valley fault has become a predominantly left-lateral fault.

4.6.4 Earthquake potential of the Longitudinal Valley fault

From the ages of the Hsiukuluan River terraces we have calculated the minimal millennial slip rate on the Longitudinal Valley fault. Using this rate and our limited

knowledge of historical earthquakes along the fault, we can start to evaluate preliminary earthquake recurrence intervals of the fault.

The most recent earthquake with surface ruptures occurred on the Longitudinal Valley fault is the earthquake couplet in 1951 [*Shyu et al.*, 2005c] (Figure 4.2). This earthquake was produced by rupture of two separate sections of the fault, about 45 km in total length but 20 km apart, with a maximum co-seismic offset of up to 2.1 m. Average co-seismic uplift along the fault is approximately 0.5-1 m. From the river terraces we know that the long-term uplift rate near the fault is about 20 mm/yr. Therefore, if the 0.5-1 m event in 1951 is a characteristic event on the fault, the recurrence interval will be merely about 50 yr!

It is interesting that the segment of the Longitudinal Valley fault near Hsiukuluan canyon did not rupture during the 1951 earthquakes [*Shyu et al.*, 2005c] (Figure 4.2). It was the segments both to the north and to the south that ruptured. Therefore, this central segment may behave differently, perhaps because it is actually a separate structure as we have suggested above. Characteristic rupture events with larger co-seismic offsets, for example, would result in a longer recurrence interval for this segment.

On the other hand, the long-term shortening may not be absorbed entirely by co-seismic deformations. If aseismic creep also releases some component of accumulated strain, longer earthquake recurrence intervals or smaller characteristic events would result. This may be the case for the southern part of the Longitudinal Valley fault near Chihshang, where rapid aseismic creep is well documented [e.g., *Angelier et al.*, 1997; *Lee et al.*, 2001, 2003]. Around Hsiukuluan canyon, however, current data is not adequate to determine if significant aseismic creep occurs [*Yu and Liu*, 1989].

Paleoseismic studies can also help us determine the seismic behavior of the fault. Preliminary paleoseismic works on the segment of the Longitudinal Valley fault north of Hsiukuluan canyon indicate that the fault may have ruptured twice before the 1951 event,

with intervals of about 160 yr [*Fengler et al.*, in preparation]. If the fault ruptures at similar intervals near Hsiukuluan canyon, the characteristic rupture of the fault should have co-seismic slips greater than 3.5 m. More studies are needed along the central segment of the fault in order to understand better about the strain accumulation and release there.

4.7 Conclusions

Numerous fluvial terraces with ages up to 10 kyr are present along the Hsiukuluan River valley across the Coastal Range in eastern Taiwan. The ages of these terraces provide the basis for calculating the bedrock incision rate, and therefore rock uplift rate along the river valley, in the hanging-wall block of the Longitudinal Valley fault. Using this information, we have constructed the subsurface geometry of the fault and calculated its millennial slip rate.

Near Hsiukuluan canyon, the Longitudinal Valley fault likely dips about 50° at its uppermost km or so, but its dip shallows to about 30° by about 2.5 km. Slip rate on the fault is approximately 23 mm/yr, which is also the maximum value of the horizontal shortening rate.

Our proposed subsurface geometry is very different from what has been suggested further south. This indicates that the fault near Hsiukuluan canyon and further to the south may not be at the same structural depth, a result of the evolution of the Longitudinal Valley suture. Moreover, our calculation suggests that the fault may have been present for only several hundred thousand years, and a significant part of the horizontal shortening may be absorbed by the underthrusting of the Longitudinal Valley basement. More geodetic, seismic, and paleoseismic studies are needed in order to test our hypothesis and to further understand the earthquake potential of the Longitudinal Valley fault.

4.8 Acknowledgments

We are grateful for valuable discussions with H.-H. Chen, H.-T. Chu, M.-L. Hsieh, Y.-J. Hsu, J.-C. Lee, W.-T. Liang, M.-S. Lin, R.-J. Rau, C.P. Stark, Y.-M. Wu, and S.-B. Yu. We were fortunate to have the significant help of our friends and students from the National Taiwan University, especially C.-H. Chen, Y.-C. Chen, L.-H. Chung, C. Huang, S.-H. Huang, P.-N. Li, T. Watanuki, Y. Wang, B.C.-C. Yang, and Y.-C. Yen for the heavy and arduous field works of this research. Radiocarbon dating by M. Kashgarian in the Center for Accelerator Mass Spectrometry, LLNL, was crucial for this research. Y.-J. Hsu and Y.-M. Wu kindly provided their GPS and seismicity information to us. Our project in Taiwan was supported by National Science Foundation (NSF) grant EAR-0208505 and partly by project 92EC2A380204 of the Central Geological Survey, MOEA, Taiwan. This research was also supported in part by the Gordon and Betty Moore Foundation through the Tectonics Observatory at California Institute of Technology (Caltech). This is contribution #13 of Caltech Tectonics Observatory.

4.9 References

Angelier, J., H.-T. Chu, and J.-C. Lee (1997), Shear concentration in a collision zone: kinematics of the Chihshang Fault as revealed by outcrop-scale quantification of active faulting, Longitudinal Valley, eastern Taiwan, *Tectonophysics*, *274*, 117-143.

Biq, C. (1965), The East Taiwan Rift, *Pet. Geol. Taiwan*, *4*, 93-106.

Bonilla, M. G. (1975), A review of recently active faults in Taiwan, *Open File Rep. 75-41*, 58pp., U. S. Geol. Surv., Menlo Park, Calif.

Bonilla, M. G. (1977), Summary of Quaternary faulting and elevation changes in Taiwan, *Mem. Geol. Soc. China*, *2*, 43-55.

Bull, W. B. (1990), Stream-terrace genesis: implications for soil development, *Geomorphology*, *3*, 351-367.

Bull, W. B., and P. L. K. Knuepfer (1987), Adjustments by the Charwell River, New Zealand, to uplift and climatic changes, *Geomorphology*, *1*, 15-32.

Chang, C. P., J. Angelier, C. Y. Huang, and C. S. Liu (2001), Structural evolution and significance of a mélange in a collision belt: the Lichi Mélange and the Taiwan arc-continent collision, *Geol. Mag.*, *138*, 633-651.

Chang, H. H. (1988), *Fluvial Processes in River Engineering*, 432pp., John Wiley & Sons, New York.

Chang, J.-C., T.-T. Shih, S.-M. Shen, and C.-L. Chang (1992), A geomorphological study of river terrace in northern Huatung Longitudinal Valley (in Chinese with English abstract), *Geogr. Res.*, *18*, 1-51.

Chemenda, A. I., R. K. Yang, C.-H. Hsieh, and A. L. Groholsky (1997), Evolutionary model for the Taiwan collision based on physical modelling, *Tectonophysics*, *274*, 253-274.

Chen, H.-H., and R.-J. Rau (2002), Earthquake locations and style of faulting in an active arc-continent plate boundary: the Chihshang fault of eastern Taiwan, *EOS, Trans., Am. Geophys. Uni.*, *83*(47), Fall Meet. Suppl., Abstract T61B-1277.

Chen, W.-S. (1988), Tectonic evolution of sedimentary basins in Coastal Range, Taiwan (in Chinese), Ph.D. thesis, 304pp., Natl. Taiwan Univ., Taipei.

Chen, W.-S., and Y. Wang (1988), Development of deep-sea fan systems in Coastal Range Basin, eastern Taiwan, *Acta Geol. Taiwanica*, *26*, 37-56.

Chen, W.-S., M.-T. Huang, and T.-K. Liu (1991), Neotectonic significance of the Chimei fault in the Coastal Range, eastern Taiwan, *Proc. Geol. Soc. China*, *34*, 43-56.

Chen, Y.-G. (1988), C-14 dating and correlation of river terraces along the lower reach of

the Tahan-chi, northern Taiwan (in Chinese), M.S. thesis, 88pp., Natl. Taiwan Univ., Taipei.

Chen, Y.-G. (1993), Sea-level change and neotectonics in southern part of Taiwan region since Late Pleistocene (in Chinese), Ph.D. thesis, 158pp., Natl. Taiwan Univ., Taipei.

Chen, Y.-G., and T.-K. Liu (1996), Sea level changes in the last several thousand years, Penghu Islands, Taiwan Strait, *Quat. Res.*, *45*, 254-262.

Chen, Y.-G., and T.-K. Liu (2000), Holocene uplift and subsidence along an active tectonic margin southwestern Taiwan, *Quat. Sci. Rev.*, *19*, 923-930.

Chen, Y.-G., W.-S. Chen, J.-C. Lee, Y.-H. Lee, C.-T. Lee, H.-C. Chang, and C.-H. Lo (2001), Surface rupture of 1999 Chi-Chi earthquake yields insights on active tectonics of central Taiwan, *Bull. Seismol. Soc. Am.*, *91*, 977-985.

Cheng, S. N., and Y. T. Yeh (1989), *Catalog of the Earthquakes in Taiwan from 1604 to 1988* (in Chinese), 255pp., Inst. Earth Sci., Acad. Sinica, Taipei, Taiwan.

Cheng, S.-N., Y. T. Yeh, and M.-S. Yu (1996), The 1951 Taitung earthquake in Taiwan, *J. Geol. Soc. China*, *39*, 267-285.

Chi, W.-R., J. Namson, and J. Suppe (1981), Stratigraphic record of plate interactions in the Coastal Range of eastern Taiwan, *Mem. Geol. Soc. China*, *4*, 155-194.

Dadson, S. J., et al. (2003), Links between erosion, runoff variability and seismicity in the Taiwan orogen, *Nature*, *426*, 648-651.

Fengler, K. P., C. M. Rubin, W.-S. Chen, Y.-G. Chen, and C. L. Madden, Similar slip per event on the Longitudinal Valley fault, Eastern Taiwan, manuscript in preparation.

Friberg, M., C. Juhlin, M. Beckholmen, G. A. Petrov, and A. G. Green (2002), Palaeozoic tectonic evolution of the Middle Urals in the light of the ESRU seismic experiments, *J. Geol. Soc. London*, *159*, 295-306.

Fuller, C. W., S. D. Willett, N. Hovius, and R. Slingerland (2003), Erosion rates for Taiwan mountain basins: New determinations from suspended sediment records and a stochastic model of their temporal variation, *J. Geol.*, *111*, 71-87.

Ho, C. S. (1986), A synthesis of the geologic evolution of Taiwan, *Tectonophysics*, *125*, 1-16.

Ho, C. S. (1988), *An Introduction to the Geology of Taiwan, Explanatory Text of the Geologic Map of Taiwan*, 2nd ed., 192pp., Cent. Geol. Surv., Ministry Econ. Affairs, Taipei, Taiwan.

Hovius, N., and C. Stark (2001), Actively meandering bedrock rivers, *EOS, Trans., Am. Geophys. Uni.*, *82*(47), Fall Meet. Suppl., Abstract H52B-0389.

Hovius, N., C. P. Stark, H.-T. Chu, and J.-C. Lin (2000), Supply and removal of sediment in a landslide-dominated mountain belt: Central Range, Taiwan, *J. Geol.*, *108*, 73-89.

Hsieh, M.-L., T.-H. Lai, and P.-M. Liew (1994), Holocene climatic river terraces in an active tectonic-uplifting area, middle part of the Coastal Range, eastern Taiwan, *J. Geol. Soc. China*, *37*, 97-114.

Hsieh, M.-L., C. P. Stark, and C.-C. Liu (2003), New radiocarbon dates from the Hsiu-ku-luan River crossing the Coastal Range, eastern Taiwan, and their tectonic implications (in Chinese), *Program with Abstracts, 2003 Ann. Meet. Geol. Soc. Located in Taipei*, 51, Taipei, Taiwan.

Hsu, M.-T. (1980), *Earthquake Catalogues in Taiwan (from 1644 to 1979)* (in Chinese), 77pp., Natl. Taiwan Univ., Taipei.

Hsu, T. L. (1962), Recent faulting in the Longitudinal Valley of eastern Taiwan, *Mem. Geol. Soc. China*, *1*, 95-102.

Hsu, Y.-J., M. Simons, S.-B. Yu, L.-C. Kuo, and H.-Y. Chen (2003), A two-dimensional dislocation model for interseismic deformation of the Taiwan mountain belt, *Earth Planet. Sci. Lett.*, *211*, 287-294.

Huang, C.-Y., W.-Y. Wu, C.-P. Chang, S. Tsao, P. B. Yuan, C.-W. Lin, and K.-Y. Xia (1997), Tectonic evolution of accretionary prism in the arc-continent collision terrane of Taiwan, *Tectonophysics*, *281*, 31-51.

Juhlin, C., M. Friberg, H. P. Echtler, T. Hismatulin, A. Rybalka, A. G. Green, and J. Ansorge (1998), Crustal structure of the Middle Urals: Results from the (ESRU) Europrobe seismic reflection profiling in the Urals experiments, *Tectonics*, *17*, 710-725.

Kelson, K. I., K.-H. Kang, W. D. Page, C.-T. Lee, and L. S. Cluff (2001), Representative styles of deformation along the Chelungpu fault from the 1999 Chi-Chi (Taiwan) earthquake: Geomorphic characteristics and responses of man-made structures, *Bull. Seismol. Soc. Am.*, *91*, 930-952.

Kim, K.-H., J.-M. Chiu, H. Kao, Q. Liu, and Y.-H. Yeh (2004), A preliminary study of crustal structure in Taiwan region using receiver function analysis, *Geophys. J. Int.*, *159*, 146-164.

Kuo, C.-M., and P.-M. Liew (2000), Vegetational history and climatic fluctuations based on pollen analysis of the Toushe peat bog, central Taiwan since the Last Glacial Maximum, *J. Geol. Soc. China*, *43*, 379-392.

Kuochen, H., Y.-M. Wu, C.-H. Chang, J.-C. Hu, and W.-S. Chen (2004), Relocation of the eastern Taiwan earthquakes and its tectonic implications, *Terr. Atmos. Oceanic Sci.*, *15*, 647-666.

Lallemand, S., and C.-S. Liu (1998), Geodynamic implications of present-day kinematics in the southern Ryukyus, *J. Geol. Soc. China*, *41*, 551-564.

Lavé, J., and J. P. Avouac (2000), Active folding of fluvial terraces across the Siwaliks Hills, Himalayas of central Nepal, *J. Geophys. Res.*, *105*, 5,735-5,770.

Lavé, J., and J. P. Avouac (2001), Fluvial incision and tectonic uplift across the Himalayas of central Nepal, *J. Geophys. Res.*, *106*, 26,561-26,591.

Lee, J.-C., J. Angelier, H.-T. Chu, J.-C. Hu, and F.-S. Jeng (2001), Continuous monitoring of an active fault in a plate suture zone: a creepmeter study of the Chihshang Fault, eastern Taiwan, *Tectonophysics*, *333*, 219-240.

Lee, J.-C., J. Angelier, H.-T. Chu, J.-C. Hu, F.-S. Jeng, and R.-J. Rau (2003), Active fault creep variations at Chihshang, Taiwan, revealed by creep meter monitoring, 1998-2001, *J. Geophys. Res.*, *108*(B11), 2528, doi:10.1029/2003JB002394.

Liew, P.-M., and M.-L. Hsieh (2000), Late Holocene (2 ka) sea level, river discharge and climate interrelationship in the Taiwan region, *J. Asian Earth Sci.*, *18*, 499-505.

Lin, C.-H. (2005), Identification of mantle reflections from a dense linear seismic array: Tectonic implications to the Taiwan orogeny, *Geophys. Res. Lett.*, *32*, L06315, doi:10.1029/2004GL021814.

Liu, C.-C., and S.-B. Yu (1990), Vertical crustal movements in eastern Taiwan and their tectonic implications, *Tectonophysics*, *183*, 111-119.

Malavieille, J., S. E. Lallemand, S. Dominguez, A. Deschamps, C.-Y. Lu, C.-S. Liu, P. Schnürle, and the ACT Scientific Crew (2002), Arc-continent collision in Taiwan: new marine observations and tectonic evolution, *Geol. Soc. Am. Spec. Paper*, *358*, 187-211.

McIntosh, K., Y. Nakamura, T.-K. Wang, R.-C. Shih, A. Chen, and C.-S. Liu (2005), Crustal-scale seismic profiles across Taiwan and the western Philippine Sea, *Tectonophysics*, *401*, 23-54.

Miall, A. D. (1991), Stratigraphic sequences and their chronostratigraphic correlation, *J. Sedi. Petrol.*, *61*, 497-505.

Muñoz, J. A. (1992), Evolution of a continental collision belt: ECORS-Pyrenees crustal balanced cross-section, in *Thrust Tectonics*, edited by K. R. McClay, pp. 235-246, Chapman and Hall, London, UK.

Roure, F., P. Choukroune, X. Berastegui, J. A. Munoz, A. Villien, P. Matheron, M. Bareyt, M. Seguret, P. Camara, and J. Deramond (1989), ECORS deep seismic data and balanced cross sections: Geometric constraints on the evolution of the Pyrenees, *Tectonics*, *8*, 41-50.

Schnürle, P., C.-S. Liu, S. E. Lallemand, and D. Reed (1998), Structural controls of the Taitung Canyon in the Huatung Basin east of Taiwan, *Terr. Atmos. Oceanic Sci.*, *9*, 453-472.

Schumm, S. A. (1993), River response to baselevel change: implications for sequence

stratigraphy, *J. Geol.*, *101*, 279-294.

Seguret, M., and M. Daignieres (1986), Crustal scale balanced cross-sections of the Pyrenees; discussion, *Tectonophysics*, *129*, 303-318.

Sella, G. F., T. H. Dixon, and A. Mao (2002), REVEL: A model for Recent plate velocities from space geodesy, *J. Geophys. Res.*, *107*(B4), 2081, doi:10.1029/2000JB000033.

Shyu, J. B. H., K. Sieh, L.-H. Chung, Y.-G. Chen, and Y. Wang (2002), The active tectonics of eastern Taiwan—new insights from the two geomorphic tablelands ("the Feet") in the Longitudinal Valley, *EOS, Trans., Am. Geophys. Uni.*, *83*(47), Fall Meet. Suppl., Abstract T61B-1278.

Shyu, J. B. H., K. Sieh, Y.-G. Chen, and C.-S. Liu (2005a), Neotectonic architecture of Taiwan and its implications for future large earthquakes, *J. Geophys. Res.*, *110*, B08402, doi:10.1029/2004JB003251.

Shyu, J. B. H., K. Sieh, and Y.-G. Chen (2005b), Tandem suturing and disarticulation of the Taiwan orogen revealed by its neotectonic elements, *Earth Planet. Sci. Lett.*, *233*, 167-177.

Shyu, J. B. H., L.-H. Chung, Y.-G. Chen, J.-C. Lee, and K. Sieh (2005c), Re-evaluation of the surface ruptures of the November 1951 earthquake series in eastern Taiwan, and its neotectonic implications, *J. Asian Earth Sci.*, submitted for publication.

Shyu, J. B. H., K. Sieh, Y.-G. Chen, and L.-H. Chung (2005d), Geomorphic analysis of the Central Range fault, the second major active structure of the Longitudinal Valley suture, eastern Taiwan, *Geol. Soc. Am. Bull.*, submitted for publication.

Simoes, M., and J.-P. Avouac, Investigating the kinematics of mountain-building in an arc-continent collision zone: example of Taiwan, manuscript in preparation.

Steer, D. N., J. H. Knapp, L. D. Brown, H. P. Echtler, D. L. Brown, and R. Berzin (1998), Deep structure of the continental lithosphere in an unextended orogen: An explosive-source seismic reflection profile in the Urals (Urals Seismic Experiment and Integrated Studies (URSEIS 1995)), *Tectonics*, *17*, 143-157.

Stuiver, M., and P. J. Reimer (1993), Extended ^{14}C data base and revised CALIB 3.0 ^{14}C age calibration program, *Radiocarbon*, *35*, 215-230.

Suppe, J. (1984), Kinematics of arc-continent collision, flipping of subduction, and back-arc spreading near Taiwan, *Mem. Geol. Soc. China*, *6*, 21-33.

Suppe, J. (1987), The active Taiwan mountain belt, in *Anatomy of Mountain Chains*, edited by J. P. Schaer, and J. Rodgers, pp. 277-293, Princeton Univ. Press, Princeton, N.J.

Tang, J.-C., A. I. Chemenda, J. Chéry, S. Lallemand, and R. Hassani (2002),

Compressional subduction regime and initial arc-continent collision: Numerical modeling, *Geol. Soc. Am. Spec. Paper*, *358*, 177-186.

Teng, L. S. (1980), Lithology and provenance of the Fanshuliao Formation, northern Coastal Range, eastern Taiwan, *Proc. Geol. Soc. China*, *23*, 118-129.

Teng, L. S. (1982), Stratigraphy and sedimentation of the Suilien Conglomerate, northern Coastal Range, eastern Taiwan, *Acta Geol. Taiwanica*, *21*, 201-220.

Teng, L. S. (1987), Stratigraphic records of the late Cenozoic Penglai orogeny of Taiwan, *Acta Geol. Taiwanica*, *25*, 205-224.

Teng, L. S. (1990), Late Cenozoic arc-continent collision in Taiwan, *Tectonophysics*, *183*, 57-76.

Teng, L. S. (1996), Extensional collapse of the northern Taiwan mountain belt, *Geology*, *24*, 949-952.

Teng, L. S., W.-S. Chen, Y. Wang, S.-R. Song, and H.-J. Lo (1988), Toward a comprehensive stratigraphic system of the Coastal Range, eastern Taiwan, *Acta Geol. Taiwanica*, *26*, 19-35.

Yu, S.-B., and C.-C. Liu (1989), Fault creep on the central segment of the Longitudinal Valley fault, eastern Taiwan, *Proc. Geol. Soc. China*, *32*, 209-231.

Yu, S.-B., H.-Y. Chen, and L.-C. Kuo (1997), Velocity field of GPS stations in the Taiwan area, *Tectonophysics*, *274*, 41-59.

Yue, L.-F., J. Suppe, and J.-H. Hung (2005), Structural geology of a classic thrust belt earthquake: the 1999 Chi-Chi earthquake Taiwan (M_w = 7.6), *J. Struct. Geol.*, *27*, 2,058-2,083.

Chapter 5

Geomorphic Analysis of the Central Range Fault, the Second Major Active Structure of the Longitudinal Valley Suture, Eastern Taiwan

An earlier version of this chapter has been submitted as:

Shyu, J.B.H., K. Sieh, Y.-G. Chen, and L.-H. Chung, 2005, *Geological Society of America Bulletin*, submitted for publication.

5.1 Abstract

Numerous landforms along the Longitudinal Valley suture of eastern Taiwan indicate that two opposing reverse faults currently dominate the suturing process. The east-dipping Longitudinal Valley fault, on the eastern flank of the valley, is well known. The west-dipping Central Range reverse fault, on the western flank of the valley, is more obscure. Nonetheless, it has produced many uplifted lateritic fluvial terraces along the eastern flank of the Central Range in the central reach of the valley, from just north of the Wuhe Tableland to near Chihshang. The fault appears to be active but blind south of Chihshang and inactive along the northern part of the Longitudinal Valley. The maximum slip rate of the fault through the late Quaternary Period is lower than 13.6 mm/yr. This constraint means that the fault is absorbing far less than half of the horizontal shortening across the Longitudinal Valley suture. The fault is an expression of shallow brittle deformation along the eastern edge of the Central Range, which is probably rising rapidly by pervasive ductile crustal thickening.

Keywords: Taiwan, tectonic geomorphology, Central Range fault, Longitudinal Valley, sutures.

5.2 Introduction

The island of Taiwan is the product of the collision of the Eurasian and the Philippine Sea plates over the past several million years [e.g., *Ho*, 1986; *Teng*, 1987, 1990, 1996; and references therein]. This collision involves three lithospheric pieces: the Eurasian continental margin on the west, the Luzon volcanic arc on the east, and a thin continental sliver, part of which forms the Central Range of Taiwan [*Shyu et al.*, 2005a] (Figure 5.1). Demarcating these three blocks are two sutures. The eastern suture, along the Longitudinal Valley of eastern Taiwan, has long been known as one of the world's most tectonically active belts. Seismic activity and active structures are abundant along this linear, N-S trending valley.

The principal active structure in the valley is the Longitudinal Valley fault [e.g., *Shyu et al.*, 2005b] (Figure 5.2). This east-dipping oblique-slip fault, running along the eastern edge of the valley, is slipping at a high rate and creating rapid uplift of the Coastal Range in its hanging-wall block [e.g., *Yu and Liu*, 1989; *Hsu et al.*, 2003; *Shyu et al.*, 2005c]. This high rate of activity has attracted numerous geodetic [e.g., *Yu and Liu*, 1989; *Liu and Yu*, 1990; *Angelier et al.*, 1997; *Lee et al.*, 2001, 2003; *Yu and Kuo*, 2001] and seismologic [e.g., *Cheng et al.*, 1996; *Chen and Rau*, 2002; *Kuochen et al.*, 2004; *Lin*, 2004] investigations. These studies have shown that one part of the Longitudinal Valley fault is creeping aseismically at a high rate but is also capable of coseismic rupture. Ruptures of the fault produced large earthquakes in 1951 and many moderate earthquakes subsequently, including those in 1972, 1995, and 2003 [*Chan*, 1985; *Chen and Rau*, 2002; *Lin*, 2004; *Kuochen et al.*, 2004, 2005]. Aftershocks of these moderate earthquakes appear to illuminate the fault plane as a listric surface [*Chen and Rau*, 2002; *Kuochen et al.*, 2004].

Although much is known and accepted about the activity of the Longitudinal Valley fault, a related structure on the western edge of the valley remains very controversial.

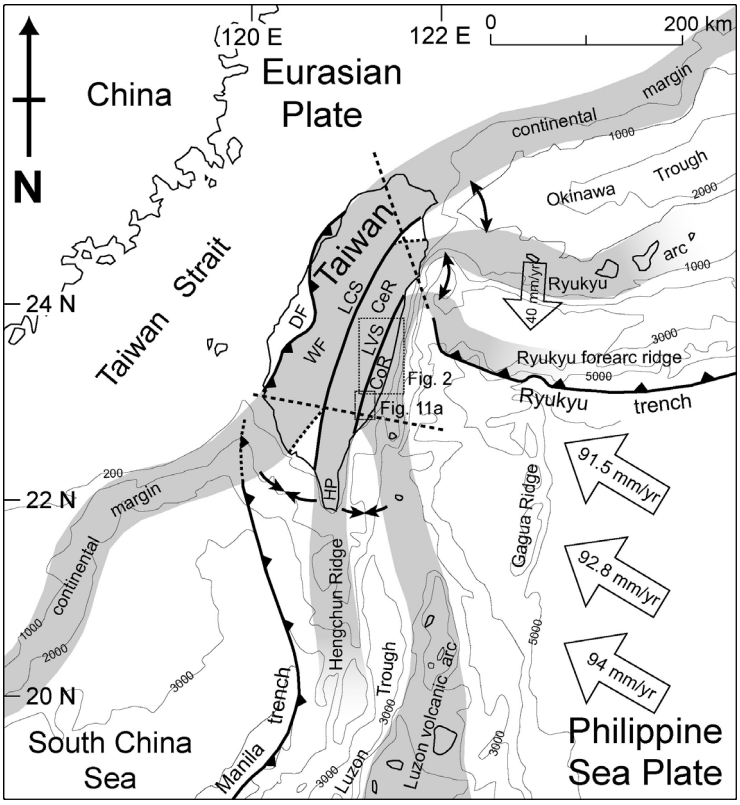

Figure 5.1. The island of Taiwan is being created by a tandem suturing of the Luzon volcanic arc and a sliver of continental crust to the Chinese continental margin. In eastern Taiwan, the Longitudinal Valley suture (LVS) is the eastern of the two sutures. This suture joins the Coastal Range (CoR), the docked part of the Luzon volcanic arc, and the continental sliver of the Central Range (CeR), the mountainous backbone of the island. Current velocity vectors of the Philippine Sea plate relative to South China, at 124°E and 20°, 21°, and 22°N, are calculated using the Recent plate velocity model (REVEL) of *Sella et al.* [2002]. Current velocity vector of the Ryukyu arc is adapted from *Lallemand and Liu* [1998]. Black dashed lines are the northern and western limits of the Wadati-Benioff zone of the two subduction zones taken from the seismicity database of the Central Weather Bureau, Taiwan. DF: deformation front; LCS: Lishan-Chaochou suture; WF: Western Foothills; HP: Hengchun Peninsula. Adapted from *Shyu et al.* [2005a].

Many believe that a west-dipping reverse fault is present along the western edge of the valley, making the valley a "ramp valley" flanked by reverse faults. *Biq* [1965] named this east-vergent reverse fault the Central Range thrust. However, some believe there is, instead, a normal fault which accommodates subsidence of the Longitudinal Valley floor with respect to the Central Range [e.g., *Crespi et al.*, 1996; *Lee et al.*, 2001, 2003]. Extending the spectrum of opinion, others maintain that there is no fault at all and that the eastern flank of the Central Range is being covered by the sediments of the valley [e.g., *Malavieille et al.*, 2002].

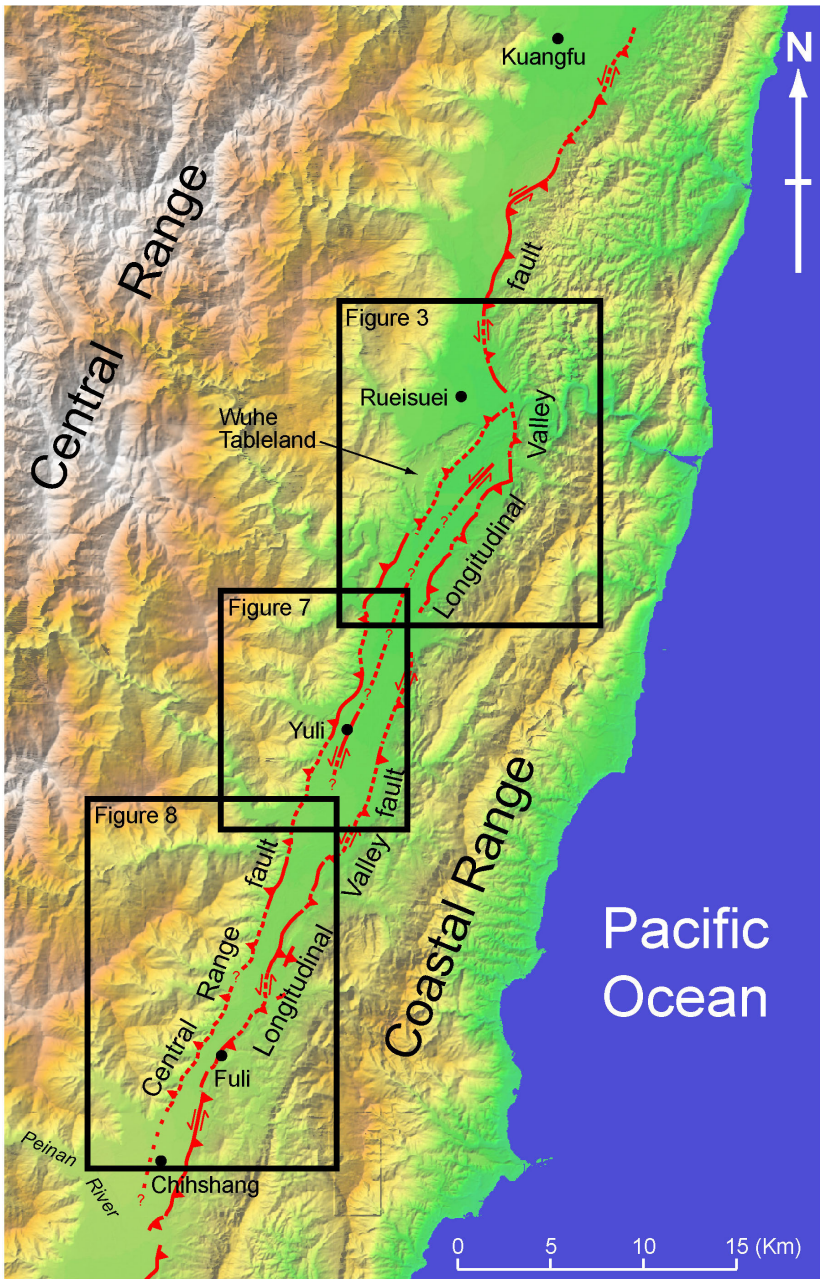

Figure 5.2. Map of major structures in the middle part of the Longitudinal Valley adapted from *Shyu et al.* [2005d]. The east-dipping Longitudinal Valley fault is an obliquely slipping reverse fault along which the Coastal Range is rising rapidly and moving toward the Central Range. In this paper we present geomorphic evidence for the less prominent Central Range fault. This fault is a west-dipping reverse fault, above which many fluvial terraces and the Wuhe Tableland are rising slowly.

In this paper we present a geomorphic analysis of the eastern flank of the Central Range, which supports the existence of a reverse fault along at least part of the western edge of the valley. Following *Biq* [1965], we call this structure the Central Range fault.

Our principal means for geomorphic analysis are two sets of digital elevation model (DEM), one with a 40-m resolution and the other with a 5-m resolution, followed by mapping and investigation of fluvial landforms in the field. We have also augmented our geomorphic analysis with published information from geodetic and seismologic analyses.

5.3 Geologic setting

Taiwan is forming at the boundary between the Philippine Sea plate and the South China block of the Eurasian plate. South of Taiwan, the two blocks are converging at about 90 mm/yr [*Sella et al.*, 2002; *Shyu et al.*, 2005c] (Figure 5.1), and the convergence is being absorbed by subduction of the South China Sea along the Manila trench. At the latitude of southern Taiwan, subduction has ceased because oceanic lithosphere of the South China Sea has been wholly consumed, and the Chinese continental margin impinges upon the trench. Thus, the convergence gives way to collisional deformation of the continental margin, resulting in the formation of the mountainous island of Taiwan.

The Taiwan orogen is made more complicated by the existence of an intervening continental sliver, comprising the submarine Hengchun Ridge and the Central Range backbone of Taiwan. As a result, the orogen is forming by a tandem suturing of the Chinese continental margin, the continental sliver, and the Luzon volcanic arc [*Shyu et al.*, 2005a] (Figure 5.1). In eastern Taiwan, the Longitudinal Valley suture is the eastern of the two sutures, separating the docked volcanic arc of the Coastal Range and the metamorphic core of the Central Range continental sliver.

Along the east-dipping Longitudinal Valley fault, the highly shortened volcanic rocks and forearc and intra-arc basin sedimentary rocks are thrusting over the current sediments of the Longitudinal Valley at rates up to several tens of mm/yr. These geodetically determined rates extend back through at least the past 10 kyr [*Shyu et al.*,

2005c]. Along one segment of the fault many small earthquakes illuminate a listric shape of the fault plane [e.g., *Kuochen et al.*, 2004]. Seismic activity along the Central Range fault is less impressive. Thus, the existence of the fault has been controversial for many years.

The Central Range, on the hanging-wall block of the proposed Central Range fault, consists of metamorphosed sedimentary rocks and basement rocks. Structural analysis indicates that the range is fundamentally an anticlinorium, with slates and other slightly metamorphosed sedimentary rocks overlying a more highly metamorphosed core [e.g., *Ho*, 1988]. The underlying basement rocks include shallow marine sedimentary rocks that contain late-Paleozoic fossils [*Yen et al.*, 1951; *Yen*, 1953], and Eocene to Miocene deep marine foraminifera fossils have been recovered from the overlying slates [e.g., *Chang*, 1971]. Thus the range is likely to be the metamorphosed product of what is now the submarine Hengchun Ridge: A continental sliver, with shallow marine sediments, is mantled by deep marine sediments of the forearc region.

5.4 Geomorphic analysis near the Wuhe Tableland

The most prominent landforms that lead us to suspect the existence of the Central Range fault are between the Fuyuan and Taiping Rivers, about halfway between the northern and southern ends of the Longitudinal Valley near the town of Rueisuei (Figures 5.2 and 5.3). There, rising anticlines in the hanging-wall block of the Central Range fault have produced the Wuhe Tableland in the north and a series of river terraces and a bedrock ridge in the south. The growth of these anticlines has diverted the Hungyeh River to the north and the Taiping River to the south.

The Wuhe Tableland is an uplifted fluvial terrace formed by the Hsiukuluan River, one of the largest rivers in eastern Taiwan. The tableland surface is about 170 m above the present riverbed. Its top surface is gently warped, and its highest point is near

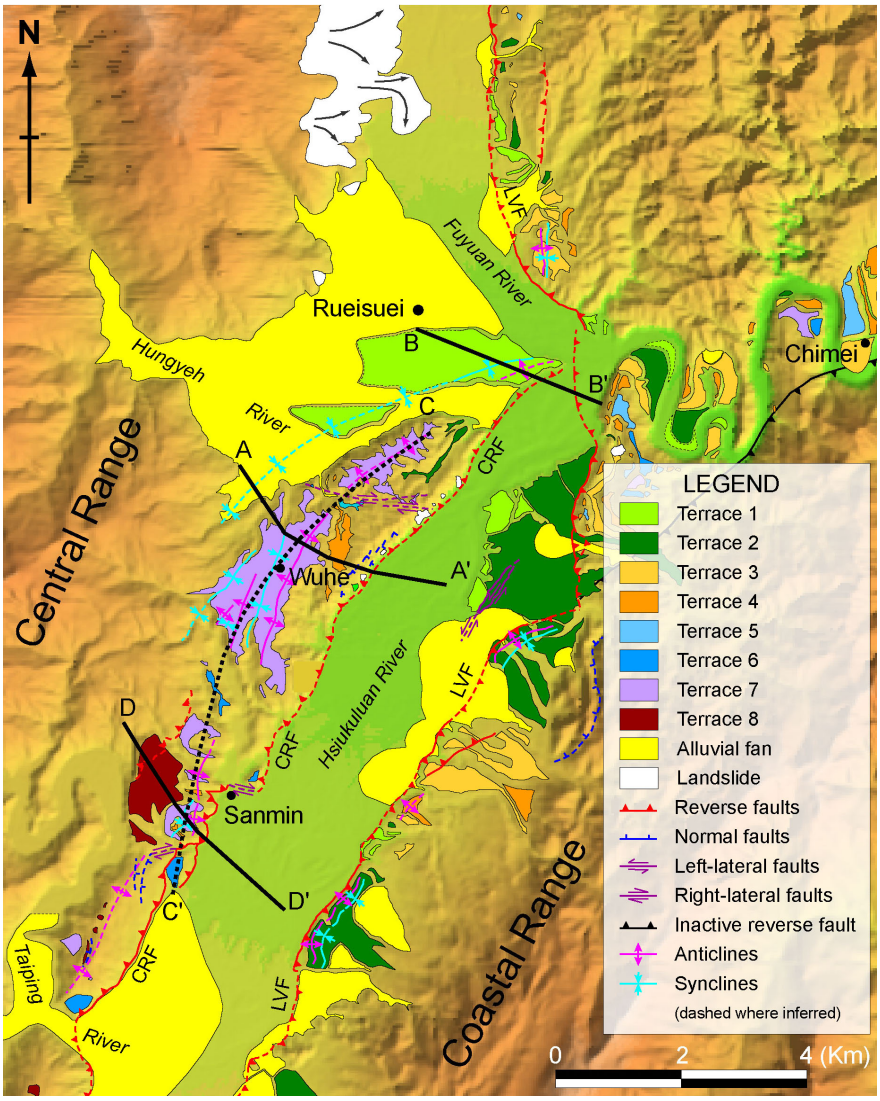

Figure 5.3. Detailed map of geomorphic and neotectonic features on and around the Wuhe Tableland shows deformations by young anticlines extending 13 km between the Fuyuan and Taiping Rivers. A syncline in young sediments flanks the anticlines on the northwest. These folds are formed in the hanging-wall block of the west-dipping Central Range fault (CRF). The Wuhe Tableland is a long, nearly contiguous patch of uplifted lateritic fluvial terrace on the crest of a major anticline. Undulations on the broadly anticlinal shape of the surface of the tableland reflect the existence of secondary folds. A deformed lower and younger fluvial terrace shows that the fold extends nearly 2 km northeast of the tableland and may plunge beneath the Longitudinal Valley fault (LVF). Lateritic fluvial strath terraces along the eastern flank of the Central Range and a bedrock ridge show that the anticlines extend several kilometers southwest of the tableland. Fluvial terraces along the western flank of the Coastal Range, deformed by the east-dipping LVF, also appear in the figure.

its southern end.

About 1.5 to 2.5 m of lateritic soil caps the surface of the Wuhe Tableland. Underlying the soil are layers of gravels and sand. These fluvial deposits comprise the

entire northwestern flank of the tableland, along the cut bank of the Hungyeh River (Figures 5.4 and 5.5a). In contrast, along the southeastern flank of the tableland, cut by the Hsiukuluan River, are scattered outcrops of metamorphic rocks, mostly slates, below the fluvial sediments (Figure 5.5b).

The fluvial deposits consist of mostly cobbles and boulders with rare thin layers of sand. It is of interest that the fluvial deposits on the Hungyeh River side of the tableland are very different from those on the Hsiukuluan River side. On the Hungyeh River side, matrix-supported gravel beds with larger and more-angular clasts suggest that the sediments were deposited by the Hungyeh River (Figure 5.5a). On the Hsiukuluan side, clast-supported gravel beds with smaller and more-rounded clasts, more frequent fine-grained layers, and even rare mud layers with tree trunks suggest that the sediments formed in the much larger and wider Hsiukuluan River and its marginal slack-water environments (Figures 5.5c and 5.5d). Therefore, there appears to be a sedimentary boundary between facies of the two rivers beneath the surficial lateritic soil of the tableland.

The age of the tableland is poorly constrained. The overlying lateritic soil implies that the surface formed at least a few tens of thousand years ago, judging from the dates of similar lateritic terraces in other parts of Taiwan [e.g., *Chen*, 1988]. The tree trunks found within the fluvial sediments of the tableland are older than the 50-kyr limit to ^{14}C dating. However, there are no further constraints on the age of the tableland. Preliminary dating from optically stimulated luminescence (OSL) of the fluvial sediments suggests that the age of the sediments may be about 45 kyr old, but large errors limit the usefulness of these analyses [*Chen et al.*, 2004].

The fluvial sediments of the Wuhe Tableland clearly formed in the Hsiukuluan and Hungyeh Rivers and were then uplifted along a west-dipping Central Range reverse fault. The tableland surface, once the riverbed, has risen at least 170 m since its formation several tens of thousand years ago. The gently-warped tableland surface has been

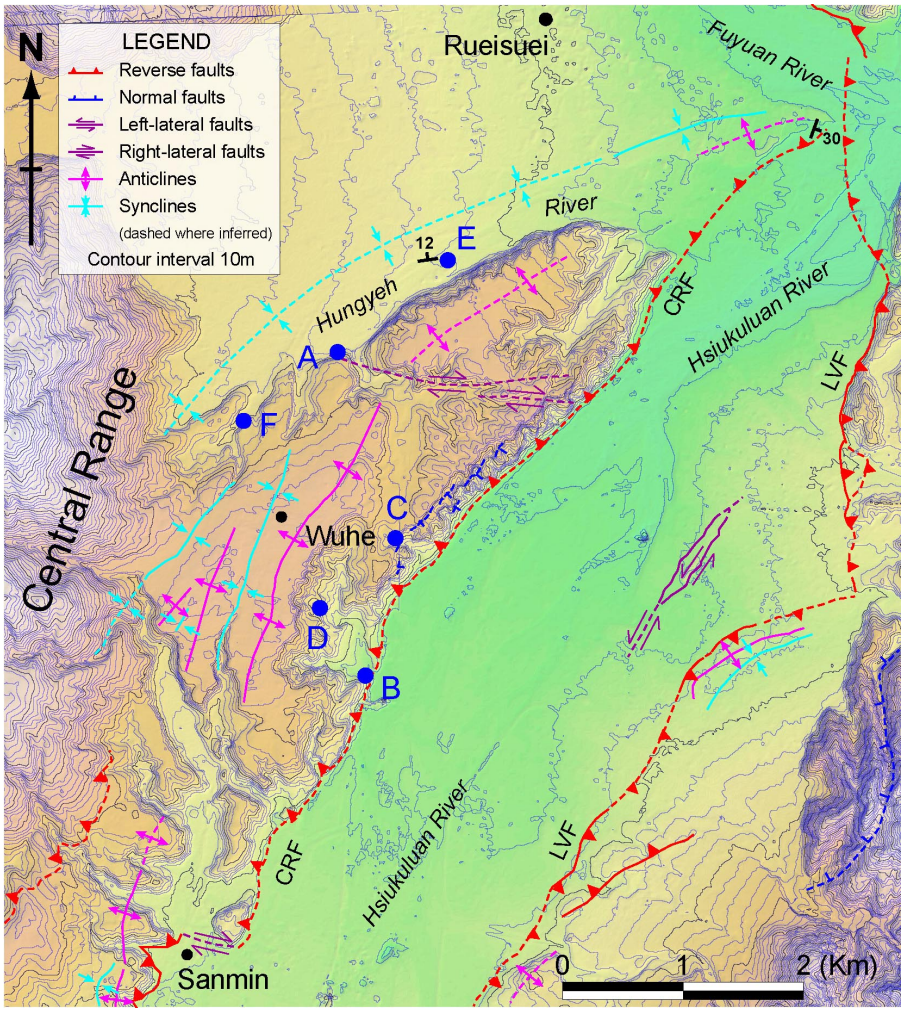

Figure 5.4. Index map of locations where photographs shown in Figure 5.5 were taken in the Wuhe Tableland area.

warped into an anticline with secondary folds on the hanging-wall block of the fault (Figures 5.4 and 5.6a). The exposed slate basement below the fluvial deposits on the eastern flank of the tableland formed at depths far below the land surface. Since the thickness of fluvial sediments in the Longitudinal Valley is greater than 1 km [*Chen et al.*, 1974; *Chen*, 1976], this suggests a minimum total offset of several kilometers across the fault.

In the present Hungyeh River bed we have found an outcrop of gently tilted indurated gravels and sand (Figures 5.4 and 5.5e). The mild induration of these sediments indicates that they are old and perhaps correlative with sediments beneath the

Figure 5.5. Selected photographs showing fluvial sediments and bedrocks of the Wuhe Tableland. (a) Along the cut bank of the Hungyeh River at the northwestern side of the tableland the entire outcrop below the surface of the tableland (T) is composed of matrix-supported fluvial gravels with large and angular clasts. Total height of the outcrop is about 40 m. The photo was taken at site A in Figure 5.4. (b) Along the Hsiukuluan River at the southeastern side of the tableland, scattered metamorphic rocks, mostly slates, crop out as the basement of the fluvial sediments. Length of the hammer is about 30 cm. The photo was taken at site B in Figure 5.4. (c) The southeastern part of the fluvial deposits beneath the Wuhe Tableland includes clast-supported gravels with smaller and more rounded clasts and more frequent fine-grained layers. The person is about 1.8 m tall. The photo was taken at site C in Figure 5.4. (d) The fine-grained fluvial sediments of southeastern Wuhe Tableland include occasional mud layers with tree trunks. Length of the scraper is about 25 cm. The photo was taken at site D in Figure 5.4. (e) In the current Hungyeh River bed, an outcrop of tan-colored, gently tilting indurated gravels and sand appears to be equivalent of deeper Wuhe Tableland sediments. These sediments are overlain by grayish-colored current Hungyeh River deposits. Strike and dip of the indurated beds are N82°E and 12° to the northwest. This indicates that the syncline bounding the northwestern side of the tableland should lie north of the Hungyeh River. Length of the hammer is about 30 cm. The photo was taken at site E in Figure 5.4. (f) On the western flank of the Wuhe Tableland, fluvial gravels deposit on an erosional strath (shown in dashed line) on the slate bedrock. No fault is present between the Wuhe sediments and the slate formations. Length of the hammer is about 30 cm. The photo was taken at site F in Figure 5.4.

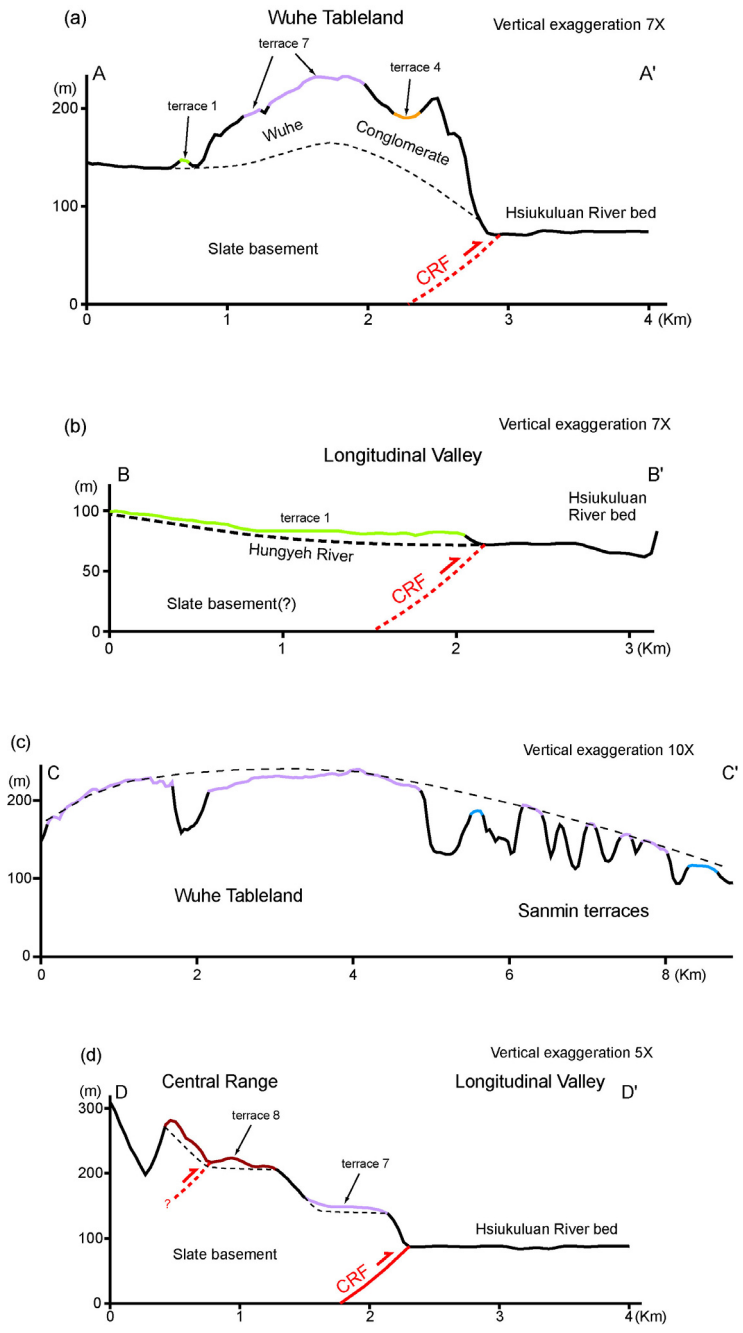

Figure 5.6. Selected topographic profiles in the Wuhe Tableland area. Locations of the profiles are shown in Figure 5.3. (a) Across the Wuhe Tableland, warped fluvial terraces on top of the tableland clearly show the deformation by the secondary folds in the hanging-wall block of the Central Range fault. The fault trace is probably very close to the eastern base of the tableland. (b) Terrace 1 of the Hungyeh River, previously part of the Hungyeh River alluvial fan, has risen and tilted upstream in association with slip along the Central Range fault. (c) A topographic profile extending from the Wuhe Tableland to the Sanmin terraces shows that most of the Sanmin terraces are correlative with the Wuhe Tableland surface, as shown by the thin dashed line. This topographic profile indicates that the anticline underlying these surfaces plunges both to the north and to the south. (d) Lateritic terraces 7 and 8 are uplifted Hsiukuluan River beds, formed by slip along the Central Range fault. A secondary reverse fault in the hanging-wall block of the fault may have deformed the terrace 8 surface.

Wuhe Tableland. The strike (N82°E) and dip (12°NW) of the beds suggest the presence of a syncline northwest of the tableland, north of the Hungyeh River (Figures 5.3 and 5.4). Therefore, the northwestern side of the Wuhe Tableland has been eroded significantly by the Hungyeh River. However, since the Wuhe sediments are still being uplifted and crop out in the Hungyeh River bed, the anticline and syncline appear to be active.

Just northeast of the tableland, a small, lower fluvial terrace provides a clear demonstration of the northeastward continuation of the Wuhe Tableland anticline, syncline, and fault (Figures 5.3 and 5.6b). The terrace formed as part of the Hungyeh River fan near its confluence with the Longitudinal Valley. Subsequent to deposition, the fluvial surface tilted toward the northwest, rising above the surrounding youngest and active alluvial fan surface. Fluvial sediments underlying the terrace surface are also tilted (Figure 5.4). The form of the terrace is an anticline-syncline pair, analogous to the topographic manifestation of the fault further to the south, on the Wuhe Tableland. The southeastern flank of the terrace is steep and may, in fact, be a fault scarp. About 3 km northwest of the scarp, the terrace merges smoothly with the active alluvial fan. This indicates that the age of the terrace and its deformation are very young.

Some published maps depict the Wuhe Tableland lying on the hanging-wall block of a strand of the east-dipping Longitudinal Valley fault at the western edge of the tableland [e.g., *Yu*, 1997; *Lin et al.*, 2000]. However, it is clear from field relationships that on its western flank the fluvial sediments of the tableland overlie a slate strath and that no fault is present there (Figure 5.5f).

The exact location of the Central Range fault is unclear. Although we believe the fault crops out very close to the southeastern base of the Wuhe Tableland, fluvial action by the Hsiukuluan River may have eroded the tableland edge somewhat.

The landforms of the Central Range fault continue south of the Wuhe Tableland. West of the village of Sanmin, a series of fluvial terraces perches on the eastern flank of the Central Range at heights up to 150 m above the Longitudinal Valley floor (Figure 5.3).

These are strath terraces, which generally have fluvial gravel caps less than 1 m thick. A topographic profile across both the Wuhe Tableland surface and the Sanmin terraces clearly shows that the majority of the Sanmin terraces are correlative with the Wuhe Tableland (Figure 5.6c). Prominent chemical and mechanical weathering of the Sanmin terrace surface appears as alteration of basement slate to reddish-colored rock fragments, consistent with the hypothesis that the Sanmin terraces are similar in age to those of the Wuhe Tableland. Lateritic soil, however, is poorly developed on top of the Sanmin terraces, probably because of the lack of thick fluvial sediments.

The fluvial terraces west of Sanmin represent uplifted riverbed of the Hsiukuluan River. Their uplift is due to slip along the Central Range fault beneath the eastern flank of the range since the terraces are the southward extension of the Wuhe Tableland. The fact that the terraces are strath terraces with just a thin cap of fluvial gravels suggests that the hanging-wall block had been rising along the fault since the time of formation of the terrace. Moreover, the presence of slates beneath the thin fluvial sediment cover of the terraces clearly shows that the terrace straths had risen at least several tens of meters prior to fluvial down-cutting. A small right-lateral tear may be present near Sanmin, where the fault steps slightly to the west from the eastern edge of the tableland (Figure 5.3). Other secondary structures, including folds and a minor reverse fault, appear to be present in the hanging-wall block of the Central Range fault along this segment. South of Sanmin, the fault trace must run along the eastern base of the terraces because there is scant evidence for fluvial erosion of the hillside by the Hsiukuluan River (Figure 5.6d).

The fact that the Sanmin terraces are lower in elevation than the Wuhe Tableland indicates that the anticline beneath the terraces plunges to the south. As the anticline plunges, another anticline appears to its west and forms the linear, N-S trending ridge southwest of Sanmin (Figure 5.3). This ridge is nearly devoid of strath terraces but is also a topographic manifestation of the Central Range fault. The highest terrace west of Sanmin, north of this ridge, is likely the uplifted riverbed of the Taiping River formed at a

time when the river flowed directly southeastward into the Longitudinal Valley. The current bed of the Taiping River, however, turns southwestward and flows parallel to the ridge for about 4 km before cutting through the ridge to the valley. This geometry suggests that the river has been diverted around an actively rising anticlinal ridge on the hanging-wall block of the Central Range fault. Scattered fluvial terraces on this ridge may be uplifted remnant of the Taiping River bed during its southwestward diversion.

5.5 The Central Range fault south of the Taiping River

South of the Taiping River, uplifted lateritic strath terraces along the eastern flank of the Central Range indicate that the Central Range fault extends still further to the south. These expressions of uplift are particularly clear west and north of Yuli (Figure 5.7). The terraces near Yuli are uplifted riverbeds of the Hsiukuluan River and its tributary, the Chuo River. The majority of these terraces currently sit more than 100 m above the valley floor. The higher terraces have very thin fluvial sediment cover, less than a few meters thick. Some lower terraces, however, are underlain by thicker fluvial sediments and thus appear to be alluvial (or fill) terraces.

Between Yuli and the Lele River, geomorphic manifestations of the Central Range fault are sparse (Figure 5.7). However, very clear tectonic landforms exist south of the Lele River (Figure 5.8). Immediately south of the Lele River, west of the small village of Changliang, is a small N-S trending ridge. The southern half of the ridge consists of thick fluvial gravels surmounted by a lateritic terrace surface (Figure 5.9). The northern, higher half of the ridge, however, consists of slate topped locally by lateritic strath terraces. This geometry indicates that the southern half of the ridge represents an uplifted paleochannel of the southern branch of the Lele River, which formed at a time when the tributary flowed directly into the Longitudinal Valley. As the eastern flank of the Central Range rose along the Central Range fault, the tributary was forced to flow

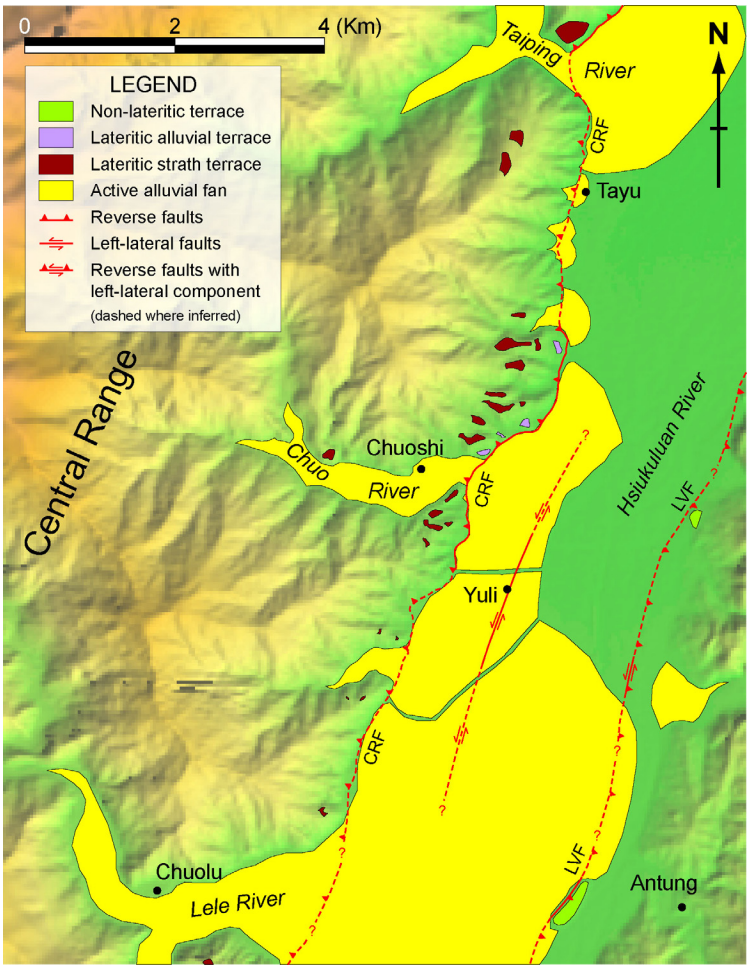

Figure 5.7. Detailed map of geomorphic and neotectonic features south of the Wuhe Tableland from the Taiping River to the Lele River. North and west of Yuli, numerous uplifted lateritic strath terraces along the eastern flank of the Central Range indicate the presence of the Central Range fault (CRF) along the western edge of the Longitudinal Valley. Some fluvial terraces along the eastern side of the Longitudinal Valley, deformed by the east-dipping Longitudinal Valley fault (LVF), as well as the left-lateral surface rupture of November 1951 that runs through the town of Yuli [*Shyu et al.*, 2005d], are also shown in the figure.

northward and join the Lele River just south of Chuolu. This is analogous to the diversion of the Taiping River mentioned above. The trace of the Central Range fault must be very close to the base of the eastern flank of the Central Range because the Hsiukuluan River currently flows along the eastern side of the Longitudinal Valley and is therefore unlikely to have eroded the fault scarp.

Farther to the south, another well-constrained location of the Central Range fault is just north of the village of Kufeng (site G in Figure 5.8). An uplifted alluvial fan there

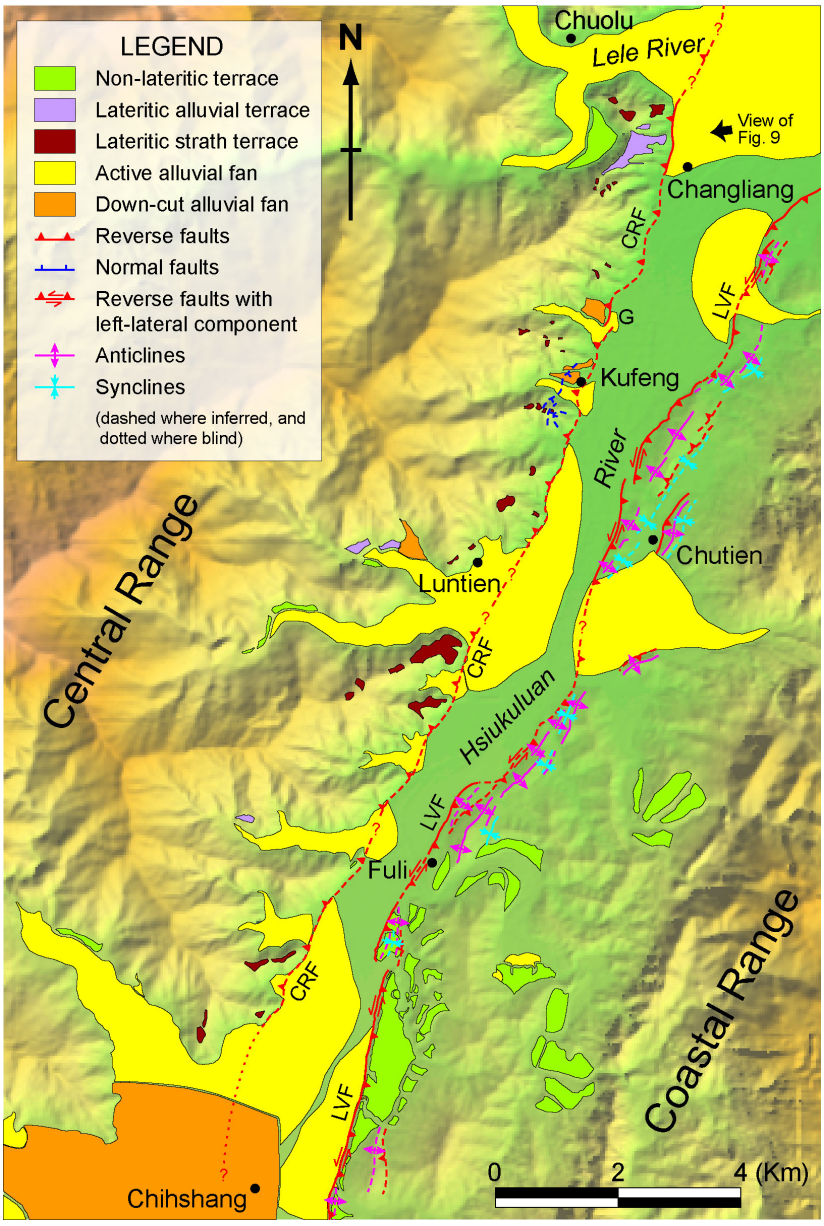

Figure 5.8. Detailed map of geomorphic and neotectonic features between the Lele River and Chihshang. As to the north, numerous uplifted lateritic strath terraces and deformed alluvial fans along the eastern flank of the Central Range indicate that the Central Range fault (CRF) is present along the western edge of the Longitudinal Valley. Fluvial terraces and neotectonic landforms of the east-dipping Longitudinal Valley fault (LVF) along the eastern side of the Longitudinal Valley are also shown in the figure.

is warped at the mountain-front, forming a scarp on the alluvial fan that is steeper than the original fan slope (Figure 5.10). Offset across the scarp is at least 10 m. The broad, shallow nature of the scarp suggests that the fault does not break the surface; instead, the deformation of the alluvial fan is likely the manifestation of a fault-propagation fold

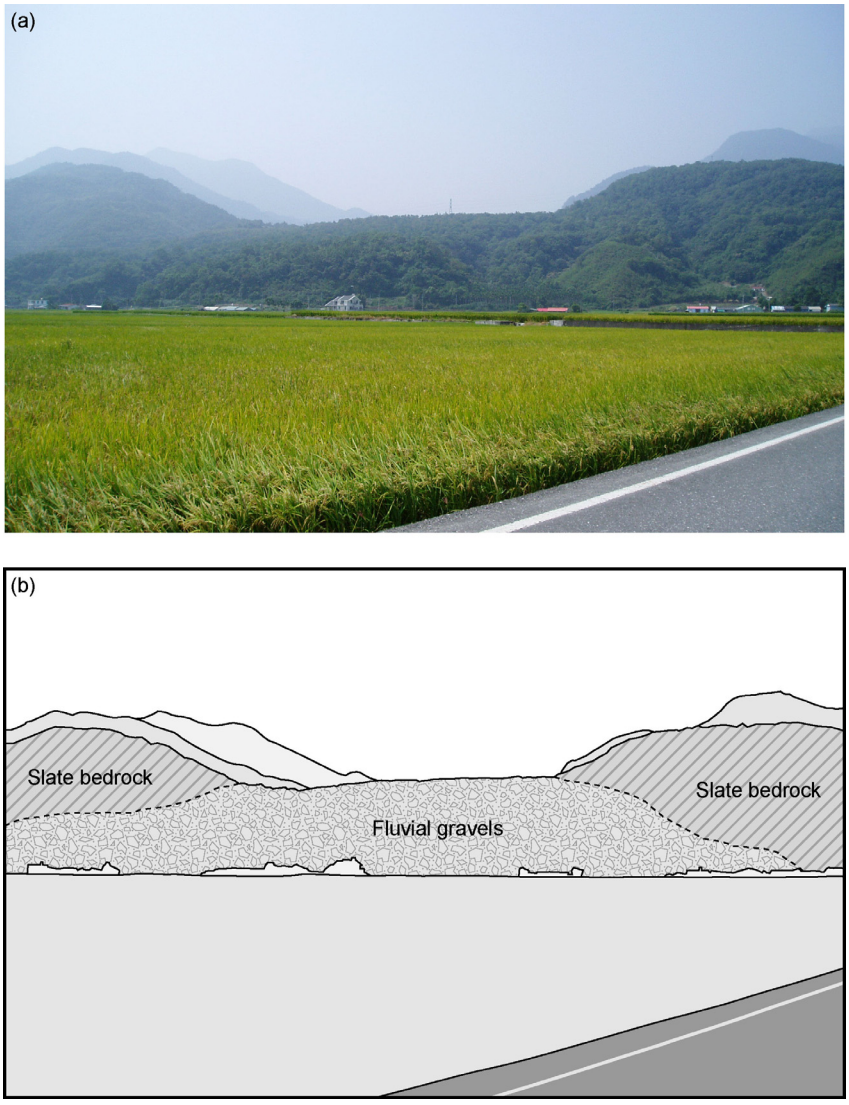

Figure 5.9. Photograph (a) and sketch (b) of a large N-S trending ridge south of the Lele River and west of Changliang. View is toward the west as shown by the black arrow in Figure 5.8. The southern half of the ridge is an alluvial terrace underlain almost entirely by fluvial gravels. It appears to be an uplifted paleochannel of the southern tributary of the Lele River, formed at a time when the tributary flowed directly into the Longitudinal Valley.

above a blind Central Range fault.

Numerous lateritic strath terraces on the eastern flank of the Central Range show that the Central Range fault extends still farther to the south from Kufeng to near Chihshang. These terraces are especially large near the village of Luntien (Figure 5.8). The exact location of the fault in this segment is again unclear, due to possible fluvial erosion of the eastern flank of the Central Range by the Hsiukuluan River.

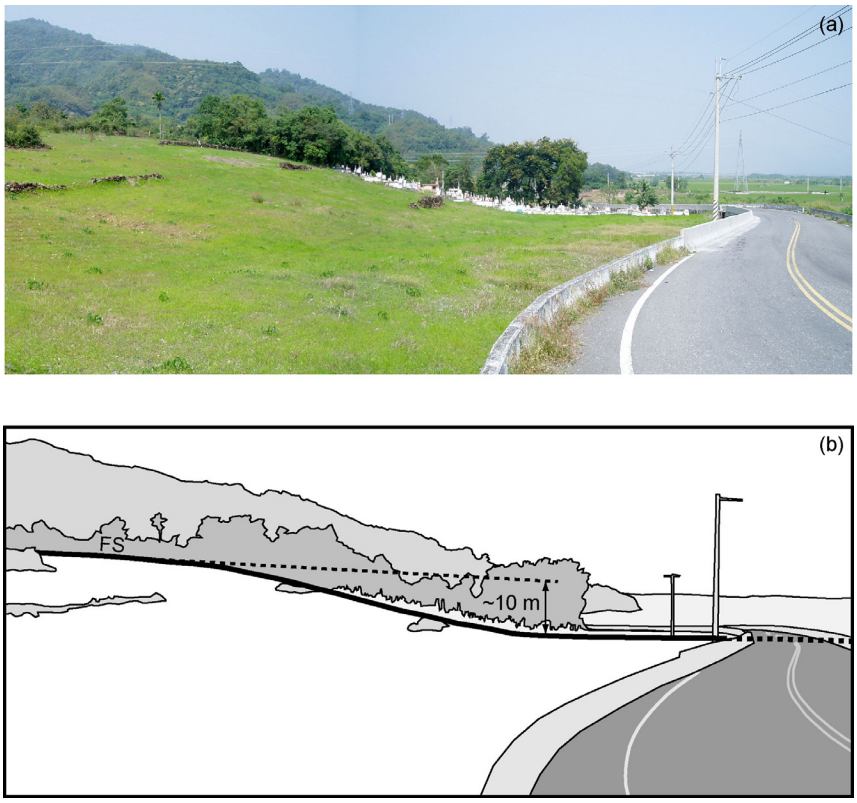

Figure 5.10. Photograph (a) and sketch (b) of a deformed alluvial fan surface (FS) at site G in Figure 5.8. View is toward the north. The undeformed part of the fan surface dips eastward about 3.2°, and the deformed part of the fan surface dips much steeper, at about 14°. We interpret this gentle monocline to be the eastern flank of a fault-propagation fold, caused by about 10 m of slip on the Central Range fault in the shallow subsurface.

5.6 The blind Central Range fault south of Chihshang

Uplifted lateritic terraces are very scarce along the eastern flank of the Central Range south of Chihshang. Thus the Central Range fault there must be either inactive or blind. We favor the latter hypothesis because many of the major Central Range rivers south of Chihshang have incised into their large alluvial fans in the Longitudinal Valley (Figure 5.11a). The large alluvial fan terrace of the Peinan River, on which the town of Chihshang sits, is a prominent example [*Chang et al.*, 1994] (Figure 5.11). This is consistent with regional uplift of the western Longitudinal Valley above a blind Central Range fault.

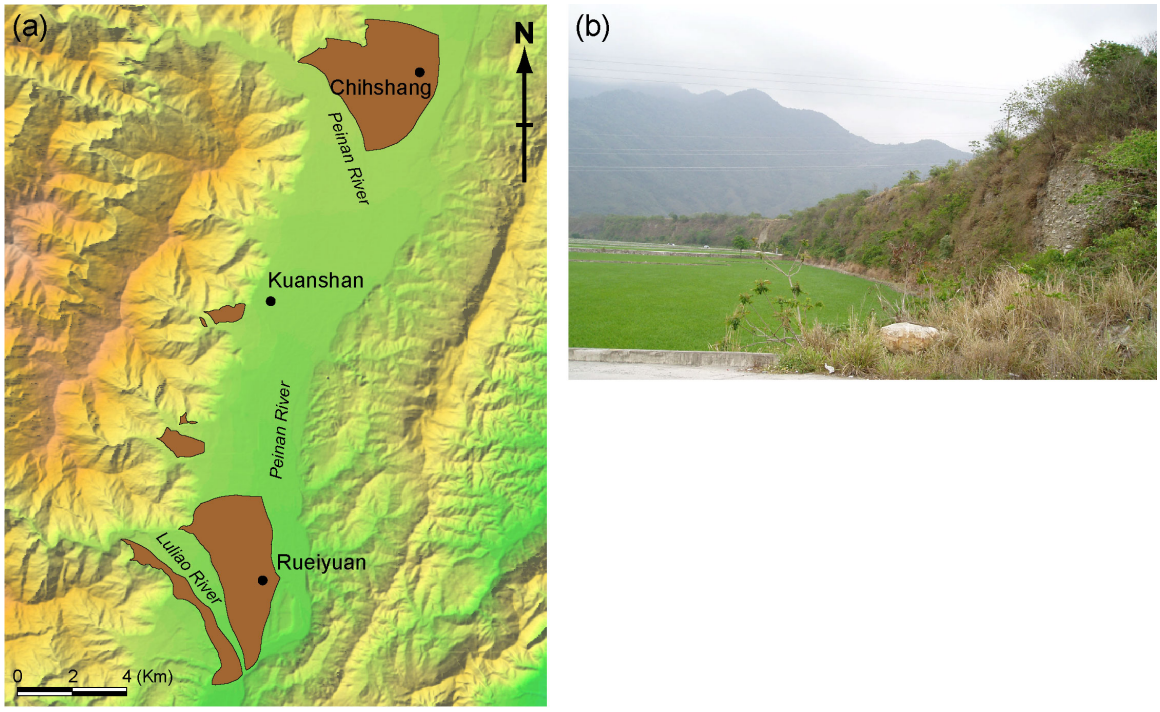

Figure 5.11. (a) South of Chihshang most major rivers draining from eastern Central Range develop large incised alluvial fans (shown in brown). (b) The Peinan River fan where the river flows out of the Central Range was incised for more than 15 m. The town of Chihshang sits on this incised alluvial fan.

Farther to the south, near the southern end of the Longitudinal Valley, our previous mapping [*Shyu et al.*, 2002] suggests that the active Central Range fault is overridden by a western branch of the Longitudinal Valley fault. Thus the Central Range fault is probably active but blind from Chihshang to the southern end of the Longitudinal Valley.

5.7 Discussion

5.7.1 Geodetic and Seismic Evidence

Several other, independent lines of evidence support the existence of the Central Range fault. In fact, it was this other evidence that compelled us to search for tectonic landforms along the eastern flank of the Central Range. The evidence includes geodetic measurements and seismic refraction lines across the eastern flank of the Central Range,

mostly done more than a decade ago. More recently, relocated earthquake hypocenters of background seismicity and aftershocks of the Chengkung earthquake of 10 December 2003 (M_L 6.5) provide additional insight about the Central Range fault.

A leveling line that extends 16 km into the Central Range near Chihshang shows tilt of the easternmost 16 km of the range at about 0.8 μradian/yr between 1984 and 1987 [*Liu and Yu*, 1990]. Thus the westernmost point of the leveling profile, 16 km into the range, is rising about 13 mm/yr relative to the Longitudinal Valley floor. This would be consistent with strain accumulating across a locked Central Range reverse fault beneath the eastern flank of the range. Unfortunately, the short length of leveling profile hampered further modeling of the result; therefore we could not discriminate the possibility of an east-dipping normal fault for producing the tilting pattern. More recent leveling west of Yuli shows similar but less well constrained eastward tilting of the eastern Central Range [*Yu and Kuo*, 2001].

Since the Longitudinal Valley is underlain by a thick pile of coarse fluvial gravels, seismic surveys have not been able to provide much useful information about the subsurface structure of the valley. About three decades ago, though, a seismic-refraction survey revealed that at the western edge of the Longitudinal Valley a high-speed (~6.2 km/s) unit exists in the shallow subsurface, in direct contact with a low-speed (3.2-4.3 km/s) unit to the east. This contact may be the Central Range fault [*Chen et al.*, 1974; *Chen*, 1976]. However, since the survey had good resolution only to a depth of about 1 km, the precise geometry and nature of the contact is not known.

Eastern Taiwan has long been an abundantly active seismic area. In fact, much of our knowledge about the subsurface geometry of the Longitudinal Valley fault has come from clusters of small earthquakes. The Central Range fault, on the other hand, is not as seismically active as the Longitudinal Valley fault, probably because the slip rate of the Central Range fault is much lower. A small cluster of earthquakes near Yuli, however, appears to illuminate a west-dipping plane beneath the eastern flank of the Central Range

[*Carena et al.*, 2001]. This plane may be a piece of the Central Range fault. Moreover, another small cluster of relocated aftershocks of the 2003 Chengkung earthquake near the southern end of the Longitudinal Valley may also illuminate another piece of the Central Range fault; some of the aftershocks in this cluster show earthquake focal mechanisms consistent with a west-dipping reverse fault [*Kuochen et al.*, 2005].

5.7.2 Sense of Slip and Slip Rate of the Central Range Fault

One of the major controversies about the Central Range fault, at least among those who believe in its existence, is the fault's sense of slip. Some maintain that it is an east-dipping normal fault [e.g., *Crespi et al.*, 1996; *Lee et al.*, 2001, 2003]. Normal dip-slip would provide a mechanism for the exhumation of high-pressure metamorphic rocks found locally in the eastern Central Range. The mechanism would therefore be similar to the "return flow" or "upward extrusion" mechanisms for the ascent of high-pressure metamorphic rocks to Earth's surface as proposed for the Alps and predicted by physical models [e.g., *Michard et al.*, 1993; *Chemenda et al.*, 1995; *Gerya et al.*, 2002]. However, since the ages of formation and exposure of the high-pressure metamorphic rocks of the eastern Central Range are quite controversial [e.g., *Jahn and Liou*, 1977; *Jahn et al.*, 1981], the exhumation of those rocks may have occurred earlier and might not have involved the Central Range fault.

Our geomorphic analysis of the Central Range fault indicates that the fault is a west-dipping reverse fault, at least in its shallow part. The secondary folds that exist west of the fault on the Wuhe Tableland and around the Taiping River and the monoclinally warped surface near Kufeng are all consistent with a reverse sense of slip along the Central Range fault. An east-dipping normal fault along the eastern Central Range front could also produce the uplifted river terraces that we see on the eastern flank of the Range, but the anticlines and monoclines would not be expected.

Furthermore, geodetic and seismic evidence supports the proposition that the Central Range fault is a west-dipping reverse fault. The eastward tilt of the eastern Central Range revealed from leveling measurements [*Liu and Yu*, 1990; *Yu and Kuo*, 2001] is consistent with surface deformation by a locked west-dipping reverse fault beneath the range front. The clusters of small earthquakes also show west-dipping planes with reverse focal mechanisms beneath the eastern Central Range [*Carena et al.*, 2001; *Kuochen et al.*, 2005].

At present, the slip rate of the Central Range fault is poorly constrained. The surface of the Wuhe Tableland is probably older than 50 kyr and is now about 170 m above the Hsiukuluan River bed. If the current Hsiukuluan River bed were correlative with the Wuhe Tableland surface, the uplift rate of the tableland surface would be limited to no more than about 3.4 mm/yr. However, our recent investigation on the slip rate of the Longitudinal Valley fault suggests that the Longitudinal Valley floor may be subsiding and underthrusting along both the Longitudinal Valley fault and the Central Range fault [*Shyu et al.*, 2005c]. This indicates that the total uplift of the Wuhe Tableland surface is greater than 170 m, and the uplift rate of the tableland surface should be higher. A 3 mm/yr subsidence rate of the Longitudinal Valley floor was proposed in our investigation of the Longitudinal Valley fault near Rueisuei [*Shyu et al.*, 2005c]. Assuming this value, the maximum uplift rate of the Wuhe Tableland surface should be about 6.8 mm/yr. If the Central Range fault dips at 30° westward, a typical dip for a reverse fault, the maximum slip rate along the fault would be about 13.6 mm/yr. The resulting horizontal shortening rate of about 11.8 mm/yr, plus the ~29 mm/yr maximum horizontal shortening proposed for the Longitudinal Valley fault [*Shyu et al.*, 2005c], would be consistent with the ~40 mm/yr total shortening across the Longitudinal Valley observed in GPS [*Hsu et al.*, 2003]. However, this calculation may significantly over-estimate the actual rate if, for example, the fault dip is steeper or the Wuhe Tableland surface is much older than 50 kyr.

The constraint of less than 13.6 mm/yr for the slip rate of the Central Range fault suggests that the fault is absorbing much less than half of the shortening across the Longitudinal Valley suture since we [*Shyu et al.*, 2005c] have shown that the slip rate along the Longitudinal Valley fault is about 23 mm/yr. The constraint also indicates that the earthquake potential of the Central Range fault is smaller than that of the Longitudinal Valley fault. That is, for a given magnitude of slip, an earthquake should occur on the Longitudinal Valley fault at least twice as frequently as on the Central Range fault. This probably explains the much sparser seismicity along the western flank of the Longitudinal Valley.

5.7.3 The Evolution of the Longitudinal Valley Suture

Although the Central Range fault is absorbing only a small portion of the horizontal shortening across the Longitudinal Valley suture at present, we believe it may have played a more important role in the evolution of the suture. We have recently proposed a model for the northward maturation of the suturing between the Luzon volcanic arc and the Central Range continental sliver in which the development of multiple reverse-fault wedges facilitates the thickening of the margins of both non-oceanic blocks at the suture and creates a "Christmas tree" shape for the Longitudinal Valley suture [*Shyu et al.*, 2005c] (Figure 5.12). In such a model, the current Central Range fault is likely to be the youngest of several generations of reverse-faults on the western side of the suture.

Farther to the south, near the southern tip of Taiwan, bathymetric evidence suggests that a west-dipping thrust fault along the eastern edge of the forearc basin is the major structure responsible for the closure of the forearc basin [*Shyu et al.*, 2005b] (Figure 5.12a). This would be the first generation of this family of west-dipping faults. As the suture becomes more developed to the north, the east-dipping Longitudinal Valley fault appears at the southern end of the Longitudinal Valley (Figure 5.12b). There the Central

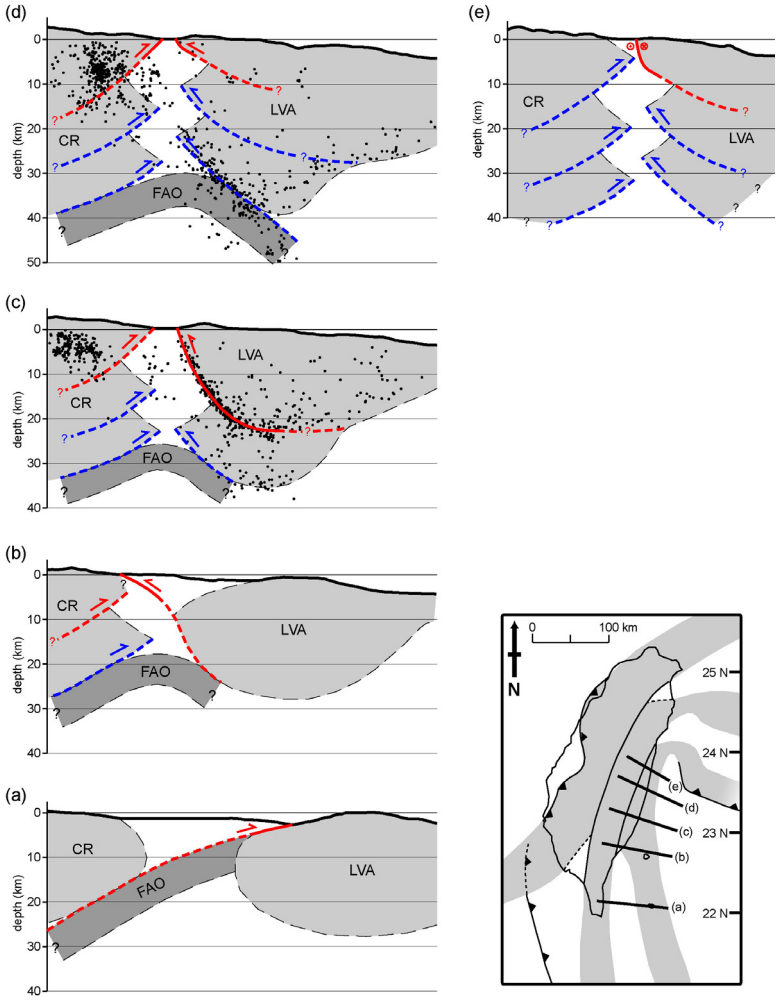

Figure 5.12. Schematic crustal cross sections show our hypothesis for the evolution of the Longitudinal Valley suture. Each section is drawn using current topography and observations along the lines specified on the index map, with no vertical exaggeration. (a) Before suturing, the Luzon forearc oceanic lithosphere (FAO) subducts beneath the Central Range continental sliver (CR). This is currently occurring at about the latitude of the southern tip of Taiwan, about 22°N. (b) As the Luzon volcanic arc lithosphere (LVA) approaches the Central Range, an east-dipping thrust fault appears, allowing the FAO to also subduct underneath the LVA. Contemporaneously on the west side of the valley, the proximity of the LVA to the CR induces formation of a newer, shallower west-dipping thrust fault above the original one. This is the current structural geometry near the southern end of the Longitudinal Valley between about 22°40'N and 22°50'N. (c) As the suture matures, the two non-oceanic lithospheric blocks both start to thicken by evolving multiple reverse-fault wedges, with the younger ones at shallower depth. This is the current structural geometry at the latitude of Chihshang, about 23°10'N. (d) At the latitude of the Wuhe Tableland, about 23°30'N, the suture is nearing maturity. The suture has evolved into a "Christmas tree" shape, with a thick pile of sediments between the two non-oceanic lithospheric blocks and underlain by the subducted forearc oceanic lithosphere. (e) In northern Longitudinal Valley, at the latitude about 23°45'N, the dominantly sinistral Longitudinal Valley fault appears to be the only major active structure. The west-dipping Central Range fault has become inactive, and sediments in the Longitudinal Valley are lapping on the eastern flank of the Central Range. Red indicates the youngest and currently active faults in each time frame, and blue indicates older faults which may still be active. Faults are dashed where inferred. Frames (a) to (d) are from *Shyu et al.* [2005c]. Relocated earthquake hypocenters in (c) and (d) are adapted from *Kuochen et al.* [2004].

Range fault appears to be blind and overridden by the Longitudinal Valley fault [*Shyu et al.*, 2002]. As our geomorphic analysis suggests, the Central Range fault becomes emergent father to the north (Figures 5.12c and 5.12d).

The geometry of the Central Range fault near Rueisuei suggests that it may be overridden again by the Longitudinal Valley fault north of the Wuhe Tableland (Figure 5.3). Although part of the overridden segment of the Central Range fault may still be active, we believe that the fault becomes inactive immediately north of this point. Between Rueisuei and the northern end of the Longitudinal Valley, the eastern flank of the Central Range is notably more sinuous than it is to the south (Figure 5.2). The higher sinuosity indicates that rates of uplift of the range are much lower than rates of alluvial deposition. This hypothesis is supported by the rarity of lateritic fluvial terraces along the eastern flank of the range along this reach of the valley [*Chang et al.*, 1992]. Thus it appears that the Longitudinal Valley fault is the solitary major active structure along the northern part of the Longitudinal Valley suture (Figure 5.12e). The inactivity of all reverse-fault wedges on the suture's western side would be an indication that the suture is fully developed; that is, the volcanic arc would have docked fully with the continental sliver of the Central Range.

5.7.4 The Central Range Fault and the Uplift of the Central Range

The Central Range is the mountainous backbone of Taiwan, with highest peaks rising nearly 4 km above sea level. Yet the mechanism responsible for the growth of such a large mountain range remains poorly understood. Rapid exhumation of the Central Range, at rates as high as about 6 mm/yr over the past several million years, has been suggested by thermochronological studies of the metamorphic rocks of the range [e.g., *Jahn et al.*, 1986; *Liu et al.*, 2001; *Willett et al.*, 2003]. This rate is coincident with directly measured recent erosion and fluvial incision rate over the past couple of years

[e.g., *Hovius et al.*, 2000; *Hartshorn et al.*, 2002]. Therefore the current annual uplift rate of the range which produced the fluvial incision is also about several mm/yr. Decadal and millennial uplift rates of the range are poorly constrained, however, and they may be very different from the abovementioned annual and million-year rate of several mm/yr.

Hsu et al. [2003] analyzed horizontal and vertical GPS displacements in profiles across Taiwan drawn parallel to the direction of relative plate motion. They used a moderately complex elastic dislocation geometry to show that the horizontal motion could be explained well with a shallow-dipping thrust fault under the western flank of the Central Range (such as the Chelungpu thrust fault that ruptured in 1999) and a steeply east-dipping Longitudinal Valley fault. They noted, however, that the rapid uplift of the Central Range is not explained by this model. The best alternative explanation may be pervasive ductile crustal thickening of the rocks of the Central Range [*Shyu et al.*, 2005a, 2005b].

Although our analysis indicates that the uplift rate of the Wuhe Tableland surface caused by the slip along the Central Range fault is comparable to the uplift and exhumation rate of the range, we suspect that the fault may only be locally important in the uplift of the range. It is unlikely that the slip along the Central Range fault, along the eastern front of the range, is responsible for uplift of the core of the range, much further to the west. Therefore, we suggest that pervasive crustal thickening of the Central Range produces the rapid uplift and the overall anticlinorial shape of the range and that reverse slip on the Central Range fault represents shallow brittle deformation, localized along the eastern edge of this anticlinorium.

5.8 Conclusions

An abundance of young tectonic landforms along the eastern flank of the Central

Range, as well as geodetic and seismic observations, reveal the presence of a west-dipping reverse fault along the western side of the Longitudinal Valley in eastern Taiwan. This Central Range fault crops out for a distance of about 40 km, from just north of the Wuhe Tableland to near Chihshang (Figure 5.2). South of Chihshang, the fault is also active, but blind. The Central Range fault appears to veer toward and plunge beneath the east-dipping Longitudinal Valley fault northeast of the Wuhe Tableland, and is inactive along the more northern reaches of the Longitudinal Valley.

Although millennial slip rate of the Central Range fault is not well established, the maximum rate is about 13.6 mm/yr, and it is likely to be an over-estimation. This slip rate indicates that the fault is absorbing a smaller portion of the 40 mm/yr of horizontal shortening across the Longitudinal Valley suture. Furthermore, whereas the slip rate of the fault is comparable to the exhumation rate of the Central Range for the past several million years, we believe the exhumation and uplift of the range is likely due to pervasive ductile thickening of the crust and that the Central Range fault represents only the shallow brittle deformation at the eastern edge of the range.

5.9 Acknowledgements

We greatly appreciate the assistance of Y. Wang and T. Watanuki in the field and are grateful for valuable discussions with J.-P. Avouac, O. Beyssac, Y.-C. Chan, H.-T. Chu, J.-C. Lee, W.-T. Liang, M. Simons, Y.-M. Wu, and S.-B. Yu. We have also benefited from stimulating discussions with the students of a binational field class of the National Taiwan University and California Institute of Technology (Caltech), held in eastern Taiwan in 2002. Our mapping was facilitated by J. Giberson, manager of the Caltech's Geographic Information Systems (GIS) laboratory. The 5-m DEM was generously provided by the Central Geological Survey, MOEA, Taiwan. Our project in Taiwan was supported by National Science Foundation (NSF) grant EAR-0208505. This research was also supported in part by the Gordon and Betty Moore Foundation. This is Caltech Tectonics Observatory Contribution #22.

5.10 References

Angelier, J., H.-T. Chu, and J.-C. Lee (1997), Shear concentration in a collision zone: kinematics of the Chihshang Fault as revealed by outcrop-scale quantification of active faulting, Longitudinal Valley, eastern Taiwan, *Tectonophysics*, *274*, 117-143.

Biq, C. (1965), The East Taiwan Rift, *Pet. Geol. Taiwan*, *4*, 93-106.

Carena, S., J. Suppe, and H. Kao (2001), Imaging the main detachment under Taiwan: implications for the critical-taper mechanics and large-scale topography, *EOS, Trans., Am. Geophys. Uni.*, *82*(47), Fall Meet. Suppl., Abstract T32A-0863.

Chan, C.-W. (1985), The Rueisuei, Hualien earthquake series on 24 April 1972 (in Chinese), M.S. thesis, 92pp., Natl. Taiwan Univ., Taipei.

Chang, J.-C., T.-T. Shih, S.-M. Shen, and C.-L. Chang (1992), A geomorphological study of river terrace in northern Huatung Longitudinal Valley (in Chinese with English abstract), *Geogr. Res.*, *18*, 1-51.

Chang, J.-C., T.-T. Shih, S.-C. Yang, Y.-F. Lin, and H.-L. Chen (1994), A geomorphological study of alluvial fan in Huatung Longitudinal Valley (in Chinese with English abstract), *Geogr. Res.*, *21*, 43-74.

Chang, L.-S. (1971), A biostratigraphic study of the so-called Slate Formation in Taiwan based on smaller foraminifera: I. The E-W cross-mountain highway, *Proc. Geol. Soc. China*, *14*, 45-61.

Chemenda, A. I., M. Mattauer, J. Malavieille, and A. N. Bokun (1995), A mechanism for syn-collisional rock exhumation and associated normal faulting: Results from physical modeling, *Earth Planet. Sci. Lett.*, *132*, 225-232.

Chen, H.-H., and R.-J. Rau (2002), Earthquake locations and style of faulting in an active arc-continent plate boundary: the Chihshang fault of eastern Taiwan, *EOS, Trans., Am. Geophys. Uni.*, *83*(47), Fall Meet. Suppl., Abstract T61B-1277.

Chen, J.-S. (1976), The analysis and design of refraction and reflection seismic survey of the Taitung area, *Pet. Geol. Taiwan*, *13*, 225-246.

Chen, J.-S., J.-N. Chou, Y.-C. Lee, and Y.-S. Chou (1974), Seismic survey conducted in eastern Taiwan (in Chinese with English abstract), *Pet. Geol. Taiwan*, *11*, 147-163.

Chen, Y.-G. (1988), C-14 dating and correlation of river terraces along the lower reach of the Tahan-chi, northern Taiwan (in Chinese), M.S. thesis, 88pp., Natl. Taiwan Univ., Taipei.

Chen, Y.-G., W.-S. Chen, and Y.-W. Chen (2004), Thermoluminescence and optically stimulated luminescence dating, trenching and paleoseismologic research projects (3/5)

(in Chinese), *Cent. Geol. Surv. Rep. 93-6*, 44pp., Taipei, Taiwan.

Cheng, S.-N., Y. T. Yeh, and M.-S. Yu (1996), The 1951 Taitung earthquake in Taiwan, *J. Geol. Soc. China*, *39*, 267-285.

Crespi, J. M., Y.-C. Chan, and M. S. Swaim (1996), Synorogenic extension and exhumation of the Taiwan hinterland, *Geology*, *24*, 247-250.

Gerya, T. V., B. Stöckhert, and A. L. Perchuk (2002), Exhumation of high-pressure metamorphic rocks in a subduction channel: A numerical simulation, *Tectonics*, *21*(6), 1056, doi:10.1029/2002TC001406.

Hartshorn, K., N. Hovius, W. B. Dade, and R. L. Slingerland (2002), Climate-driven bedrock incision in an active mountain belt, *Science*, *297*, 2,036-2,038.

Ho, C. S. (1986), A synthesis of the geologic evolution of Taiwan, *Tectonophysics*, *125*, 1-16.

Ho, C. S. (1988), *An Introduction to the Geology of Taiwan, Explanatory Text of the Geologic Map of Taiwan*, 2nd ed., 192pp., Cent. Geol. Surv., Ministry Econ. Affairs, Taipei, Taiwan.

Hovius, N., C. P. Stark, H.-T. Chu, and J.-C. Lin (2000), Supply and removal of sediment in a landslide-dominated mountain belt: Central Range, Taiwan, *J. Geol.*, *108*, 73-89.

Hsu, Y.-J., M. Simons, S.-B. Yu, L.-C. Kuo, and H.-Y. Chen (2003), A two-dimensional dislocation model for interseismic deformation of the Taiwan mountain belt, *Earth Planet. Sci. Lett.*, *211*, 287-294.

Jahn, B.-M., and J. G. Liou (1977), Age and geochemical constraints of glaucophane schists of Taiwan, *Mem. Geol. Soc. China*, *2*, 129-140.

Jahn, B.-M., J. G. Liou, and H. Nagasawa (1981), High-pressure metamorphic rocks of Taiwan: REE geochemistry, Rb-Sr ages and tectonic implications, *Mem. Geol. Soc. China*, *4*, 497-520.

Jahn, B. M., F. Martineau, J. J. Peucat, and J. Cornichet (1986), Geochronology of the Tananao Schist Complex and crustal evolution of Taiwan, *Mem. Geol. Soc. China*, *7*, 383-404.

Kuochen, H., Y.-M. Wu, C.-H. Chang, J.-C. Hu, and W.-S. Chen (2004), Relocation of the eastern Taiwan earthquakes and its tectonic implications, *Terr. Atmos. Oceanic Sci.*, *15*, 647-666.

Kuochen, H., Y.-M. Wu, Y.-G. Chen, and R.-Y. Chen (2005), 2003 Mw6.8 Chengkung earthquake and its related seismogenic structure, *J. Asian Earth Sci.*, in press.

Lallemand, S., and C.-S. Liu (1998), Geodynamic implications of present-day kinematics in the southern Ryukyus, *J. Geol. Soc. China*, *41*, 551-564.

Lee, J.-C., J. Angelier, H.-T. Chu, J.-C. Hu, and F.-S. Jeng (2001), Continuous monitoring

of an active fault in a plate suture zone: a creepmeter study of the Chihshang Fault, eastern Taiwan, *Tectonophysics*, *333*, 219-240.

Lee, J.-C., J. Angelier, H.-T. Chu, J.-C. Hu, F.-S. Jeng, and R.-J. Rau (2003), Active fault creep variations at Chihshang, Taiwan, revealed by creep meter monitoring, 1998-2001, *J. Geophys. Res.*, *108*(B11), 2528, doi:10.1029/2003JB002394.

Lin, C.-H. (2004), Repeated foreshock sequences in the thrust faulting environment of eastern Taiwan, *Geophys. Res. Lett.*, *31*, L13601, doi:10.1029/2004GL019833.

Lin, C.-W., H.-C. Chang, S.-T. Lu, T.-S. Shih, and W.-J. Huang (2000), *An Introduction to the Active Faults of Taiwan, 2nd ed., Explanatory Text of the Active Fault Map of Taiwan* (in Chinese with English abstract), *Spec. Pub. Cent. Geol. Surv.*, *13*, 122pp., Taipei, Taiwan.

Liu, C.-C., and S.-B. Yu (1990), Vertical crustal movements in eastern Taiwan and their tectonic implications, *Tectonophysics*, *183*, 111-119.

Liu, T.-K., S. Hsieh, Y.-G. Chen, and W.-S. Chen (2001), Thermo-kinematic evolution of the Taiwan oblique-collision mountain belt as revealed by zircon fission track dating, *Earth Planet. Sci. Lett.*, *186*, 45-56.

Malavieille, J., S. E. Lallemand, S. Dominguez, A. Deschamps, C.-Y. Lu, C.-S. Liu, P. Schnürle, and the ACT Scientific Crew (2002), Arc-continent collision in Taiwan: new marine observations and tectonic evolution, *Geol. Soc. Am. Spec. Paper*, *358*, 187-211.

Michard, A., C. Chopin, and C. Henry (1993), Compression versus extension in the exhumation of the Dora-Maira coesite-bearing unit, Western Alps, Italy, *Tectonophysics*, *221*, 173-193.

Sella, G. F., T. H. Dixon, and A. Mao (2002), REVEL: A model for Recent plate velocities from space geodesy, *J. Geophys. Res.*, *107*(B4), 2081, doi:10.1029/2000JB000033.

Shyu, J. B. H., K. Sieh, L.-H. Chung, Y.-G. Chen, and Y. Wang (2002), The active tectonics of eastern Taiwan—new insights from the two geomorphic tablelands (“the Feet”) in the Longitudinal Valley, *EOS, Trans., Am. Geophys. Uni.*, *83*(47), Fall Meet. Suppl., Abstract T61B-1278.

Shyu, J. B. H., K. Sieh, and Y.-G. Chen (2005a), Tandem suturing and disarticulation of the Taiwan orogen revealed by its neotectonic elements, *Earth Planet. Sci. Lett.*, *233*, 167-177.

Shyu, J. B. H., K. Sieh, Y.-G. Chen, and C.-S. Liu (2005b), Neotectonic architecture of Taiwan and its implications for future large earthquakes, *J. Geophys. Res.*, *110*, B08402, doi:10.1029/2004JB003251.

Shyu, J. B. H., K. Sieh, J.-P. Avouac, W.-S. Chen, and Y.-G. Chen (2005c), Millennial slip

rate of the Longitudinal Valley fault from river terraces: Implications for convergence across the active suture of eastern Taiwan, *J. Geophys. Res.*, submitted for publication.

Shyu, J. B. H., L.-H. Chung, Y.-G. Chen, J.-C. Lee, and K. Sieh (2005d), Re-evaluation of the surface ruptures of the November 1951 earthquake series in eastern Taiwan, and its neotectonic implications, *J. Asian Earth Sci.*, submitted for publication.

Teng, L. S. (1987), Stratigraphic records of the late Cenozoic Penglai orogeny of Taiwan, *Acta Geol. Taiwanica*, *25*, 205-224.

Teng, L. S. (1990), Late Cenozoic arc-continent collision in Taiwan, *Tectonophysics*, *183*, 57-76.

Teng, L. S. (1996), Extensional collapse of the northern Taiwan mountain belt, *Geology*, *24*, 949-952.

Willett, S. D., D. Fisher, C. Fuller, E.-C. Yeh, and C.-Y. Lu (2003), Erosion rates and orogenic-wedge kinematics in Taiwan inferred from fission-track thermochronometry, *Geology*, *31*, 945-948.

Yen, T. P. (1953), On the occurrence of the late Paleozoic fossils in the metamorphic complex of Taiwan, *Bull. Geol. Surv. Taiwan*, *4*, 23-26.

Yen, T. P., C. C. Sheng, and W. P. Keng (1951), The discovery of fusuline limestone in the metamorphic complex of Taiwan, *Bull. Geol. Surv. Taiwan*, *3*, 23-25.

Yu, M.-S. (1997), Active faults in the Taitung Longitudinal Valley (in Chinese), Ph.D. thesis, 141pp., Natl. Taiwan Univ., Taipei.

Yu, S.-B., and L.-C. Kuo (2001), Present-day crustal motion along the Longitudinal Valley Fault, eastern Taiwan, *Tectonophysics*, *333*, 199-217.

Yu, S.-B., and C.-C. Liu (1989), Fault creep on the central segment of the Longitudinal Valley fault, eastern Taiwan, *Proc. Geol. Soc. China*, *32*, 209-231.

Chapter 6

Neotectonic Geomorphology of Southernmost Longitudinal Valley Fault, Eastern Taiwan, and Its Tectonic Implications

6.1 Abstract

In order to fully understand the deformational patterns of the Longitudinal Valley fault system, a major structure along the eastern suture of Taiwan, we mapped detailed geomorphic features near the southern end of the Longitudinal Valley where many well-developed fluvial landforms have recorded the deformations by the multiple strands of the fault. Our geomorphic analysis shows that the Longitudinal Valley fault branches into two major strands in the area. The Luyeh strand in the west has predominantly reverse motion. The Peinan strand in the east has significant left-lateral component. Between the two strands, late Quaternary fluvial sediments and surfaces are progressively deformed. The Luyeh strand dies out to the north and steps to the east, joining with the Peinan strand to become the main strand of the reverse sinistral Longitudinal Valley fault near the Pingting terraces. To the south, the Luyeh strand becomes an E-W trending monocline at the southern end of the Peinanshan. This suggests that the reverse motion on the Longitudinal Valley system decreases drastically at that point, and, together with the end of the Coastal Range, may represent the southern termination of the Taitung Domain.

Keywords: Taiwan, tectonic geomorphology, Longitudinal Valley fault, river terraces, sutures.

6.2 Introduction

The island of Taiwan, at the plate boundary between the Eurasian and the Philippine Sea plate, is the product of the ongoing collision between the two plates [e.g., *Ho*, 1986; *Teng*, 1987, 1990; *Shyu et al.*, 2005a; and references therein] (Figure 6.1). As one of the very few places on Earth that is undergoing active suturing of two lithospheric blocks, Taiwan provides valuable opportunities for understanding the suturing processes. The collision involves three lithospheric blocks and has created two sutures on the island [*Shyu et al.*, 2005a]. Of the two sutures, the eastern one, the Longitudinal Valley in eastern Taiwan, is the active suture between the docked Luzon volcanic arc and a continental sliver that includes the Central Range, the mountainous backbone of Taiwan. The valley is characterized by numerous earthquakes and many active structures and is dominated by the Longitudinal Valley fault, one of the most active structures in the world [e.g., *Angelier et al.*, 1997; *Shyu et al.*, 2005b].

As the suturing processes gets more mature from south to north, active structures of the Taiwan orogen manifest different characteristics, separating the island into several discreet neotectonic domains [*Shyu et al.*, 2005b] (Figure 6.2). Along the Longitudinal Valley, there are two domains: the Hualien and the Taitung Domains. In the Hualien Domain which includes the northern third of the Longitudinal Valley fault, the fault appears to be more sinistral-dominated and slipping at a lower rate. In the Taitung Domain, farther to the south, the fault slips obliquely at a much higher rate and causes the rapid uplift of the Coastal Range in the hanging-wall block of the fault [*Yu and Liu*, 1989; *Hsu et al.*, 2003; *Shyu et al.*, 2005c].

Although the activeness of the Longitudinal Valley fault has been known for decades and attracted numerous geodetic and seismologic investigations [e.g., *Angelier et al.*, 1997; *Lee et al.*, 2001, 2003; *Yu and Kuo*, 2001; *Kuochen et al.*, 2004], there have been very few detailed geomorphic analyses of the fault. Most of the maps of the fault are

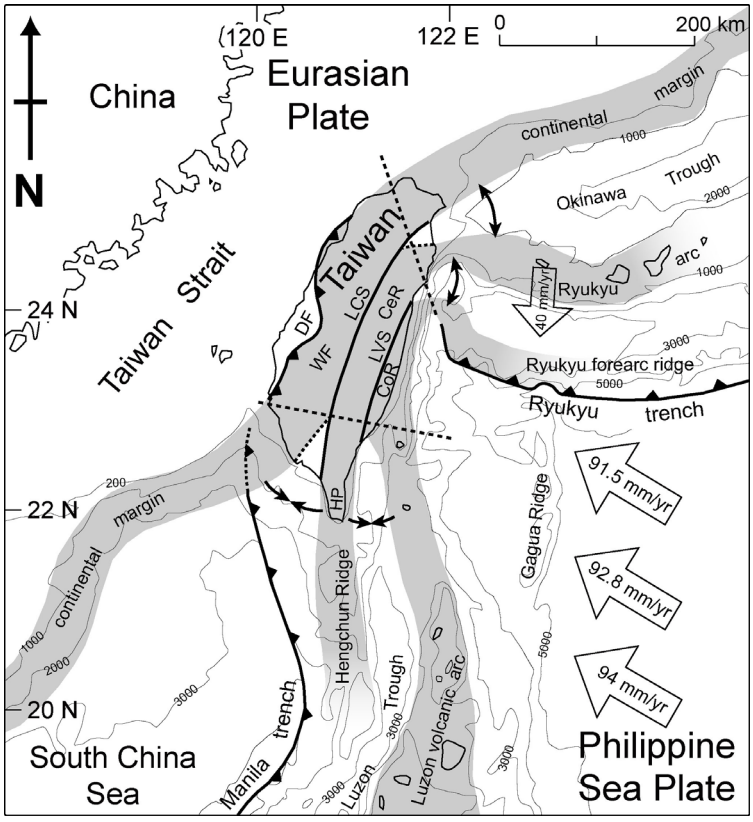

Figure 6.1. The island of Taiwan is being created by a tandem suturing of the Luzon volcanic arc and a sliver of continental crust to the Chinese continental margin. In eastern Taiwan, the Longitudinal Valley suture (LVS) is the eastern of the two sutures. This suture joins the Coastal Range (CoR), the docked part of the Luzon volcanic arc, and the continental sliver of the Central Range (CeR), the mountainous backbone of the island. Current velocity vectors of the Philippine Sea plate relative to South China, at 124°E and 20°, 21°, and 22°N, are calculated using the Recent plate velocity model (REVEL) of *Sella et al.* [2002]. Current velocity vector of the Ryukyu arc is adapted from *Lallemand and Liu* [1998]. Black dashed lines are the northern and western limits of the Wadati-Benioff zone of the two subduction zones, taken from the seismicity database of the Central Weather Bureau, Taiwan. DF: deformation front; LCS: Lishan-Chaochou suture; WF: Western Foothills; HP: Hengchun Peninsula. The figure is adapted from *Shyu et al.* [2005a].

large-scaled maps of the entire Longitudinal Valley, with very little detail on any of the secondary features of the fault [e.g., *Wang and Chen*, 1993; *Lin et al.*, 2000]. As a result, most current knowledge of the fault was limited to the main fault trace, which may absorb only a portion of the total deformation across the entire fault system. Without the knowledge of the deformational pattern of the fault system, it is difficult to design proper experiment to observe the fault. For example, many of the current short-aperture geodetic experiments focus on the main fault trace only [e.g., *Lee et al.*, 2001, 2003] and may significantly underestimate the rate of the fault.

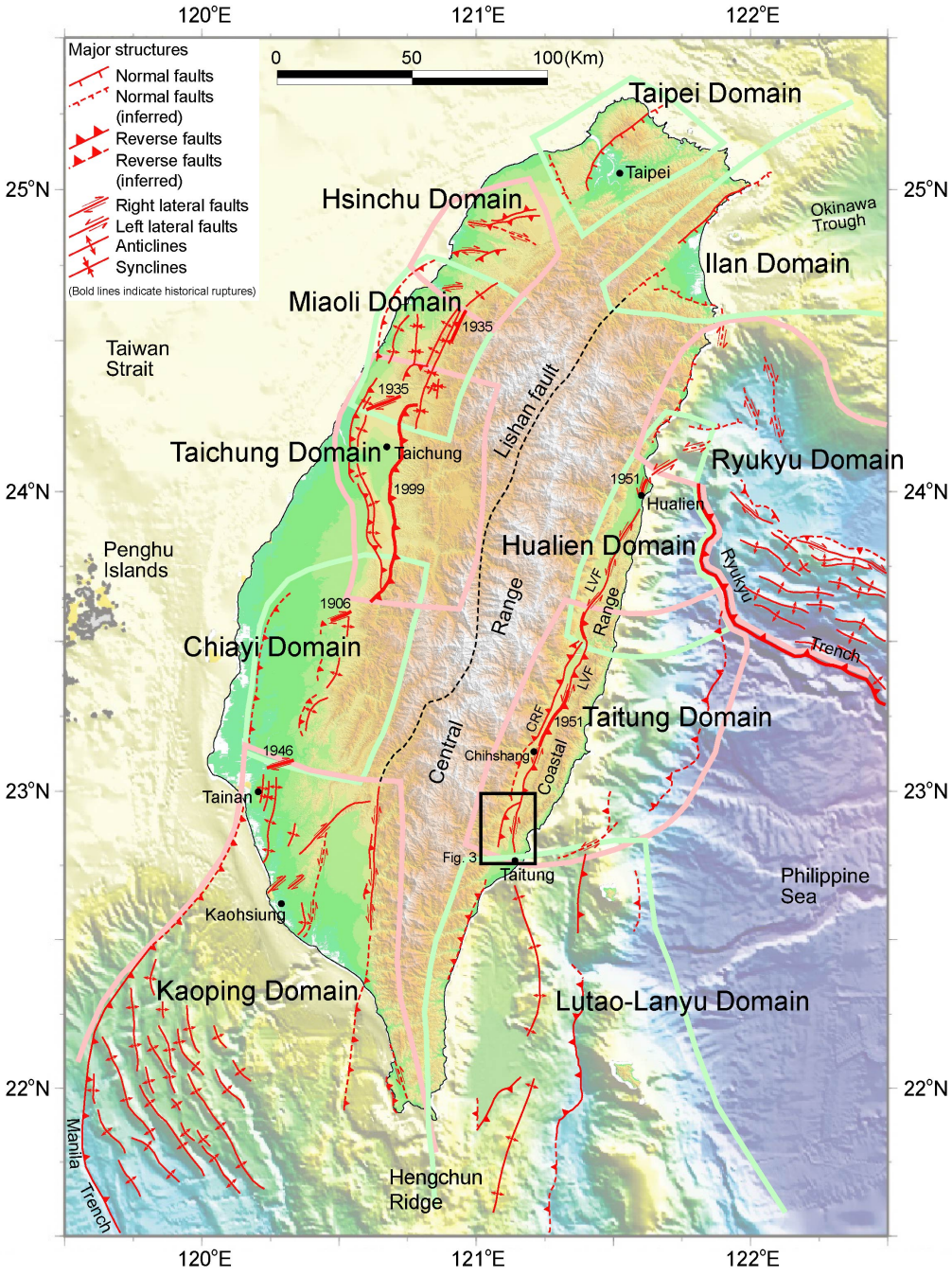

Figure 6.2. Map of neotectonic domains of Taiwan. Each domain contains a distinct assemblage of active structures. The map is adapted from *Shyu et al.* [2005b]. Two domains, the Hualien and Taitung Domains, are present in eastern Taiwan along the Longitudinal Valley suture. LVF: Longitudinal Valley fault; CRF: Central Range fault. Bold light green and pink lines are boundaries of domains.

Near the southern end of the Longitudinal Valley, well-developed fluvial surfaces provide a useful tool for mapping the Longitudinal Valley fault system in great detail

[*Shih et al.*, 1983, 1984]. Distinct deformational patterns of these fluvial surfaces enabled us to further understand the characteristics of each of the multiple strands of the fault. We believe such systematic and detailed mapping of the geomorphic features of the fault is the foundation for designing any detailed experiment to understand the kinematics of the fault.

Our principal mean for geomorphic analysis is a set of digital elevation model (DEM) with a 40-m resolution. Although a more recent 5-m resolution DEM covers only part of our study area, it significantly improved our ability to identify small features and secondary structures of the fault. In this paper we present the combined result of our mapping using these two sets of DEM. Our DEM analysis was followed by mapping and investigation of fluvial landforms in the field.

6.3 Tectonic setting

Taiwan is formed at the boundary between the Philippine Sea plate and the South China block of the Eurasian plate (Figure 6.1). South of Taiwan, the oceanic South China Sea plate is subducting eastward beneath the Philippine Sea plate along the Manila trench, forming the Luzon volcanic arc. At the latitude of Taiwan, however, the oceanic lithosphere of the South China Sea is consumed entirely, and the Chinese continental margin begins to impinge upon the trench, creating the mountainous island of Taiwan.

This collision is further complicated by an intervening continental sliver which forms the submarine Hengchun Ridge and the Central backbone Range of Taiwan (Figures 6.1 and 6.2). Therefore, the orogen is formed by a tandem suturing and tandem disarticulation between the Eurasian continental margin, the continental sliver, and the Luzon volcanic arc [*Shyu et al.*, 2005a]. In eastern Taiwan, the Longitudinal Valley suture is the suture between the docked volcanic arc of the Coastal Range and the Central Range, the metamorphic core of the continental sliver.

The east-dipping Longitudinal Valley fault is the major structure along this suture (Figure 6.2). Along the fault, the highly shortened volcanic rocks and forearc and intraarc basin sedimentary rocks of the Coastal Range are thrusting over the current sediments of the Longitudinal Valley. Slip rate along the fault is up to several tens of mm/yr [*Angelier et al.*, 1997; *Shyu et al.*, 2005c], making it one of the fastest slipping faults in the world. Uplifted fluvial terraces in the Coastal Range suggest that the fault is slipping at such high rates, at least for the Holocene [*Shyu et al.*, 2005c]. Along a segment of the fault, many small earthquakes illuminate the subsurface listric shape of the fault plane [*Chen and Rau*, 2002; *Kuochen et al.*, 2004].

At the western side of the Longitudinal Valley, the west-dipping Central Range fault slips at a lower rate than the Longitudinal Valley fault and is active along the southern two-thirds of the valley [*Shyu et al.*, 2005d] (Figure 6.2). Although currently not slipping at a high rate, geomorphic evidence of the fault is clear and widespread along the western side of the valley, and the fault appears to also play important roles during the evolution of the Longitudinal Valley suture.

Along the southwestern flank of the Coastal Range, the Lichi Formation crops out as a very distinct stratigraphic unit. This unit consists of various and abundant blocks, sometimes tens of kilometers in size, within highly sheared, chaotic sand and mud matrix [*Ho*, 1988]. The Lichi Formation can be considered as highly shortened and sheared deep marine forearc or intraarc basin sediments [e.g., *Biq*, 1971; *Teng*, 1981; *Hsü*, 1988; *Huang et al.*, 1992; *Chang et al.*, 2001] or as slump deposits associated with collapse of sediments on the steeper slopes around these basins [e.g., *Page and Suppe*, 1981; *Barrier and Muller*, 1984; *Barrier and Angelier*, 1986].

6.4 Major geomorphic features at southernmost Longitudinal Valley

At the southernmost part of the Longitudinal Valley, instead of a low and flat valley between the Central and Coastal Ranges, several uplifted fluvial terraces, locally up to 300 m above the current valley floor, exist between the two ranges (Figure 6.3). These terraces are underlain by late Quaternary alluvial deposits, mostly gravels and sand. Distinct members of these fluvial landforms, from south to north, are the Peinanshan, the Kaotai and surrounding terraces, and the smaller Pingting terraces southeast of the town of Rueiyuan.

South of the eastward flowing Luyeh River, the Peinanshan is a N-S elongated hill that perches up to 300 m above the Longitudinal Valley floor (Figure 6.3). This feature is also known as “The Foot” due to its peculiar shape in map view. Lateritic soils overlie most of the western part of the Peinanshan. Judging from the dates of similar lateritic terraces in other parts of Taiwan [e.g., *Chen*, 1988], this indicates that fluvial terraces atop western Peinanshan formed at least a couple tens of thousand years ago. Below the lateritic soils and in the eastern part of the Peinanshan, late Quaternary Peinanshan Conglomerate crops out as the bedrock of the fluvial terraces. This stratigraphic unit consists mostly of rounded fluvial cobbles of metamorphic rocks from the Central Range, including schist and marble clasts [*Hsu*, 1956; *Teng and Wang*, 1981; *Barrier et al.*, 1982]. Volcanic rock and sandstone clasts, probably from the Coastal Range, are found locally. In the eastern part of the Peinanshan, the Peinanshan Conglomerate is indurated and dips steeply. This suggests that part of the Peinanshan Conglomerate has been buried and deformed extensively.

Between the Luyeh and Luliao Rivers are the Kaotai terraces and several steps of lower terraces. The Kaotai terraces are also overlain by lateritic soils. This and the fact that the Kaotai terraces have a similar elevation above the Longitudinal Valley floor

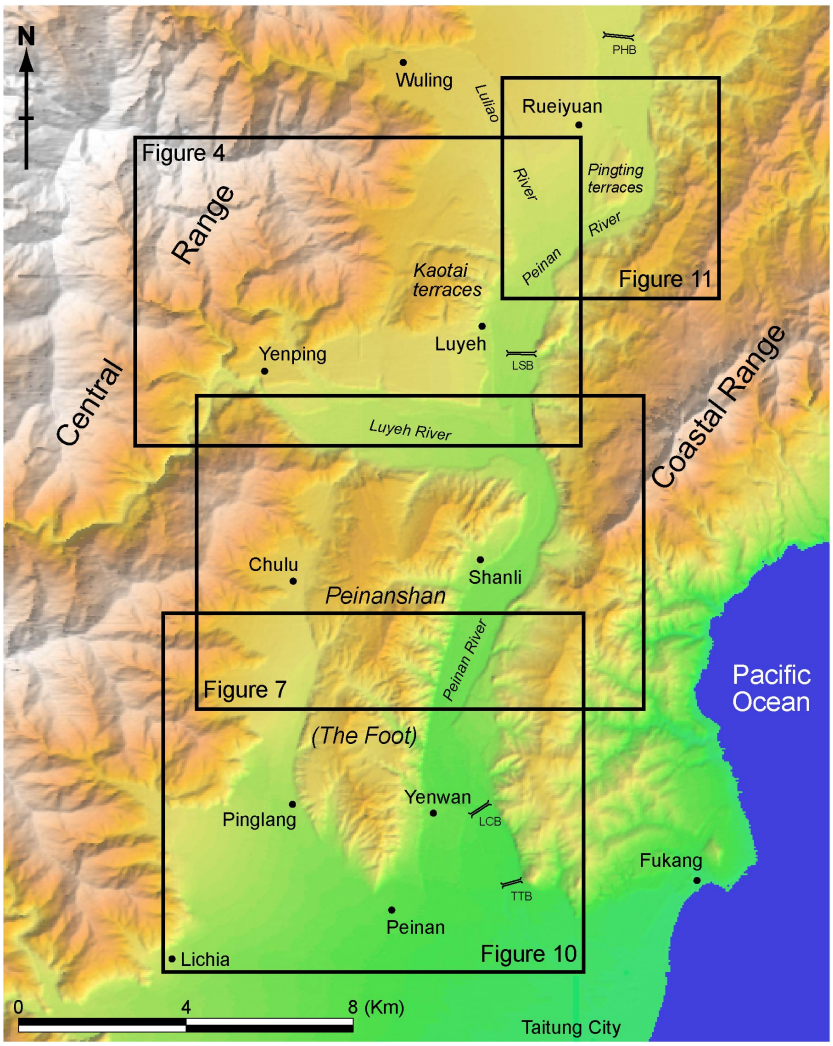

Figure 6.3. Major fluvial landforms near the southernmost Longitudinal Valley. Between the Central and Coastal Ranges, several uplifted fluvial surfaces are present. The Peinanshan south of the Luyeh River is a N-S elongated hill overlain by lateritic fluvial terraces, with the fluvial Peinanshan Conglomerate as the bedrock. The Kaotai terraces north of the Luyeh River consist of lateritic fluvial surfaces that may be correlative with the highest surfaces of the Peinanshan. The lower Pingting terraces east of the Luliao River are surfaces of uplifted Peinan River bed, with a thin layer of fluvial gravels overlying the Lichi Formation.

as the Peinanshan suggest that they are probably similar in age. The lateritic soils of the Kaotai terraces are also underlain by fluvial cobbles derived mostly from the Central Range, possibly comparable with the Peinanshan Conglomerate.

East of the Luliao River, the small Pingting terraces appear to be uplifted Peinan River bed (Figure 6.3). The terraces have two major steps, with the higher one, about 50 m above the current riverbed, at the eastern side. Due to the uplift of the Pingting

terraces, the current Peinan River narrows significantly when flowing around the terraces. The lower elevation of the Pingting terraces suggests that the age of the terraces is much younger than the Peinanshan and the Kaotai terraces. This is consistent with the fact that no lateritic soil appears above the Pingting terraces. The terraces are overlain by only a thin layer of fluvial gravels, locally up to 10 m thick. At outcrops both on the north and south sides of the terraces, the Lichi Formation crops out underlying the thin fluvial gravels as the bedrock of the terraces.

6.5 Neotectonic geomorphology of the Kaotai and surrounding terraces

North of the Luyeh River, geomorphic features clearly indicate that a major reverse fault cuts across the large river terrace 4 on which the village of Lungtien sits (Figure 6.4). This reverse fault extends further to the north and forms the approximate boundary of the Kaotai terraces and the Central Range. Still farther to the north, the fault appears to die out and ends just short of the Luliao River.

A very clear monoclinal scarp, up to 15 m high, runs N-S through the large terrace 4 in the northern bank of the Luyeh River, just west of Lungtien (Figures 6.4 and 6.5a). Between Lungtien and the scarp, the surface of Lungtien terrace forms an anticlinal warp. Other than the scarp and the warp, the Lungtien terrace surface shows a gentle eastward slope that is consistent with its Luyeh River origin. Therefore, we believe the scarp and the anticline are manifestations of a fault-propagation fold of an east-dipping blind reverse fault beneath the eastern part of the Lungtien terrace. In fact, this clear feature was identified as an active structure long ago and has been named as the Luyeh fault by several investigators [*Shih et al.*, 1983, 1984, 1986; *Yang*, 1986; *Chu and Yu*, 1997]. It has been generally considered to be a thrust strand of the Longitudinal Valley fault. With a sinistral strand to the east, this would be a typical slip-partitioning of the oblique

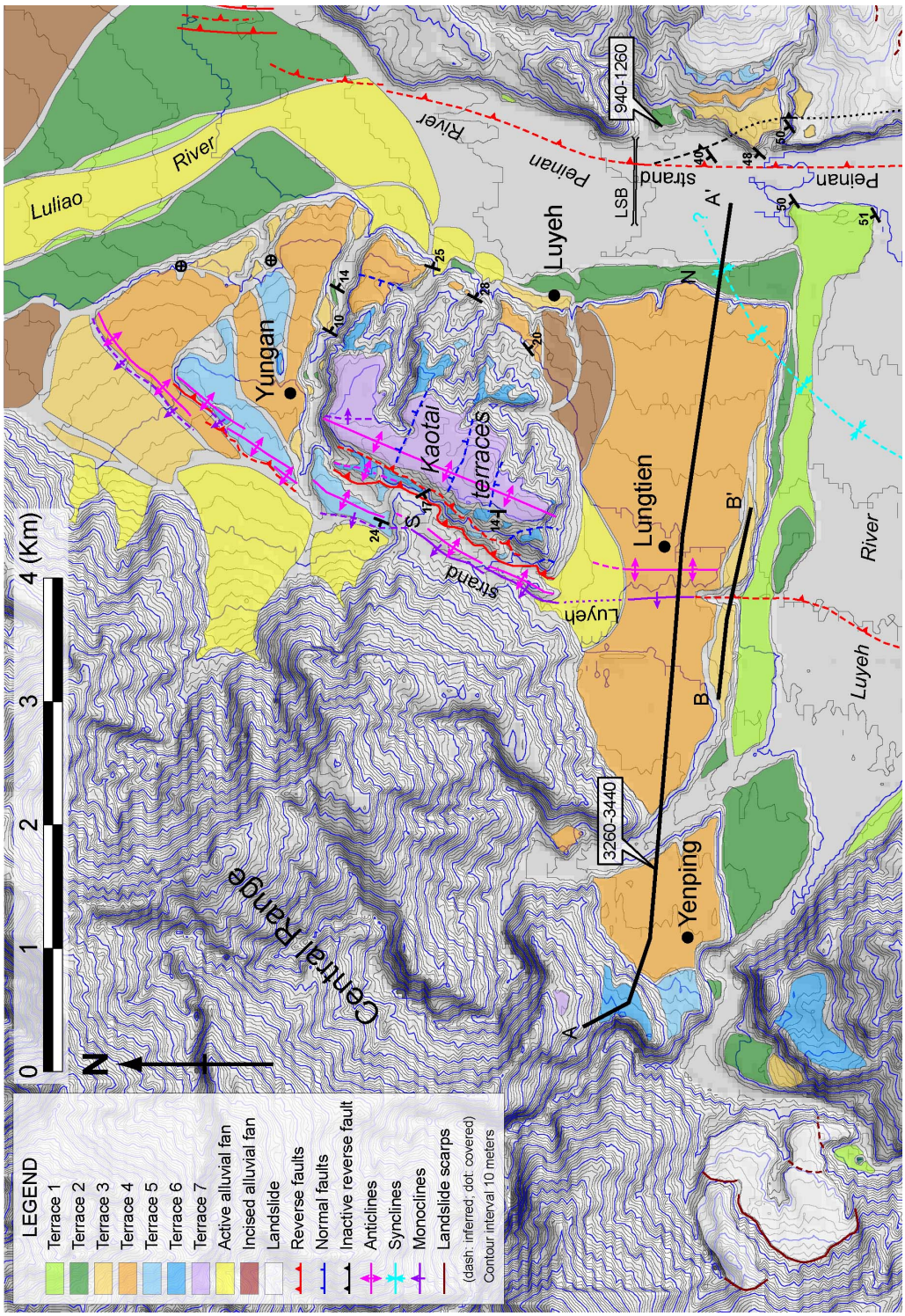

Figure 6.4. Detailed map shows geomorphic features and active structures of the Kaotai terraces area. The Luyeh strand, a major strand of the Longitudinal Valley fault, runs along the western edge of the Kaotai terraces and produces a monoclinal scarp on the Lungtien terrace to the south. To the north the Luyeh strand dies out just south of the Luliao River. The other strand of the Longitudinal Valley fault, the Peinan strand, runs within the Peinan River valley and through the Luanshan Bridge (LSB) at about 200 m to the eastern end of the bridge. Ages of terraces are calibrated ages (2σ) in cal BP.

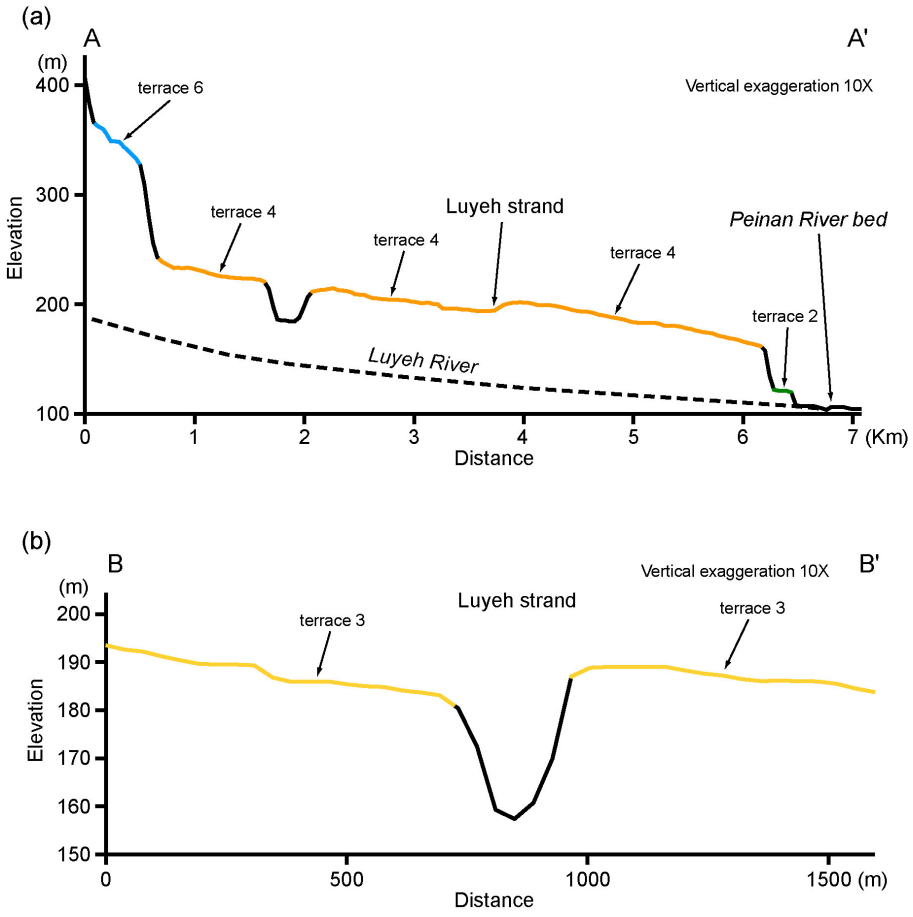

Figure 6.5. Selected topographic profiles of the Kaotai terraces area. Locations of the profiles are shown in Figure 6.4. (a) A topographic profile across the Lungtien and other terraces. The Luyeh strand produced a monoclinal scarp about 15 m high at about halfway downstream on the Lungtien terrace (terrace 4). Other than the scarp, the terrace surface shows a gentle eastward slope that is consistent with the Luyeh River bed. Notice that at the downthrown (west) side of the Luyeh strand the Lungtien terrace is still about 60 m above the current Luyeh River bed. We hypothesize that the Longitudinal Valley and eastern flank of the Central Range are on the hanging-wall block of a deeper Central Range fault that dips west, under the Central Range. (b) A short topographic profile across the Luyeh strand on terrace 3. The terrace east of the Luyeh strand is about 10 m higher than its counterpart west of the strand.

slipping Longitudinal Valley fault system [*Lee et al.*, 1998; *Hu et al.*, 2001]. Since this reverse fault is essentially a strand of the Longitudinal Valley fault, we call this structure the Luyeh strand hereinafter.

From a shallow pit dug into terrace surface east of Yenping, we successfully collected a charcoal sample from the gravel beds that underlie terrace 4. The sample yielded an age of about 3.35 kyr (Figure 6.4; Table 6.1), representing the maximum age

Table 6.1. List and analytical results of the charcoal samples dated in this research.

Sample number	Site name	GPS location of site		Corresponding figure	Terrace level	Age (yrBP)*	Calibrated age (2σ)(cal BP)#
		X	Y				
BN-02B	BN	258439	2534148	6.4	4	3130±30	3260-3440
20010917-2	CYB	264514	2533951	6.4	2	1170±80	940-1260
RY2-05	RY2	266018	2538348	6.11	4	1700±30	1530-1690

* All samples were dated in Lawrence Livermore National Laboratory (LLNL) using accelerator mass spectrometry (AMS).
# Calibrated using the CALIB program [*Stuiver and Reimer*, 1993].

of terrace 4 surface. Since the terrace surface was offset about 15 m by the Luyeh strand, the minimum vertical component of the slip rate of the strand is therefore about 4.5 mm/yr.

To the south, the Luyeh strand appears to follow the small southward flowing canyon and extend toward the Luyeh River bed (Figure 6.4). Terrace 3, which is about 10 m lower than terrace 4, was clearly offset by the Luyeh strand since the small patch of terrace 3 east of the canyon is about 10 m higher than its counterpart west of the canyon (Figure 6.5b). The much lower terrace 1, however, does not show offset by the Luyeh strand. This is likely due to the much younger age, and thus much smaller offset, of terrace 1.

North of the Lungtien terrace, the Luyeh strand extends into the valley between the Kaotai terraces and the Central Range (Figure 6.4). The Kaotai terraces appear to be underlain by a large, wide anticline, as shown by both their sloping surfaces and the bedding attitude measurements of the underlying gravels beds. This large anticline may be the northern extension of the small anticline west of Lungtien and may also be formed as the fault-propagation fold of the Luyeh strand.

West of the Kaotai terraces, the Luyeh strand appears to branch into several sub-strands (Figure 6.4). At least one of these sub-strands, along the western front of the terraces, appears to break the surface as a reverse fault. The westernmost strand, however, appears to be a monocline. This monoclinal strand produced a series of

anticlinal ridges of colluvium along the valley between the Kaotai terraces and the Central Range and cuts through an E-W trending ridge of metamorphic slates of the Central Range (point S in Figure 6.4). Therefore, although most of the deformation caused by the Luyeh strand concentrates in late Quaternary gravels underlying the Kaotai terraces, the westernmost sub-strand has broken a small piece of the Central Range. This may be the only place where part of the Longitudinal Valley fault system extends so far to the west that it deforms the Central Range.

Above the highest surface of the Kaotai terraces (terrace 7), several gentle E-W striking scarps are present (Figure 6.4). These scarps are likely to be minor normal fault scarps formed on the anticlinal axis and parallel to the convergence direction, similar to those found in southern Tibet [e.g., *Molnar and Tapponnier*, 1978; *Yin et al.*, 1999; *Blisniuk et al.*, 2001]. Alternatively, these gentle scarps may reflect the geometrical change of the shape of the underlying fault when the footwall block has an irregular upper surface.

Since the minimum vertical slip component of the Luyeh strand is about 4.5 mm/yr, we can calculate the minimum age of the highest Kaotai terraces. Assuming that the floor of the canyon between the Kaotai terraces and the Central Range is correlative with the highest surface (terrace 7) above the Kaotai terraces, the surface has been uplifted for at least 135 m. This indicates that the Kaotai terrace 7 is at least 30 kyr old, consistent with the appearance of lateritic soils above the terraces.

The Kaotai terrace 7 ends abruptly at an E-W trending drainage just south of the village of Yungan (Figure 6.4). North of the drainage, the Luyeh strand extends northeastward as a series of anticlinal ridges that develop on several lower terraces. The height of these ridges decreases to the north. Since bedding attitude measurements of the underlying gravel beds indicate that the sediments below the terraces are generally horizontal, we believe the decreasing height of the anticlinal ridges may in fact indicates the decreasing deformation by the underlying Luyeh strand northeastward. The

northernmost and lowest anticlinal ridge ends just south of terrace 2 of the Luliao River. No deformation of any kind can be found on the lower terraces along the Luliao River or farther to the northeast. Thus, we believe the slip along the Luyeh strand diminishes northward quickly north of the Kaotai terraces and stops at the southern bank of the Luliao River.

Since the Luyeh strand appears to be a predominantly reverse fault from its geomorphic manifestations, it is reasonable to suggest that there is at least another strand of the Longitudinal Valley fault east of the Luyeh strand. We are uncertain about the exact location of this eastern strand of the Longitudinal Valley fault in the Kaotai terraces area. No deformation is present on the lower terraces west of the Peinan River, and no clear geomorphic evidence is present for a fault within the Coastal Range. Therefore, we believe the strand should be within the Peinan River valley (Figure 6.4). We hereinafter call this strand the Peinan strand.

Although it is difficult to locate the Peinan strand by topographic features, several bridges across the Peinan River may help us identify its location. Southeast of Luyeh, the Luanshan Bridge (LSB in Figure 6.4) crosses the Peinan River. At about 200 m from its eastern end, the bridge was fractured by compression, with its eastern side moving westward (Figure 6.6a). Since the bridge was last fixed in early 2003, the fracture is believed to be caused by deformation from small induced slip of the Peinan strand during the M_L 6.5 Chengkung earthquake of 10 December 2003 [*H.-T. Chu*, unpublished data]. Because the fracture of the bridge localizes only at this point and the bridge is supposed to be built out of identical sections, we suggest that the Peinan strand should run through the point, about 200 m from the eastern end of the Luanshan Bridge (Figure 6.4).

The existence of the two strands of the Longitudinal Valley fault led many to believe that this is a typical slip-partitioning of the fault with a reverse Luyeh strand and a sinistral Peinan strand [*Lee et al.*, 1998; *Hu et al.*, 2001]. However, it may not be this

Figure 6.6. Field photographs of several deformed bridges across the Peinan River. (a) At about 200 m from its eastern end, the Luanshan Bridge was fractured with its eastern part moved westward. View is toward the south. (b) Near the eastern end of the Lichi Bridge, an eastern section of the bridge appears to have moved upward and caused deformation of its contact with its western neighboring section. The lower part of the contact appears to have been opened and the upper part of the contact appears to have been squeezed. View is toward the north. (c) At about 100 m from its eastern end, the Paohua Bridge was deformed by the Longitudinal Valley fault. The eastern part of the bridge has moved upward with respect to its western part. View is toward the west.

simple. The deformation of the Luanshan Bridge indicates that the Peinan strand has significant reverse motion. Moreover, the vertical slip component of the Luyeh strand, at about 4.5 mm/yr, is much less than the vertical slip component of the Longitudinal Valley fault observed along its other segments, which may be as high as more than 20 mm/yr [Y*u and Liu*, 1989; *Angelier et al.*, 1997; *Lee et al.*, 2001, 2003; *Shyu et al.*, 2005c]. Therefore, we believe that although the Longitudinal Valley fault branches into two strands, at least north of the Luyeh River its slip is not entirely partitioned.

6.6 Neotectonic geomorphology of the northern Peinanshan area

South of the Luyeh River, the Luyeh strand appears to extend along the western edge of the Peinanshan and produces a large anticline-syncline pair, as shown by the deformed highest terrace surface above the Peinanshan (Figure 6.7). The Peinan strand appears to become more predominantly sinistral and cuts the northeastern corner of the Peinanshan.

Geomorphic features indicate that the Luyeh strand extends southward along the western edge of the Peinanshan (Figures 6.7 and 6.8). At several points, such as east of the village of Chulu, the strand appears to be emerged and produces clear fault scarps. The northwestern corner of the Peinanshan buttresses against a ridge of metamorphic rocks of the Central Range. Since the ridge does not seem to be deformed, we believe the Luyeh strand should locate along the small canyon flowing northward between the ridge and the Peinanshan. Therefore, unlike west of the Kaotai terraces, the southern part of the Luyeh strand does not appear to have broken any piece of the Central Range.

In the hanging-wall block of the Luyeh strand, an anticline-syncline pair is present (Figure 6.7). These two folds are clearly manifested by the deformed surface of terrace 7 above northern Peinanshan (Figure 6.8a) as well as bedding attitude measurements of the underlying gravel beds. The degree of deformation by the two folds on younger terraces such as terrace 4 on the northern side of the Peinanshan are smaller than the older terrace 7 (Figure 6.8b). Moreover, the bedrock gravels have steeper dipping beds than terrace 7 surface. These features indicate that the folds are active and growing during the deposition of the gravels and the subsequent incision of the Luyeh River.

The two folds appear to turn slightly to the southwest and are truncated by the Luyeh strand south of Chulu (Figure 6.7). The horizontal gravel beds found along the small southwestward flowing canyon south of Chulu suggest that the synclinal axis may follow the canyon and connect with the Luyeh strand further south.

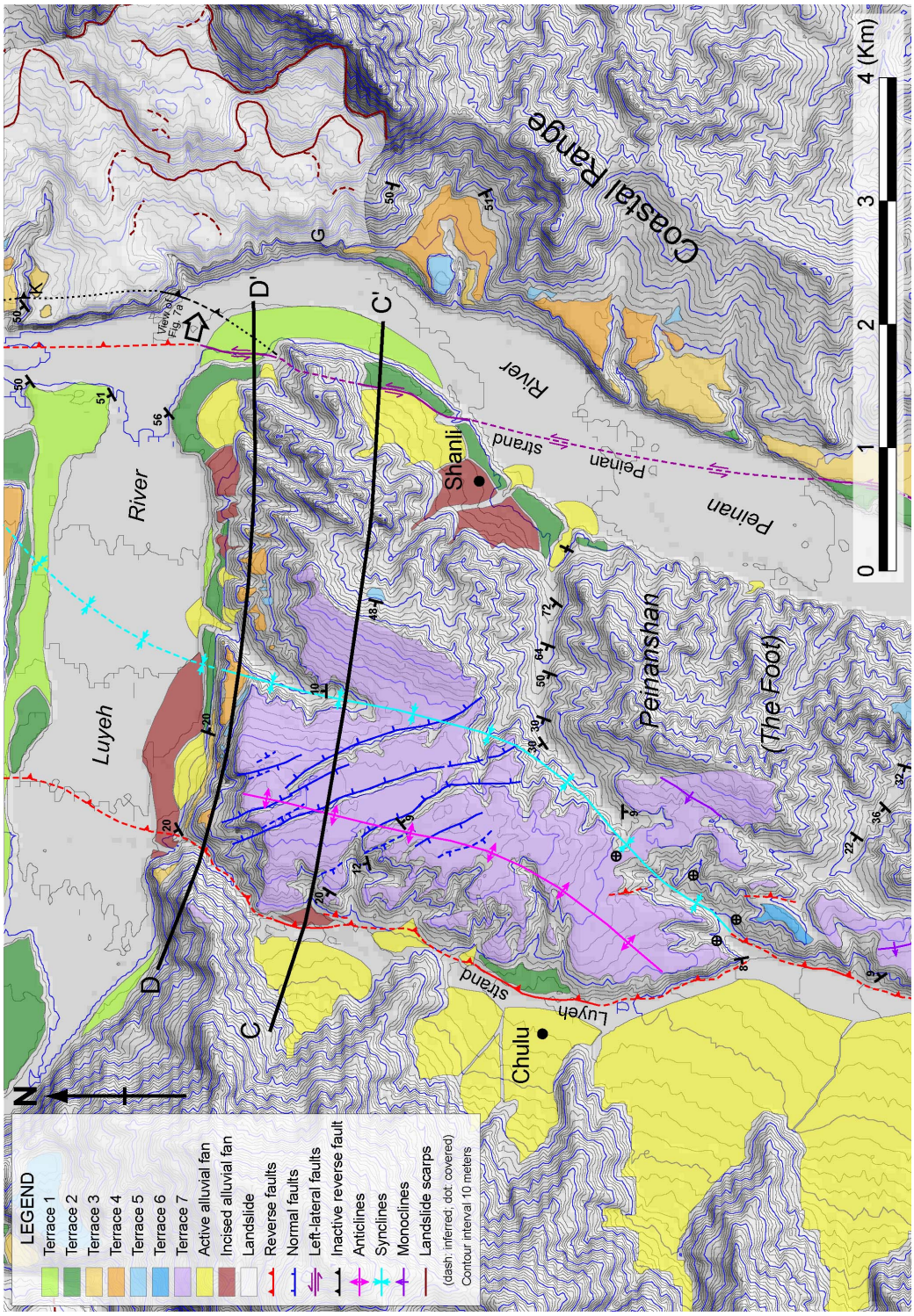

Figure 6.7. Detailed map shows geomorphic features and active structures of the northern Peinanshan area. The Luyeh strand runs along the western front of the Peinanshan. An anticline and a syncline in the hanging-wall block of the Luyeh strand clearly deformed the highest terrace 7 above northern Peinanshan. The Peinan strand cuts through the northeastern corner of the Peinanshan and appears to be predominantly left-lateral. An immense landslide deposit covers a fluvial strath, at about 80 m above the current Peinan River bed, east of the Peinan River on the western flank of the Coastal Range.

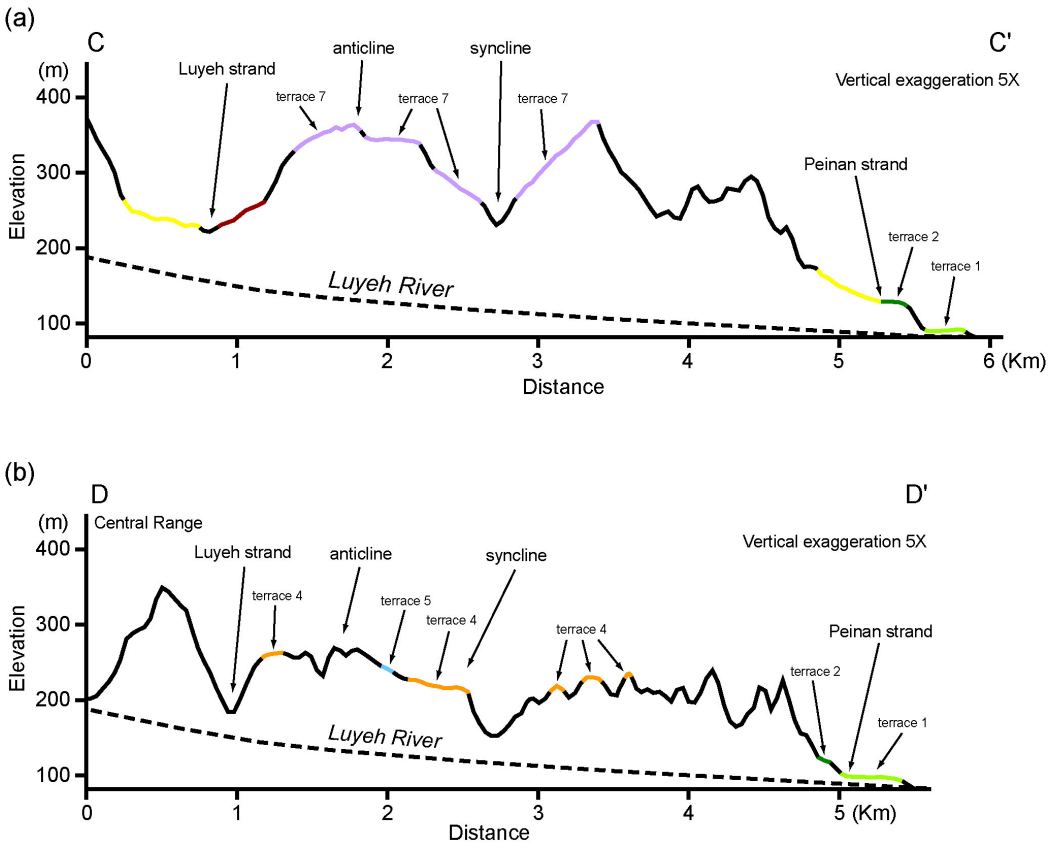

Figure 6.8. Selected topographic profiles of the northern Peinanshan area. Locations of the profiles are shown in Figure 6.7. (a) A topographic profile of terraces 7 on northern Peinanshan. The fluvial surface has been deformed into an asymmetrical syncline in the east and an anticline in the west. (b) The topographic profile of lower terraces on the south side of the Luyeh River north of terrace 7 indicates that these lower terraces are also deformed by the folds, with smaller degrees of deformation. This suggests that the folds are growing during the incision of the Luyeh River.

We are not sure if the anticlinal axis extends further north over the Luyeh River and connects with the anticlines west of Lungtien or beneath the Kaotai terraces. The synclinal axis, however, appears to extend to the north and turns northeastward (Figures 6.4 and 6.7). Several outcrops of the Peinanshan Conglomerate, such as along the eastern wall of the Peinan River and as the bedrock of terrace 1 at the confluent of the Luyeh and Peinan Rivers, indicate the synclinal axis trends more to the east north of the Luyeh River.

East of the synclinal axis the dip of the Peinanshan Conglomerate steepens to the east, and eventually becomes vertical at the easternmost part of the Peinanshan (Figure

6.7). This is evident by the presence of clear bedding plane ridges near the northeastern corner of the Peinanshan and by the bedding attitude measurements along the eastward flowing canyon south of the village of Shanli. The presence of very steep beds in the eastern limb of the syncline and the fact that the synclinal axis connects with the Luyeh strand suggest that the syncline may have formed as a fault-propagation fold at depth. The gentle limbs of the anticline, on the other hand, suggest that the anticline may be a fault-bend fold. Therefore, the two folds found in northern Peinanshan may represent structures developed in different stages. The syncline may have developed first as a fault-propagation fold of a deeper Luyeh strand. Later, when the tip of Luyeh strand gets closer to the surface, a shallow bend along the fault plane produced the gentle anticline. Along the southern part of the Peinanshan, the Luyeh strand did not bend; thus no anticline developed and the fault broke the surface along the synclinal axis.

Above the surface of terrace 7, many NNW-SSE striking scarps are present (Figure 6.7). The origin of these scarps is controversial. Some believe that they are terrace risers formed by the eastward migrating Luyeh River during the uplift of the Peinanshan [*Shih et al.*, 1986; *Yang*, 1986], while others suggest that they may represent active fault scarps [*Shih et al.*, 1983, 1984]. The presence of several west-facing scarps, however, seems to be contradictory with the terrace riser origin for the scarps. Furthermore, at least along the westernmost scarps we found that the paleo-current direction is perpendicular to the scarps. Therefore, we favor the fault scarp origin for these scarps. Due to the steepness of the scarps and the horst-and-graben-like topography, we suspect that they are normal faults. The limited distribution of these normal faults and their striking direction suggest that they may have formed due to the indentation of the metamorphic rock ridge against the northwestern corner of the Peinanshan.

The Peinan strand appears to cut through the northeastern corner of the Peinanshan (Figures 6.7 and 6.8). South of the confluent of the Luyeh and Peinan Rivers, a small N-S striking scarp with its western side about 5 m higher is present on terrace 1. The

scarp appears to extend to the south into the hills and connects with another scarp on terrace 2 just northeast of Shanli. In fact, the latter scarp has been identified previously as the Shanli fault [*Shih et al.*, 1983, 1984, 1986; *Yang*, 1986]. Since the eastern side of the Shanli scarp is higher, we suspect that the Peinan strand south of the Luyeh River has predominantly strike-slip. The Peinan strand is likely to extend within the Peinan River valley again south of Shanli.

On the eastern side of the Peinan River, across from the Luyeh River junction, an enormous landslide complex is present on the western flank of the Coastal Range (Figure 6.7). This landslide complex originated very close to the Coastal Range crest, and deposited above a bedrock strath about 80 m above the current Peinan River bed (Figure 6.9a). The thickness of the landslide deposits locally exceeds 100 m. A thin fluvial gravel layer of rounded clasts is present above this strath, below the landslide deposits (Figure 6.9b). Therefore, the strath may be an uplifted Peinan River bed right before the landslide occurred. Above terrace 2 strath just east of Luanshan Bridge, about 18 m above the current Peinan River bed, we found a charcoal sample with an age of about 1.1 kyr (Figure 6.4; Table 6.1). Thus the incision rate of the Peinan River is about 16.4 mm/yr. If the incision rate of the Peinan River stays constant, the age of the landslide deposits is therefore about 4.9 kyr.

In some previous maps, the contact between the Lichi Formation and the Peinanshan Conglomerate has been considered the major fault plane of the Longitudinal Valley fault [e.g., *Wang and Chen*, 1993]. An outcrop of this highly sheared contact is present on the eastern Peinan River wall across the junction of the Luyeh River (Figures 6.7 and 6.9a). The same contact can also be found in the small westward flowing canyon further north (Figure 6.9c). Although this highly sheared contact may have been a major fault plane because it is covered by the landslide deposits and no offset of the overlying landslide deposits is present, the fault has ceased activity at least after the occurrence of the landslide. However, at the northeastern corner of the Peinanshan

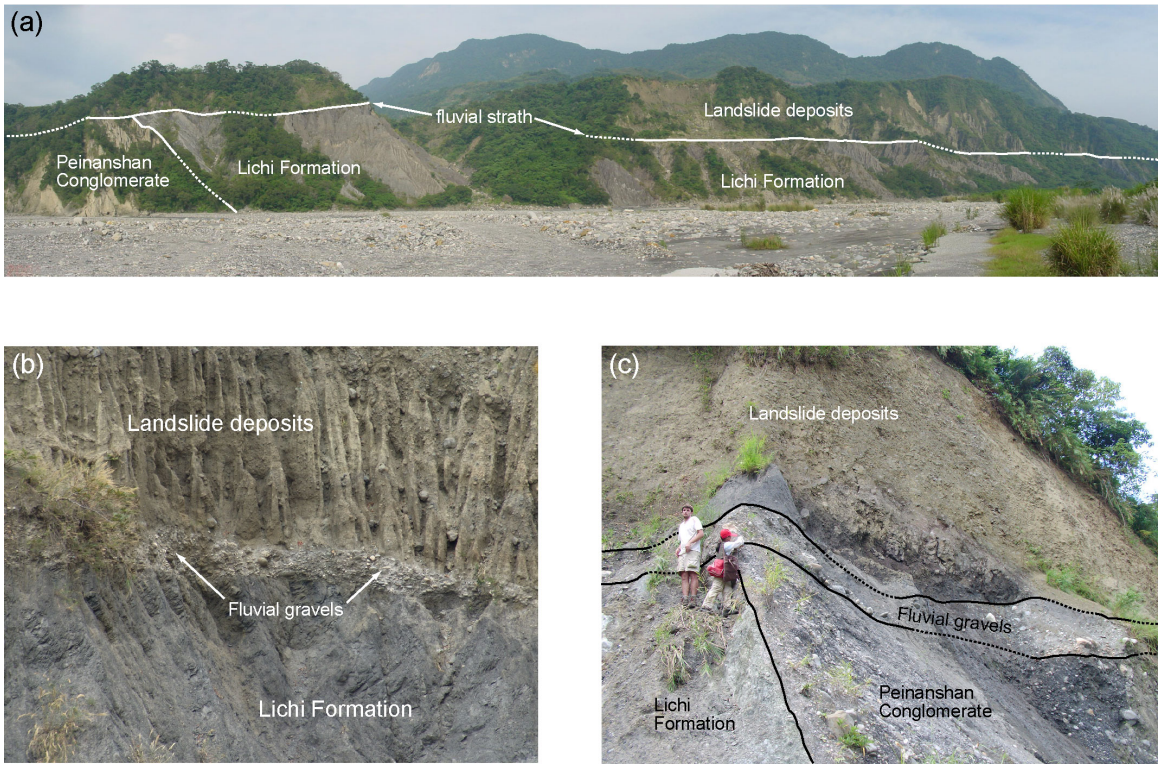

Figure 6.9. Photographs of the landslide deposits on the eastern bank of the Peinan River. (a) The landslide deposits sit on a fluvial strath, now at about 80 m above the Peinan River bed, above the bedrocks of the Lichi Formation and the Peinanshan Conglomerate. The view of the photo is shown in Figure 6.7. (b) A thin fluvial gravel layer of rounded clasts about 1-2 m thick overlies the strath and underlies the landslide deposits. The photo was taken at point G in Figure 6.7 with view to the north. (c) The contact between the Lichi Formation and the Peinanshan Conglomerate, which may be an old fault, is covered by the fluvial gravels and the landslide deposits. No offset along this contact is present in the fluvial gravels or the landslide deposits. The photo was taken in a small westward flowing canyon at point K in Figure 6.7 with view to the south.

where the Peinan strand cuts through a hill, the eastern side of the Peinan strand is a large limestone block of the Lichi Formation, and the strand in fact runs along the contact between the block and the Peinanshan Conglomerate. Therefore, the active Peinan strand may indeed follow the Lichi-Peinanshan contact south of this point.

6.7 Neotectonic geomorphology of the southern Peinanshan area

Along the western front of the southern half of the Peinanshan the Luyeh strand appears to be an emerged fault, locally producing fault scarps on young alluvial surfaces

(Figure 6.10). The southernmost part of the Luyeh strand wraps southern Peinanshan and turns into an E-W trending monocline, creating a series of southward tilting terraces. To the east, the Peinan strand runs mostly in the Peinan River bed but also through the triangular-shaped terraces near the village of Lichi.

South of the point where the syncline of northern Peinanshan ends, the Luyeh strand runs along the western front of the Peinanshan as the emerged fault that produced the fault-propagation fold (Figure 6.10). The total motion on the fault plane appears to decrease significantly to the south, as shown by the southward decrease in elevation of terrace 7 surface. Several minor monoclines deformed terrace 7 surface, generally creating steeper eastern surfaces and gentler western surfaces.

One of the monoclines appears to extend along the large N-S trending canyon and replaces the fault as the major structure of the southernmost Luyeh strand (Figure 6.10). At the southernmost part of the Peinanshan, several southwestward tilting surfaces of terrace 7 are present. The bedding attitude of the gravel beds underlying the easternmost one appears to be very similar to the slope of the surface itself. Further east, surfaces of terraces 3 and 2 are progressively less tilted. Since we have found steeply dipping Peinanshan Conglomerate bedrock underlying both terraces near the village of Yenwan, the two terraces are thus strath terraces, and the tilting surfaces would have to be produced by active deformation. Therefore, we believe the southernmost Luyeh strand becomes an E-W trending monocline, and created this series of tilted terraces.

West of the small village of Pinglang, a N-S trending anticlinal ridge with a monoclinal western front breaks the alluvial surfaces (Figure 6.10). The ridge has a maximum height of about 10 m and gradually dies out to the south before ending just north of the Taiping River bed on the active Taiping River fan. Although current knowledge of this feature is very limited, we believe that this feature is created by a young, westernmost secondary sub-strand of the Luyeh strand.

North of Lichi, a small N-S striking scarp separate terraces 2 and 3 (Figure 6.10).

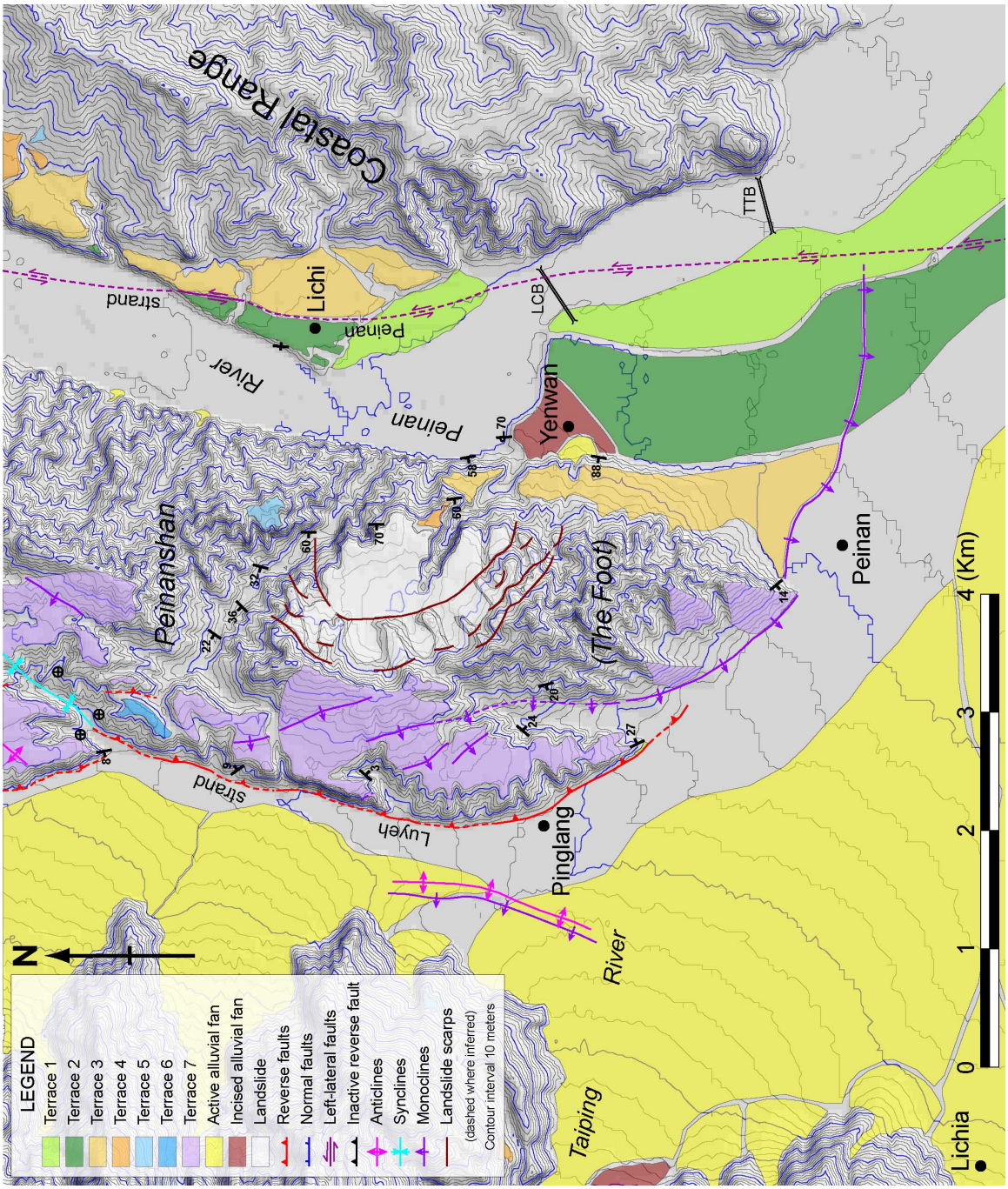

Figure 6.10. Detailed map shows geomorphic features and active structures of the southern Peinanshan area. The Luyeh strand still runs along the western front of the Peinanshan, but becomes an E-W trending monocline wrapping around the southernmost part of the Peinanshan. The Peinan strand runs mostly in the Peinan River valley, but produces a small N-S scarp on the terraces near Lichi.

Although this scarp may simply be a terrace riser, our field investigation revealed that the scarp is also coincident with the contact between the Lichi Formation and the Peinanshan

Conglomerate. Since the mud-rich Lichi Formation in the eastern side should be much more erodable, it is odd that a terrace riser should follow this contact. Therefore, we believe the scarp is where the Peinan strand cuts through the terraces near Lichi.

The southern extension of the Peinan strand is again difficult to determine and is likely to run within the Peinan River valley for most of its length (Figure 6.10). Close to the eastern end of the Lichi Bridge (LCB in Figure 6.10) the bridge appears to be slightly deformed (Figure 6.6b), but the deformation may be simply due to poor construction. Farther to the south, geodetically measured left-lateral creep of about 25 mm/yr near the Taitung Bridge [*Yu et al.*, 1992] (TTB in Figure 6.10) indicates that the Peinan strand runs very close to the bridge.

We had much difficulty when interpreting the series of large, high, and slightly westward tilting surfaces northwest of Yenwan (Figure 6.10). The presence of several truncated ridges and triangular facets west of the surfaces led us to believe that they are created by a series of landslides. However, the presence of undisturbed fluvial gravels on the surfaces indicates that the surfaces are originally fluvial terraces, and the landslides have to be cohesive slide blocks to preserve the fluvial gravel beds. Although it is odd to develop slide surfaces in the Peinanshan Conglomerate, we did find several normal faults in the two southeastward flowing canyons. Moreover, the presence of landslides may help explain the odd terrace 2 of Yenwan, which rises in the middle of the Peinan River bed. If the toe of the landslides has extended out to the east into the Peinan River bed, the river may have been forced to flow more to the east and left the Yenwan terrace behind.

6.8 Neotectonic geomorphology of the Pingting terraces

Since the Luyeh strand does not continue further north than the Luliao River, we believe the Luyeh strand steps to the east and joins the Peinan strand to become the main

strand of the Longitudinal Valley fault just southwest of the Pingting terraces. Below the thin fluvial gravels of the Pingting terraces, the Lichi Formation crops out at several outcrops as the underlying bedrock of the terraces. This indicates that the Pingting terraces are formed east of and in the hanging-wall block of the Longitudinal Valley fault system. The two-stepped Pingting terraces appear to be formed by several smaller sub-strands of the Longitudinal Valley fault (Figure 6.11). Some of these sub-strands clearly exhibit sinistral as well as reverse motion, consistent with the characteristics of the Longitudinal Valley fault.

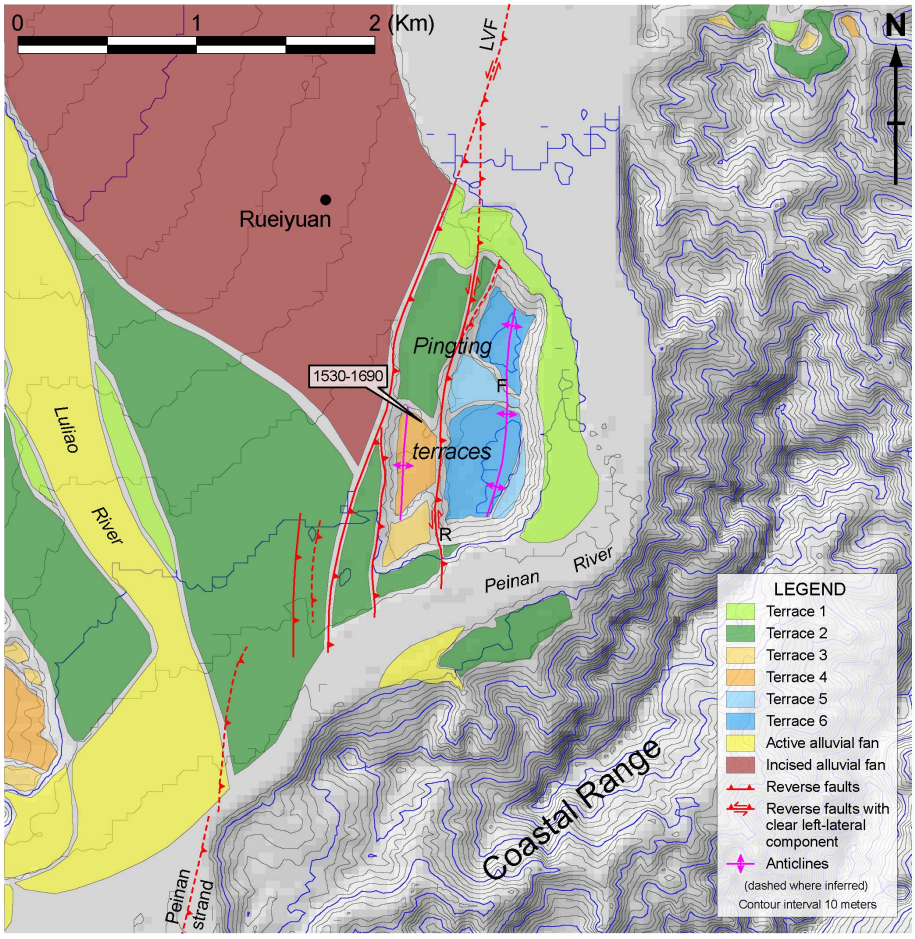

Figure 6.11. Detailed map shows geomorphic features and active structures of the Pingting terraces area. The Luyeh strand steps to the east and joins with the Peinan strand to form the main strand of the Longitudinal Valley fault. The fault has several sub-strands along the western side of the major steps of the Pingting terraces. The eastern sub-strand clearly shows sinistral as well as reverse offset. The age of a terrace is shown in calibrated ages (2σ) in cal BP.

There are two major steps of the Pingting terraces (Figure 6.11). Since the current Peinan River flows east of the Pingting terraces further into the hanging-wall block of the Longitudinal Valley fault, if the scarps between these major steps are simply terrace risers, it is odd that the Peinan River would later abandon these channels and develop a new channel in the rapidly uplifting hanging wall of the Longitudinal Valley fault. Therefore, we believe that the western scarps of Pingting steps are mostly sub-strands of the Longitudinal Valley fault and that both of the two major steps are likely to be correlative fluvial terraces formed by previous Peinan River bed.

During our field investigation we found an outcrop of the eastern sub-strand which separates the two major Pingting steps in a recent man-made excavation site (point R in Figure 6.11). In the outcrop, the Lichi Formation clearly thrusts over fluvial gravels along this strand, which dips steeply at about 70° to the east. South of point R, the terrace risers of terrace 2 were clearly offset left-laterally by this sub-strand. Similar left-lateral offset by this sub-strand can also be observed in the terrace risers between terraces 1 and 2 near the northern end of the Pingting terraces. Therefore, this sub-strand clearly has both reverse and sinistral motions.

Along the western edge of the western Pingting step is another sub-strand of the Longitudinal Valley fault (Figure 6.11). Although this strand may also have a sinistral component, there is no good geomorphic evidence for left-lateral offset by this sub-strand. To the southwest of the Pingting terraces the fault appears to form a series of *en echelon* sub-strands to step slightly to the west and connects with the Peinan strand. These smaller sub-strands have produced several minor scarps, all of which are less than 5 m high, on terrace 2. Although some of these sub-strands may extend further south to the southern side of the Peinan River and into the Coastal Range, the highly sheared and chaotic nature of the Lichi Formation cropping out in this area makes it very difficult to test this hypothesis.

The highest terrace (terrace 6) of the eastern Pingting step is warped by the eastern

sub-strand into an anticline (Figure 6.11). In the middle of this terrace a slightly lower triangular surface is present. Paleo-current direction of this surface, found at point F in Figure 6.11, indicates that the flow was flowing toward southeast. Therefore, this surface is likely to be a slightly younger terrace, probably formed by a small channel of the southeastward flowing Luliao River. The shape of this terrace, with a wider upstream part and a much narrower downstream part, indicates that the terrace formed while the anticline is growing. The narrowest part of this terrace is coincident with the anticlinal axis. As the rapidly growing anticline outpaced the incision of the river channel, the terrace was abandoned entirely.

According to a charcoal sample found at an outcrop of the western Pingting step, the age of the surfaces is about 1.6 kyr (Figure 6.11; Table 6.1). Since the western Pingting step has been uplifted for about 20 m, the uplift rate by the western sub-strand is about 12.5 mm/yr. Furthermore, if we assume that both Pingting steps are correlative, from the elevation difference of about 25 m between the two steps the uplift rate by the eastern sub-strand is about 15.6 mm/yr. Therefore, total vertical slip component of the Longitudinal Valley fault at the Pingting terraces is at least about 28 mm/yr. If the fault dips at 70° to the east, the minimum slip rate along the fault would be about 30 mm/yr.

North of the Pingting terraces, the many sub-strands of the Longitudinal Valley fault are likely to join together into a single main strand of the fault in the Peinan River bed (Figure 6.11). The fault appears to extend to the north and run through about 100 m from the eastern end of the Paohua Bridge (PHB in Figure 6.3) where the bridge was clearly deformed by the fault (Figure 6.6c), probably during the December 2003 earthquake [*H.-T. Chu*, unpublished data].

6.9 Discussion

6.9.1 The Central Range fault at the southernmost Longitudinal Valley

All of the neotectonic features we have mapped in the Peinanshan area are produced by the east-dipping Longitudinal Valley fault system. The west-dipping Central Range fault, active and emerged in the middle part of the Longitudinal Valley [*Shyu et al.*, 2005d] (Figure 6.2), does not appear to break the surface and produce any surface offset in this area. However, the fluvial terraces along the northern bank of the Luyeh River provide the evidence for showing that the Central Range fault may be active but blind.

West and in the footwall block of the Luyeh strand, the Lungtien terrace (terrace 4) is still up to 60 m above the current Luyeh River bed (Figure 6.5a). Since we did not find any other strand of the Longitudinal Valley fault west of the Luyeh strand, the incision of the Luyeh River to produce the Lungtien and other terraces west of the Luyeh strand is likely to be caused by the uplift of the eastern flank of the Central Range. In fact, the surface break of the Lungtien terrace by the Luyeh strand appears to be just a small irregularity overprinting on the general incision of the Luyeh River. Therefore, we believe the overall uplift of the eastern Central Range flank and the Luyeh River terraces is produced by the slip of a deep Central Range fault. The fault appears to be overridden by the Luyeh strand which breaks the surface and produced the monoclinal scarp on the Lungtien terrace (Figure 6.12).

However, the large amount of incision by the Luyeh River, in comparison with the height of the Luyeh strand scarp, indicates that the Central Range fault should be slipping at a much higher rate than the Luyeh strand. This is contradictory to the current knowledge of the slip rate along the Central Range fault [e.g., *Shyu et al.*, 2005d] and is likely because the Lungtien terrace is not a strath terrace. Although terraces 1 and 2 south of Luyeh appear to be strath terraces with the Peinanshan Conglomerate cropping

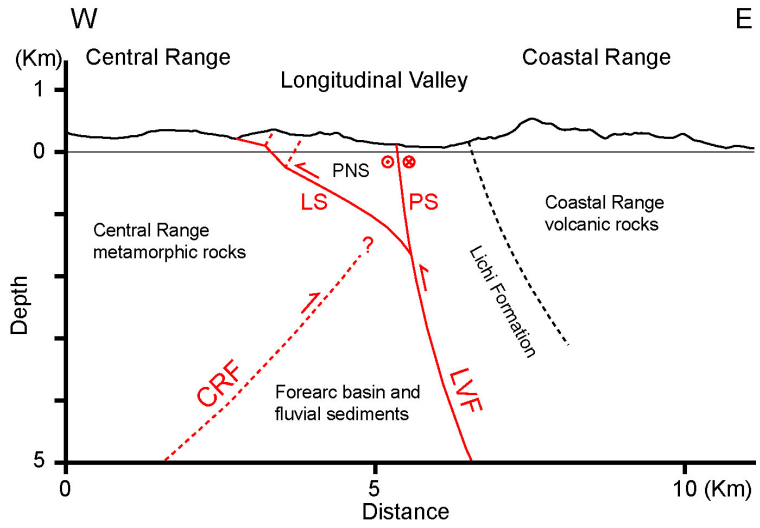

Figure 6.12. A schematic tectonic E-W cross section at the latitude of the Peinanshan showing the proposed tectonic model for the southern end of the Taitung Domain. The east-dipping Longitudinal Valley fault (LVF) branches into the Luyeh strand (LS) and the Peinan strand (PS), between which late Quaternary fluvial surfaces and the Peinanshan Conglomerate (PNS) are progressively deformed. The Luyeh strand crops out along the western edge of the Peinanshan, while the Peinan strand crops out approximately along the Peinan River. The west-dipping Central Range fault appears to be blind in this area and overridden by the Longitudinal Valley fault. However, the uplifted and deformed terraces along the upper reach of the Luyeh River suggest the Central Range fault is also active.

out as the bedrock, an outcrop at point N in Figure 6.4 shows that above terrace 2, the Lungtien terrace consists of entirely young fluvial gravels. Thus the thickness of fluvial gravels underlying the Lungtien terrace is about 40 m. As a result, the net bedrock uplift of the Lungtien terrace west of the Luyeh strand is only about 20 m. From the age of the Lungtien terrace, this yields an uplift rate of the eastern Central Range flank of about 6 mm/yr, consistent with the suggested uplift rate caused by the slip of the Central Range fault elsewhere [*Shyu et al.*, 2005d].

6.9.2 The southern termination of the Taitung Domain

A major characteristic of the neotectonic domains of Taiwan is that between neighboring domains, major structures behave distinctively [*Shyu et al.*, 2005b]. This significant change in behavior sometimes occurs through a transition zone, where

characteristics of both neighboring domains are present. Since the Peinanshan area locates at the southernmost part of the Taitung Domain (Figure 6.2), the structures present in this area may provide information of how the Taitung Domain ends to the south.

Our geomorphic analysis of southern Peinanshan indicates that the total reverse motion on the Luyeh strand decreases significantly to the south. The elevation of terrace 7 becomes much lower in southern Peinanshan, and the southernmost part of the Luyeh strand turns into a monocline wrapping around southern Peinanshan. Although the Peinan strand, with its sinistral motion, may extend further to the south, the reverse motion on the Luyeh strand clearly becomes zero at the monocline. Coincidentally, east of the Peinan strand the elevation of the Coastal Range decreases dramatically and disappears at this point.

Therefore, we believe that the southern end of the Peinanshan and the Coastal Range, with the end of reverse motion on the Luyeh strand, all represent the southern termination of the Taitung Domain. To the south, the major structure in the Lutao-Lanyu Domain is a west-dipping thrust fault beneath the forearc basin sediments, and no east-dipping structure equivalent to the Longitudinal Valley fault is present [*Shyu et al.*, 2005b] (Figure 6.2). Only at the latitude of Taitung where the colliding Luzon arc gets close enough to the Central Range continental sliver does the west-vergent Longitudinal Valley fault begin to appear. This structure then produces the uplift of the Luzon arc into Coastal Range and the formation of the Longitudinal Valley suture.

6.9.3 Stress release of the southernmost Longitudinal Valley fault

It is well-known that the Longitudinal Valley fault is creeping aseismically at a high rate up to 20 mm/yr [*Angelier et al.*, 1997; *Lee et al.*, 2001, 2003] along the segment near Chihshang, about 30 km north of the Peinanshan (Figure 6.2). Other segments of the fault, however, may be locked. In the Peinanshan area, the locking depth of the two

major strands of the fault appears to be very shallow, but the evidence for the strands to be creeping at the surface is very scarce.

Along the entire length of the Luyeh strand, we found no place where any man-made structure is broken by the strand. This suggests that the Luyeh strand is not creeping at the surface. A preliminary leveling investigation across the Luyeh strand scarp on the Lungtien terrace, however, shows that the deformation by the strand occurs only at a small distance across the strand. Therefore, the tip of the creeping part of the Luyeh strand is likely to be very close to the surface.

The Peinan strand may actually be creeping at the surface. Many bridges that built across the strand do show fractures by the strand. However, most of the fracture may have occurred during the December 2003 earthquake by small induced slip of the strand [*H.-T. Chu*, unpublished data]. Preliminary results of a short-aperture GPS transect across the Peinan strand at the northeastern corner of the Peinanshan show that no significant near-field velocity difference is present across the strand. This indicates that currently the strand is not creeping at the surface at that point.

A short-aperture GPS transect across the many sub-strands near the Pingting terraces shows that large near-field velocity differences are present across the two major sub-strands. Since we did not find any broken man-made structure in this area, we believe that these sub-strands may be similar to the Luyeh strand, that they have a very shallow locking depth but are not creeping at the surface.

6.9.4 Lichi Formation and the Longitudinal Valley fault

Due to its deep marine depositional environment, the Lichi Formation is generally considered as part of the Coastal Range [e.g., *Ho*, 1988]. Therefore, the western boundary of the Lichi Formation is usually mapped as the Longitudinal Valley fault [e.g., *Wang and Chen*, 1993]. Several previous field investigations have also mapped the

contact between the Lichi Formation and younger sediments as the location of the fault [*Yang*, 1986; *Chu and Yu*, 1997].

In the Peinanshan area, our field investigation indicates that the contact between the Lichi Formation and the Peinanshan Conglomerate or younger fluvial sediments is indeed generally coincident with the Peinan strand. This is consistent with the idea of previous maps: Although the Luyeh strand clearly breaks the Peinanshan Conglomerate much farther to the west, the Peinan strand, a major strand of the Longitudinal Valley fault, still follows the western boundary of the Lichi Formation.

However, near the confluent of the Luyeh and Peinan Rivers, the Peinan strand clearly deviates from the Lichi-Peinanshan contact, and the contact, probably an old fault, has evidently not been active for the last several thousand years because it is covered by the landslide deposits. It is interesting that, however, the old contact locates in the middle of an old Peinan River bed, very similar to the current situation, where most of the Peinan strand locates within the present Peinan River bed. Therefore we suspect that the covered Lichi-Peinanshan contact may have been the active Longitudinal Valley fault strand right before the landslide occurred. Reverse faults are known to be sensitive to overlying topography and break into new branches if there is a significant overburden. The additional load of the landslide deposits may thus cause the strand to break further to the west. If this is the case, the current Peinan strand near the confluent of the Luyeh and Peinan Rivers would be a young feature, probably just a couple of thousand years old. This would be consistent with the obscure topographic features of the strand there.

6.10 Conclusions

Plenty of fluvial landforms helped us to map the Longitudinal Valley fault system in great detail ay the southernmost part of the Longitudinal Valley, in the Peinanshan area. In this area, the Longitudinal Valley fault branches into two major strands: the Luyeh

strand in the west and the Peinan strand in the east. The Luyeh strand has predominantly reverse motion, whereas the Peinan strand has a significant sinistral component. Complete slip-partitioning, however, does not appear to occur at least north of the Luyeh River, since the Peinan strand may also have a large reverse component there.

The Luyeh strand produces a monoclinal scarp on the Lungtien terrace. Both to the north and to the south of the Lungtien terrace, old fluvial surfaces of the Kaotai terraces and the Peinanshan are moving upward and westward against the eastern Central Range flank along the Luyeh strand. From the age of the Lungtien terrace, the minimum vertical slip component of the Luyeh strand is about 4.5 mm/yr. The southernmost part of the Luyeh strand becomes an E-W trending monocline that wraps around southern Peinanshan.

The Peinan strand appears to run within the current Peinan River bed for most of its length. The only exceptions are northeast of Shanli and on the terraces near Lichi, where the strand offsets the terraces and produces small scarps. South of the Luyeh River, the Peinan strand appears to have more left-lateral component.

The Luyeh strand steps to the east south of the Luliao River and joins with the Peinan strand to form the main strand of the Longitudinal Valley fault, which runs along the western edge of the Pingting terraces and extend to the north. The southern end of the Luyeh strand, on the other hand, is coincident with the southern end of the Coastal Range, and is likely to represent the southern termination of the Taitung Domain. Most of the active strands in the Peinanshan area have very shallow locking depths, but do not seem to be creeping at the surface.

6.11 Acknowledgments

We greatly appreciate the assistance of Y.-C. Chen and T. Watanuki in the field. We have benefited significantly from the information collected by and the stimulating discussions with the students of two binational field classes of the National Taiwan University and California Institute of Technology (Caltech), held in the Peinanshan area in 2001 and 2005. We are also grateful for valuable discussions with H.-T. Chu, J.-C. Lee, W.-T. Liang, D.V. Wiltschko, Y.-M. Wu, and S.-B. Yu. Our mapping was facilitated by J. Giberson, manager of the Caltech's Geographic Information Systems (GIS) laboratory. The 5-m DEM was generously provided by the Central Geological Survey, MOEA, Taiwan. Radiocarbon dating by M. Kashgarian in the Center for Accelerator Mass Spectrometry, LLNL, is greatly appreciated. Our project in Taiwan was supported by National Science Foundation (NSF) grant EAR-0208505. This research was also supported in part by the Gordon and Betty Moore Foundation. This is Caltech Tectonics Observatory Contribution #28.

6.12 References

Angelier, J., H.-T. Chu, and J.-C. Lee (1997), Shear concentration in a collision zone: kinematics of the Chihshang Fault as revealed by outcrop-scale quantification of active faulting, Longitudinal Valley, eastern Taiwan, *Tectonophysics*, *274*, 117-143.

Barrier, E., and J. Angelier (1986), Active collision in eastern Taiwan: the Coastal Range, *Mem. Geol. Soc. China*, *7*, 135-159.

Barrier, E., and C. Muller (1984), New observations and discussion on the origin and age of the Lichi Mélange, *Mem. Geol. Soc. China*, *6*, 303-325.

Barrier, E., J. Angelier, H. T. Chu, and L. S. Teng (1982), Tectonic analysis of compressional structure in an active collision zone: the deformation of the Pinanshan Conglomerates, eastern Taiwan, *Proc. Geol. Soc. China*, *25*, 123-138.

Biq, C. (1971), Comparison of mélange tectonics in Taiwan and in some other mountain belts, *Pet. Geol. Taiwan*, *9*, 79-106.

Blisniuk, P. M., B. R. Hacker, J. Glodny, L. Ratschbacher, S. Bi, Z. Wu, M. O. McWilliams, and A. Calvert (2001), Normal faulting in central Tibet since at least 13.5 Myr ago, *Nature*, 412, 628-632.

Chang, C. P., J. Angelier, C. Y. Huang, and C. S. Liu (2001), Structural evolution and significance of a mélange in a collision belt: the Lichi Mélange and the Taiwan arc-continent collision, *Geol. Mag.*, *138*, 633-651.

Chen, H.-H., and R.-J. Rau (2002), Earthquake locations and style of faulting in an active arc-continent plate boundary: the Chihshang fault of eastern Taiwan, *EOS, Trans., Am. Geophys. Uni.*, *83*(47), Fall Meet. Suppl., Abstract T61B-1277.

Chen, Y.-G. (1988), C-14 dating and correlation of river terraces along the lower reach of the Tahan-chi, northern Taiwan (in Chinese), M.S. thesis, 88pp., Natl. Taiwan Univ., Taipei.

Chu, H.-T., and M.-S. Yu (1997), The relationships between earthquakes and faults in the Taitung Longitudinal Valley (in Chinese), *Natl. Sci. Council Project Rep., No. NSC-86-2116-M-047-002*, 133pp., Natl. Sci. Council, Taipei, Taiwan.

Ho, C. S. (1986), A synthesis of the geologic evolution of Taiwan, *Tectonophysics*, *125*, 1-16.

Ho, C. S. (1988), *An Introduction to the Geology of Taiwan, Explanatory Text of the Geologic Map of Taiwan*, 2nd ed., 192pp., Cent. Geol. Surv., Ministry Econ. Affairs, Taipei, Taiwan.

Hsü, K. J. (1988), Mélange and the mélange tectonics of Taiwan, *Proc. Geol. Soc. China*,

31(2), 87-92.

Hsu, T. L. (1956), Geology of the Coastal Range, eastern Taiwan, *Bull. Geol. Surv. Taiwan*, *8*, 39-63.

Hsu, Y.-J., M. Simons, S.-B. Yu, L.-C. Kuo, and H.-Y. Chen (2003), A two-dimensional dislocation model for interseismic deformation of the Taiwan mountain belt, *Earth Planet. Sci. Lett.*, *211*, 287-294.

Hu, J.-C., J. Angelier, C. Homberg, J.-C. Lee, and H.-T. Chu (2001), Three-dimensional modeling of the behavior of the oblique convergent boundary of southeast Taiwan: friction and strain partitioning, *Tectonophysics*, *333*, 261-276.

Huang, C.-Y., C.-T. Shyu, S. B. Lin, T.-Q. Lee, and D. D. Sheu (1992), Marine geology in the arc-continent collision zone off southeastern Taiwan: Implications for Late Neogene evolution of the Coastal Range, *Mar. Geol.*, *107*, 183-212.

Kuochen, H., Y.-M. Wu, C.-H. Chang, J.-C. Hu, and W.-S. Chen (2004), Relocation of the eastern Taiwan earthquakes and its tectonic implications, *Terr. Atmos. Oceanic Sci.*, *15*, 647-666.

Lallemand, S., and C.-S. Liu (1998), Geodynamic implications of present-day kinematics in the southern Ryukyus, *J. Geol. Soc. China*, *41*, 551-564.

Lee, J.-C., J. Angelier, H.-T. Chu, S.-B. Yu, and J.-C. Hu (1998), Plate-boundary strain partitioning along the sinistral collision suture of the Philippine and Eurasian plates: Analysis of geodetic data and geological observation in southeastern Taiwan, *Tectonics*, *17*, 859-871.

Lee, J.-C., J. Angelier, H.-T. Chu, J.-C. Hu, and F.-S. Jeng (2001), Continuous monitoring of an active fault in a plate suture zone: a creepmeter study of the Chihshang Fault, eastern Taiwan, *Tectonophysics*, *333*, 219-240.

Lee, J.-C., J. Angelier, H.-T. Chu, J.-C. Hu, F.-S. Jeng, and R.-J. Rau (2003), Active fault creep variations at Chihshang, Taiwan, revealed by creep meter monitoring, 1998-2001, *J. Geophys. Res.*, *108*(B11), 2528, doi:10.1029/2003JB002394.

Lin, C.-W., H.-C. Chang, S.-T. Lu, T.-S. Shih, and W.-J. Huang (2000), *An Introduction to the Active Faults of Taiwan, 2nd ed., Explanatory Text of the Active Fault Map of Taiwan* (in Chinese with English abstract), *Spec. Pub. Cent. Geol. Surv.*, *13*, 122pp., Taipei, Taiwan.

Molnar, P., and P. Tapponnier (1978), Active tectonics of Tibet, *J. Geophys. Res.*, *83*, 5,361-5,375.

Page, B. M., and J. Suppe (1981), The Pliocene Lichi Mélange of Taiwan: its plate-tectonic and olistostromal origin, *Am. J. Sci.*, *281*, 193-227.

Sella, G. F., T. H. Dixon, and A. Mao (2002), REVEL: A model for Recent plate

velocities from space geodesy, *J. Geophys. Res.*, *107*(B4), 2081, doi:10.1029/2000JB000033.

Shih, T.-T., J.-C. Chang, C.-E. Hwang, C.-D. Shih, G.-S. Yang, and Y.-M. Sunlin (1983), A geomorphological study of active fault in northern and eastern Taiwan (in Chinese with English abstract), *Geogr. Res.*, *9*, 20-72.

Shih, T.-T., J.-C. Chang, C.-E. Hwang, C.-D. Shih, and G.-S. Yang (1984), A geomorphological study of active fault in northern and eastern Taiwan, *Geogr. Studies*, *8*, 1-30.

Shih, T.-T., K.-H. Teng, J.-C. Chang, C.-D. Shih, and G.-S. Yang (1986), A geomorphological study of active fault in Taiwan (in Chinese with English abstract), *Geogr. Res.*, *12*, 1-44.

Shyu, J. B. H., K. Sieh, and Y.-G. Chen (2005a), Tandem suturing and disarticulation of the Taiwan orogen revealed by its neotectonic elements, *Earth Planet. Sci. Lett.*, *233*, 167-177.

Shyu, J. B. H., K. Sieh, Y.-G. Chen, and C.-S. Liu (2005b), Neotectonic architecture of Taiwan and its implications for future large earthquakes, *J. Geophys. Res.*, *110*, B08402, doi:10.1029/2004JB003251.

Shyu, J. B. H., K. Sieh, J.-P. Avouac, W.-S. Chen, and Y.-G. Chen (2005c) Millennial slip rate of the Longitudinal Valley fault from river terraces: Implications for convergence across the active suture of eastern Taiwan, *J. Geophys. Res.*, submitted for publication.

Shyu, J. B. H., K. Sieh, Y.-G. Chen, and L.-H. Chung (2005d) Geomorphic analysis of the Central Range fault, the second major active structure of the Longitudinal Valley suture, eastern Taiwan, *Geol. Soc. Am. Bull.*, submitted for publication.

Stuiver, M., and P. J. Reimer (1993), Extended ^{14}C data base and revised CALIB 3.0 ^{14}C age calibration program, *Radiocarbon*, *35*, 215-230.

Teng, L. S. (1981), On the origin and tectonic significance of the Lichi Formation, Coastal Range, eastern Taiwan (in Chinese with English abstract), *Ti-Chih*, *3*, 51-61.

Teng, L. S. (1987), Stratigraphic records of the late Cenozoic Penglai orogeny of Taiwan, *Acta Geol. Taiwanica*, *25*, 205-224.

Teng, L. S. (1990), Late Cenozoic arc-continent collision in Taiwan, *Tectonophysics*, *183*, 57-76.

Teng, L. S., and Y. Wang (1981), Island arc system of the Coastal Range, eastern Taiwan, *Proc. Geol. Soc. China*, *24*, 99-112.

Wang, Y., and W.-S. Chen (1993), Geologic map of eastern Coastal Range, scale 1:100,000, Cent. Geol. Surv., Ministry Econ. Affairs, Taipei, Taiwan.

Yang, G.-S. (1986), A geomorphological study of active faults in Taiwan – especially on

the relation between active faults and geomorphic surfaces (in Chinese), Ph.D. thesis, 178pp., Chinese Culture Univ., Taipei, Taiwan.

Yin, A., P. A. Kapp, M. A. Murphy, C. E. Manning, T. M. Harrison, M. Grove, L. Ding, X.-G. Deng, and C.-M. Wu (1999), Significant late Neogene east-west extension in northern Tibet, *Geology*, *27*, 787-790.

Yu, S.-B., and L.-C. Kuo (2001), Present-day crustal motion along the Longitudinal Valley Fault, eastern Taiwan, *Tectonophysics*, *333*, 199-217.

Yu, S.-B., and C.-C. Liu (1989), Fault creep on the central segment of the Longitudinal Valley fault, eastern Taiwan, *Proc. Geol. Soc. China*, *32*, 209-231.

Yu, S.-B., G.-K. Yu, L.-C. Kuo, and C. Lee (1992), Crustal deformation in the southern Longitudinal Valley area, eastern Taiwan, *J. Geol. Soc. China*, *35*, 219-230.

Chapter 7

Conclusions and Implications

7.1 Neotectonic framework of Taiwan and earthquake scenarios

The lack of a systematic understanding of active structures in Taiwan, revealed by the fact that the disastrous 1999 Chi-Chi earthquake was an utter surprise, led us to prepare a map of the active structures of the island as the first major product of this thesis (Figure 7.1). Based upon this active-structure map, we have also produced a rudimentary map of future earthquake sources in and around Taiwan (Figure 7.2). Although this is just an initial attempt and we have ignored many details, this is a major step forward, and information in this map provides an important foundation for future hazard-mitigation projects.

The characteristics of the active structures in and around Taiwan inspired us to propose a new tectonic model for the active orogen (Figure 7.3). Based upon the apparent topographic and structural continuity of the Hengchun Ridge, the Central Range, and the westernmost Ryukyu volcanic arc, we conclude that these three units constitute a continental sliver drifted away from southeastern China during the opening of the South China Sea (Figure 7.4). We hypothesize that the Taiwan orogen reflects a tandem suturing and disarticulation of the Luzon volcanic arc, the Eurasian continental margin, and the continental sliver. Suturing of these three lithospheric blocks is occurring at the southernmost part of Taiwan, forming the Longitudinal Valley suture in the east and the western Taiwan deformational belt in the west. The three blocks detach again along the two sutures in northern and northeastern Taiwan due to the flip of subduction polarity.

This new model can be subjected to further tests. In fact, we hope our proposition of the model will stimulate further investigations to do just that. For example, although distinctive gravity pattern and P-wave velocity across the Hengchun Ridge suggest that the underlying rocks of the ridge may have continental affinity [e.g., *Chi et al.*, 1998; *Nakamura et al.*, 1998], a well-designed ocean-drilling project on the ridge could confirm or refute the hypothesis. High-resolution tomographic investigations should be very

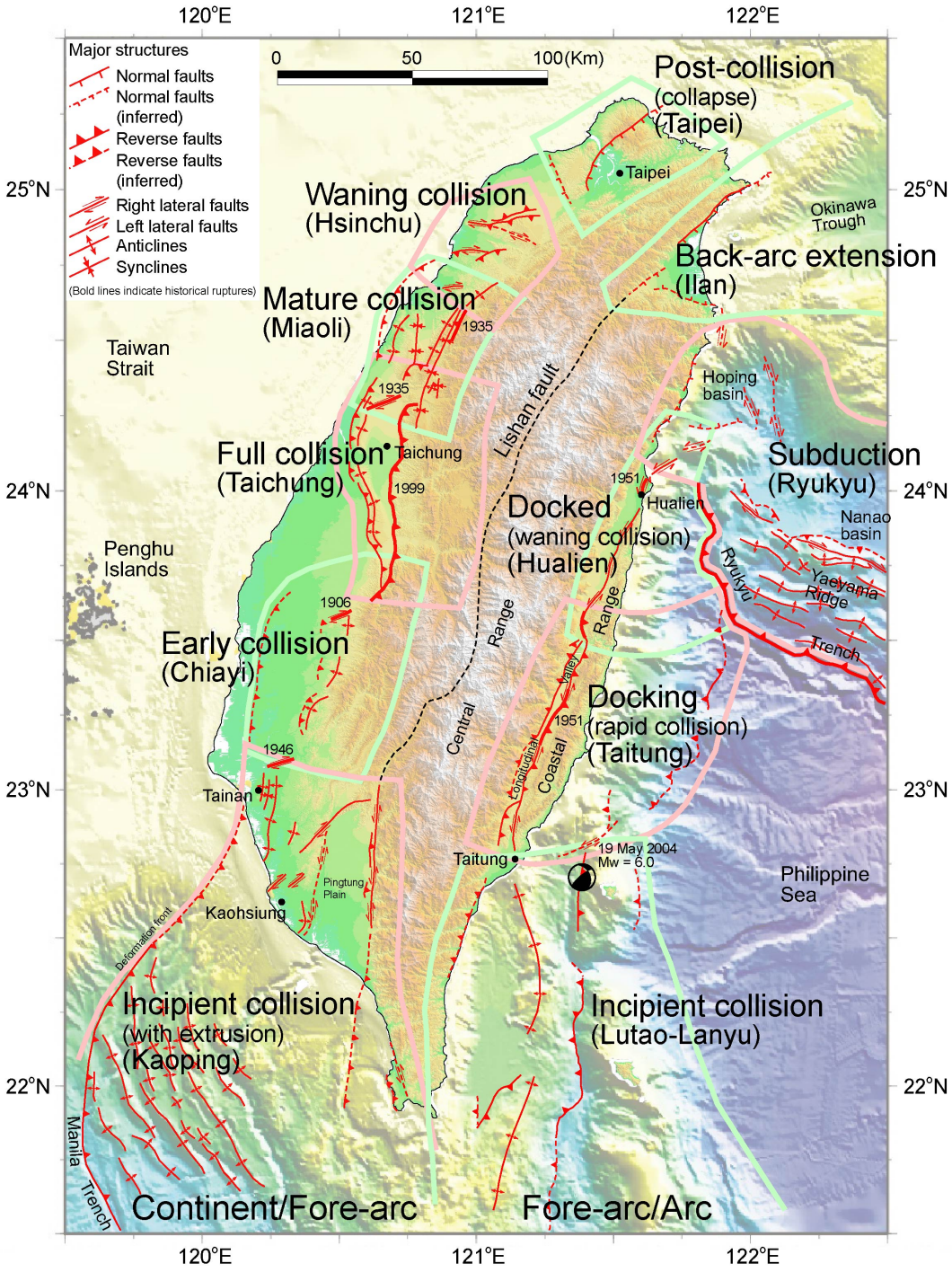

Figure 7.1. Map of major active faults and folds of Taiwan (in red) shows that the two sutures are producing separate western and eastern neotectonic belts. Each collision belt matures and then decays progressively from south to north. This occurs in discrete steps, manifested as seven distinct neotectonic domains along the western belt and four along the eastern. A distinctive assemblage of active structures defines each domain. The Lishan fault (dashed black line) is the suture between forearc ridge and continental margin. Bold light green and pink lines are boundaries of domains. Focal mechanism and magnitude of the 19 May 2004 earthquake adapted from the BATS (http://bats.earth.sinica.edu.tw/) database.

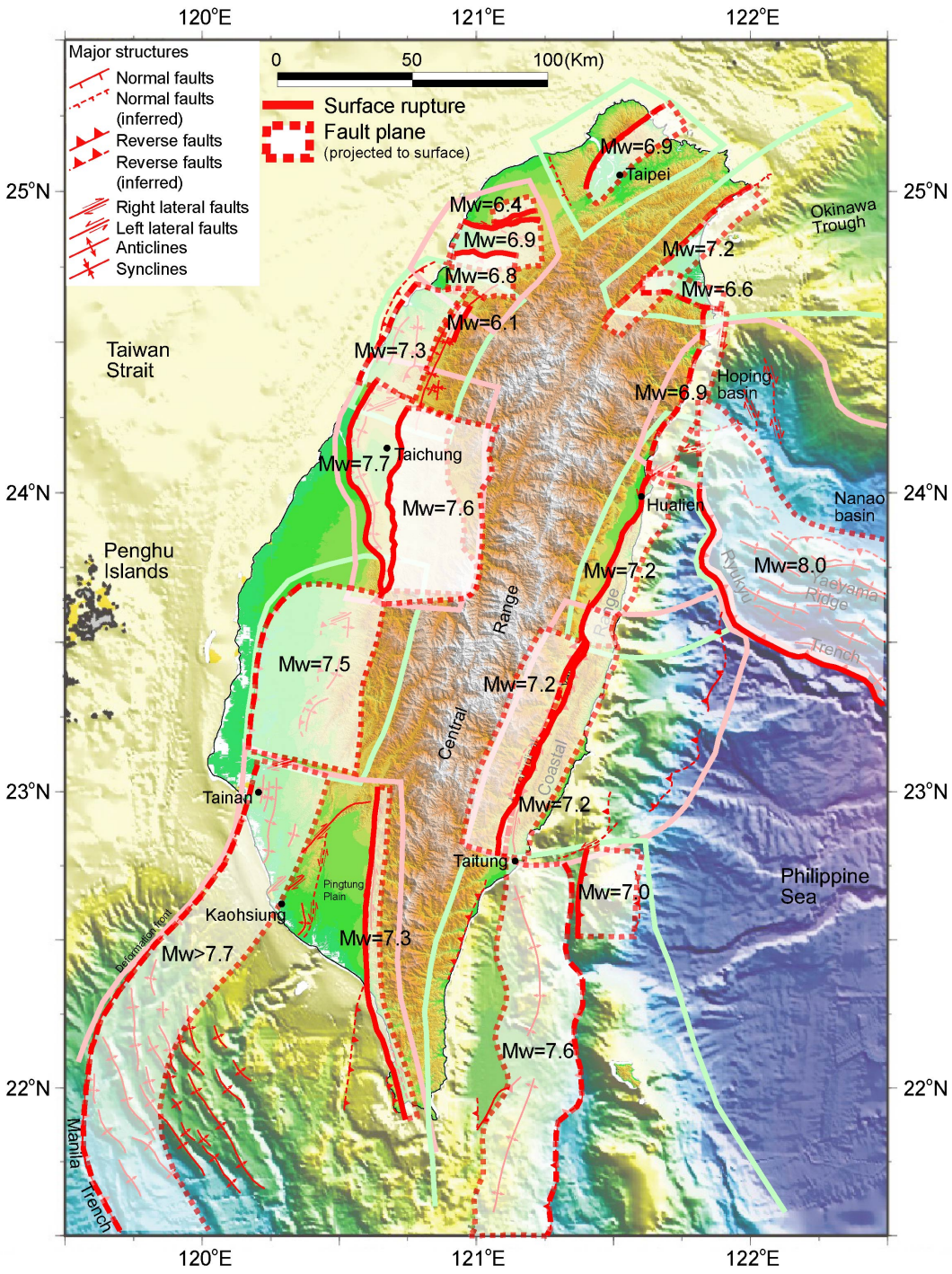

Figure 7.2. Proposed major sources for future large earthquakes in and around Taiwan. Bold red lines are proposed future ruptures, and the light patches are rupture planes projected to the surface. Earthquake magnitude of each scenario is predicted value from our calculation.

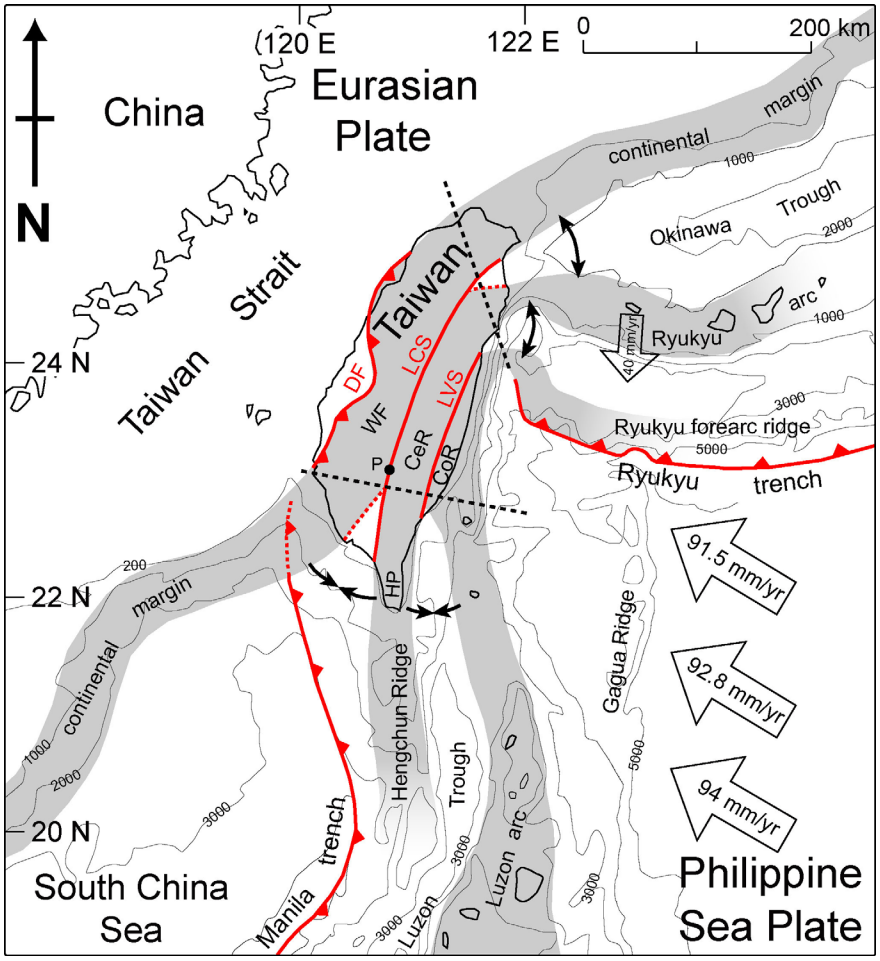

Figure 7.3. Taiwan is experiencing a tandem suturing of a volcanic arc and a sliver of continental crust to continental margin. In the south, the Luzon volcanic arc is converging on the Hengchun forearc ridge, which is, in turn, converging on the Chinese continental margin. Suturing of these three elements occurs in the middle of the island. In the north, both sutures are disarticulating, to form both the Okinawa Trough and troughs south of the Ryukyu island arc. Current velocity vectors of the Philippine Sea plate relative to South China, at 124°E and 20°, 21°, and 22°N, are calculated using the Recent plate velocity model (REVEL) of *Sella et al.* [2002]. Current velocity vector of the Ryukyu arc is adapted from *Lallemand and Liu* [1998], relative to the Penghu Islands in the Taiwan Strait. Black dashed lines are the northern and western limits of the Wadati-Benioff zone of the two subducting systems taken from the seismicity database of the Central Weather Bureau, Taiwan. DF: deformation front; LCS: Lishan-Chaochou suture; LVS: Longitudinal Valley suture; WF: Western Foothills; CeR: Central Range; CoR: Coastal Range; HP: Hengchun Peninsula; P: Outcrops of pillow lava along the western suture.

helpful for determining if the Taiwan orogen incorporates a distinctive continental sliver. Our hypothesis that no structural break exists between the Central Range and the Hengchun Peninsula/Ridge, based mainly on their geometrical continuation, can also be tested by detailed mapping of bedrock between these two regions. Any alternative to our tandem-suturing model must explain the geomorphologic and kinematic features of

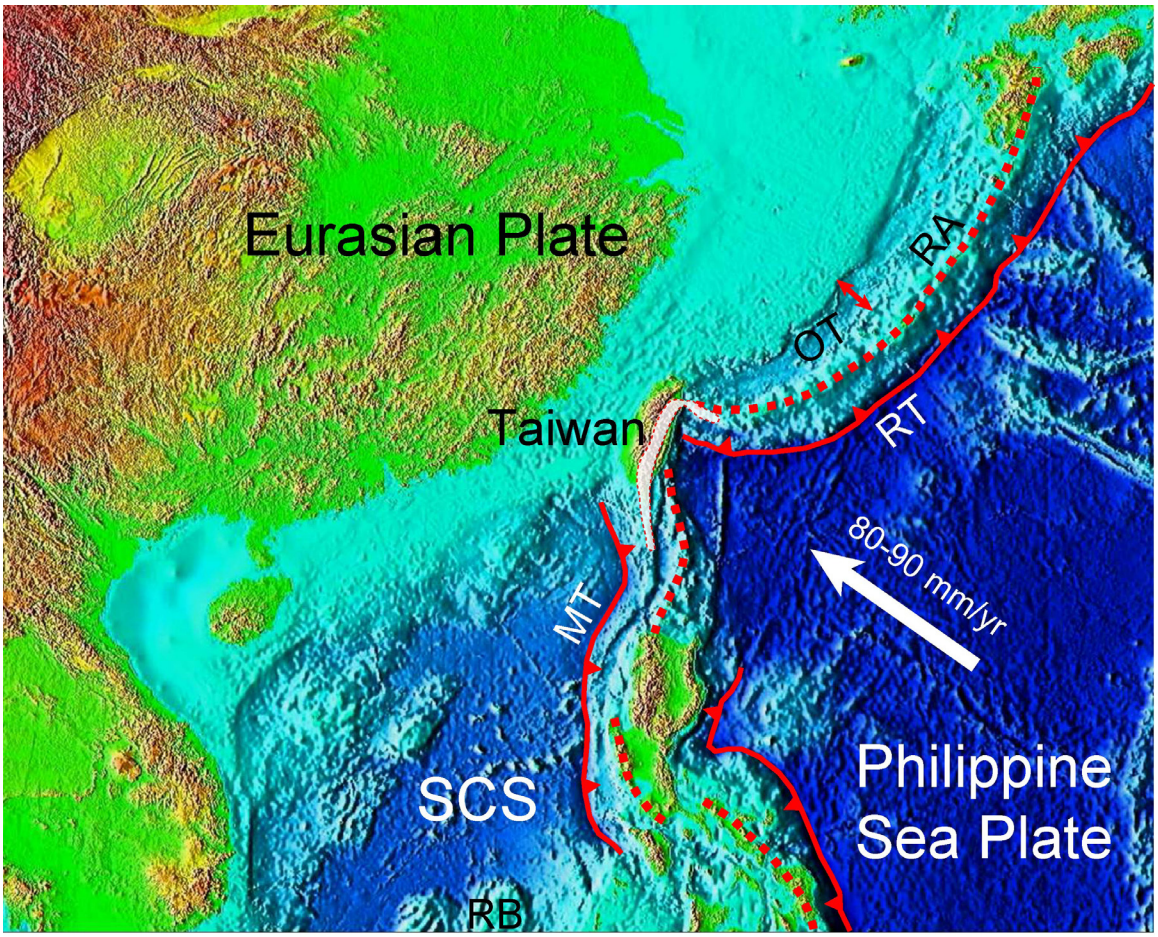

Figure 7.4. Major tectonic elements in southeastern Asia. The Philippine Sea Plate is moving toward the Eurasian Plate at a rate of about 80-90 mm/yr and is subducting underneath the Eurasian Plate along the Ryukyu trench (RT), creating the Ryukyu arc (RA) and the back-arc Okinawa Trough (OT). The South China Sea (SCS) Plate is subducting eastward beneath the Philippine Sea Plate along the Manila trench (MT). Several continental blocks, including the Reed Bank (RB) were split away and drifted from southeastern China during the opening of the South China Sea. We propose that another continental sliver, marked by the white patch including part of Taiwan, formed in a similar way and was sandwiched between the Luzon arc and the Eurasian continental margin during the collision that produced the island of Taiwan. Red dots indicate volcanic arcs. Bathymetry is obtained from National Geophysical Data Center.

the island, such as the extrusion and foundering of the Pingtung Plain and the presence of pillow lavas along our proposed western suture [*Kuo*, 1984]. Further investigations of the pillow lavas could support or refute our contention that this is a remnant of South China Sea oceanic crust.

Some new information suggests that a slight modification of our tandem suturing model may be necessary. Structural analysis of Neogene sedimentary rocks in the

Western Foothills of Taiwan indicates that total shortening of the rocks is more than 60 km [*Yue et al.*, 2005]. Since these rocks are mostly shallow continental shelf sedimentary rocks, they must have been scraped off of about 60 km of Eurasian continental shelf. Thus the shelf should have extended some 60 km east of the present position of the Western Foothills, almost as far east as the eastern flank of the Central Range. If such a reconstruction is correct, it means that Eurasian continental lithosphere in central Taiwan must extend underneath at least the western Central Range. This implies a protrusion eastward from the gently arcuate shape we show in Figure 7.3.

Such a configuration might require that our Central Range continental sliver is merely a thin continental fragment rather than the thick lithospheric block that we have proposed. In this case, this thin continental fragment would override the margin of the Eurasian continental shelf. The resulting active crustal duplexing could be the cause of the observed rapid uplift of the Central Range (Figure 7.5). The submarine character of the Hengchun Ridge is also consistent with the hypothesis of a thin continental sliver: A thick continental block should be buoyant enough to emerge above sea level. Moreover, other large continental blocks within the South China Sea, such as the Reed Bank (Figure 7.4), are capped by post-rift carbonate rocks, indicative of shallow water [e.g., *Schlüter et al.*, 1996]. The lack of Neogene carbonate rocks in the Central Range suggests that our proposed Central Range continental sliver was not thick enough (i.e. buoyant enough) to rise to reef-forming water depths.

Our tandem suturing and disarticulation model of Taiwan has some significant implications for understanding the orogenic processes of Taiwan. For a long time, the Taiwan orogen has been considered the classic example of critical taper wedge mechanics, as illustrated by the well-known “bulldozer” model [e.g., *Dahlen et al.*, 1984]. However, the presence of the continental sliver within the Taiwan orogen indicates that the wedge mechanics may not be applicable for the entire mountain belt. Instead, the wedge mechanics may be valid only in the Western Foothills, and the exhumation and uplift of

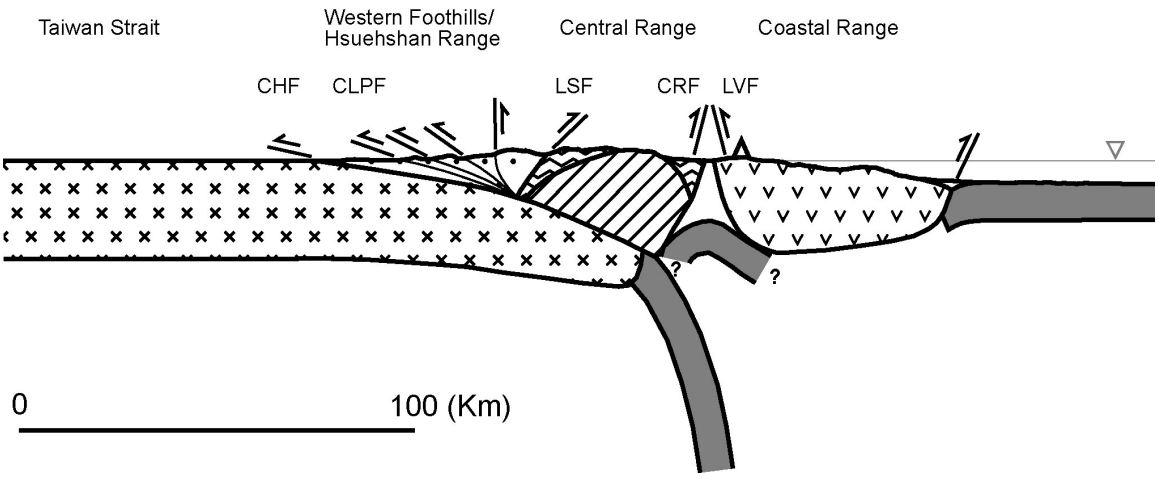

Figure 7.5. An alternative model for the E-W crustal cross section across central Taiwan. The Central Range continental sliver may be a small piece of continental fragment and this small fragment may override the margin of the Eurasian continental shelf, resulting in crustal duplex and creating the rapid uplifting Central Range.

the Central Range may be produced by pervasive ductile thickening of the crust. Recent models of horizontal and vertical GPS displacements have also shown that the rapid uplift of the Central Range is difficult to explain by a simple two-dimensional elastic dislocation model [e.g., *Hsu et al.*, 2003]. Furthermore, many recent wedge mechanical models of Taiwan involve the Coastal Range (collided Luzon arc) as a backstop, which leads to an eastern Central Range that rises much faster than the Coastal Range [e.g., *Willett et al.*, 2003]. Although this phenomenon may have been occurring before, it clearly contradicts current observations of that the Coastal Range is also rising rapidly, even much faster than the Central Range.

Our elucidation of the orogenic processes of Taiwan may provide significant insight into other active orogens. For example, similar continental fragments are widespread throughout the South China Sea, and the tandem suturing model of Taiwan illustrates a potential role that these continental fragments might play when incorporated into a collisional belt. In fact, collision of such blocks played an important role in the formation of the island of Palawan [e.g., *Yumul et al.*, 2003]. One cannot argue that the Central Range/Hengchun Ridge is too narrow and long to be a continental sliver, because

similar-shaped continental fragments do occur elsewhere. The Seychelles microcontinent in the Indian Ocean is one example [e.g., *Plummer*, 1995; *Plummer and Belle*, 1995]. The incorporation of such long and narrow continental slivers into collisional belts may therefore be an important process in Earth's tectonic history. Besides, the lessons learned from Taiwan are certainly very valuable in understanding the future tectonic evolution of other arc-continental collision zones, such as Timor.

Our proposed scenarios for future earthquakes in Taiwan obviously need refinement. In fact, a database of all future earthquake sources in Taiwan would likely require decades to complete. Detailed subsurface geometry of major active structures would be one of the most important constraints on such a database, but is currently poorly known for many of the structures. Our calculations of future earthquake scenarios would also be significantly improved with better constraints on geothermal gradients and, thus, the depths of the brittle-ductile transition for different areas of Taiwan. We assume that each major structure breaks along its entire length. Yet recent paleoseismologic studies are showing that the Chelungpu fault has not always ruptured along its entire length [e.g., *Chen et al.*, 2001a, 2001b, 2001c]. This means that we have overestimated the size of some future earthquakes and underestimated the recurrence interval. Scores of paleoseismologic investigations, at different sites along the major faults, will be needed to document systematically the past behavior of each major fault.

Nonetheless, our proposed earthquake scenarios should serve as initial guidelines for future land-use planning in Taiwan. For example, in southwestern Taiwan the paucity of historical earthquakes has led to the conventional wisdom that the region is seismically less dangerous than other areas. Our results, however, indicate the Manila megathrust could produce very large subduction earthquakes in that region (Figure 7.2). Such events would have a major impact on Kaohsiung and Tainan, the largest and most densely populated cities in the region.

7.2 Active tectonics of the Longitudinal Valley suture

Our geomorphic and neotectonic investigations in the Longitudinal Valley revealed that the valley has two major structures: the east-dipping Longitudinal Valley fault and the west-dipping Central Range fault (Figure 7.6). The Longitudinal Valley fault slips obliquely at a higher rate, up to 30 mm/yr, and thus absorbs most of the horizontal shortening between the Central Range and the Coastal Range. Part of the fault broke during the November 1951 earthquake series. The slip rate of the Central Range reverse fault, on the other hand, is lower, and the fault appears to be active only south of Rueisuei. Our reconstructed subsurface geometry of the Longitudinal Valley fault, near Hsiukuluan canyon, shows a much shallower listric fault plane than that illuminated by earthquake hypocenters farther to the south. This fundamental along-strike difference in geometry of the fault may be a manifestation of the northward maturation of the suturing of the Luzon volcanic arc to the Central Range continental sliver (Figure 7.7).

This model, too, should be subjected to further tests. High-resolution tomographic and gravity investigations could provide better constraints on the cross sections we proposed in Figure 7.7, and more well-relocated earthquakes could help test the validity of the cross-sections in the figure. Better mapping and dating of the blueschists cropping out on the eastern flank of the Central Range might help us figure out the tectonic history of those rocks, as well as the mechanism for their emplacement.

A clear implication of the model we proposed in Figure 7.7 is that there needs to be many accommodation structures between each of the panels. A major accommodation structure is especially necessary between panels (a) and (b), where the vergence of major structures changes direction. Based upon a series of linearly distributed small earthquakes, a major tear fault was in fact proposed along the Taitung canyon, between Lutao and Lanyu [e.g., *Kao et al.*, 2000]. Geomorphic evidence for such a fault, however, is obscure at best. The shallow M_w 6.0 earthquake north of Lutao on 19 May

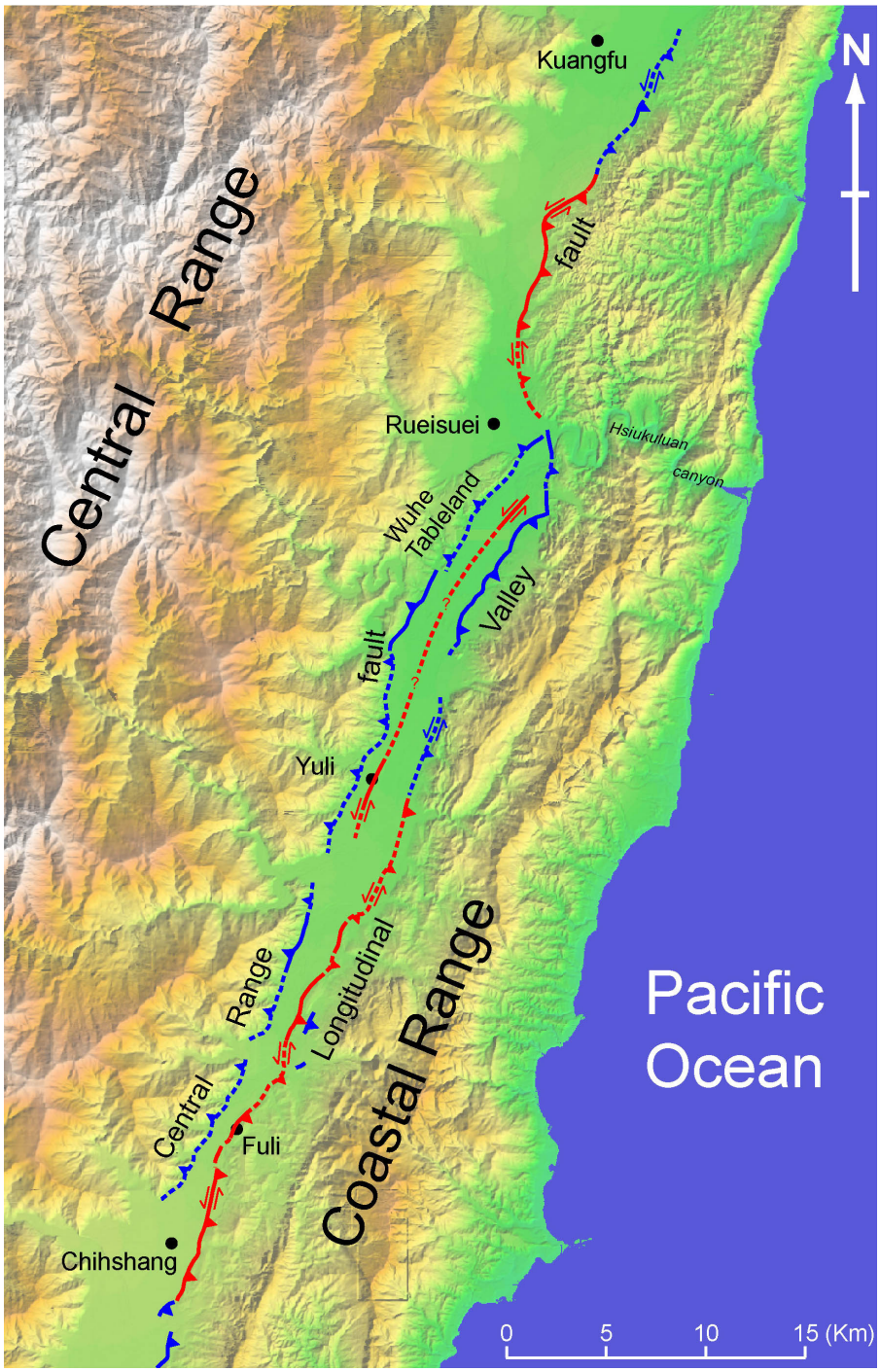

Figure 7.6. Map of major structures in the middle part of the Longitudinal Valley. The Longitudinal Valley fault is an east-dipping, obliquely slipping reverse fault, along which the Coastal Range is rising rapidly and moving toward the Central Range. The less prominent Central Range fault is a west-dipping reverse fault, above which many fluvial terraces and the Wuhe Tableland are rising slowly. Part of the Longitudinal Valley fault ruptured during the November 1951 earthquakes (in red). Major faults and flexures that did not rupture in 1951 but are known to be active are colored blue.

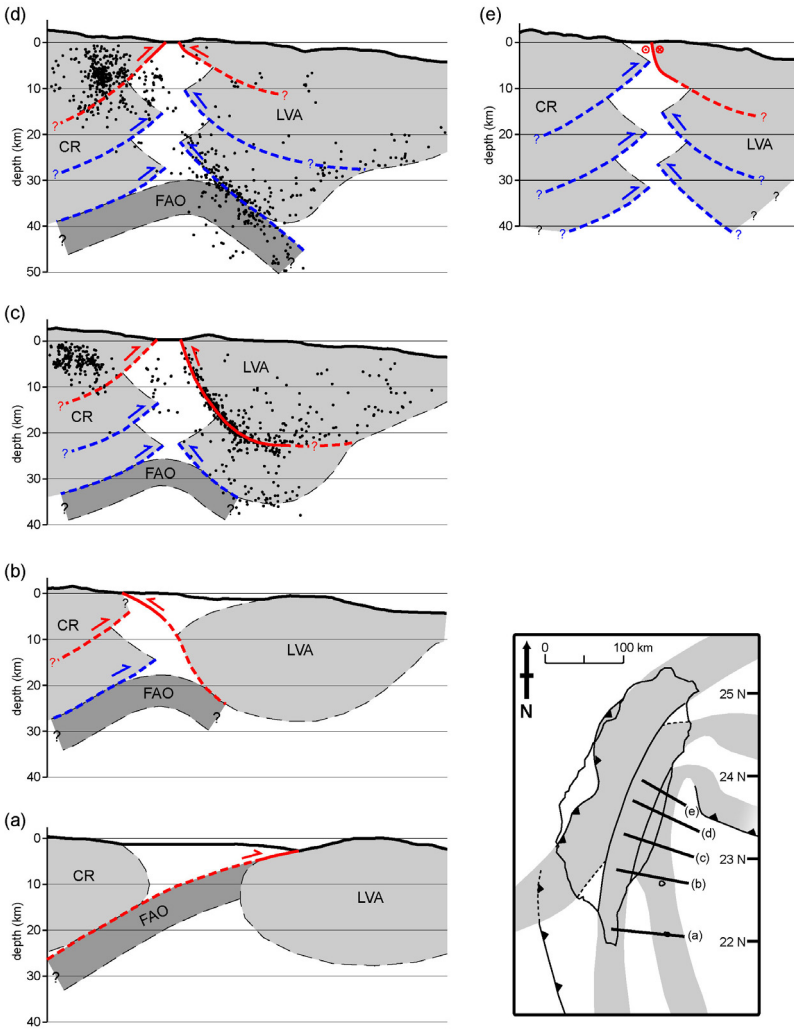

Figure 7.7. Schematic crustal cross sections show our hypothesis for the evolution of the Longitudinal Valley suture. Each section is drawn using current topography and observations along the lines specified on the index map, with no vertical exaggeration. (a) Before suturing, the Luzon forearc oceanic lithosphere (FAO) subducts beneath the Central Range continental sliver (CR). This is currently occurring at about the latitude of the southern tip of Taiwan, about 22°N. (b) As the Luzon volcanic arc lithosphere (LVA) approaches the Central Range, an east-dipping thrust fault appears, allowing the FAO to also subduct underneath the LVA. Contemporaneously on the west side of the valley, the proximity of the LVA to the CR induces formation of a newer, shallower west-dipping thrust fault above the original one. This is the current structural geometry near the southern end of the Longitudinal Valley between about 22°40'N and 22°50'N. (c) As the suture matures, the two non-oceanic lithospheric blocks both start to thicken by evolving multiple reverse-fault wedges, with the younger ones at shallower depth. This is the current structural geometry at the latitude of Chihshang, about 23°10'N. (d) At the latitude of the Wuhe Tableland, about 23°30'N, the suture is nearing maturity. The suture has evolved into a "Christmas tree" shape, with a thick pile of sediments between the two non-oceanic lithospheric blocks and underlain by the subducted forearc oceanic lithosphere. (e) In northern Longitudinal Valley, at the latitude about 23°45'N, the dominantly sinistral Longitudinal Valley fault appears to be the only major active structure. The west-dipping Central Range fault has become inactive, and sediments in the Longitudinal Valley are lapping on the eastern flank of the Central Range. Red indicates the youngest and currently active faults in each time frame, and blue indicates older faults which may still be active. Faults are dashed where inferred. Relocated earthquake hypocenters in (c) and (d) are adapted from *Kuochen et al.* [2004].

2004 might represent rupture of a NE-SW striking tear fault (Figure 7.1).

Although the Longitudinal Valley fault is absorbing most of the horizontal shortening across eastern Taiwan at present, it is likely to be a fairly new structure. Not only is the Coastal Range much lower than the Central Range, but the presence of high-grade metamorphic rocks in the Central Range also indicates that the Central Range has a much longer history of exhumation. Our model, indeed, suggests that the Longitudinal Valley fault system does not appear until the Luzon arc and the Central Range continental sliver are very close, like the current situation near the southern end of the Longitudinal Valley. Before this close approach, most of the shortening between the two blocks would be absorbed by a west-dipping fault system like the one now on the sea floor in the Lutao-Lanyu domain. Therefore, it is likely that the much older west-dipping fault systems, including the Central Range fault, produced the longer history and larger amount of exhumation and uplift of the Central Range.

7.3 References

Chen, W.-S., et al. (2001a), 1999 Chi-Chi earthquake: A case study on the role of thrust-ramp structures for generating earthquakes, *Bull. Seismol. Soc. Am.*, *91*, 986-994.

Chen, W.-S., Y.-G. Chen, and H.-C. Chang (2001b), Paleoseismic study of the Chelungpu fault in the Mingjian area, *Western Pacific Earth Sci.*, *1*, 351-358.

Chen, W.-S., Y.-G. Chen, H.-C. Chang, Y.-H. Lee, and J.-C. Lee (2001c), Paleoseismic study of the Chelungpu fault in the Wanfung area, *Western Pacific Earth Sci.*, *1*, 499-506.

Chi, W.-C., D. L. Reed, C.-S. Liu, and N. Lundberg (1998), Distribution of the bottom-simulating reflector in the offshore Taiwan collision zone, *Terr. Atmos. Oceanic Sci.*, *9*, 779-794.

Dahlen, F. A., J. Suppe, and D. Davis (1984), Mechanics of fold-and-thrust belts and accretionary wedges: cohesive Coulomb theory, *J. Geophys. Res.*, *189*, 10,087-10,101.

Hsu, Y.-J., M. Simons, S.-B. Yu, L.-C. Kuo, and H.-Y. Chen (2003), A two-dimensional dislocation model for interseismic deformation of the Taiwan mountain belt, *Earth Planet. Sci. Lett.*, *211*, 287-294.

Kao, H., G.-C. Huang, and C.-S. Liu (2000), Transition from oblique subduction to collision in the northern Luzon arc-Taiwan region: Constraints from bathymetry and seismic observations, *J. Geophys. Res.*, *105*, 3,059-3,079.

Kuo, C.-S. (1984), Geochemistry and isotopic analysis of spilite in the Paolai area (in Chinese), M.S. thesis, 96pp., Natl. Taiwan Univ., Taipei.

Kuochen, H., Y.-M. Wu, C.-H. Chang, J.-C. Hu, and W.-S. Chen (2004), Relocation of the eastern Taiwan earthquakes and its tectonic implications, *Terr. Atmos. Oceanic Sci.*, *15*, 647-666.

Lallemand, S., and C.-S. Liu (1998), Geodynamic implications of present-day kinematics in the southern Ryukyus, *J. Geol. Soc. China*, *41*, 551-564.

Nakamura, Y., K. McIntosh, and A. T. Chen (1998), Preliminary results of a large offset seismic survey west of Hengchun Peninsula, southern Taiwan, *Terr. Atmos. Oceanic Sci.*, *9*, 395-408.

Plummer, P. S. (1995), Ages and geological significance of the igneous rocks from Seychelles, *J. Afr. Earth Sci.*, *20*, 91-101.

Plummer, P. S., and E. R. Belle (1995), Mesozoic tectono-stratigraphic evolution of the Seychelles microcontinent, *Sediment. Geol.*, *96*, 73-91.

Schlüter, H. U., K. Hinz, and M. Block (1996), Tectono-stratigraphic terranes and detachment faulting of the South China Sea and Sulu Sea, *Mar. Geol.*, *130*, 39-78.

Sella, G. F., T. H. Dixon, and A. Mao (2002), REVEL: A model for Recent plate velocities from space geodesy, *J. Geophys. Res.*, *107*(B4), 2081, doi:10.1029/2000JB000033.

Willett, S. D., D. Fisher, C. Fuller, E.-C. Yeh, and C.-Y. Lu (2003), Erosion rates and orogenic-wedge kinematics in Taiwan inferred from fission-track thermochronometry, *Geology*, *31*, 945-948.

Yue, L.-F., J. Suppe, and J.-H. Hung (2005), Structural geology of a classic thrust belt earthquake: the 1999 Chi-Chi earthquake Taiwan (M_w = 7.6), *J. Struct. Geol.*, *27*, 2,058-2,083.

Yumul, G. P., Jr., C. B. Dimalanta, R. A. Tamayo, Jr., and R. C. Maury (2003), Collision, subduction and accretion events in the Philippines: A synthesis, *Island Arc*, *12*, 77-91.